Draft

Climate Change Modeling Appendix

Shasta Lake Water Resources Investigation, California

Prepared by:

United States Department of the Interior
Bureau of Reclamation
Mid-Pacific Region

U.S. Department of the Interior
Bureau of Reclamation

June 2013

Contents

Tables

Figures

Abbreviations and Acronyms

°C	degrees Celsius
°F	degrees Fahrenheit
ANN	artificial neural network
B	site-specific parameter
Bay-Delta	San Francisco Bay/Sacramento-San Joaquin Delta
BDCP	Bay Delta Conservation Plan
BO	Biological Opinion
CDF	cumulative distribution function
cfs	cubic feet per second
CIMIS	California Irrigation Management Information System
cm	centimeter
CMIP3	Coupled Model Intercomparison Project Phase 3
CO_2	carbon dioxide
CP	comprehensive plan
CT	Current Trends
CT-noCC	Current Trends-no climate change
CVP IRP CalLite	Central Valley Project Integrated Resources Plan version of the California Lite Simulation Model
CVP	Central Valley Project
CVPIA	Central Valley Project Improvement Act
CWP	California Water Plan
DCP	downscaled climate projection
DEIS	Draft Environmental Impact Statement
Delta	Sacramento-San Joaquin Delta
DSM2	Delta Simulation Model Version 2
DWR	California Department of Water Resources
EG	Expansive Growth
ENSO	El Nino Southern Oscillation
ET	evapotranspiration
FACE	Free Air Carbon Exchange
GCM	Global Circulation Model
GHG	greenhouse gas
GIS	geographical information system
GWh	gigawatt hours

in/yr	inches per year
IPCC	Intergovernmental Panel on Climate Change
IRP	Integrated Resource Plan
kg	kilogram
km	kilometer
Ko	dew point depression
LAWS	Land Atmosphere Water Simulator
LCPSIM	Least Cost Planning Simulation Model
LOD	level of development
LTGen	LongTermGen
M&I	municipal and industrial
MAF	million acre-feet
mm/yr	millimeters per year
msl	mean sea levels
mT CO_2e	metric tons of carbon dioxide equivalents
OMWEM	Other Municipal Water Economics Model
ppm	parts per minute
RBPP	Red Bluff Pumping Plant
Reclamation	U.S. Department of the Interior, Bureau of Reclamation
RH	relative humidity
Ro	clear radiation
Rs	solar radiation
SBWQM	South Bay Water Quality Model
SG	Slow Growth
SJRWQM	San Joaquin River Water Quality Model
SLWRI	Shasta Lake Water Resources Investigation
SOD	south-of-Delta
SRWQM	Sacramento River Water Quality Model
SWAP	Statewide Agricultural Production Model
SWE	Snow Water Equivalent
SWP Power	State Water Project Power
SWP	State Water Project
TAF	thousand acre feet
Tdew	dew point temperature
Tmax	daily maximum temperature
Tmin	daily minimum temperature
VIC	Variable Infiltration Capacity
VPD	vapor pressure deficit

WCRP	World Climate Research Program
WEAP	Water Evaluation and Planning

Chapter 1 Introduction

Historical warming of the climate system, including Earth's near-surface air and ocean temperatures, is now considered to be unequivocal (IPCC, 2007) with global surface temperature increasing approximately 1.33 degrees Fahrenheit (°F) over the last 100 years. Continued warming is projected to increase global average temperature between 2°F and 11°F over the next 100 years.

The causes of this warming have been identified as both natural processes and human actions. The Intergovernmental Panel on Climate Change (IPCC) concludes that variations in natural phenomena, such as solar radiation and volcanoes, produced most of the warming from preindustrial times to 1950, and had a small cooling effect afterward. However, after 1950, greenhouse gas (GHG) concentrations resulting from human activity, such as fossil fuel burning and deforestation, have been responsible for most of the observed temperature increase (CEC, 2006). These conclusions have been endorsed by more than 45 scientific societies and academies of science, including all of the national academies of science of the major industrialized countries. Since 2007, no scientific body of national or international standing has maintained a dissenting opinion.

The average mean annual temperature is projected to increase by 5 to 6°F during this century, though with substantial variability in warming in the Central Valley (ICF, 2012). Northern California is expected to experience changes to the physical environment as a result of climate change. Climatic modeling results indicate that climate change will result in a change from snow to rain in winter, leading to reduced snowpack, earlier snowmelt, and reduced river flows and reservoir storage in summer (Knowles and Cayan 2002; Miller et al. 2003; Mote et al. 2005), causing changes to the seasonal timing of flows in rivers (ICF, 2012).

A projected increased in surface temperatures and changes in timing and magnitude of stream runoff will have important implications for California's water supply and are also expected to affect aquatic species due to changes in river flows and water temperatures. Projected changes in climate are likely to influence the potential benefits of the Shasta Lake Water Resources Investigation (SLWRI) project.

The focus of this document is to present an assessment of the potential to achieve the objectives of the SLWRI under projected future climate change.. The primary objectives of the alternatives identified in the SLWRI are (1) increase survival of anadromous fish populations in the Sacramento River primarily upstream from the Red Bluff Pumping Plant; and, (2) increase water supply and water supply reliability for agricultural, municipal and industrial, and environmental purposes, to help meet current and future water demands, with a focus on enlarging Shasta Dam and Reservoir.

To assess the potential to achieve these objectives these under projected future climate change, two SLWRI comprehensive plans (i.e., alternatives) were selected. Comprehensive Plan 4 (CP4) maximizes anadromous fish survival, and was therefore selected to assess the potential to benefit anadromous fish survival under climate change. Comprehensive Plan 5 (CP5) maximizes the potential benefits to water supply reliability, and was therefore selected to assess the potential to benefit water supply reliability under climate change.

The potential to benefit water supply reliability under climate change was evaluated using climate modeling tools developed by U.S. Department of the Interior, Bureau of Reclamation (Reclamation) for the Central Valley Project (CVP) Integrated Resource Plan (IRP). Under the CVP IRP, transient changes in projected climatic conditions in the future are applied. The transient method assumes gradual warming as the simulation moves forward based on an interpolation between current and projected future conditions. For evaluating the potential to benefit anadromous fish survival under climate change, a different method based on the mean state of projected climate changes (“delta” method) was applied. Unlike the transient method, the delta method assumes a constant change in climate for simulation of future scenarios. In this method, temperature and/or precipitation are adjusted by the mean shift from one historical 30-year period to a future 30-year period. These two methods apply different hydrologic and CVP/State Water Project (SWP) system operations modeling tools, but use the same future climatic projections.

This appendix is organized as follows:

- Chapter 2 of this appendix presents information on a summary of global climate projections and relevant research on climate change implications for California water resources, particularly those for Shasta Lake.

- Chapter 3 of this appendix presents the results of the transient method analysis of the potential to benefit water supply reliability under climate change, using CP5.

- Chapter 4 presents the results of the delta method analysis of the potential to benefit anadromous fish survival under climate change, using CP4.

- Chapter 5 contains the technical references list.

This appendix provides context for the consideration of climate change within resource areas and cumulative condition chapters of the SLWRI Draft Environmental Impact Statement (DEIS). Assessments of specific impacts of climate change on environmental resource areas are discussed in the DEIS.

While it is unlikely that any single project could have a significant impact on the projected production of GHG, the cumulative effect of human activities has been clearly linked to quantifiable changes in the composition of the atmosphere, which in turn have been shown to be the main cause of global climate change (IPCC, 2007). Possible effects of the SLWRI on GHG production are discussed in the “Air Quality and Climate” chapter of the DEIS. The regulatory framework pertaining to air quality, climate change, and the emission of GHGs is also described in the “Air Quality and Climate” chapter of the DEIS.

This page left blank intentionally.

Chapter 2 Summary of Previous Studies of Climate Change in the Study Area

This chapter provides a summary of global climate projections and relevant research on climate change implications for California water resources, including a summary of key findings on the sensitivity of California water resources to climate changes, particularly those for Shasta Lake.

Study Area Setting

Shasta Dam and Shasta Lake are located on the upper Sacramento River in Northern California, approximately 9 miles northwest of Redding in Shasta County. The SLWRI includes both a primary and extended study area because of the potential influence of the proposed modification of Shasta Dam and Reservoir and subsequent system operations and water deliveries on resources over a large geographic area. This area is represented by the Sacramento and San Joaquin rivers and the Delta system, plus the CVP and SWP facilities and water service areas.

The Sacramento River drains the northern portion and the San Joaquin drains the central and southern portions of the Central Valley, a large north to south trending alluvial basin extending over 450 miles from the southern Cascade Mountains near the City of Redding to the Tehachapi Mountains south of the City of Bakersfield. The basin is about 40 to 60 miles wide and is bounded by the Coast Range to the west and the Sierra Nevada Mountains on the east. Hydrologically, the Central Valley is divided into three hydrographic regions including the Sacramento, San Joaquin and Tulare Lake Basins. Both the Sacramento and San Joaquin rivers flow into the Sacramento-San Joaquin Delta (Delta). This region is the largest estuary on the west coast of the United States. Typically, the Tulare Lake Basin is internally drained. However, in some wetter than normal years, flow from the Tulare Lake region reaches the San Joaquin River. Together, the Sacramento and San Joaquin rivers drain and area of approximately 59,000 square miles.

The Sacramento River is the largest river in California with an historic mean annual flow of 22 million acre-feet. It drains an area of about 27,000 square miles. The Sacramento River arises in the volcanic plateaus of northern California where it is joined by the Pit River above Shasta Dam, a Reclamation facility. Below Shasta Dam, transmountain diversions from the Trinity River (tributary to the Klamath River) along with many small-and moderate-sized tributaries join the river as it flows south through the Sacramento Valley. Major tributaries also join the river from the east including the Feather, Yuba, and American Rivers. Major facilities on these rivers include Oroville Dam operated by the California State Water Project on the Feather River and Folsom Dam operated by Reclamation on the American River. After a journey of over 400 miles, the river reaches Suisun Bay in the Sacramento-San Joaquin Delta before discharging into San Francisco Bay and the Pacific Ocean.

The San Joaquin River is the second largest river in California with an historic mean annual flow of 7.5 million acre-feet. It drains an area of 32,000 square miles. The San Joaquin originates in the high Sierra Nevada Mountains in east-central California. The river initially flows westward reaching Friant Dam, a Reclamation facility, before entering the San Joaquin Valley. At Friant Dam, diversions are made to the Friant Division of the Central Valley Project, which is primarily located in the Tulare Lake Basin. Before implementation of the San Joaquin Restoration Program, flows below the dam were minimal except during flood conditions. Releases from the dam flow initially westward until reaching the Chowchilla Bypass (a constructed flood control facility) or the Mendota Pool (a managed irrigation water control facility). From there, the river turns northward and begins receiving returns flows from agricultural and wildlife refuge areas upstream from its confluence with the Merced River, a major tributary. As the river continues northward, it receives inflows from several eastside tributaries including the Toulumne, Stanislaus, Calaveras, and Mokelumne Rivers, each of which have major dams that store water and regulate flows. After a distance of 330 miles, the San Joaquin joins the Sacramento River near Suisun Bay in the Sacramento-San Joaquin Delta.

Reclamation’s major role in the Central Valley began in 1933 with the construction of the CVP. Today the CVP consists of 20 dams, 11 powerplants and more than 500 miles of canals that serve many purposes including providing, on average, 5 million acre-feet of water per year to irrigate approximately 3 million acres of land in the Sacramento, San Joaquin, and Tulare Lake basins, 600,000 acre-feet per year of water for urban users, and 800,000 acre-feet of annual supplies for environmental purposes.

Historical Climate

The historical climate of the Central Valley is characterized by hot and dry summers and cool and damp winters. Summer daytime temperatures can reach 90ºF with occasional heat waves bringing temperatures exceeding 115ºF. The majority of precipitation occurs from mid-autumn to mid-spring. The Sacramento Valley receives greater precipitation than the San Joaquin and Tulare Lake basins. In winter, temperatures below freezing may occur, but snow in the valley lowlands is rare. The Central Valley typically has a frost-free growing season ranging from 225 to 300 days.

During the growing season, relative humidity is characteristically low; in the winter, values are usually moderate to high, and ground fog may form. The Central Valley is located within the zone of prevailing westerly winds, but local terrain exerts a significant influence on wind directions. Warmer-than-normal temperatures often are associated with more northerly winds flowing out of the Great Basin to the east. During summer, strong westerly winds driven by the large temperature difference between the San Francisco Bay and interior Great Valley often occur in the Sacramento-San Joaquin Delta.

The inter-annual variability of the Central Valley climate is strongly influenced by conditions occurring in the Pacific Ocean including the El Nino Southern Oscillation (ENSO) and the existence of a semipermanent high-pressure area in the northern Pacific Ocean. During the summer season, the northerly position of the Pacific high blocks storm tracks well to the north and results in little summertime precipitation. During the winter months, the Pacific high typically moves southward allowing storms into the Central Valley. Such storms often bring widespread, moderate rainfall to the Central Valley lowlands and the accumulation of snow in the surrounding mountainous regions. When strong ENSO global circulation patterns occur, storm centers can approach the California coast from a southwesterly direction, transporting large amounts of tropical moisture with resulting heavy rains that can produce high runoff and the potential for widespread flooding in the Central Valley.

Over the course of the 20th century, warming has been prevalent over the Sacramento and San Joaquin River basins. Basin average mean-annual temperature has increased by approximately 2°F during the course of the 20th century for just the Sacramento River basin above the Delta (Figure 2-1) or the San Joaquin River basin above the Delta (Figure 2-2).

Warming has not occurred steadily throughout the 20th century. Increases in air temperatures occurred primarily during the early part of the 20th century between 1910 and 1935. Subsequently, renewed warming began again in the mid-1970s and appears to be continuing at present, as shown for the Sacramento River basin in Figure 2-1. Similar results are apparent for the San Joaquin River basin (Figure 2-2) and have been reported in other studies. Cayan et al. (2001) reported that Western United States spring temperatures have increased 1 to 3 degrees Celsius (°C) (1.8 to 5.4°F) since the 1970s; whereas, increased winter temperature trends in central California were observed to average about 0.5°C (0.9°F) per decade (Dettinger and Cayan 1995). In both the Sacramento and San Joaquin basins, the overall 20th century warming has been about 3°F.

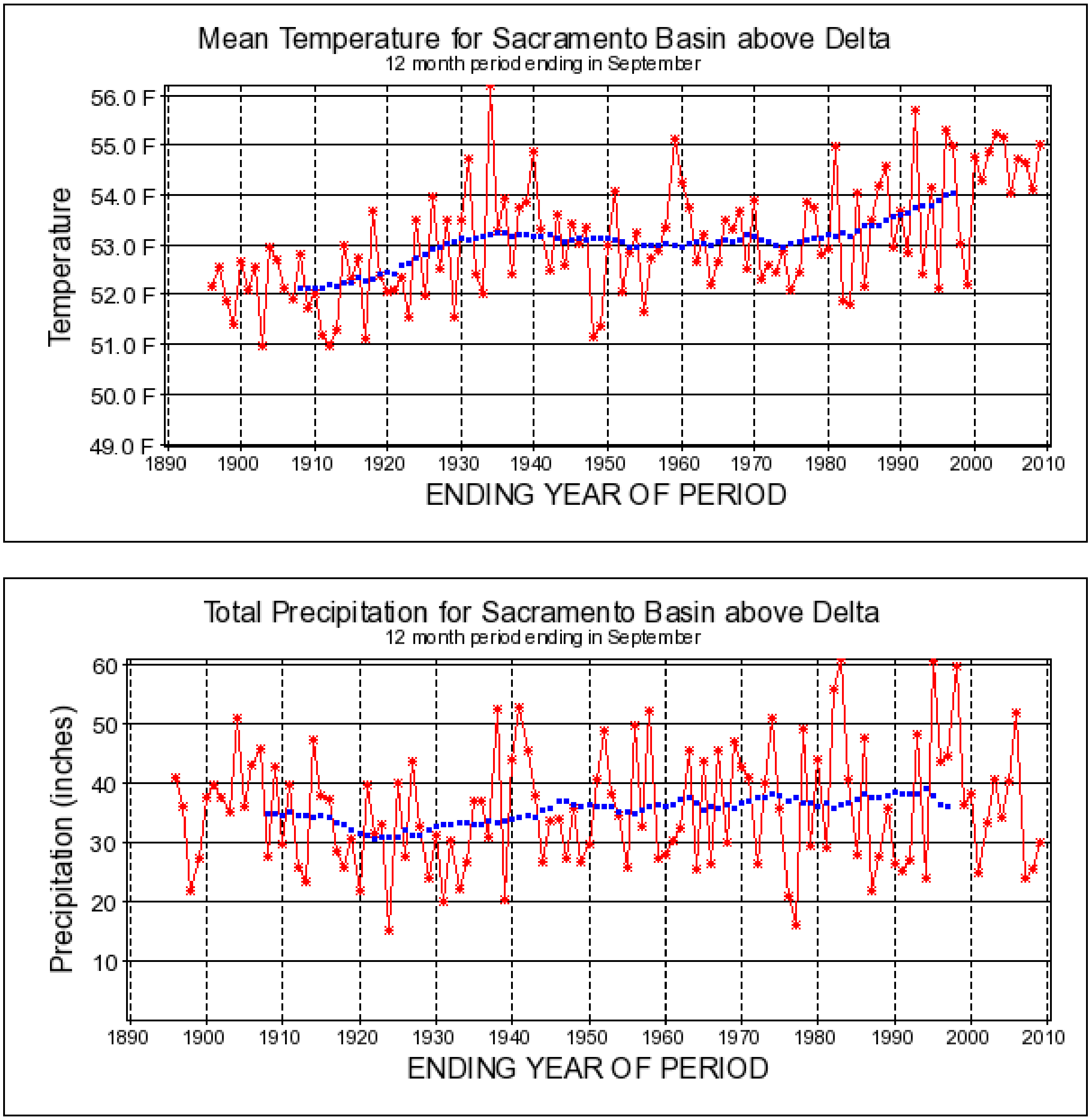

Source: Western Climate Mapping Initiative (WestMap) available at: http://www.cefa.dri.edu/ Westmap/. Red line indicates annual time series for the given geographic region. Blue line indicates 25-year moving annual mean values, where each value is plotted on the center year of its respective 25-year period. WestMap data are derived from the PRISM climate mapping system (Daly et al. 1994; Gibson et al. 2002).

Figure 2-1. Observed Annual (red) and Moving-Mean Annual (blue) Temperature and Precipitation, Averaged over the Sacramento River Basin

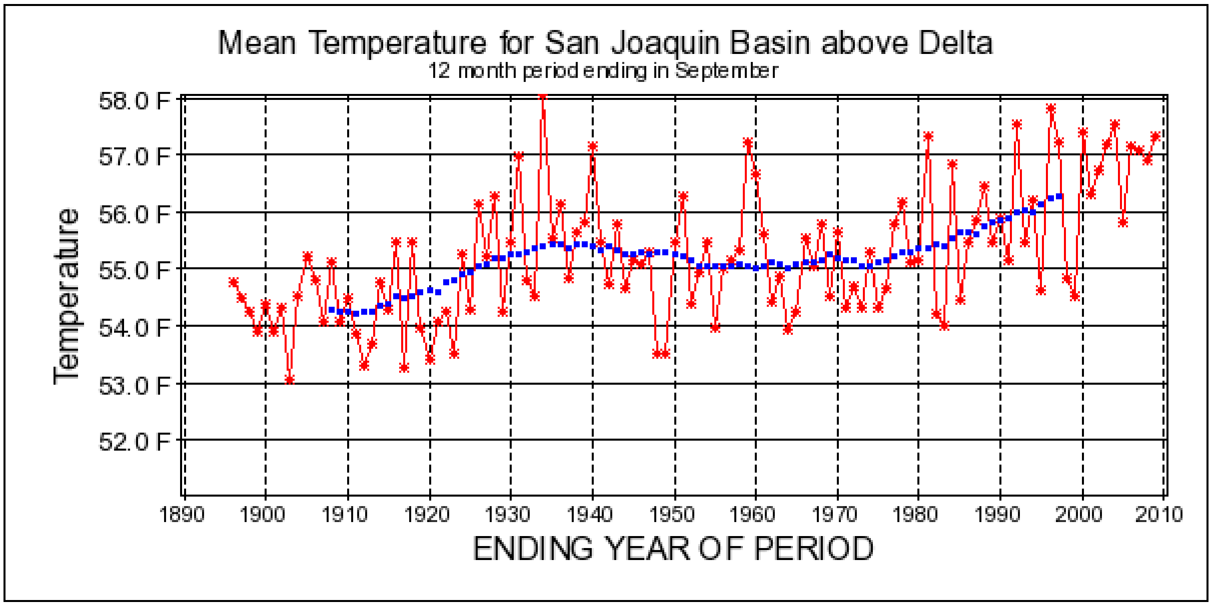

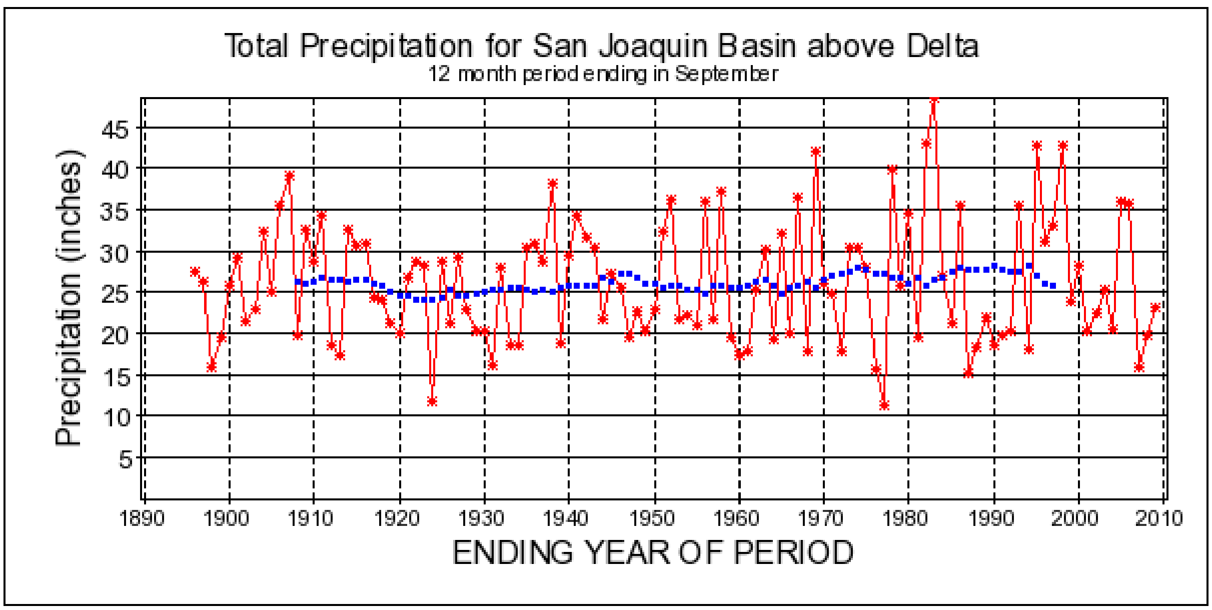

Source: Western Climate Mapping Initiative (WestMap) available at: http://www.cefa.dri.edu/ Westmap/. Red line indicates annual time series for the given geographic region. Blue line indicates 25-year moving annual mean values, where each value is plotted on the center year of its respective 25-year period. WestMap data are derived from the PRISM climate mapping system (Daly et al. 1994; Gibson et al. 2002).

Figure 2-2. Observed Annual (red) and Moving-Mean Annual (blue) Temperature and Precipitation, Averaged over the San Joaquin River Basin

In the Sacramento basin, the warming trend also has been accompanied by a gradual trend starting in the 1930s toward increasing precipitation (Figure 2-1, bottom panel). However, a similar precipitation trend is not evident in the San Joaquin basin (Figure 2-2). Other studies have shown similar results.

Regonda et al. (2005) reported increased winter precipitation trends from 1950 to 1999 at many Western United States locations, including several in California's Sierra Nevada; but a consistent region-wide trend was not apparent. The variability of annual precipitation appears to have increased in the latter part of the 20th century, as can be seen by comparing the range of differences in high and low values of the solid red line in Figure 2-1 and Figure 2-2. These extremes in wet and dry years have been especially frequent since the mid-1970s in both the Sacramento and San Joaquin basins.

Historical Hydrology

Streamflow in the Sacramento River and San Joaquin River basins has historically varied considerably from year to year. Runoff also varies geographically; during any particular year, some portions of the basin may experience relatively greater runoff conditions while others areas experience relatively less runoff (e.g., more abundance runoff in the northern Sacramento Valley versus relatively drier conditions in southern San Joaquin Valley). On a monthly to seasonal basis, runoff is generally greater during the winter to early summer months, with winter runoff generally originating from rainfall-runoff events and spring to early summer runoff generally supported by snowmelt from the Cascade Mountains and Sierra Nevada.

The historical changes in climate described in preceding sections have resulted in several important effects on Sacramento and San Joaquin basin hydrology. Although annual precipitation may have slightly increased or remained relatively unchanged, corresponding increases in mean annual runoff in the Sacramento and San Joaquin rivers did not occur (Dettinger and Cayan 1995). One change that has been observed is a change in the seasonal timing of runoff. In the Sacramento River basin, a decrease of about 10 percent in the fraction of total runoff occurring between April through July has been observed over the course of the 20th century (Roos 1991). Similar results were obtained from analyses of the combined basin runoffs for both the Sacramento and San Joaquin basins by Dettinger and Cayan (1995).

Along with the declining spring runoff, corresponding increases in winter runoff have been observed. Analysis of data for 18 Sierra Nevada river basins found earlier runoff trends (Peterson et al. 2008). Of the potential climatic factors that could produce such changes, analyses indicated that increasing spring temperatures rather than increased winter precipitation was the primary cause of the observed trends (Cayan 2001). Studies by these researchers and others showed that the magnitude of the decreases in April through July runoff was correlated with the altitude of the basin watershed. High altitude basins like the San Joaquin exhibited less decrease in spring runoff than lower elevation watersheds such as the Sacramento. However, it is noted that the appearance of runoff trends in the basins depends on location and period of record being assessed. For example, runoff trends were evaluated for this report during the last half of the 20th century; and although similar trend directions were founds, they were found to be statistically weak.[1]

Other studies of the magnitude of spring snowpack changes during the 20th century found that snowpack as measured by April 1st Snow Water Equivalent (SWE) showed a decreasing trend in the latter half of the 20th century (Mote 2005). Coincident with these trends, reduced snowpack and snowfall ratios were indicated by analyses SWE measurements made from 1948 through 2001 at 173 Western United States stations (Knowles et al. 2007). Regonda et al. (2005) reported decreasing spring SWE trends in 50 percent of Western United States locations evaluated.

The changes discussed in the previous paragraphs over regional drainages such as the Sacramento and San Joaquin River basins are sensitive to the uncertainties of station measurements as well as the periods of analyses and analyzed locations. For the entire Western United States, observed trends of temperature, precipitation, snowpack, and streamflow might be partially explained by anthropogenic influences on climate (e.g., Barnett et al. 2008; Pierce et al. 2008; Bonfils et al. 2008; Hidalgo et al. 2009; and Das et al. 2009). However, it remains difficult to attribute observed changes in hydroclimate to historical human influences or anthropogenic forcings. This is particularly the case for trends in precipitation (Hoerling et al. 2010) and for trends in basin-scale conditions rather than at the larger Western United States scale (Hidalgo et al. 2009).

Sea level change is also an important factor in assessing the effect of climate on California's water resources because of its effect on water quality in the Sacramento-San Joaquin Delta. Higher mean sea levels (msl) are associated with increasing salinity in the Delta, which influences the suitability of its water for agricultural, urban, and environmental uses. The global rate of msl change was estimated by IPCC (2007) to be 1.8 +/- 0.5 millimeters per year (mm/yr) (0.07 +/- 0.02 inches per year (in/yr)) from 1961–2003 and 3.1 +/- 0.7 mm/yr (0.12 +/0.03 in/yr) during 1993–2003. During the 20th century, msl at Golden Gate Bridge in San Francisco Bay has risen by an average of 2 mm/yr (0.08 in/yr) (Anderson et al. 2008). These rates of sea level rise appear to be accelerating based on tidal gauges and remote sensing measurements (Church and White 2006; Beckley et al. 2007).

[1] Trend significance was assessed using statistical testing during the period from 1951 through 1999 applied to historical simulated runoff results under observed historical weather conditions (Reclamation 2011a). Trends were computed and assessed for four Missouri basin locations, focusing on annual and April–July runoff. In all cases, computed trends were judged to not be statistically significant with 95 percent confidence.

Future Changes in Climate and Hydrology

This section summarizes results from studies focused on future climate and hydrologic conditions within the Sacramento and San Joaquin River basins. The first subsection summarizes literature relevant to the study area. The subsequent section focuses on results from Reclamation (2011c), which were produced within the context of a western United States-wide hydrologic analysis to identify risks to water supplies in a consistent manner throughout the Colorado, Columbia, Klamath, Missouri, Rio Grande, Sacramento, San Joaquin, and Truckee river basins consistent with Public Law 111-11, Subtitle F (the SECURE Water Act).

Summary of Future Climate and Hydrology Studies in Study Area

Future changes in Central Valley climate and hydrology have been the subject of numerous studies. For the Central Valley watersheds, Moser et al (2009) reports specifically on future climate possibilities over California and suggest that warmer temperatures are expected during the 21st century, with an end-of-century increase of 3°F to 10.5°F. For mean annual precipitation in northern California, the study indicates a generally decreasing trend of between 10 percent and 15 percent by the end of the century.

The effects of projected changes in future climate were assessed by Maurer (2007) for four river basins in the western Sierra Nevada contributing to runoff in the Central Valley. These results indicate a tendency toward increased winter precipitation; this was quite variable among the models, while temperature increases and associated SWE projections were more consistent. The effect of increased temperature was shown by Kapnick and Hall (2009) to result in a shift in the date of peak of snowpack accumulation from 4 and 14 days earlier in the winter season by the end of the century. Null et al. (2010) reported on climate change impacts for 15 western-slope watersheds in the Sierra Nevada under warming scenarios of 2°C, 4°C, and 6°C increase in mean-annual air temperature relative to historical conditions. Under these scenarios, total runoff decreased; earlier runoff was projected in all watersheds relative to increasing temperature scenarios; and decreased runoff was most severe in the northern part of the Central Valley. This study also indicated that the high elevation southern-central region was more susceptible to earlier runoff, and the central region was more vulnerable to longer low flow periods.

Sea level changes also have been projected to occur during the 21st century due to increasing air temperatures causing thermal expansion of the oceans and additional melting of the land-based Greenland and Antarctic ice sheets (IPCC 2007). The CALFED Independent Science Board estimated a range of sea level rise at Golden Gate of 1.6 feet to 4.6 feet by the end of the century (CALFED ISB 2007). The California Department of Water Resources (DWR) used the 12 future climate projections to estimate future sea levels. Their estimates indicate sea level rise by mid-century ranges from 0.8 feet to 1.0 feet with an uncertainty range spanning 0.5 feet to 1.3 feet. By the end of the century, sea level was projected to rise between 1.8 feet and 3.1 feet, with an uncertainty range spanning from 1.0 feet to 3.9 feet. There is also the potential for increased extremely high sea level events to occur when high tides coincide with winter storms (Moser et al. 2009).

Projections of Future Climate

This section summarizes climate projections developed by Reclamation (2011c) consistent with the SECURE Water Act. The methods and assumptions used to develop the projections discussed below are described in detail in a report titled *West-Wide Climate Risk Assessments: Bias-Corrected and Spatially Downscaled Surface Water Projections* (2011a).

First, basin-wide averages of projected climate conditions are presented and, secondly, those projected climate conditions as they may be distributed throughout the basin is presented. A summary of snow-related effects under future climate conditions as they may be distributed throughout the basin is then presented; and, finally, climate and snowpack changes translated into effects on annual and seasonal runoff as well as acute runoff events relevant to flood control and ecosystems management are discussed. Runoff-Reporting locations described in this section are shown in Figure 2-3.

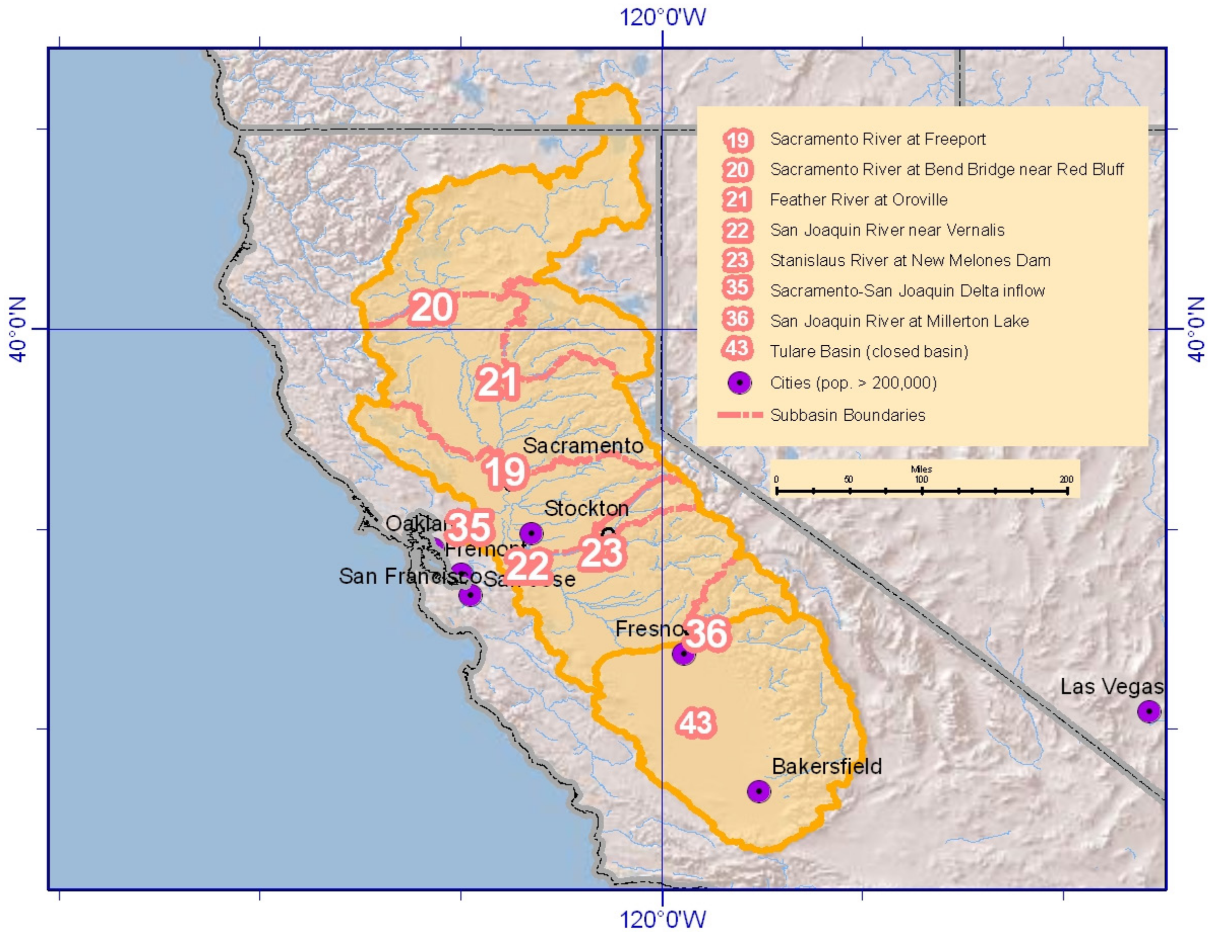

Figure 2-3. Runoff-Reporting Locations in the Sacramento River, San Joaquin River, and Tulare River Basins Described in this Section

Before summarizing climate projection and climate change information, it is noted that the projected changes have geographic variation, they vary through time, and the progression of change through time varies among climate projection ensemble members. Starting with a regional view of the time series climate projections and drawing attention to the projections' median condition through time, results suggest that temperatures throughout the Sacramento and San Joaquin basins may increase steadily during the 21st century. Focusing on the Sacramento River subbasin at Freeport, San Joaquin River subbasin at Vernalis, and on the combined basins' inflow to the Delta (Figure 2-4), the basin-average mean-annual temperature is projected to increase by roughly 5°F to 6°F during the 21st century. For each subbasin view, the range of annual possibility appears to widen through time.

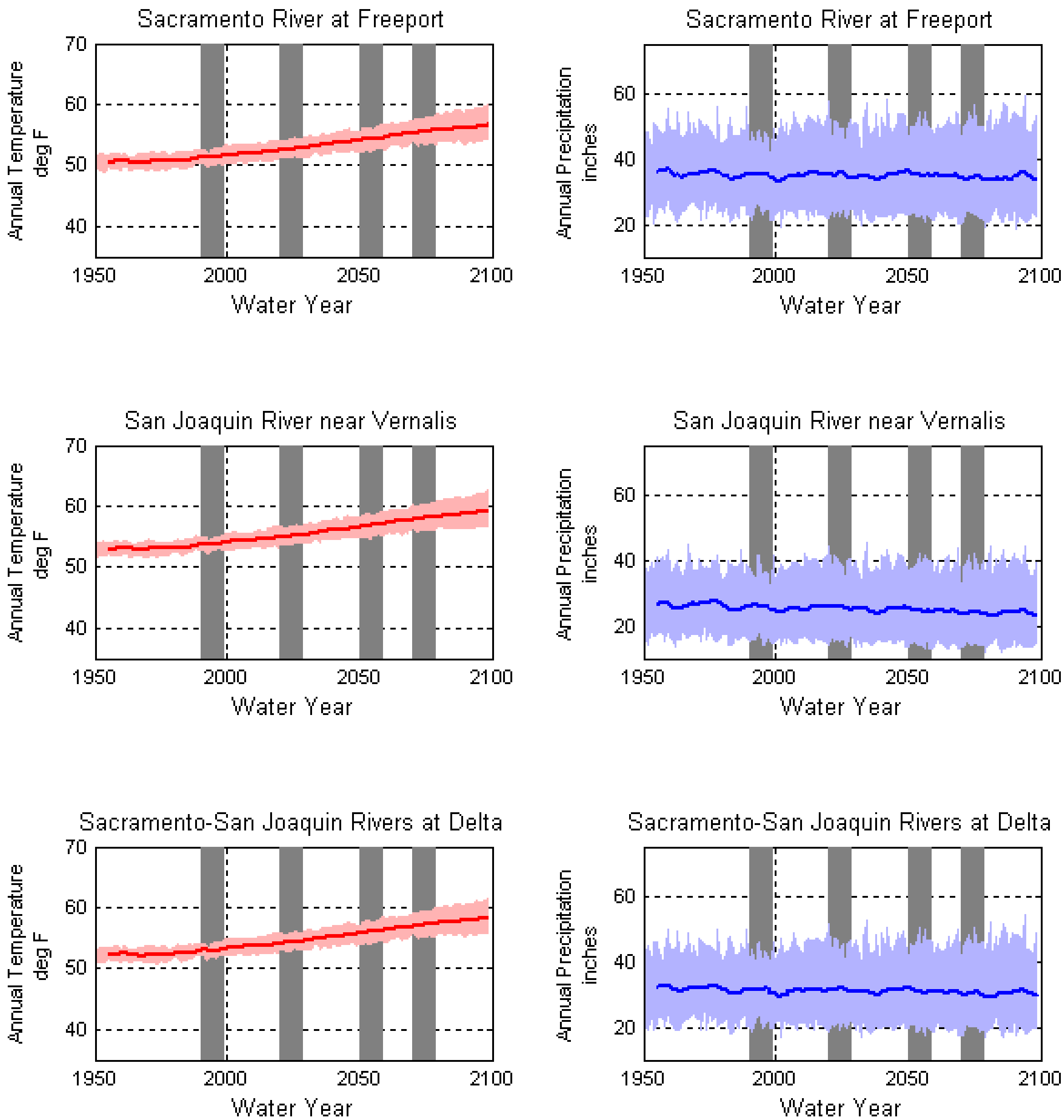

Figure 2-4. Simulated Annual Climate Averaged over Sacramento and San Joaquin River Subbasins

The ensemble mean of projections indicates that mean-annual precipitation, averaged over either subbasin (Figure 2-4), appears to stay generally steady during the 21st century, with perhaps a slight increase in the northern portion of the Central Valley (Sacramento River subbasin at Freeport) and a slight decrease within the southern portion (San Joaquin River near Vernalis). This is evident by following the ensemble median of the annual precipitation through time for both basins. The projections also suggest that annual precipitation in the Sacramento and San Joaquin basins should remain quite variable over the next century. Despite the statements about the mean of the ensemble, there is significant disagreement among the climate projections regarding change in annual precipitation over the region.

Projection of climate change is geographically complex over the Sacramento and San Joaquin River basins, particularly for precipitation. For example, consider the four decades highlighted on Figure 2-4 (vertical gray bars): the 1990s, 2020s, 2050s, and 2070s. The 1990s are proivde the baseline climate from which climate changes are assessed for the three future decades (2020s, 2050s, and 2070s). The baseline climate indicates that local climate varies considerably within the basin. For example, in the Sacramento River at Freeport (Figure 2-4, top left panel), annual average temperatures are generally cooler in the high-elevation upper reaches in the north and along the mountainous rim to the east. Warmer temperatures occur to the south and in the lower lying valley area. This is similarly the case for the San Joaquin River near Vernalis (Figure 2-4, top right panel). For precipitation, amounts are generally greater along the mountainous spine extending from the Cascades in the north-central part of the basin throughout the Sierra Nevada to the southeast (Figure 2-4, top left panel) and lesser in the interior plateau northeast of these mountain ranges and in the lower lying valley areas to the south and west. In the San Joaquin River Basin, precipitation amounts are also greater in the Sierra Nevada (Figure 2-4, top left panel).

Regarding climate change, temperature changes are generally uniform over both the Sacramento River (Figure 2-4) and San Joaquin River basins (Figure 2-4) and steadily increase through time. Changes are projected to be perhaps slightly greater in the eastern portions of the basins. For precipitation, similar geographic consistency is found, although there is a little less uniformity in the direction of change between the two basins and through the progression of 21st century decades. For example, the Sacramento River basin is projected to generally experience slight increase in precipitation during the early to mid 21st century (2020s and 2050s) followed by a reversal to slight precipitation decline (2070s). In the San Joaquin River Basin, a similar progression is projected but with the reversal occurring earlier in the 21st century (i.e., slight increase to no change in preciptation projected for the 2020s followed by slight decrease by the 2050s and continuing through the 2070s). It it important to note that, while the mean-annual amount of precipitation may only change slightly under increasing temperature projections, the character of precipitation within the Sacramento and San Joaquin River basins also is expected to change under warming conditions, resulting in more frequent rainfall events, less frequent snowfall events.

Figure 2-4 displays the ensemble of temperature and precipitation projections from Bias Corrected and Spatially Downscaled WCRP CMIP3 Climate Projections. Annual conditions represent spatially averaged results over the basin. Darker colored lines indicate the median-annual condition through time, sampled from the ensemble of 112 climate simulations, and then smoothed using a 5-year running average. Lighter-colored areas represent the time-series range of 10^{th} to 90^{th} percentile annual values within the ensemble from simulated 1950 through simulated 2099.

Figure 2-5 presents basin-distributed views of change in mean annual temperature over the Sacramento River Basin upstream from Freeport. Figure data are simulated conditions as described in Reclamation (2011a). The upper left panel shows the baseline mean-annual condition (1990s), and next three panels show changes from baseline conditions for three future decades (2020s, 2050s, and 2070s). Both historical and future conditions are from climate simulations. Mapped values for baseline conditions (1990s) are median-values from the collection of climate simulations. Mapped changes (next three panels) are median changes from the collection of climate simulations. Temperature units °F for baseline and change. Precipitation and SWE units are inches for baseline and percentage for change. For SWE, areas that are white on the plots have less 1990s decade-mean conditions of less than 0.0004 inch and are not considered in the change assessment.

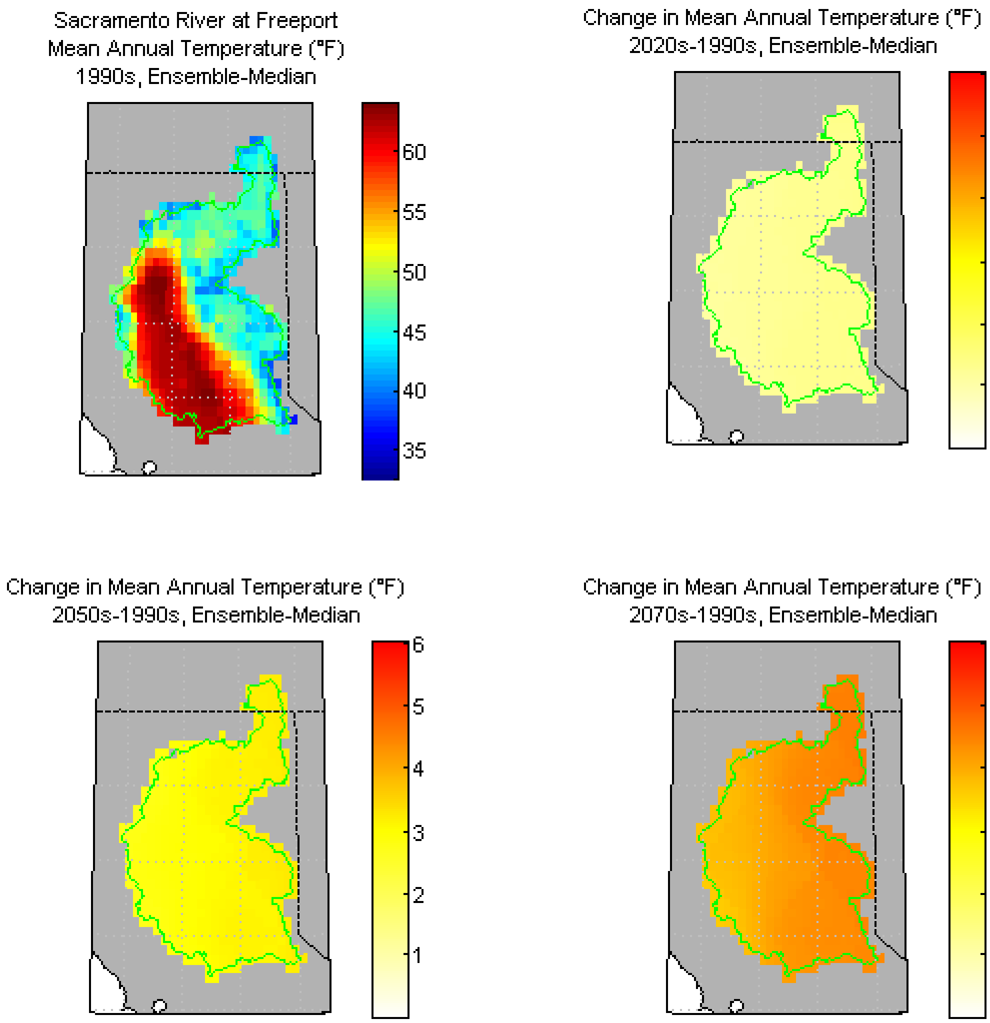

Figure 2-5. Simulated Decade-Mean Temperature over the Sacramento River Basin Above Freeport, California

Figure 2-6 presents basin-distributed views of change in mean annual temperature over the San Joaquin River Basin upstream from Vernalis. Figure data are simulated conditions as described in Reclamation (2011a). The upper left panel shows the baseline mean-annual condition (1990s), and next three panels show changes from baseline conditions for three future decades (2020s, 2050s, and 2070s). Both historical and future conditions are from climate simulations. Mapped values for baseline conditions (1990s) are median-values from the collection of climate simulations. Mapped changes (next three panels) are median changes from the collection of climate simulations.

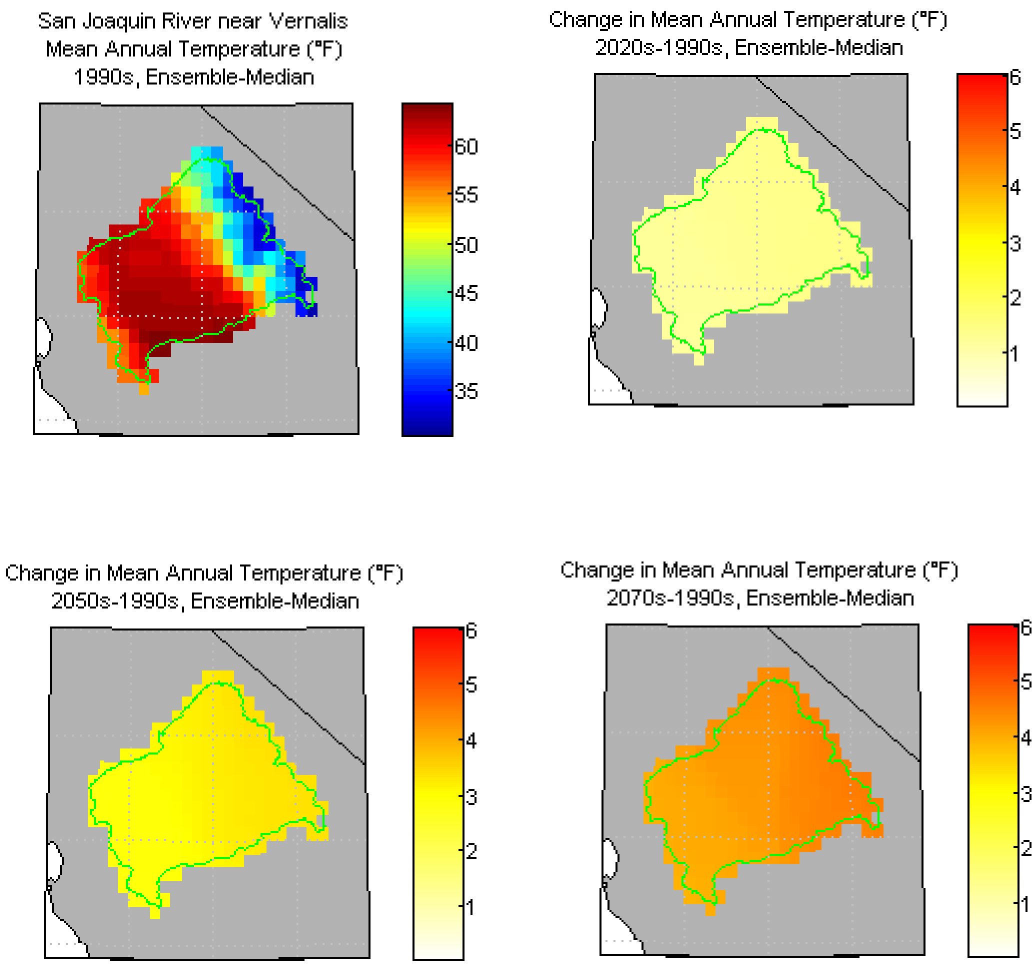

Figure 2-6. Simulated Decade-Mean Temperature over the San Joaquin River Basin Above Vernalis, California

Figure 2-7 presents basin-distributed views of change in mean annual precipitation over the Sacramento River Basin upstream from Freeport. Figure data are simulated conditions as described in Reclamation 2011a. The upper left panel shows the baseline mean-annual condition (1990s), and next three panels show changes from baseline conditions for three future decades (2020s, 2050s, and 2070s). Both historical and future conditions are from climate simulations. Mapped values for baseline conditions (1990s) are median-values from the collection of climate simulations. Mapped changes (next three panels) are median changes from the collection of climate simulations. For SWE, areas that are white on the plots have less 1990s decade-mean conditions of less than 0.0004 inch and are not considered in the change assessment.

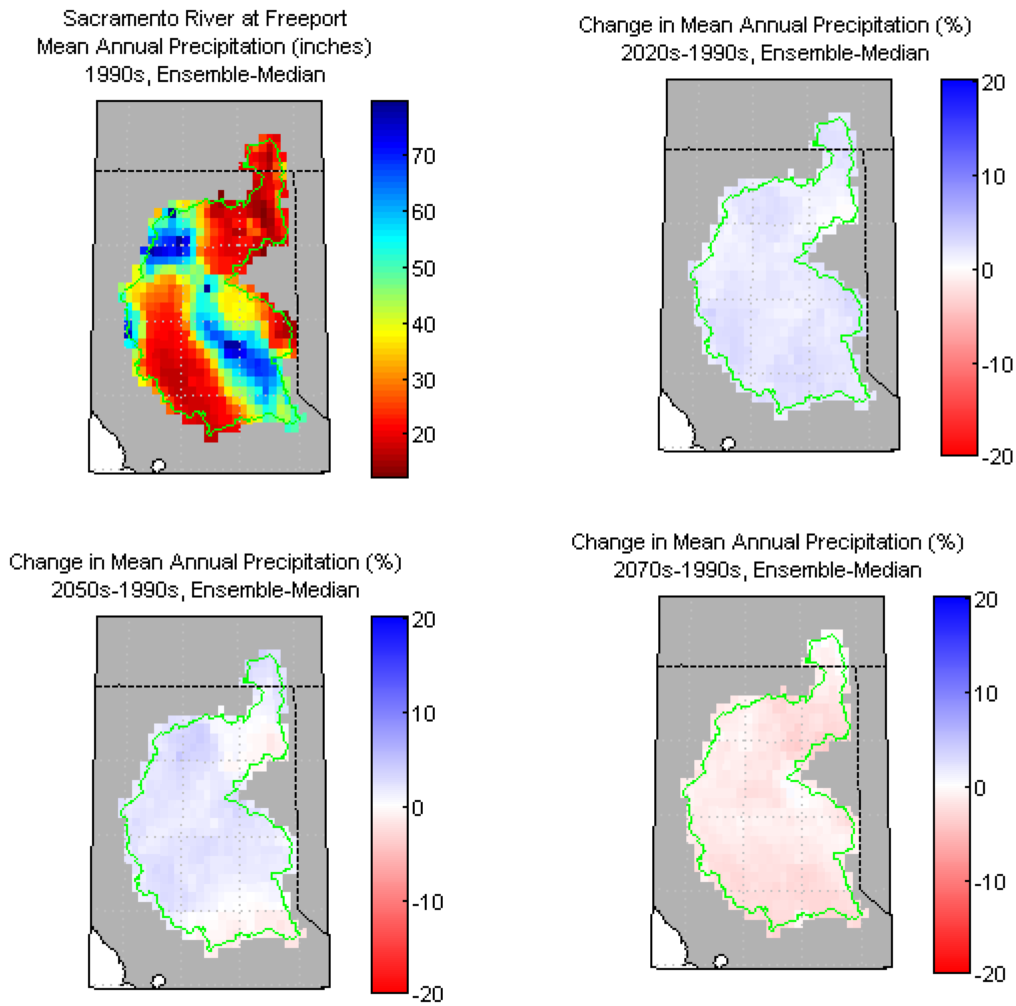

Figure 2-7. Simulated Decade-Mean Precipitation over the Sacramento River Basin Above Freeport, California

Figure 2-8 presents basin-distributed views of change mean annual precipitation over the San Joaquin River Basin upstream from Vernalis. Figure data are simulated conditions as described in Reclamation 2011a. The upper left panel shows the baseline mean-annual condition (1990s), and next three panels show changes from baseline conditions for three future decades (2020s, 2050s, and 2070s). Both historical and future conditions are from climate simulations. Mapped values for baseline conditions (1990s) are median-values from the collection of climate simulations. Mapped changes (next three panels) are median changes from the collection of climate simulations. For SWE, areas that are white on the plots have less 1990s decade-mean conditions of less than 0.0004 inch and are not considered in the change assessment.

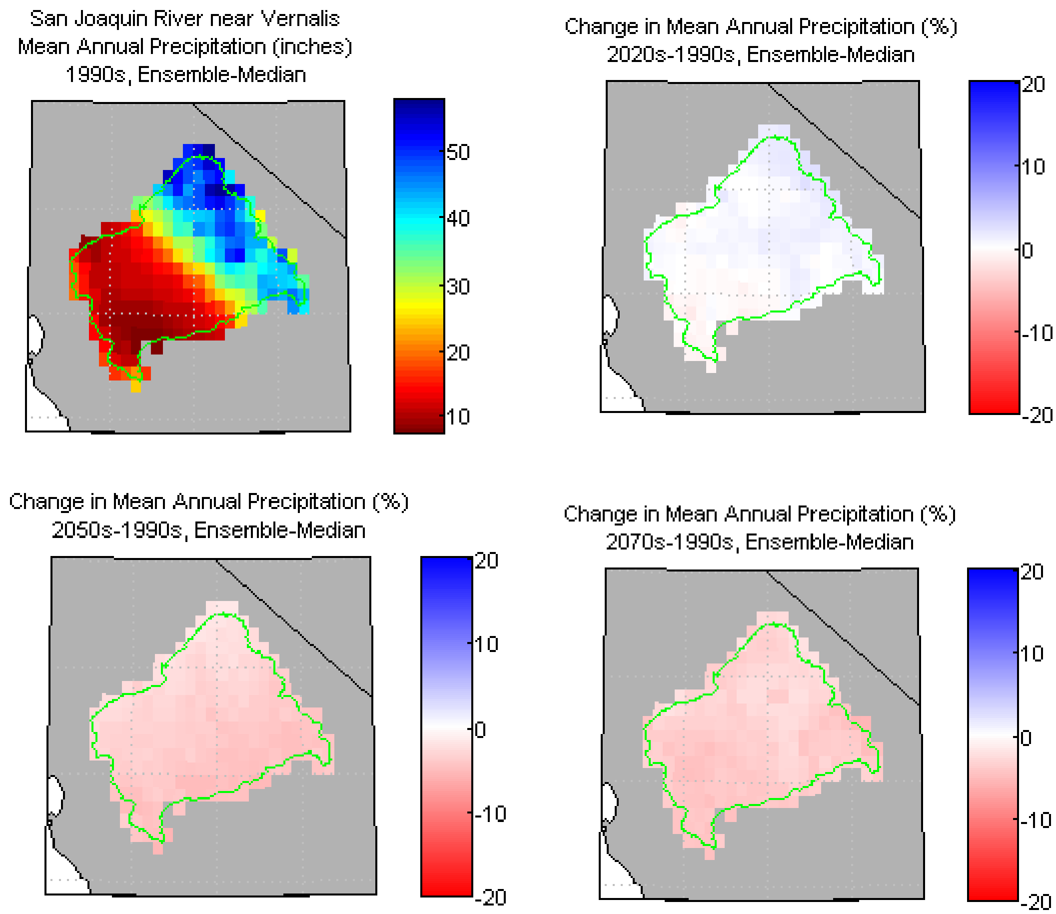

Figure 2-8. Simulated Decade-Mean Precipitation over the San Joaquin River Basin Above Vernalis, California

Temperature and precipitation changes are expected to affect hydrology in various ways including snowpack development. As noted previously, increased warming is expected to diminish the accumulation of snow during the cool season (i.e., late autumn through early spring) and the availability of snowmelt to sustain runoff during the warm season (i.e., late spring through early autumn). Although increases or decreases in cool season precipitation could somewhat offset or amplify changes in snowpack, it is apparent that the projected warming in the Sacramento River and San Joaquin River basins tends to dominate projected effects (e.g., changes in April 1st snowpack distributed over the basin, shown on Figure 2-9 and Figure 2-10 for the two basins, respectively). Snowpack decrease is projected to be more substantial over the portions of the basin where baseline cool season temperatures are generally closer to freezing thresholds and more sensitive to projected warming. Such areas include much of the northern Sierra Nevada and Cascade Mountains of the Sacramento River basin as well as lower to middle elevations in the southern Sierra Nevada of the San Joaquin River basin. However, even in the highest elevations of the southern Sierra Nevada, losses are projected to be significant by the late 21st century.

Figure 2-9 presents basin-distributed views of change SWE over the Sacramento River Basin upstream from Freeport. Figure data are simulated conditions as described in Reclamation 2011a. The upper left panel shows the baseline mean-annual condition (1990s), and next three panels show changes from baseline conditions for three future decades (2020s, 2050s, and 2070s). Both historical and future conditions are from climate simulations. Mapped values for baseline conditions (1990s) are median-values from the collection of climate simulations. Mapped changes (next three panels) are median changes from the collection of climate simulations.

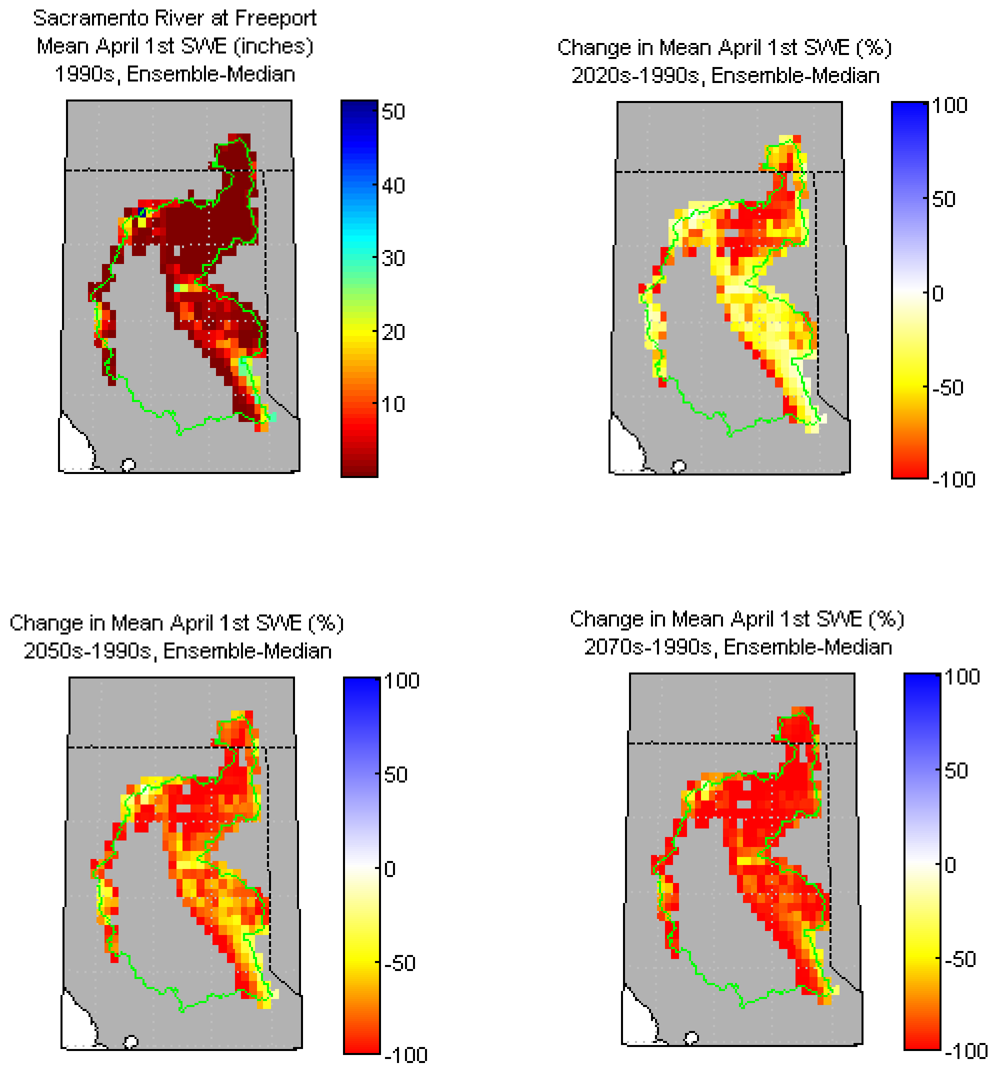

Figure 2-9. Simulated Decade-Mean April 1st Snow Water Equivalent over the Sacramento River Basin Above Freeport, California

Figure 2-10 presents basin-distributed views of change in SWE over the San Joaquin River Basin upstream from Vernalis. Figure data are simulated conditions as described in Reclamation 2011a. The upper left panel shows the baseline mean-annual condition (1990s), and next three panels show changes from baseline conditions for three future decades (2020s, 2050s, and 2070s). Both historical and future conditions are from climate simulations. Mapped values for baseline conditions (1990s) are median-values from the collection of climate simulations. Mapped changes (next three panels) are median changes from the collection of climate simulations. For SWE, areas that are white on the plots have less 1990s decade-mean conditions of less than 0.0004 inch and are not considered in the change assessment.

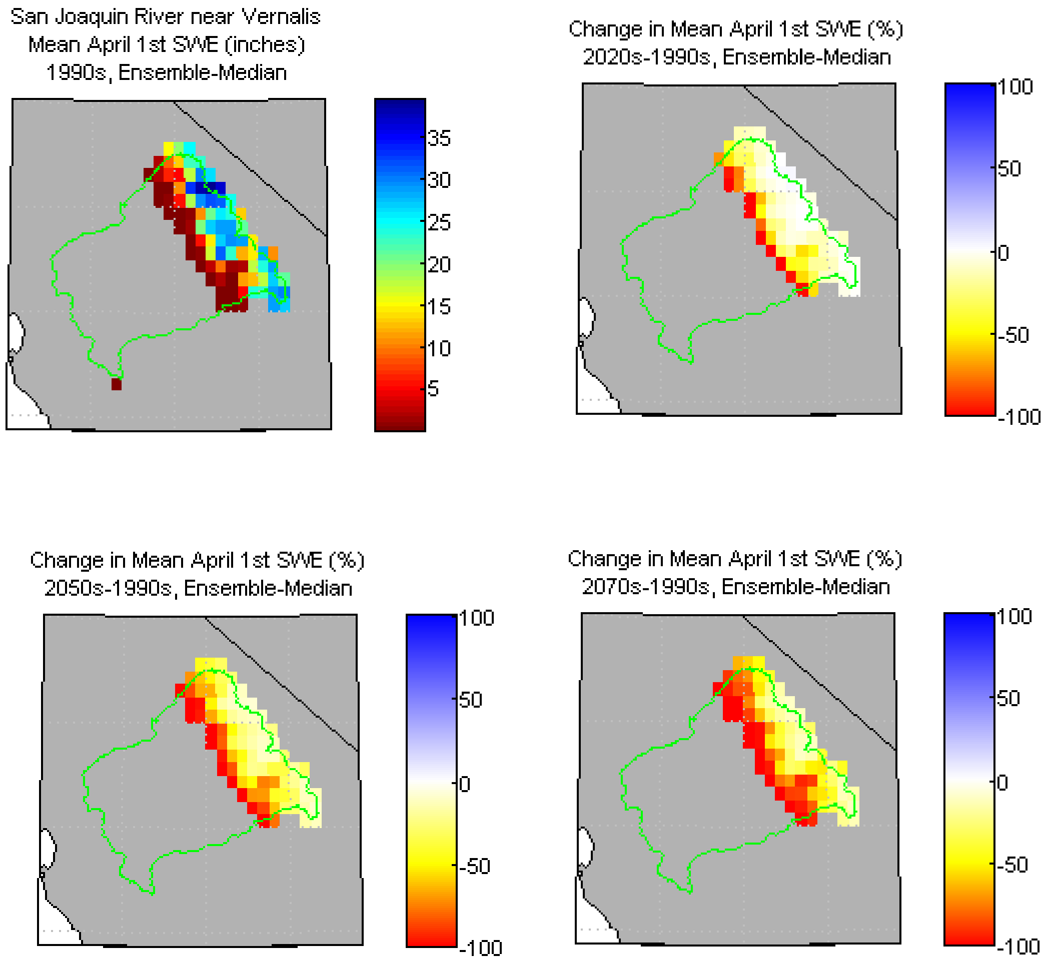

Figure 2-10. Simulated Decade-Mean April 1st Snow Water Equivalent over the San Joaquin River Basin Above Vernalis, California

Changes in climate and snowpack within the Sacramento and San Joaquin River basins will change the availability of natural water supplies. These effects may be experienced in terms of changes to annual runoff and changes in runoff seasonality. For example, warming without precipitation change may lead to increased evapotranspiration from the watershed and decreased annual runoff. Precipitation increases or decreases (either as rainfall or snowfall) offset or amplify the effect.

Figure 2-11 presents annual, December through March, and April through July runoff impacts for subbasins shown. Each panel shows percentage changes in mean runoff (annual or either season) for three future decades (2020s, 2050s, and 2070s) relative to baseline conditions (1990s).

Development of runoff information is described in Reclamation (2011a) based on climate simulations previously discussed. Results from Reclamation (2011a) suggest that annual runoff effects are generally consistent but do slightly vary by location within the basins, as shown in Figure 2-11, depending on baseline climate and the projected temperature and precipitation changes. For example, in the Sacramento River and its major tributaries, the Feather River and the American River, annual runoff increases very slightly during the early and middle part of the 21st century. However, in all of these watersheds, a slight decline is projected to occur in the latter half of the century. In the San Joaquin River basin and its major tributaries, similar results are found but with mean-annual runoff declines projected to occur by the mid-21st century.

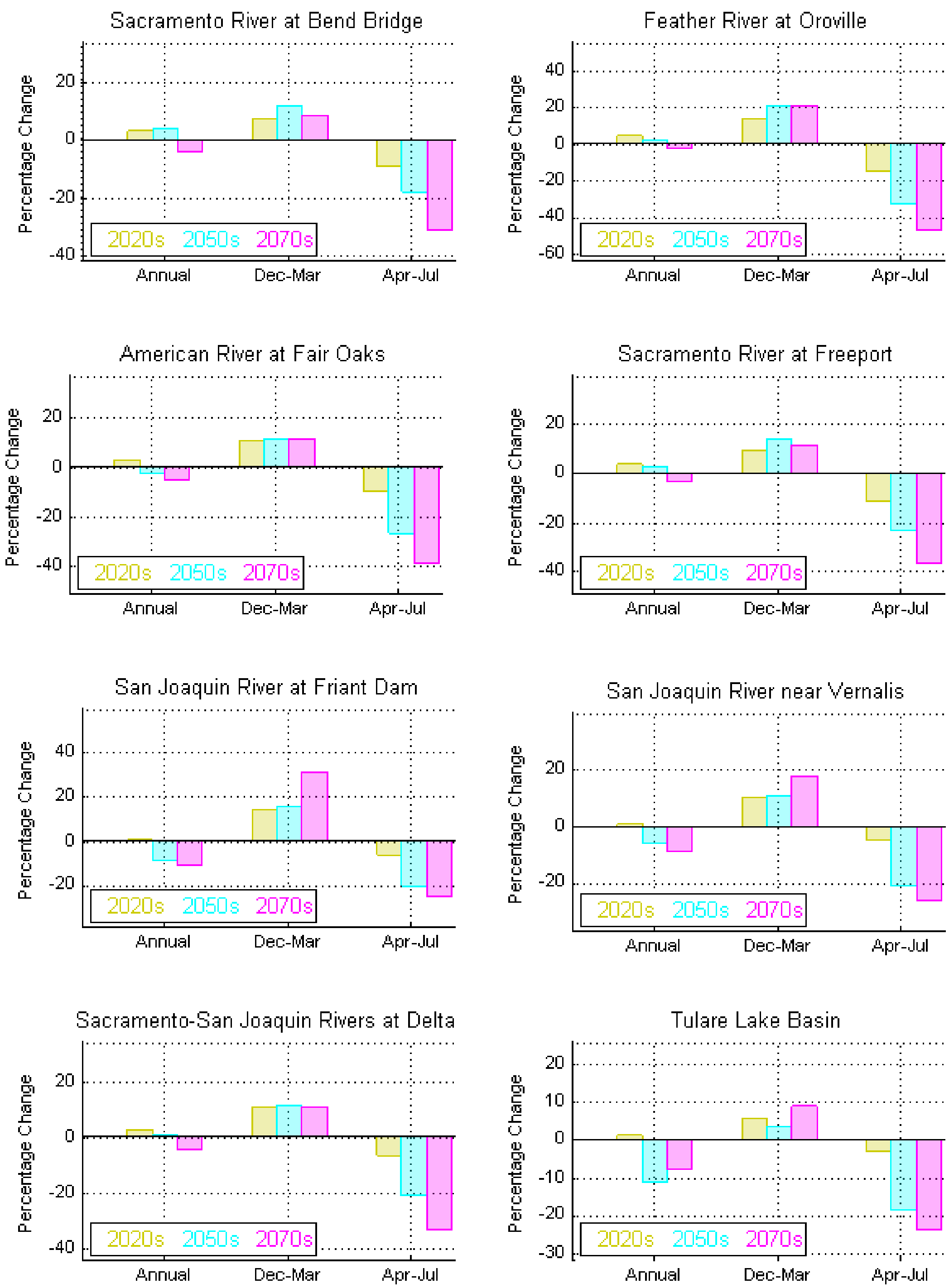

Figure 2-11. Simulated Changes in Decade-Mean Runoff for Several Subbasins in the Sacramento and San Joaquin River Basins

The seasonality of runoff is also projected to change. Warming may lead to more rainfall-runoff during the cool season rather than snowpack accumulation. This conceptually leads to increases in December through March runoff and decreases in April through July runoff. Results over the two basins suggest that this concept generally holds throughout the two basins, but the degree of seasonal change does vary by basin location (Figure 2-11).

This combination of increased winter and decreased spring runoff points to the important role of temperature in determining 21st century seasonal water supplies for both basins. In the lower left-hand corner of Figure 2-11, the combined runoff change is depicted based on runoff changes in the Sacramento River, San Joaquin River, and other Delta tributaries. Overall, the changes are more similar to those found in the Sacramento River basin and are reflective of the larger contribution of the Sacramento River (see Sacramento River at Freeport) relative to the San Joaquin River (see San Joaquin near Vernalis) to Delta flows. It may be noticed that percentage reductions in April through July runoff may appear to be small compared to some percentage reductions in lower elevation April 1st snowpack from the preceding discussion. The fact that percentage April through July runoff reductions are smaller speaks to how higher elevation snowpack contributes proportionally more to April through July runoff than lower elevation snowpack, and how percentage snow losses at higher elevations are relatively smaller than those at lower elevation.

Climate change in relation to acute runoff events are also of interest as they relate to flood control and ecosystem management in both basins. There is less certainty in the analysis of these types of acute events relative to effects in annual or seasonal runoff. Generally speaking, streamflow variability over the basin is expected to continue under changing climate conditions. For this discussion, annual maximum- and minimum-week runoff are used as metrics of acute runoff events.

Figure 2-12 displays the ensemble of annual “maximum 7-day” and “minimum 7-day” runoff projections for the subbasins shown development of runoff information is described in Reclamation (2011a) based on climate simulations previously discussed. It should be noted that these results are derived from simulations that have been computed at a daily time step, but have been calibrated to monthly natural flows. As such, there is considerable uncertainty that is reflected in the lightly shaded regions around the heavier dark line. These values are presented for qualitative, rather than quantitative analysis. The maximum weekly runoff typically occurs sometime between late fall and early summer, whereas the minimum weekly runoffs are most likely to occur between late summer and early fall. Because the selected locations are upstream from major aquifers in the Central Valley, the runoff extremes are only minimally affected by groundwater and bank storage processes.

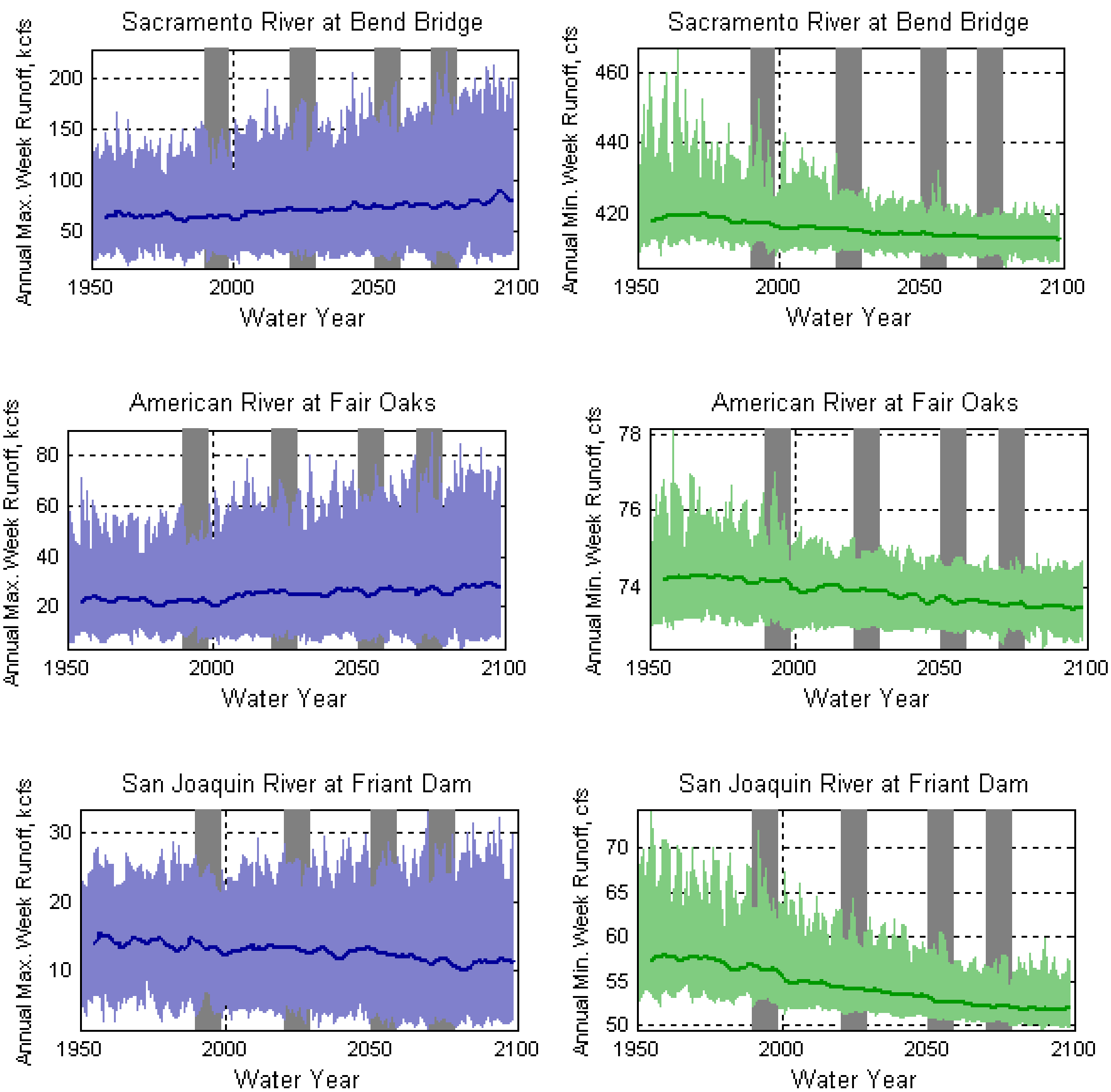

Figure 2-12. Simulated Annual Maximum and Minimum Week Runoff for Several Subbasins in the Sacramento and San Joaquin River Basins

For annual maximum-week runoff, results for the Sacramento River and San Joaquin River basins appear to differ. For the two subbasins shown in the Sacramento River basin, it appears that expected annual maximum-week runoff may gradually increase during the 21st century. The range of possibility also appears to increase during the century. These findings raise questions about whether increases in maximum weekly runoff may be indicative of potentially greater flood risks during the 21st century. However, for the San Joaquin River Basin upstream from Friant Dam, results suggest a slight decline in annual maximum-week runoff.

For annual minimum-week runoff, results suggest a gradual decrease in the expected annual value as the 21st century progresses. The range of projected possibility also reduces with time. These declines are likely the result of decreased snowpack accumulation and increased soil evaporation and plant transpiration in the upper watershed. Decreasing minimum runoff may lead to adverse effects on aquatic habitats by reducing both wetted stream perimeters and availability of aquatic habitat and through increased water temperatures detrimental to temperature-sensitive aquatic organisms.

A summary of climate and hydrologic changes is provided in Table 2-1 for four subbasins of the Sacramento River and San Joaquin River basins: Sacramento River at Bend Bridge, Sacramento River at Freeport, San Joaquin River at Friant Dam, and San Joaquin River at Vernalis. The tabulated changes reflect a subbasin-average view and are measured relative to 1990s baseline conditions, as shown on the preceding figures.

Table 2-1. Summary of Simulated Changes in Decade-Mean Hydroclimate for Several Subbasins in the Sacramento and San Joaquin River Basins

Hydroclimate Metric (change from 1990s)	2020s	2050s	2070s
Sacramento River at Bend Bridge			
Mean Annual Temperature (°F)	1.3	3.0	4.2
Mean Annual Precipitation (%)	-0.3	0.6	-2.7
Mean April 1st Snow Water Equivalent (%)	-53.4	-75.9	-88.6
Mean Annual Runoff (%)	3.5	2.5	-3.6
Mean December–March Runoff (%)	9.0	13.6	11.0
Mean April–July Runoff (%)	-11.1	-23.0	-36.1
Mean Annual Maximum Week Runoff (%)	12.9	18.4	18.3
Mean Annual Minimum Week Runoff (%)	-0.3	-0.5	-0.6
Sacramento River at Freeport			
Mean Annual Temperature (°F)	1.3	3.0	4.2
Mean Annual Precipitation (%)	-0.3	0.6	-2.7
Mean April 1st Snow Water Equivalent (%)	-53.4	-75.9	-88.6
Mean Annual Runoff (%)	3.5	2.5	-3.6
Mean December–March Runoff (%)	9.0	13.6	11.0
Mean April–July Runoff (%)	-11.1	-23.0	-36.1
Mean Annual Maximum Week Runoff (%)	12.9	18.4	18.3
Mean Annual Minimum Week Runoff (%)	-0.3	-0.5	-0.6
San Joaquin River at Friant Dam			
Mean Annual Temperature (°F)	1.4	3.3	4.5
Mean Annual Precipitation (%)	-1.3	-5.3	-8.6
Mean April 1st Snow Water Equivalent (%)	-23.1	-39.6	-48.7
Mean Annual Runoff (%)	0.7	-8.7	-10.7
Mean December–March Runoff (%)	13.9	15.8	31.0
Mean April–July Runoff (%)	-6.1	-20.2	-25.0
Mean Annual Maximum Week Runoff (%)	-2.3	-6.6	-16.0
Mean Annual Minimum Week Runoff (%)	-4.0	-6.4	-7.6

Table 2-1. Summary of Simulated Changes in Decade-Mean Hydroclimate for Several Subbasins in the Sacramento and San Joaquin River Basins (contd.)

Hydroclimate Metric (change from 1990s)	2020s	2050s	2070s
San Joaquin River at Vernalis			
Mean Annual Temperature (°F)	1.3	3.1	4.3
Mean Annual Precipitation (%)	-1.0	-4.2	-7.7
Mean April 1st Snow Water Equivalent (%)	-27.2	-45.9	-56.3
Mean Annual Runoff (%)	0.8	-5.9	-8.4
Mean December–March Runoff (%)	10.1	10.7	17.2
Mean April–July Runoff (%)	-4.8	-20.6	-25.8
Mean Annual Maximum Week Runoff (%)	1.6	-1.8	-4.9
Mean Annual Minimum Week Runoff (%)	-1.2	-1.9	-2.3

Key:
ºF = degree Fahrenheit

Chapter 3 Potential to Achieve Water Supply Reliability Objective Under Climate Change

Introduction

This chapter presents an assessment of the potential to achieve the water supply reliability objective under climate change. CP5 was selected for climate change this assessment as it maximizes water supply reliability. It is important to recognize that the complexity of the global climate system and its local scale expression precludes an accurate prediction what actual future climate changes will be. Therefore, the approach is to characterize the most significant uncertainties both climatically and socioeconomically. This objective was accomplished by combining these uncertainties into a variety of scenarios. Several different methodologies and modeling tools developed by Reclamation for the CVP IRP were employed.

In this section, the following topics are discussed:

1. Description of the CVP IRP modeling tools and methods
2. Assessment of Potential Climate Impacts on CVP and SWP operations and infrastructure under Baseline conditions
3. Assessment of Potential Climate Change Impacts on CVP and SWP operations and infrastructure with CP5

Description of the CVP IRP Modeling Tools and Methods

A description of the CVP IRP modeling tools and methods is presented here and a more detailed description is presented in Reclamation's CVP IRP Technical Modeling Report (2013). The CVP IRP employed a scenario-based analytical approach to evaluate the effects of a range of potential future uncertainties on a variety of water management actions including a simplified representation of CP5. The CVP IRP analytical framework was developed to evaluate the combined effects of climate change and socioeconomics on water supplies and urban and agricultural demands in the Sacramento, San Joaquin, and Tulare Lake basins. This basin-scale information was used to assess impacts within CVP Divisions and to evaluate impacts to the coordinated operations of the CVP-SWP system under current regulatory requirements. Critical uncertainties and scenario development included:

- Agricultural water demand and productivity

- Hydrology and systems analysis
- Performance-assessment tools
- Performance metrics
- Baseline Condition analysis
- Analysis of Water Management Actions including alternative CP5

In the analytical framework, the effects of climatic uncertainties on supply and demand are consistently evaluated. Climate impacts on supply are simulated through the use of hydrologic models. To provide consistent evaluation of agricultural and outdoor urban water requirements, the Land Atmosphere Water Simulator (LAWS) model was used to assess how climate change affects the water requirements and yields of major crops. This information was used as inputs to the Water Evaluation and Planning (WEAP) and Central Valley Project Integrated Resources Plan version of the California Lite Simulation (CVP IRP CalLite) models. The calibrated WEAP model of the Central Valley watershed (WEAP-CV) was used to generate surface water and groundwater flows and local area demands, which are used as inputs for the CVP IRP CalLite model. The CVP IRP CalLite model was then used to simulate CVP and SWP facilities, operations, and allocation decisions. The results of the hydrology and systems analysis were then used to provide inputs for additional performance-assessment tools that evaluate how potential water management actions affect economics, water quality and temperature, hydropower generation and use, and GHG emissions.

To account for a range of uncertainty in future conditions, a suite of scenarios was developed to reflect the following conditions:

- Three future socioeconomic conditions
- Six future climate conditions, including one reflecting historical conditions without climate changes and five reflecting climate change conditions

These three socioeconomic futures and six climate futures were combined to form the suite of eighteen future scenarios. Each scenario was analyzed for the period from 2011 through 2099 using a transient approach in which the climate and socioeconomic factors gradually change as the simulation moves through time. The following sections describe how the socioeconomic and climate futures are developed.

Socioeconomic Futures

The analysis uses the three socioeconomic future scenarios developed by California Department of Water Resources DWR in the California Water Plan (CWP) Update 2009 (DWR, 2009b):

- Current Trends, which assumes that recent trends will to continue into the future
- Slow Growth, which assumes that future development is less resource intensive than under recent conditions
- Expansive Growth, which assumes that future development is more resource intensive than under recent conditions

For each scenario, the CWP (DWR, 2009b) quantified population projected in 10-year increments from 2010 through 2050. The CWP used these population estimates to develop WEAP inputs relating to urban and agricultural land use. For the 2010 through 2050 period, CWP data was used directly. Through consultation with DWR CWP staff, the CWP population estimates and the WEAP urban and agricultural inputs were further extended in 10-year increments through 2100 for this analysis. Details of the methodology are presented in Reclamation (2013).

Figure 3-1 shows the population of each Central Valley Hydrologic Region (Sacramento, San Joaquin, and Tulare Lake) for the Slow Growth (SG), Current Trends (CT) and Expansive Growth (EG) scenarios in 2005 (base), 2050, and 2100.

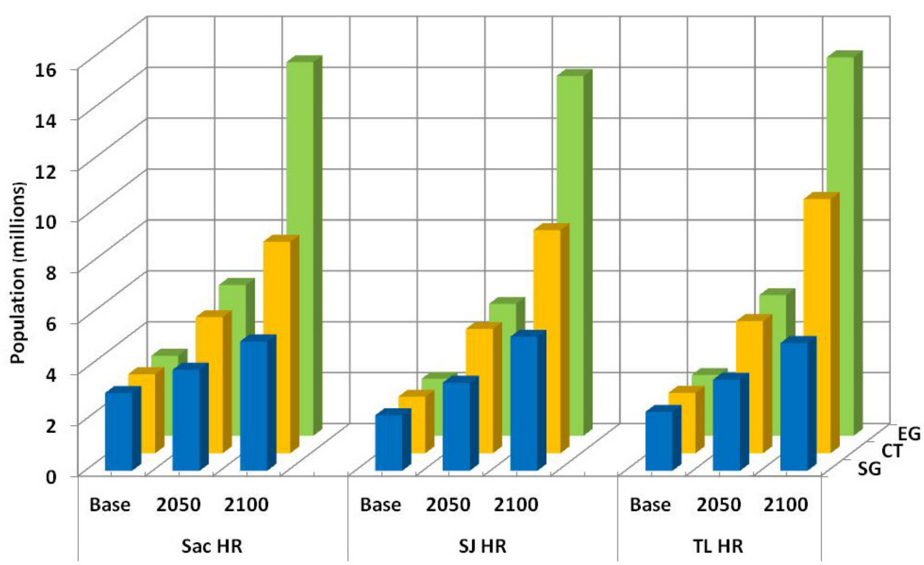

Figure 3-1. Central Valley Population Projections for 2050 and 2100 Under Each Scenario

Irrigated Land Area Projections

After the population projections were developed, the socioeconomic scenarios were used to project irrigated land areas in each county. For each scenario in the CWP, DWR developed assumptions about the relationships between population growth and urban and agricultural land use. This approach has been used to extend projected irrigated land areas beyond 2050 for use in the SLWRI analysis. Figure 3-2 shows the total irrigated land area in each Central Valley Hydrologic Region for each scenario in 2005 (base), 2050, and 2100.

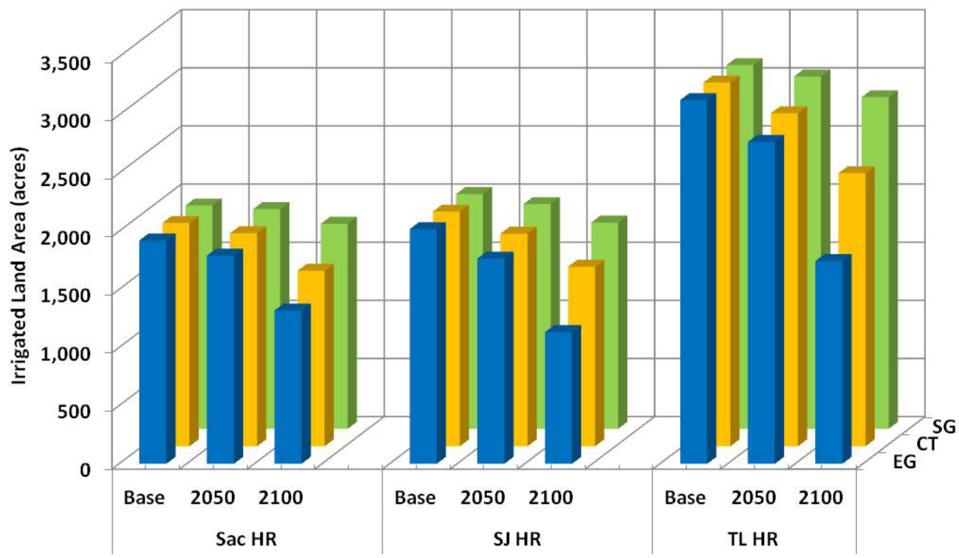

Figure 3-2. Central Valley Irrigated Land Area Projections Under Each Scenario

WEAP Urban Input Projection

The projected population projections are also used to develop residential, commercial and industrial inputs of each of the DWR Planning Area used in the WEAP_CV of the Central Valley. Figure 3-3 through Figure 3-6 show the projected numbers of single-family homes, multi-family homes, commercial employment, and industrial employment in each Central Valley Hydrologic Region for each scenario in 2005 (base), 2050 and 2100.

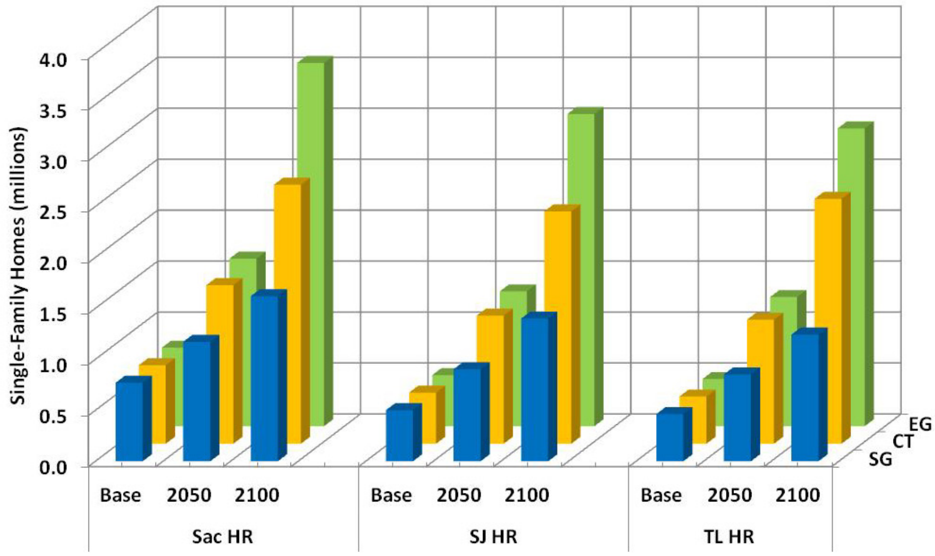

Figure 3-3. Central Valley Single-Family Home Projections Under Each Scenario

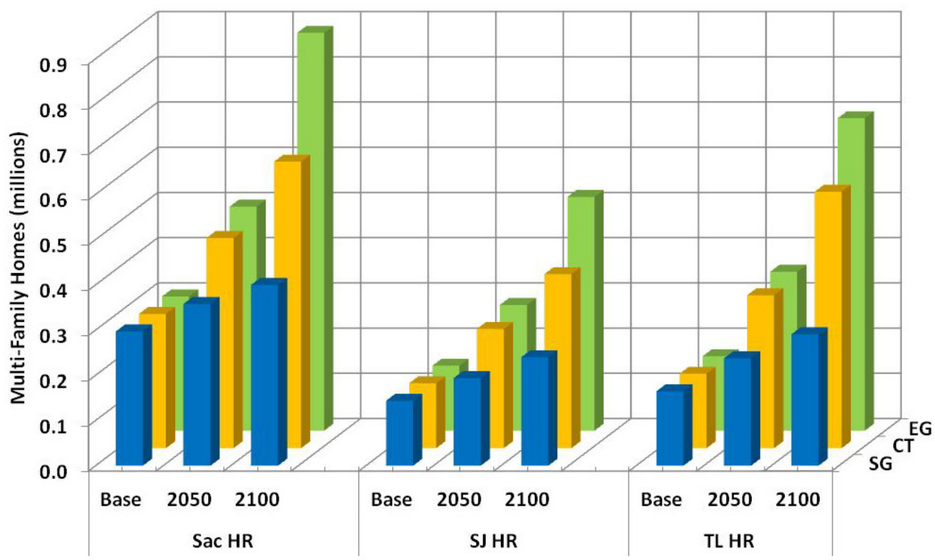

Figure 3-4. Central Valley Multi-Family Home Projections Under Each Scenario

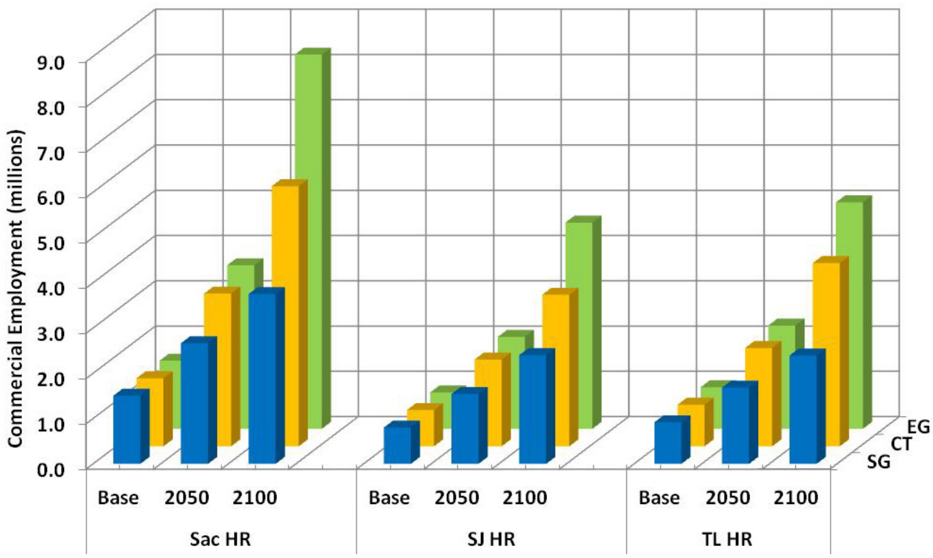

Figure 3-5. Central Valley Commercial Employment Projections under Each Scenario

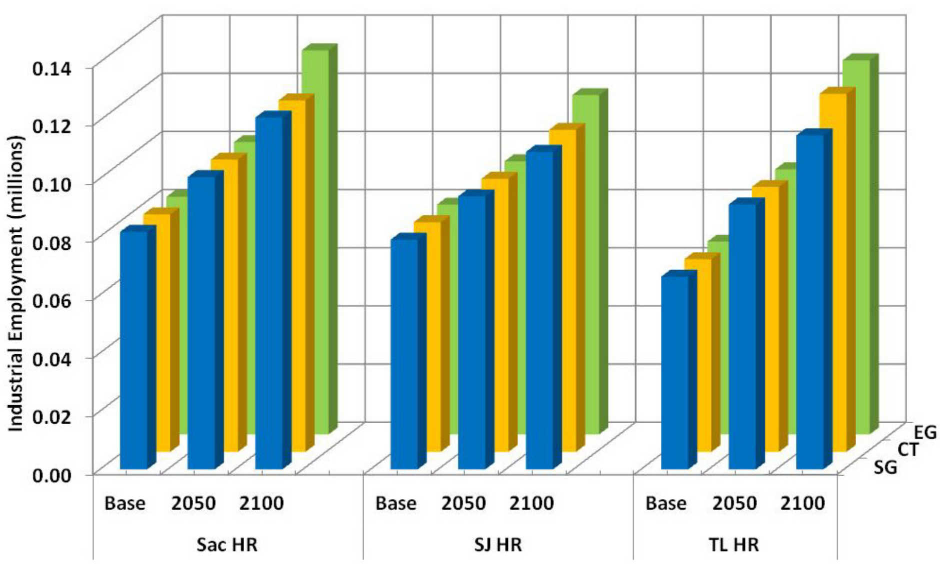

Figure 3-6. Central Valley Industrial Employment Projections Under Each Scenario

Climate Futures

The SLWRI analysis uses six climate future projections: one reflecting the historical hydrology without climate change, and five statistically representative climate change projections that employ an approach similar to the methods used for the Bay Delta Conservation Plan (BDCP). Each climate change future is characterized by changes in hydrology and sea level rise. The following sections describe how ensemble-informed climate hydrology and sea level rise inputs were developed for each climate future.

Ensemble-informed Climate Scenarios

Five climate sequences were developed using statistical techniques that consider the full range of the 112 (see Figure 3-7) bias-corrected, spatially downscaled climate change projections (Maurer et al., 2007) developed by Reclamation and others. These projections were used to develop statistically relevant climate scenarios employed in SLWRI analysis. The five representative climate sequences were developed using a multi-model hybrid delta ensemble approach in which the ensemble of future climate change projections is broken into regions representing future climate uncertainties ranging from (Q1) drier, less warming, (Q2) drier, more warming, (Q3) wetter, more warming, and (Q4) wetter, less warming scenarios than the captured by the ensemble median (Q5). These quadrants are labeled Q1 through Q4 in Figure 3-7. A fifth region (Q5) samples from inner-quartiles (25th to 75th percentile) of the ensemble and represents the central tendency of 112 projected climate changes. In each of the five regions, the subset of climate change projections, consisting of those contained within the region's boundary is identified. For the Q1 through Q4 regions, this subset consists of the 10 nearest neighbors to the 10-90 percentile points (see Figure 3-7).

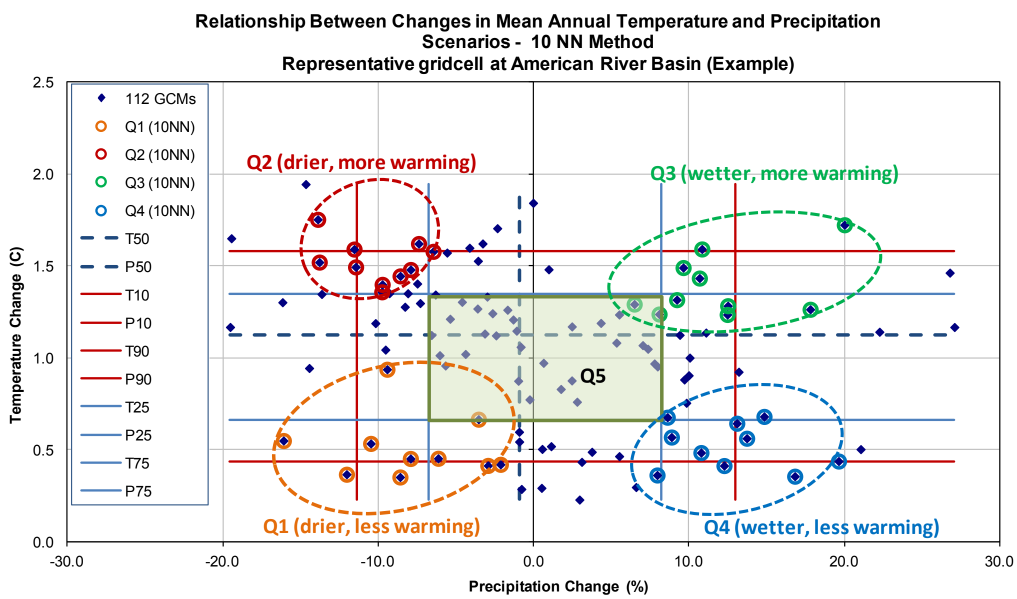

Note:
The Q5 scenario is bounded by the 25th and 75th percentile joint temperature-precipitation change. Scenarios Q1-Q4 are selected to reflect the results of the 10 projections nearest each of 10th and 90th joint temperature-precipitation change bounds.

Figure 3-7. Downscaled Climate Projections and Sub-Ensembles Used for Deriving Climate Scenarios (Q1-Q5) at a Location in the American River Basin at 2025

To develop the transient climate change scenarios for each of the five regions, a historical cumulative distribution function (CDF) was developed using a 30-year period centered around 1985 (1971 through 2000). In addition, three future

CDFs were developed using 30-year periods centered around 2025 (2011 through 2040), 2055 (2041 through 2070) and 2084 (2070 through 2099). The method uses the quantile map developed for each of these periods to redevelop a monthly time series of temperature and precipitation reflecting the observed natural variability sequence (1915 through 2003) and the projected climate change. The method applies the change for any particular year by interpolating from the two CDFs that bracket the simulation year. This process adjusts the historic observed climate records by the climate shifts projected to occur in the future.

This method was used to develop transient climate projections for each of the location shown on Figure 3-8.

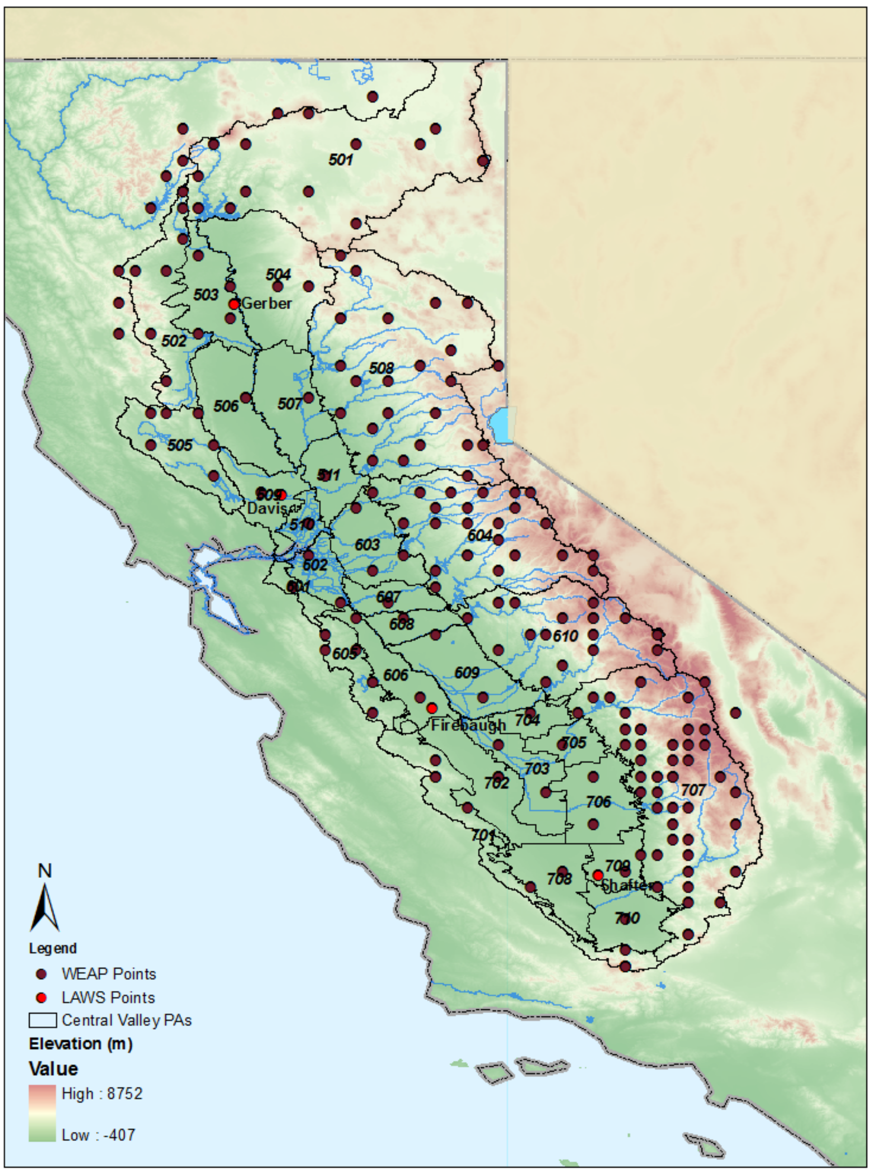

Figure 3-8. Map Showing the Climate Projection Locations Used in the WEAP Hydrologic Modeling and LAWS Modeling

Figure 3-9 shows temperature and precipitation for the transient climate scenarios Q1 through Q5 for a representative grid cell in the American River basin. The plot also contains observed historical temperature and precipitation for comparison.

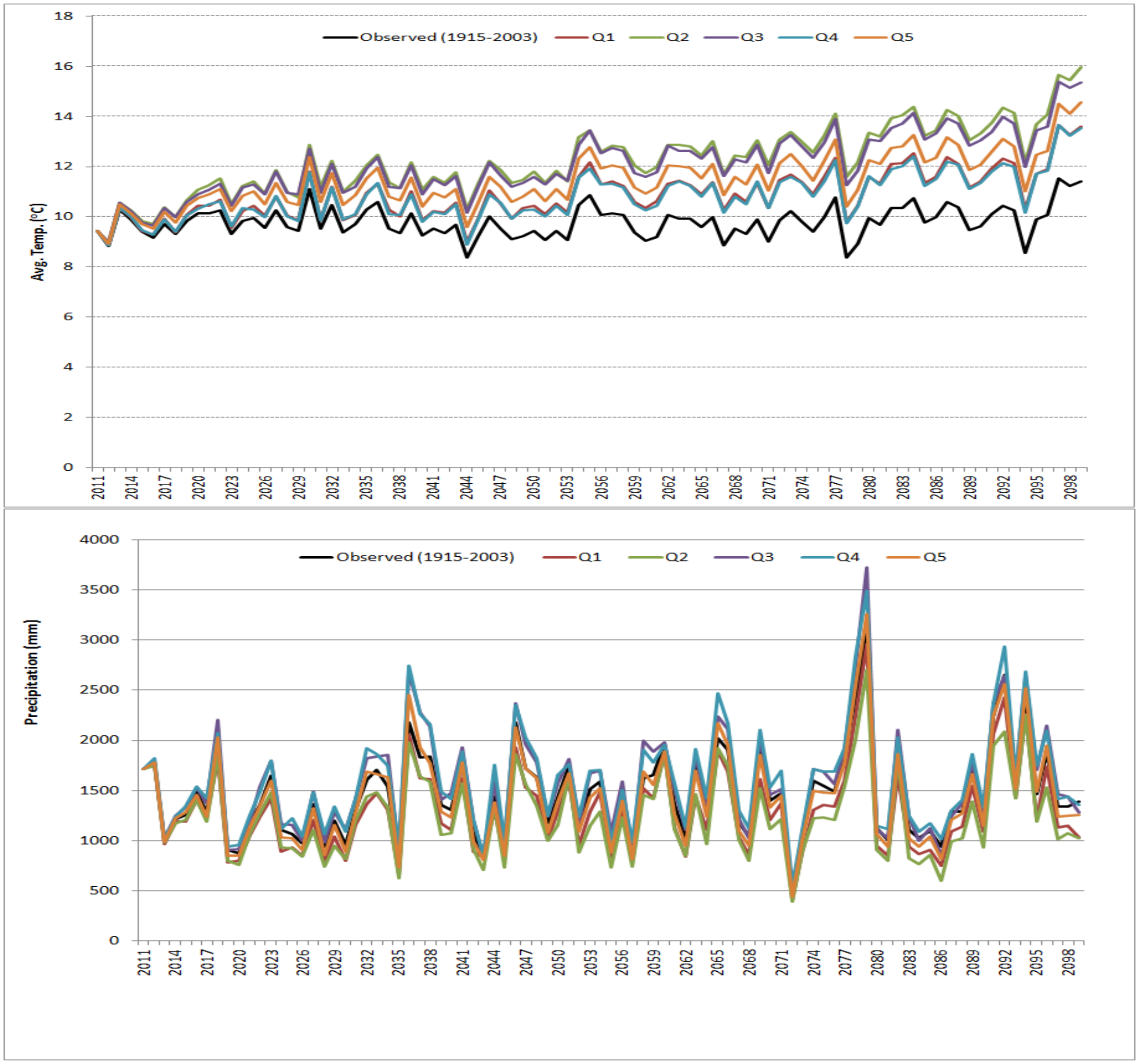

Source: Hamlet and Lettenmaier, 2005

Note:

Average annual temperature is shown in the top plot and annual precipitation in the bottom plot. Colored lines represent transient climate scenarios Q1 through Q5. Black color line represents annual average temperature and precipitation computed from historical observed data.

Figure 3-9. Transient Ensemble-Informed Climate Scenarios for a Representative Grid Cell in the American River Basin

Figure 3-10 shows the projected changes in precipitation under transient climate scenarios. Trends in precipitation projections are less steady because of naturally occurring decadal and multi-decadal precipitation variations. By construction, the transient climate scenarios method preserves the inter-annual variability as observed in the historical time series. However, the variability expands as directed by the climate projections.

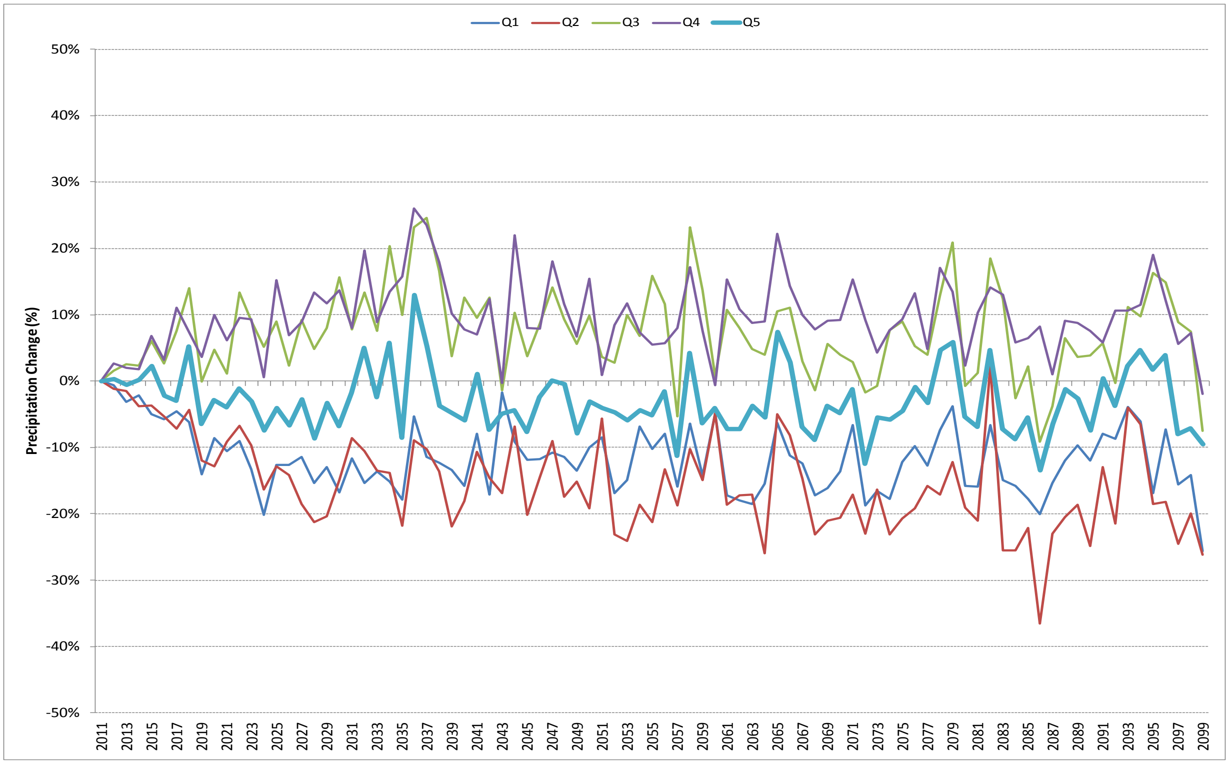

Figure 3-10. Precipitation Projections Under Transient Ensemble-Informed Climate Scenarios from 2011 Through 2099

An analysis of the effects of potential future climate changes on agricultural water demands and productivity requires more than just projections of future temperature and precipitation conditions. Crop growth, yield and evapotranspiration (ET) are also sensitive to other meteorological conditions including solar radiation, atmospheric humidity, wind speed and carbon dioxide. However, the climate projections described above did not include projections for these meteorological conditions. Consequently, several estimation methods using the Q1 through Q5 temperature and precipitation projections were employed to obtain values for these meteorological conditions corresponding to the future climate projections.

To represent the spatial variability in these meteorological conditions in the Central Valley, four locations were selected to provide representative conditions in the Central Valley. These locations are shown in bright red on Figure 3-8 above. They include existing California Irrigation Management Information System (CIMIS) stations located at Gerber, Davis, Firebaugh, and Shafter. These stations were chosen because at these locations long term observations of daily maximum and minimum temperature (Tmax, Tmin), solar radistion (Rs), dew point temperature (Tdew), relative humidity (RH), and wind speed were available . All historical data from the stations were carefully checked for erroneous values before preparing the subsequent projections.

Solar radiation is one of the primary factors effecting crop ET. It can be estimated from the Tmax and Tmin using the clear radiation (Ro) which only depends on latitude and the day of the year and a site-specific parameter (B). The CIMIS station historical records where used to calibrate B and the climate projections of Tmax and Tmin were then used to compute Rs based on the method of Thornton and Running (Thornton and Running, 1999) for each of the climate projections (Q1 through Q5).

The average Tmax, Tmin and Rs results for each of the climate projections during the early (2020), mid (2050) and late (2080) 21st century are presented in Figure 3-11 through Figure 3-13.

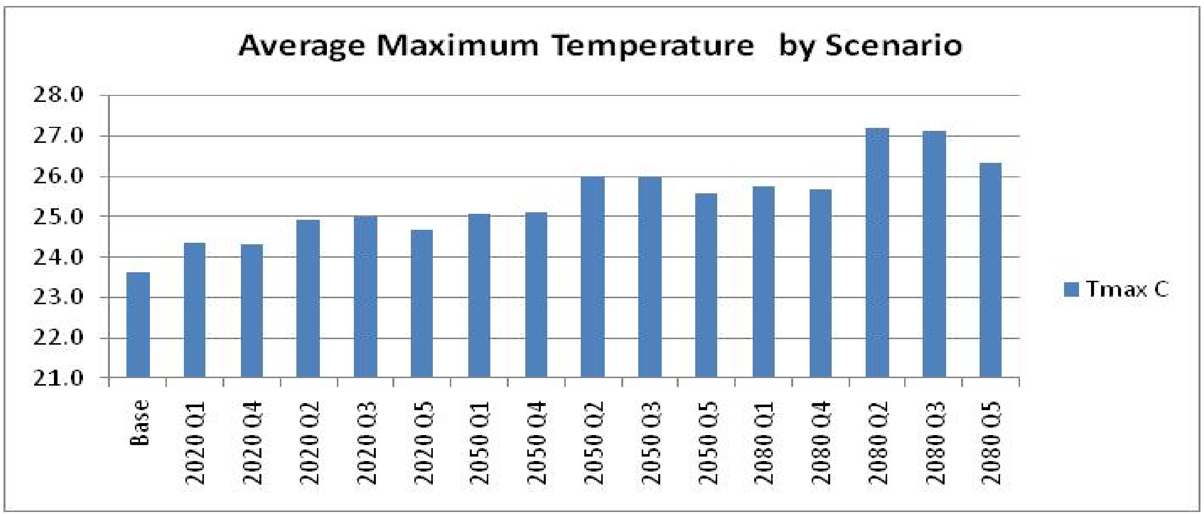

Figure 3-11. Projected Average Daily Maximum Temperatures in Degrees Celsius for Each Climate Scenario

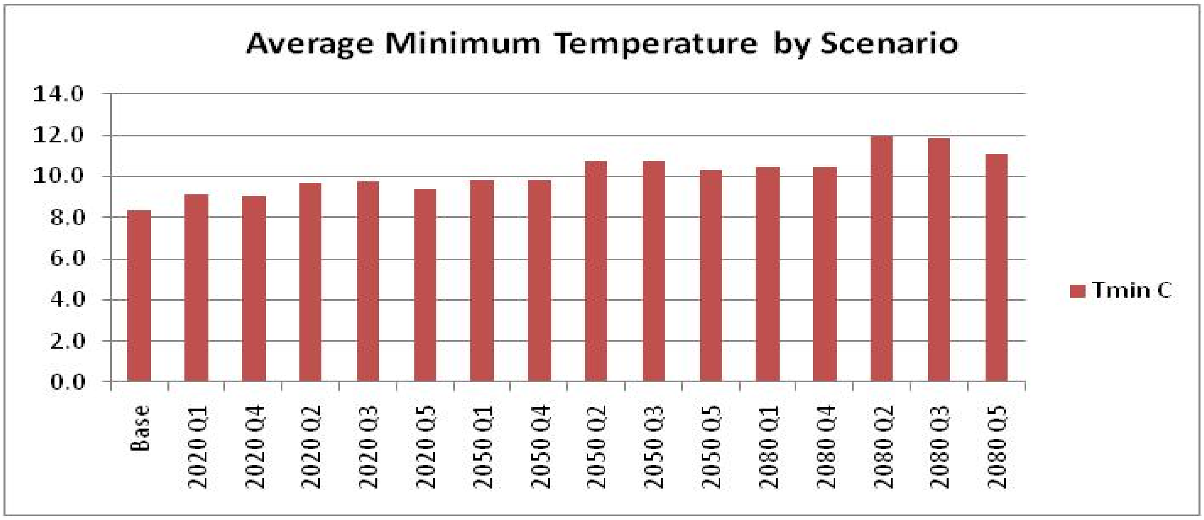

Figure 3-12. Projected Average Daily Minimum Temperatures in Degrees Celsius for Each Climate Scenario During the Early (2020), mid (2050) and late (2080) 21st Century

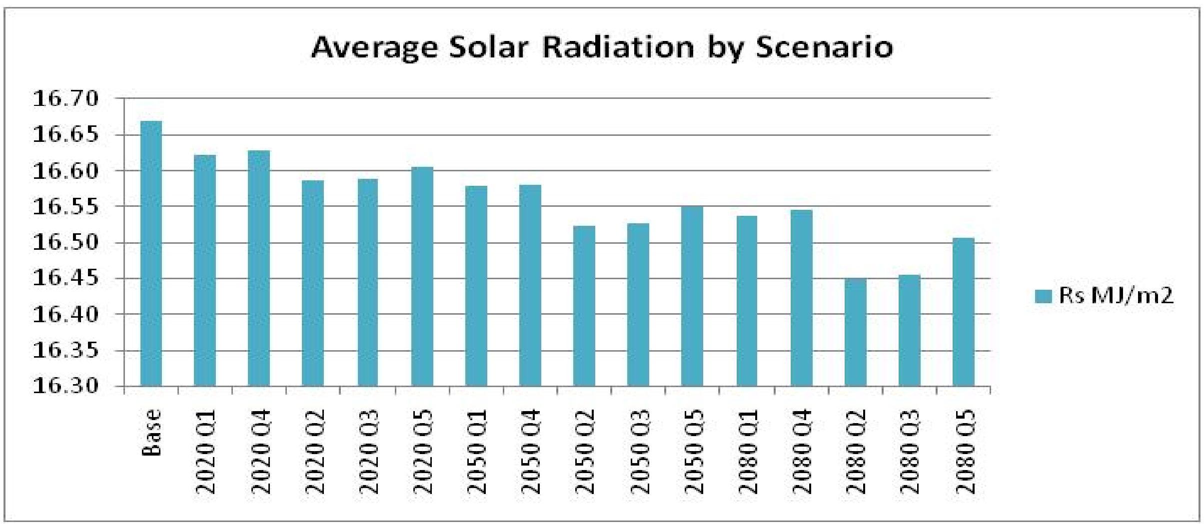

Figure 3-13. Projected Average Solar Radiation in Mega-Joules per Square Meter for Each Climate Scenario During the Early (2020), mid (2050) and late (2080) 21st Century

Atmospheric humidity is a major driver of crop ET. As the air becomes drier, ET generally increases. Tdew is an indicator of the moisture content of the air. As the atmospheric humidity increases, Tdew also increases. The daily minimum temperature is a good indicator of Tdew because cloudiness and high humidity reduce the amount of heat loss from the surface to the upper atmosphere which is reflected in higher Tmin values. To estimate projected changes in atmospheric humidity, an analysis of the CIMIS station records was made to determine the monthly average difference between the observed Tmin and Tdew values. This difference is referred to as the dew point depression (Ko). To estimate projected changes in Tdew, these monthly average observed

Ko values were subtracted for the projected Tmin values. The results are presented in Figure 3-14.

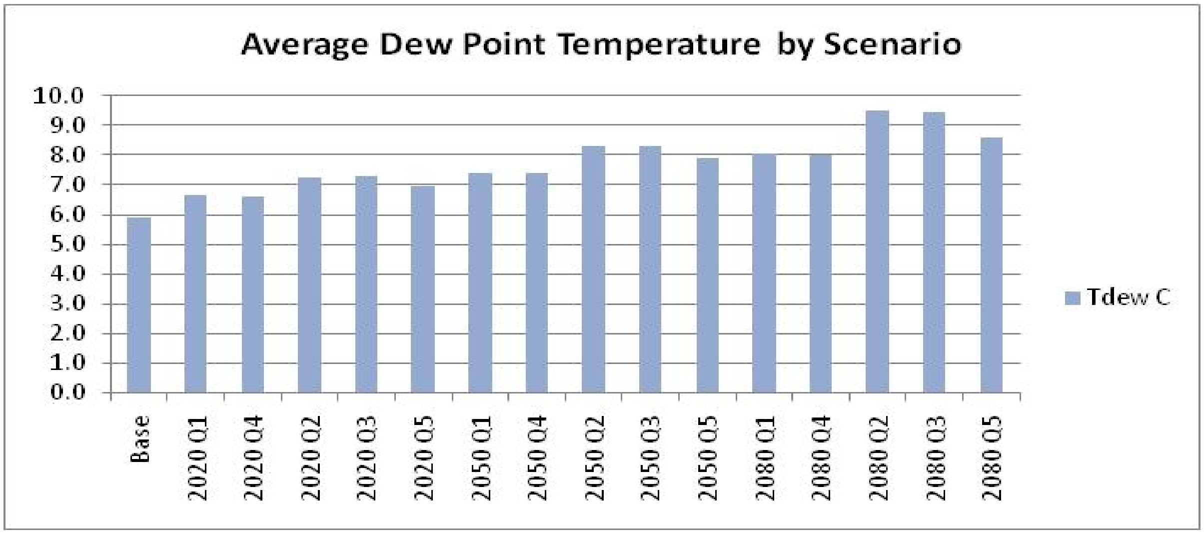

Figure 3-14. Projected Average Daily Dew Point Temperatures in Degrees Celsius for Each Climate Scenario During the Early (2020), mid (2050) and late (2080) 21st Century

The effects of atmospheric humidity are reflected in ET as the difference between the saturated vapor pressure in the moist plant leaves and the typically drier surrounding atmosphere. This difference is referred to as the vapor pressure deficit (VPD). As the VPD increases, crop ET generally increases. Because the saturation vapor pressure is a function of temperature, projections of VPD can be computed from the projections of daily Tmax, Tmin and Tdew using the results described above. Figure 3-15 shows the projected VPD results associated with each climate scenario.

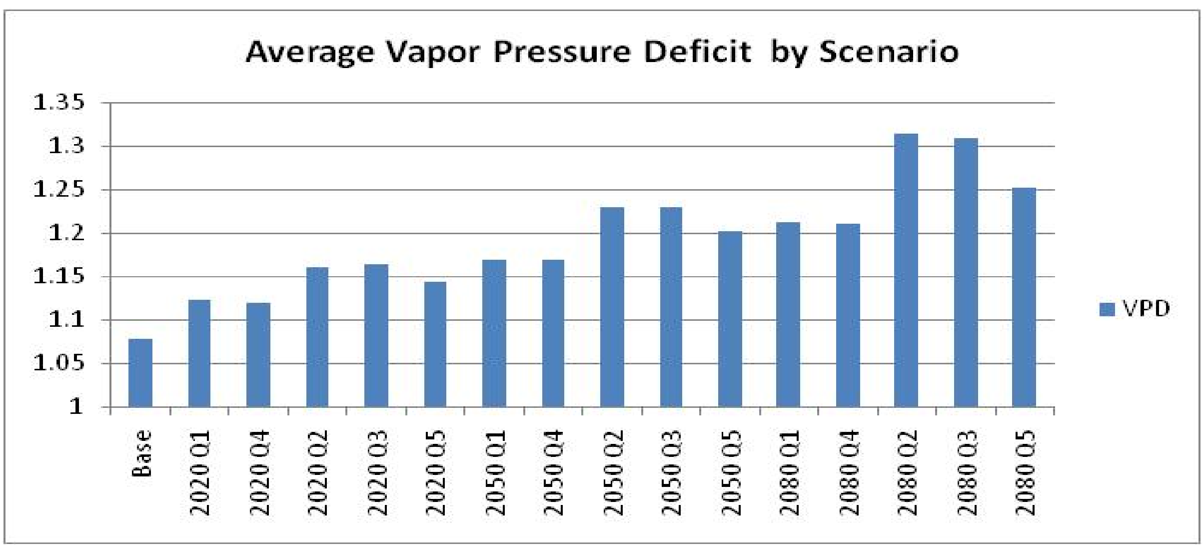

Figure 3-15. Projected Average Daily Vapor Pressure Deficits in Kilo Pascals for Each Climate Scenario During the Early (2020), mid (2050) and late (2080) 21st Century

Carbon dioxide (CO_2) has been observed to exert a strong effect on crop ET. As CO_2 concentrations increase, many crops have been demonstrated to have reduced ET. Consequently, an analysis of the Q1 through Q5 climate projections was made to determine the frequency of the different emission scenarios present in each of these ensembles. Because the CO_2 concentrations associated with each ensemble member are known, a weighted average CO_2 concentration could be computed for five projections on a decadal basis throughout the 21st century. These results are presented in Figure 3-16.

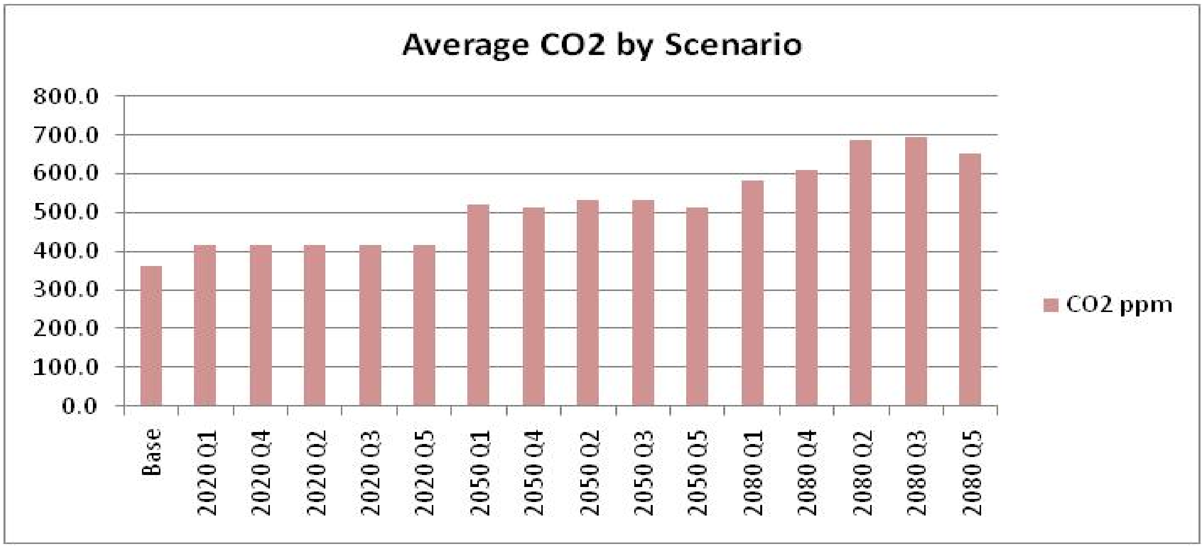

Figure 3-16. Projected Average Daily Average Carbon Dioxide Concentrations (parts per Million of CO_2 by Volume of air) for each Climate Scenario During the Early (2020), mid (2050) and late (2080) 21st Century

Sea Level Changes

The CALFED Science Program, State, National Academy of Science and others have made assessments of the range of potential future sea level rise throughout 2100. These studies indicate that as sea level rise progresses during the 21st century, the hydrodynamics of the Delta will change causing the salinity of water in the Delta to increase. This increasing salinity will most likely have significant impacts on water management throughout the Central Valley and other regions of the State.

Figure 3-17 below shows various projected ranges of potential sea level change in the San Francisco Bay/Sacramento-San Joaquin Delta (Bay-Delta) through the year 2100. Some State and Federal planning processes in the Central Valley have considered sea level rise through mid-century. In these studies, sea level rises from 60 to 90 centimeters (cm) (2 to 3 feet) have been simulated using existing hydrodynamic models. Under current conditions, sea level rise much greater than these levels would most likely inundate many of the Delta islands and would likely cause large-scale levee failures that cannot be simulated without making broad policy assumptions related to levee hardening and land use throughout the Bay-Delta.

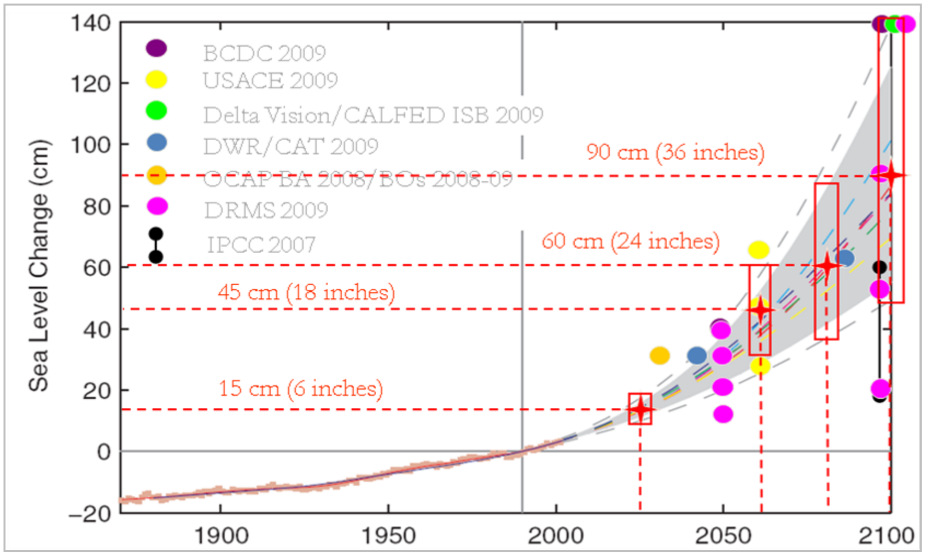

Figure 3-17. Range of Future Mean Sea Level Based on Global Mean Temperature Projections and Sea Level Rise Values

As part of the SLWRI transient climate change analysis approach, sea level rise has been assumed to gradually increase in the CVP IRP CalLite simulations from 2011 to 2099. Figure 3-18 shows the projected sea level rise used for each SLWRI climate scenarios. The highest amounts of sea level rise occur in the two warmest climate scenarios (Q2 and Q3, which have almost the same rates of rise), with the remaining differentiation corresponding to the amount of warming projected in each climate scenario. In the CalLite simulations, an artificial neural network model (ANN) reflecting a no sea level rise condition was used to determine salinity requirements and conditions in the Delta. This ANN was adjusted to reflect changes in Delta conditions due to sea level rise. For the SLWRI, sea level is projected to gradually rise up to a maximum of between 105 and 120 cm across the 5 climate scenarios. To adjust the inputs and outputs of the no sea level rise ANN, relationships between flow and salinity were developed and incorporated into the CVP IRP CalLite model to simulate the effects of the projected sea level rise on the Bay-Delta system. These relationships were developed using results derived from the UNTRIM model simulations (MacWilliams et al., 2008) and through calibration with CalSim-II simulations that incorporate sea level rise.

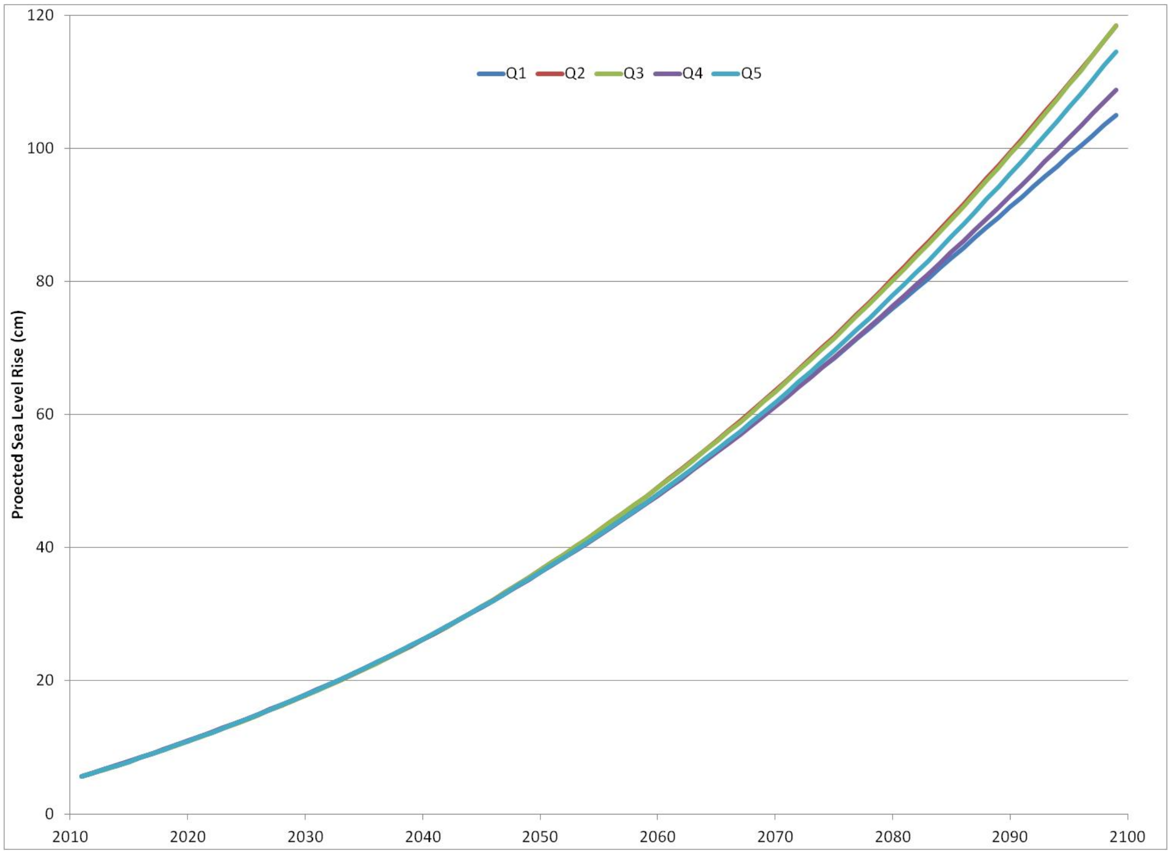

Figure 3-18. Projected Sea Level Rise Values in Five Climate Change Scenarios

Agricultural Water Demand and Productivity

In the previous sections, the approaches used to develop the projections climate change on water supply and demand were described. The projections were developed to provide a consistent assessment of how climate change affects both water supply and agricultural demands. The LAWS model (Tansey et al., 2011) was used to compute crop water requirements, growth, and yield based on climate scenarios Q1 through Q5. To accomplish this objective, the LAWS model was modified to include the biophysical processes that are needed to simulate the major effects of climate on crop ET, growth and yield. Crop growth and yield modeling are considered important because climate effects on crop yields have important implications for agricultural productivity and economics.

Before employing the projected climate changes in the LAWS model, it was calibrated using the historically observed climate data from the Gerber, Davis, Firebaugh and Shafter CIMIS stations for 20 major crops grown in the Central Valley. The "California Crop and Soil Evapotranspiration" (Irrigation Training and Research Center, 2003) study was used to provide historic period data on crop ET at the four CIMIS calibration locations. Historic crop yield data was obtained from the State Wide Agricultural Production (SWAP) model (Howitt et al., 2012). Initial estimates of crop parameters were obtained from the literature sources and adjusted to match the reported ET and yield data.

The calibrated LAWS model was used to simulate the effects of climate changes associated with the previously described Q1 through Q5 climate projections. These LAWS simulations produced the corresponding projected ET and yield data sets for the major crops grown in the Central Valley. These datasets were used in the subsequent the WEAP and SWAP modeling. Using these projected crop ET datasets in the WEAP hydrology simulations provided consistent climate based projections of both water supply and demands. By including the effects of projected climate changes on both water supply and demands, an improved representation of climate effects on the CVP/SWP system operations and performance was achieved.

These improvements in supply and demand consistency also benefit the agricultural economic evaluations performed for the SLWRI using the SWAP model. The SWAP model has been calibrated based on 15 years of observed farmers' decisions about cropping patterns, and it uses water supply and demands over time along with consideration of the costs and revenues associated with these production systems to determine optimal land and water resource allocation to maximize economic benefits. Using both the LAWS ET and major crop yield datasets in the SWAP model also provides an improved consistency between the projected economic changes for each of the Q1 through Q5 climate projections.

Hydrology and Systems Analysis

Geographic Representation of the CVP Service Area

Although CVP IRP technical analysis were designed to report modeling results for each CVP Division, the tools actually simulate the entire CVP, SWP and non-project water management system. The supply and demand information is derived primarily from WEAP model results, which are set at the CWP's Planning Area scale. Therefore, the hydrology and systems analysis models are designed to translate the Planning Area–scale data to produce data for each CVP Division.

CVP IRP Divisions

The CVP includes the following nine Divisions:

- Trinity River Division
- Shasta Division
- Sacramento River Division

- American River Division
- Delta Division
- West San Joaquin Division
- Friant Division
- East Side Division
- San Felipe Division

The geographic extent of each Division is defined by the boundaries of the CVP districts that divert water from the facilities and rivers within that Division (Figure 3-19). Similarly, the demand for each Division is equal to the sum of the demands of all of the CVP districts within the Division.

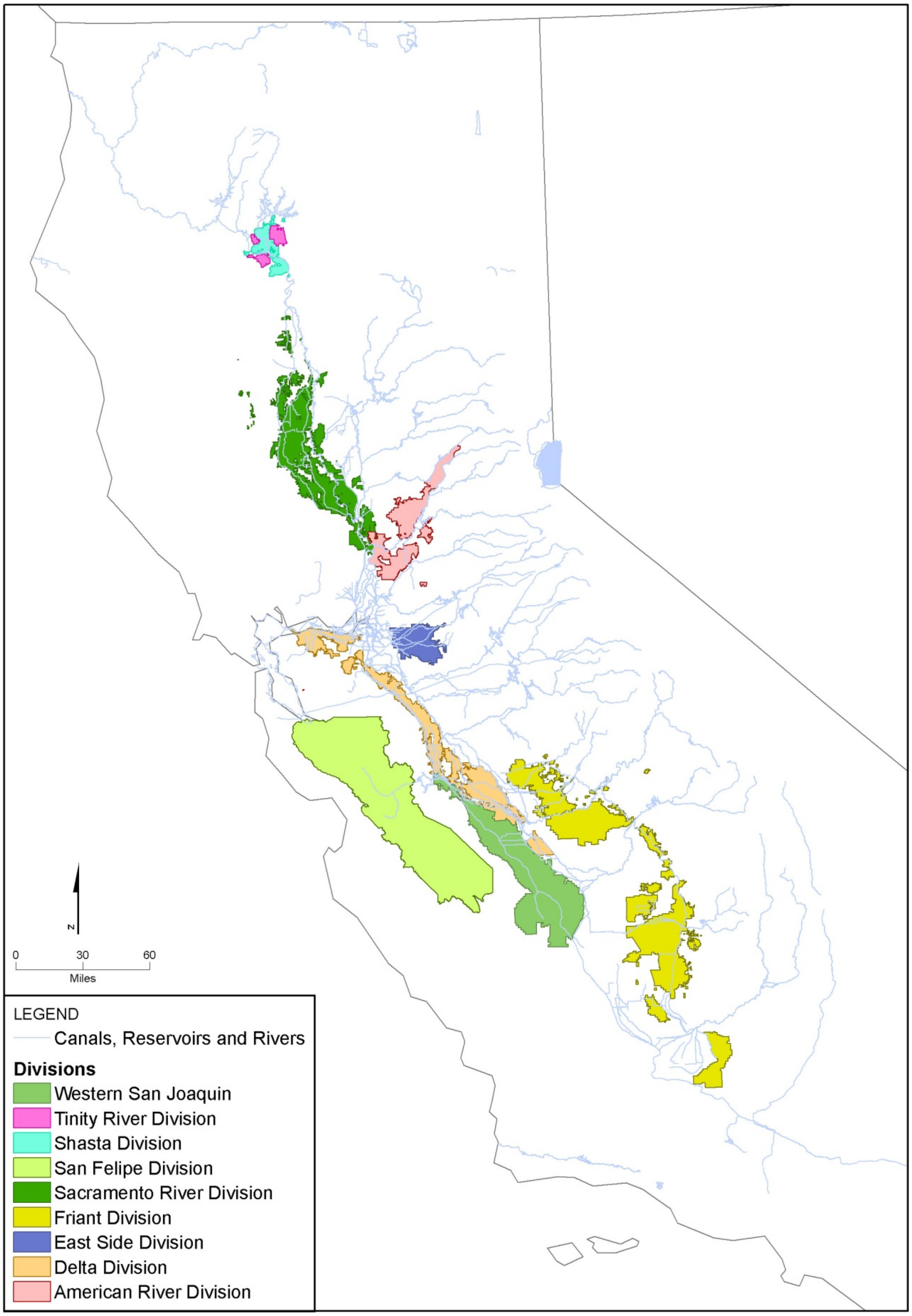

1
2 **Figure 3-19. Map of the CVP Divisions**

California Water Plan Geographic Regions

The CWP develops and uses data at the spatial scales of Hydrologic Regions and Planning Areas. California is divided into 10 Hydrologic Regions, each of which is divided into a number of Planning Areas. The CWP has used the WEAP model to develop estimates of hydrology and demand at the Planning Area–scale in the Sacramento River, San Joaquin River, and Delta Hydrologic Regions. In some cases, the Planning Areas have been subdivided into even smaller geographic units for the purpose of improved model simulations.

The Planning Area regions modeled for these Hydrologic Regions are shown in Figure 3-20. These Hydrologic Regions provide coverage for the entire CVP Service Area with the exception of the San Felipe Division. Therefore, hydrology and demand data for the San Felipe Division has been developed outside of the WEAP model as described under the following discussion.

Simulation of the CVP-SWP Integrated Water System

This section describes how simulations are performed using the CVP IRP models for the baseline socioeconomic and climate conditions and to simulate each potential water management action or suite of actions. Each scenario is analyzed for the period from 2011 through 2099 using a transient approach in which the climate and socioeconomic factors gradually change as the simulation progresses through time.

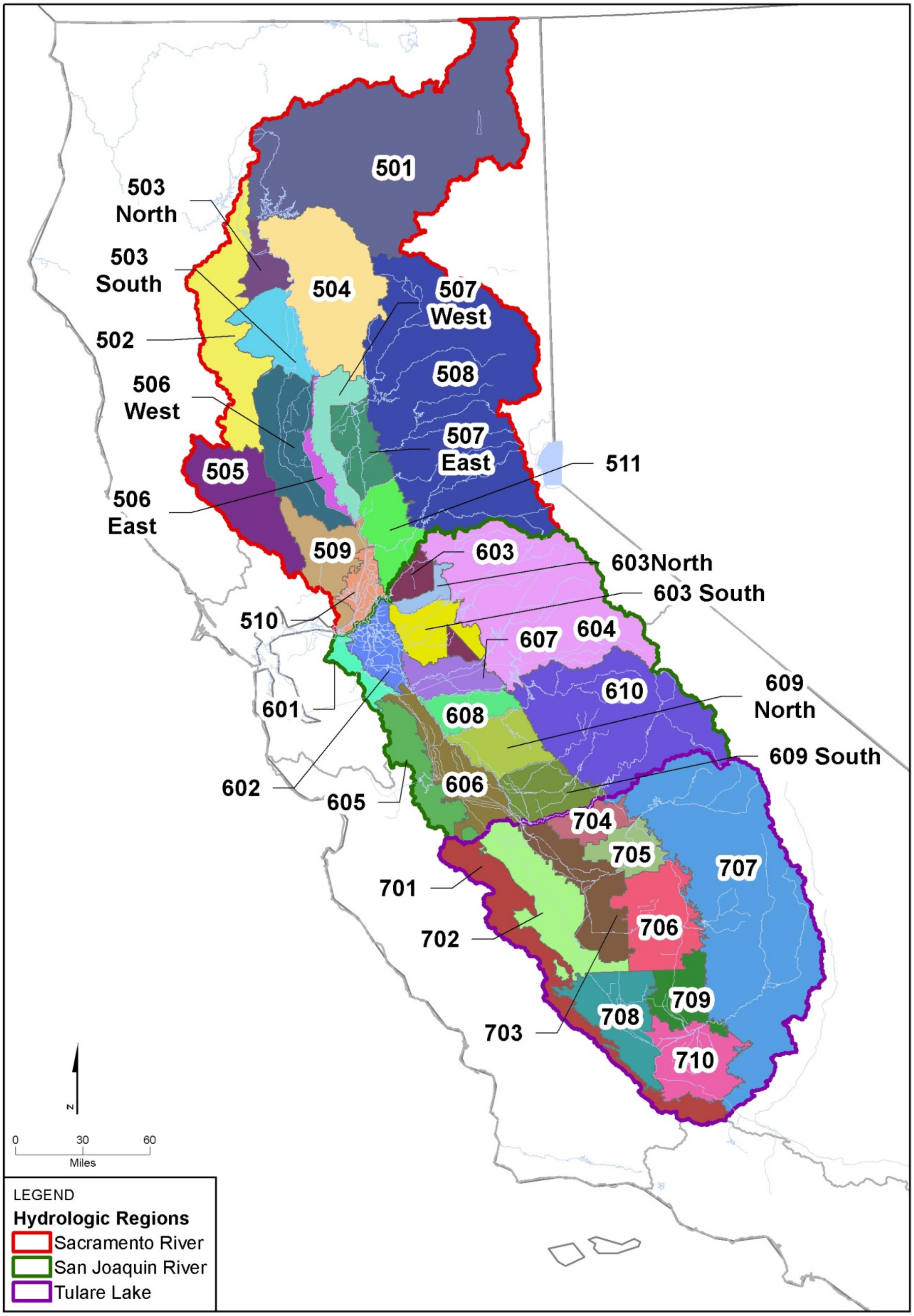

Figure 3-20. Planning Areas in the Sacramento River, San Joaquin River, and Tulare Lake Hydrologic Regions

Approach

The simulation of the SLWRI socioeconomic-climate scenarios described above was performed using the CVP IRP CalLite and WEAP-CV models in an integrated manner. The WEAP-CV model was used to develop climate-based watershed runoff for the main watersheds of the Central Valley and climate-based demand estimates for the Delta, Sacramento, San Joaquin, and Tulare Lake Hydrologic Regions. The model includes rainfall-runoff modules of the source watersheds and water demand modules for each Planning Area in the Central Valley water system. Figure 3-21 depicts a generic representation of a reservoir and river system simulated by the WEAP-CalLite integrated models. The figure depicts hydrology, demand, and operational components included in the simulation and indicates which model provides the data for each component of the analysis. Table 3-1 lists the components simulated by each model. The WEAP-CV model produces the hydrology and demand components, and the CVP IRP CalLite model produces outputs relating to system operations and local and system-wide management actions.

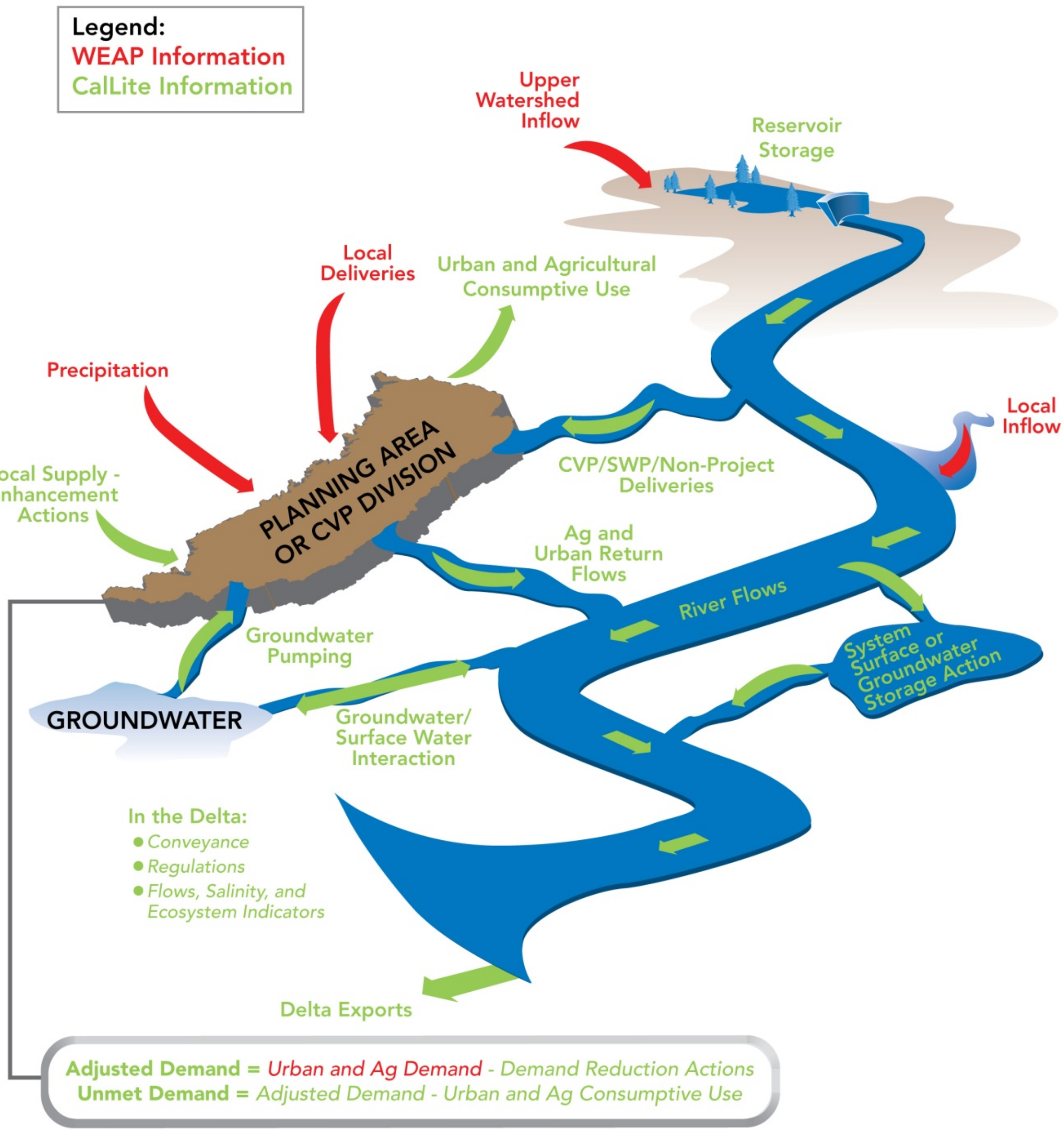

Figure 3-21. WEAP and CalLite Integration of the Supply and Demand Hydrology Components

Table 3-1. CVP IRP Simulation Components Produced by Each Model

WEAP	CalLite
Upper watershed inflow	SWP/CVP/non-project deliveries
Local inflow	River flows
Precipitation	Reservoir storage
Urban and agricultural water demand	Agricultural and urban return flows
Local deliveries	Groundwater pumping
	Local supply-enhancement actions
	Local demand-reduction actions
	Systemwide management actions
	Adjusted demand
	Unmet demand
	Delta conveyance, regulations, and exports
	Delta flow, salinity, and ecosystem indicators
	Groundwater-surface water interaction

Key:
CVP = Central Valley Project
IRP = Integrated Resource Plan
SWP = State Water Project
WEAP = Water Evaluation and Planning

Because the Planning Area–scale WEAP-CV model does not cover the San Felipe Division, the WEAP components shown in Table 3-1 were developed separately for the San Felipe Division and included as inputs into the CVP IRP CalLite simulation. Local inflow and precipitation, agricultural and urban water use, demand, return flows, local deliveries, and groundwater pumping for the San Felipe Division are estimated using county scale information for San Benito and Santa Clara Counties developed by DWR's Water Plan Update (DWR 2009b).

The CVP IRP CalLite model simulates SWP, CVP, and non-project deliveries to the San Felipe Division along with local supply-enhancement and demand-reduction actions. Therefore, local water management actions in the San Felipe Division are evaluated despite the absence of a Planning Area-scale WEAP model of the region.

The WEAP-CV model was used to simulate each of the 18 socioeconomic-climate scenarios for the period from 2011 through 2099 to evaluate the range of future uncertainties associated hydrology of the system. Each scenario was analyzed for this period using a transient approach in which the climate and socioeconomic factors gradually change as the simulation progresses through time. The climate-based supply and demand factors produced by WEAP were subsequently used as inputs to the CVP IRP CalLite model to perform simulations under different socioeconomic and climatic conditions.

The CVP IRP CalLite model was used to simulate water management in the SWP and CVP systems, with explicit representations of current Delta regulatory requirements and major CVP-SWP and non-project reservoir operations and allocation decisions. CVP IRP CalLite simulates SWP and CVP operations in the Sacramento Valley, San Joaquin River system, Tulare Lake Region, the Delta, and the south-of–Delta (SOD) export areas.

For the SLWRI, the CVP IRP CalLite model has been set up to perform simulations of the 18-scenario suite for Baseline and somewhat simplified representation of CP5. For each scenario, the CVP IRP CalLite model computes a supply-demand balance within each CVP Division and produces system wide outputs relating to flow, storage, and salinity in the SWP, CVP, and the Delta.

WEAP-CalLite Interaction

The following sections describe the WEAP-CalLite interaction required to perform CVP IRP CalLite simulations using the WEAP output data and how CalLite uses WEAP and CalLite outputs to compute a water balance for each CVP Division.

Agricultural and Urban Demands The WEAP-CV model was used to estimate agricultural and urban demands in each Planning Area. The WEAP simulation does not distinguish between CVP, SWP, and non-project demands. To use this data in the CVP IRP CalLite simulation and to compute demand information for a CVP Division, the demand data produced by WEAP must be disaggregated into different contract types and then mapped to the appropriate CVP Divisions. As an example of how CVP contractor districts relate geographically to Planning Areas, Figure 3-22 depicts the CVP contractors surrounding Planning Area 503 North. The figure shows how each Planning Area can contain multiple CVP contractors, and a CVP contractor can overlap multiple Planning Areas.

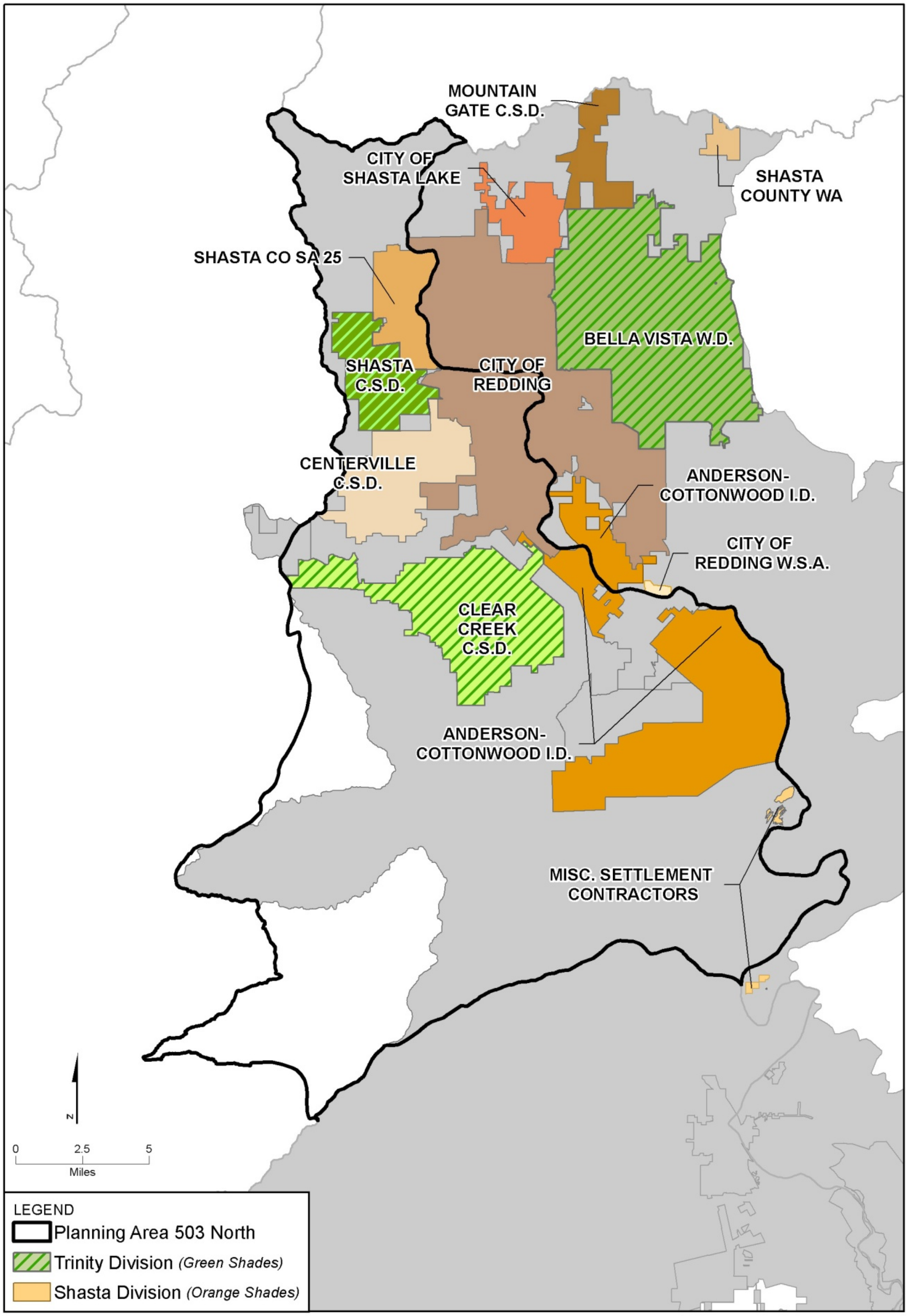

Figure 3-22. CVP Contractor Districts in Planning Area 503 North

A mapping exercise was performed using geographical information system (GIS) to convert the WEAP Planning Area–scale data to CVP Divisions. Conversion of WEAP demand data for use in by the CVP IRP in CalLite involves the following steps:

- Disaggregation of Planning Area data to CalLite nodes by contract type
- Mapping of CalLite node contract type data to CVP Divisions

The disaggregation of demand within each Planning Area is performed by using Microsoft Excel pre-processing spreadsheets that define the percent breakdown of demand types for each land use type in each Planning Area. The breakdown of demand type has been developed using data developed as part of DWR and Reclamation's joint CalSim-III model development effort. A lookup table is used to define the percent of land use for each water demand type in each Planning Area. The following demand types are used:

- CVP: agricultural, municipal and industrial (M&I), Settlement Contractors, Exchange Contractors, and refuges
- SWP: agricultural, M&I, Feather River Service Area
- Non-project: agricultural and M&I

The pre-processing spreadsheets use this information to compute the demand for each demand type in each CalLite node under each scenario. The demand breakdown in each CalLite node is also used to map the CalLite node-scale demand and delivery data to each CVP Division. This is accomplished by identifying the relevant CVP Division of each contractor in each CalLite node and cross-referencing the contract type demand delivery data to the appropriate Division. The total delivery to each CVP Division is then computed as the total for all relevant nodes.

Surface Water and Groundwater Hydrology and Return Flows The CVP IRP CalLite and WEAP models have been enhanced to allow hydrologic and return flow information developed in WEAP to be used as inputs to the CalLite model. The following steps were used to enhance the models:

- The CalLite network was overlain on a map with the Planning Areas, Hydrologic Regions, and the WEAP network.
- The overlay was examined to identify the most appropriate linkage points for integrating rim station and valley floor hydrology, return flows (non-irrigated and irrigated) and surface-groundwater interactions in CalLite and WEAP.
- A data-transfer routine was developed to convert WEAP data to CalLite inputs at each linkage point.

The following sections describe how inputs have been developed at each CalLite node for the rim station locations, for return flows and groundwater-surface water interaction and for the valley floor nodes.

Upper Watershed Hydrology The WEAP model was applied to develop upper watershed runoff values under each scenario. However, a comparison of the WEAP stream flows resulting from a historical simulation with the observed stream flows revealed biases in the modeled flows. As an example, Figure 3-23 shows the difference in monthly values between the WEAP and observed stream flows into Lake Shasta. These biases result from several factors, including spatial and temporal errors in climate model forcings, complex surface water and groundwater interactions, and other complexities normally inherent to hydrologic model parameter calibration. To address these issues, bias corrections of the WEAP stream flows were performed for all of the rim inflows into the CVP IRP CalLite model to better reflect the statistics of the observed stream flows for the historical simulation period. The resulting bias-corrected historical inflows factors were used in the CVP IRP CalLite model to exactly match the annual and monthly averages of the historical observed upper watershed flows. These bias corrections for each inflow location were also used to adjust the upper watershed inflows used for each of the SLWRI projected future socioeconomic-climate scenarios.

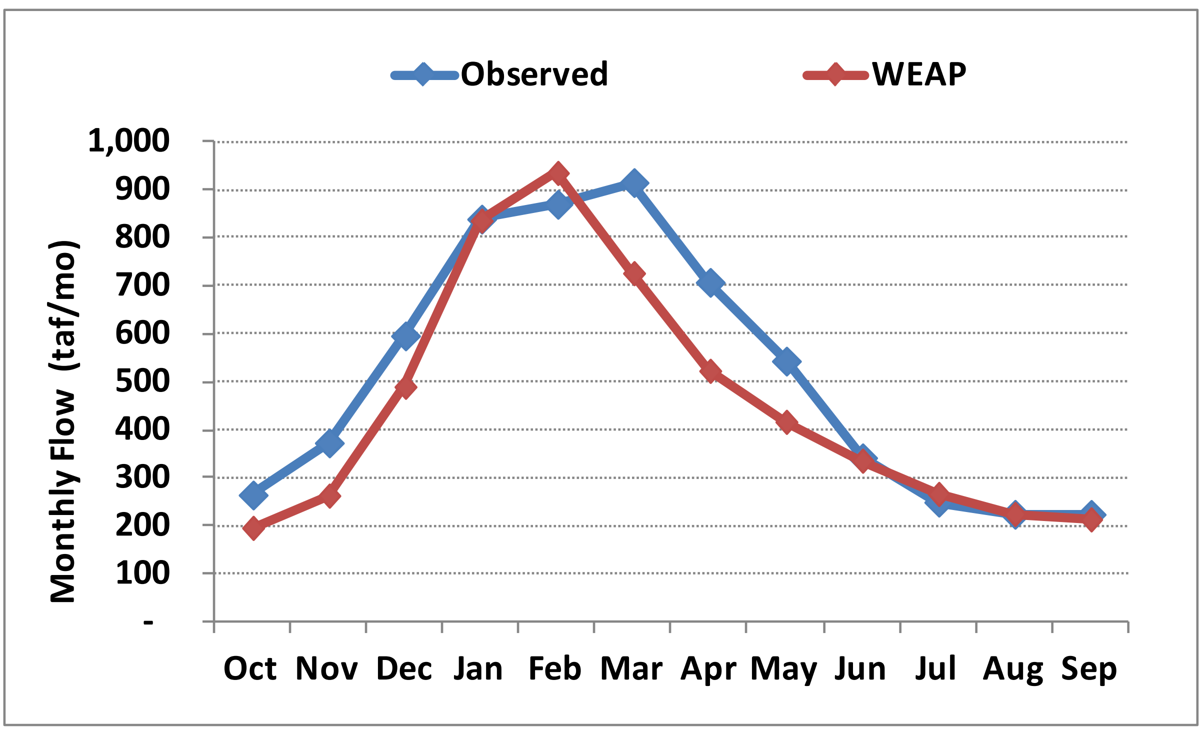

Figure 3-23. Comparison of Average Monthly Observed and Simulated Inflows into Lake Shasta on the Sacramento River Before Adjustment

Valley Floor Hydrology Valley floor hydrology inputs in CVP IRP CalLite were developed using the "Flow to GW No Irrigation" and the "Flow to River No Irrigation" outputs from WEAP. A GIS mapping process was applied to identify the percentage of the flow coming from each WEAP Planning Area that would runoff to each CalLite node and groundwater aquifer. These outputs are mapped to the corresponding CalLite groundwater aquifers and nodes and inputted directly into the CalLite model.

The irrigation return flow components are dynamically simulated in WEAP and may vary for each scenario. Therefore, the irrigation return flows are computed dynamically in the CVP IRP CalLite model using functions derived from WEAP results for each Planning Area.

Return Flows and Groundwater-Surface Water Interaction Return flows and groundwater-surface water interaction were also determined dynamically in the CVP IRP CalLite model using equations derived from WEAP results to determine the return flow quantities and groundwater-surface water flows resulting from the CalLite deliveries groundwater storage values in each month. A GIS mapping process was applied to identify the appropriate return flow destinations (i.e., river locations and groundwater aquifers) for each CalLite node. A similar mapping exercise was used to determine the appropriate surface water locations for groundwater-surface water interactions to be implemented for each groundwater aquifer.

Computing a Water Balance for a CVP Division

The water balance for each CVP Division was computed by the CVP IRP CalLite model for the 18 socioeconomic-climate scenarios using the CalLite node-scale demand and hydrology information developed for each scenario with the results of the CalLite simulations. The supply and demand components used in the water balance can be identified by focusing on the inputs and outputs to the local demand node in Figure 3-21. Those that are used to compute supply and demand are listed in Table 3-2 below. The difference between the sum of the supplies and the sum of the demands equals the unmet demand computed by CVP IRP CalLite model. The post-processing routines in CalLite are set up to produce supply and demand information for each CVP Division for each simulation of the 18-scenario suite.

Table 3-2. Components of Supply and Demand Used to Compute Water Balance for CVP Divisions

Supply	Demand
SWP/CVP/non-project deliveries	Urban and agricultural demands
Local inflow and precipitation	Local demand-reduction actions
Local deliveries	
Groundwater pumping	
Local supply-enhancement actions	

Key:
CVP = Central Valley Project
SWP = State Water Project

Application of Additional Performance Assessment Tools

In addition to using metrics available from CalLite, ranges of uncertainty for the Baseline and alternative CP5 were evaluated for water quality and temperature, agricultural and urban economics, hydro-power, and GHG metrics. The following tools were used to perform the analysis and generate reporting metric results:

- **Delta water quality** – CalLite produces monthly salinity results at compliance locations in the Bay-Delta system.
- **Urban economics** – The Least Cost Planning Simulation Model (LCPSIM) provides economic results for the San Felipe Division. In addition, the Other Municipal Water Economics Model (OMWEM) is used to perform economic analysis of other urban regions in the remainder of the CVP IRP Service Area.
- **Agricultural economics** – The SWAP model is used to perform economic analysis in agricultural regions in the Central Valley.
- **Water temperature** – The Sacramento River Water Quality Model (SRWQM) and San Joaquin River Water Quality Model (SJRWQM) are used to perform temperature analysis on rivers in the Sacramento and San Joaquin Valleys.
- **Hydro-power and GHGs** – LongTermGen (LTGen) and State Water Project Power (SWP Power) models are used to perform power generation and use analyses for the CVP and SWP systems. These models were enhanced to estimate the GHG emission changes associated with the CVP and SWP pumping and power facilities.

Each of these tools was used to simulate three selected socioeconomic-climate scenarios for the Baseline and alternative CP5 conditions. These three scenarios were selected to reflect a broad range of potential future uncertainties:

- Current Trends with median temperature change and median precipitation future climate (CT-Q5)
- Expansive Growth with higher temperature and lower precipitation than the CT-Q5 scenario (EG-Q2)
- Slow Growth with lower temperature and higher precipitation than the CT-Q5 scenario (SG-Q4)

The following sections provide a brief overview of each of the additional performance assessment tools.

Economic Models

Least Cost Planning Simulation Model LCPSIM is an annual time-step urban water service system reliability management model (DWR 2009a). Its objective is to estimate the least-cost water supply management strategy for an area, given the mix of available supplies. The model uses a shortage loss function derived from contingent valuation studies and water agency shortage allocation strategies. It accounts for the ability of shortage management (contingency) measures, including water transfers, to reduce regional costs and losses associated with shortage events. It also considers long-term regional demand reduction and supply augmentation measures in conjunction with regional carryover storage opportunities that can reduce the frequency, magnitude, and duration of those shortage events.

A shortage event, or foregone use, is the most direct consequence of water supply unreliability. Foregone use occurs when, for example, residential users or businesses have established a lifestyle or a level of economic production based on expected availability of water that is not met in a particular year or sequence of years.

Assuming that long-term supply augmentation measures are adopted in order of their cost, with lowest cost measures adopted first, LCPSIM finds the water management strategy that minimizes the sum of the total annual cost of the adopted long-term measures and the total expected annual shortage costs and losses remaining after their adoption. The value of the availability of a supply from a proposed project of future condition, can be determined from the change it produces in this least-cost mix of supply measures and shortages.

The LCPSIM, San Francisco Bay - South model was updated for the CVP IRP for three development scenarios at the 2025, 2055, and 2084 levels of development. Model preparation primarily involved updating model parameters with available population and water portfolio information from Reclamation and DWR's Water Plan Update (2009b). Parameters pertinent to the level of development not available from the Water Plan Update (2009b) were estimated using the existing 2025 and 2055 models. Model preparation also included any necessary adjustment to the model analysis period to accommodate CVP IRP CalLite model outputs.

Other Municipal Water Economics Model (OMWEM) Several M&I water providers are not covered by LCPSIM. A set of individual spreadsheet models, collectively called OMWEM, is used to estimate economic benefits of changes in SWP or CVP supplies for potentially affected M&I water providers outside the San Francisco Bay – South region. The model includes CVP M&I supplies north of Delta, SWP and CVP supplies to the Central Valley and the Central Coast, SWP supplies or supply exchanges to the desert regions east of the South Coast hydrological region, and American River contractors. The model estimates the economic value of M&I supply changes in these areas as the change in cost of shortages and alternative supplies (such as groundwater pumping or transfers).

Data available from 2010 Urban Water Management Plans were used to estimate 2025 water demand and supplies for an average condition and a dry condition, and to identify additional water supply options and their costs. Water demand estimates for 2055 and 2084, at the three development scenarios, are based on population projections developed by the CVP IRP. For each level of development and development scenario OMWEM uses project water supplies to match supply to demand. If supply is insufficient to meet demand in years categorized as below normal water supply or greater, the model calculates the cost of additional water supplies.

South Bay Water Quality Model (SBWQM) SBWQM is used by the CVP IRP to perform M&I salinity assessment for the portion of the San Francisco Bay Area region from Contra Costa County in the North to Santa Clara County in the South. The model was originally developed and used for the economic evaluation of a proposed expansion of Los Vaqueros Reservoir (Reclamation 2006). It uses estimated relationships between salinity and damages to residential appliances and fixtures to estimate the benefits from changes in salinity. Specific model outputs compare change in average salinity and change in annual salinity costs.

The model inputs include project water supply and chloride concentrations in mg/L from CalLite. Separate calculations were provided for Contra Costa Water District and agencies that use the South Bay Aqueduct. For Contra Costa Water District, water quality estimates were based on diversion volume and water quality at Old River and Rock Slough. For the other areas, water quality is based on diversion volume and salinity at Banks Pumping Plant. Changes in water quality at the City of Antioch's diversion were used to estimate additional cost of treatment or replacement supply.

The SBWQM was updated for three development scenarios at three levels of development, 2025, 2055, and 2084. Model preparation involved updating available population and water portfolio information from Reclamation and DWR's Water Plan Update (2009b).

Statewide Agricultural Production Model The SWAP model is a regional model of irrigated agricultural production and economics that simulates the decisions of agricultural producers (farmers) in California (Howitt et al. 2012). Its data coverage is most detailed in the Central Valley, but it also includes production regions in the Central Coast, South Coast, and desert areas. The model assumes that farmers maximize profit subject to resource, technical, and market constraints. Farmers sell and buy in competitive markets, and no one farmer can affect or control the price of any commodity. The model selects those crops, water supplies, and other inputs that maximize profit subject to constraints on water and land, and subject to economic conditions regarding prices, yields, and costs.

SWAP incorporates project water supplies (SWP and CVP), other local water supplies, and groundwater. As conditions change within a SWAP region (e.g., the quantity of available project water supply increases or the cost of groundwater pumping increases), the model optimizes production by adjusting the crop mix, water sources and quantities used, and other inputs. It also fallows land when that appears to be the most cost-effective response to resource conditions.

The SWAP model covers 27 agricultural subregions in the Central Valley that are analyzed by the CVP IRP. The SWAP model is used to compare the short or long-run response of agriculture to potential changes in SWP and CVP irrigation water delivery, other surface or groundwater conditions, or other economic values or restrictions. Results from the CVP IRP CalLite model are used as inputs into SWAP through a standardized data linkage tool. Groundwater analysis is used to develop assumptions, estimates, and, if appropriate, restrictions on pumping rates and pumping lifts for use in SWAP. Model output includes intensive and extensive margin production response by agriculture, input use per acre and aggregate input use, respectively.

Water Temperature Models SRWQM and SJRWQM were developed by Reclamation to simulate temperature in the upstream CVP reservoirs and river on the upper Sacramento River system and on the San Joaquin River system. A more detailed description of SRWQM and the calibration performance is included in the calibration report (RMA, 2003). The models were developed using integrated HEC-5 and HEC-5Q models. SRWQM simulates mean daily reservoir and river temperatures at Shasta, Trinity, Lewiston, Whiskeytown, Keswick and Black Butte Reservoirs and the Trinity River, Clear Creek, the upper Sacramento River from Shasta to Knights Landing, and Stony Creek based on the flow and meteorological parameters on a 6-hour time step. SJRWQM simulates mean daily reservoir and river temperatures at on all major tributaries and reservoirs in the San Joaquin River system upstream from Vernalis based on flow and meteorological parameters on a 6-hour time step.

Hydropower and GHG Models The hydro-power analysis uses spreadsheet post-processors that evaluate the power impacts of flow scenarios from CalSim-II operations studies on a monthly time step. The following post-processor tools are used in the analysis:

- LTGen: analyzes CVP facilities
- SWP_Power: analyzes SWP facilities

The tools estimate average annual energy generation and use at SWP and CVP facilities. For generation facilities, the tools estimate average annual energy generation as well as average annual peaking power capacity. For pumping facilities, the tools estimate average annual energy requirements. The tools also check to determine whether off-peak energy use targets are being met. Transmission losses are estimated for both pumping and generation facilities.

For the CVP IRP, LTGen and SWP_Power have been enhanced to estimate net GHG emissions that are related to energy use at the major project facilities so that a "relative" carbon footprint can be evaluated for each new water management scenario. The net GHG emissions are used as an additional performance metric in the CVP IRP analysis.

Climate Change Assessment Results

Performance Metrics

Performance metrics provide a common technical basis for analyzing the effects of socioeconomic-climate uncertainties. For the SLWRI, these analyses were performed the Baseline and CP5 using performance metrics related to water supply and demand, water quality (salinity and temperature), hydro-power, GHGs, socioeconomics, and ecological resources. These metrics were quantified using the outputs of the CVP IRP modeling tools for the Baseline and CP5 as described in the sections below.

Baseline Condition – Climate Change Impacts Analysis

The CVP IRP model package was used to quantify the imbalance between supply and demand in each of the CVP Divisions and to generate other performance metrics for Baseline Conditions across the range of future scenarios. The Modeling Appendix to the DEIS presents the Baseline assumptions used for the SLWRI model simulations. The Baseline assumptions reflect the requirements of the 2008 Fish and Wildlife Service and 2009 National Marine Fisheries Service Biological Opinions, along with other assumptions related to demands, water rights, facilities, regulatory standards, and operations criteria of the SWP and CVP systems. The CVP IRP CalLite model assumptions have minor differences as compared to those used in CalSim-II for the SLWRI program primarily due to the simplification inherent in the CVP IRP CalLite implementation.

Baseline system results have been developed for the following performance metric categories for each of the 18 socioeconomic-climate scenarios:

- Water Supplies
- Applied Water Demands
- CVP and SWP System Operations
- Supplies and Demands in CVP Divisions

- Results of Other Performance-Assessment Tools

These are described in the sections below.

Water Supplies

Figure 3-24 through 3-27 show the average annual runoff in the Sacramento River system upstream from Hood, the Eastside Streams and the Delta, San Joaquin River system upstream from Vernalis, and Tulare Lake region for each of the six projected climate scenarios for the period of water years from 2012 through 2099. As can be observed, there is very little difference in water supplies between the different socioeconomic scenarios (CT, EG and SG). However, there are substantial differences in runoff among the different climate scenarios. Under the no climate change condition, average annual runoff is about 20.5 million acre-feet (MAF)/year in the Sacramento River system, 1.3 MAF/year in the Eastside Streams and Delta, 6.7 MAF/year in the San Joaquin River system, and 3.4 MAF/year in the Tulare Lake region, for a total average annual runoff of 31.9 MAF/year. In the median climate scenario (Q5), average annual runoff in each region is only slightly less than the no climate change (No_CC) condition. However, the drier climate scenarios (Q1 and Q2) have average annual runoff that is substantially lower (ranging from 19-26 percent) than the no climate change scenario, while the wetter climate scenarios (Q3 and Q4) have average annual runoff that is substantially higher (ranging from 16-22 percent) than the no climate change scenario. Overall, average annual runoff for the entire water system ranges from a low of about 23.7 MAF/year in Q2 to a high of about 39.0 MAF/year in Q4 (a difference of about 64 percent).

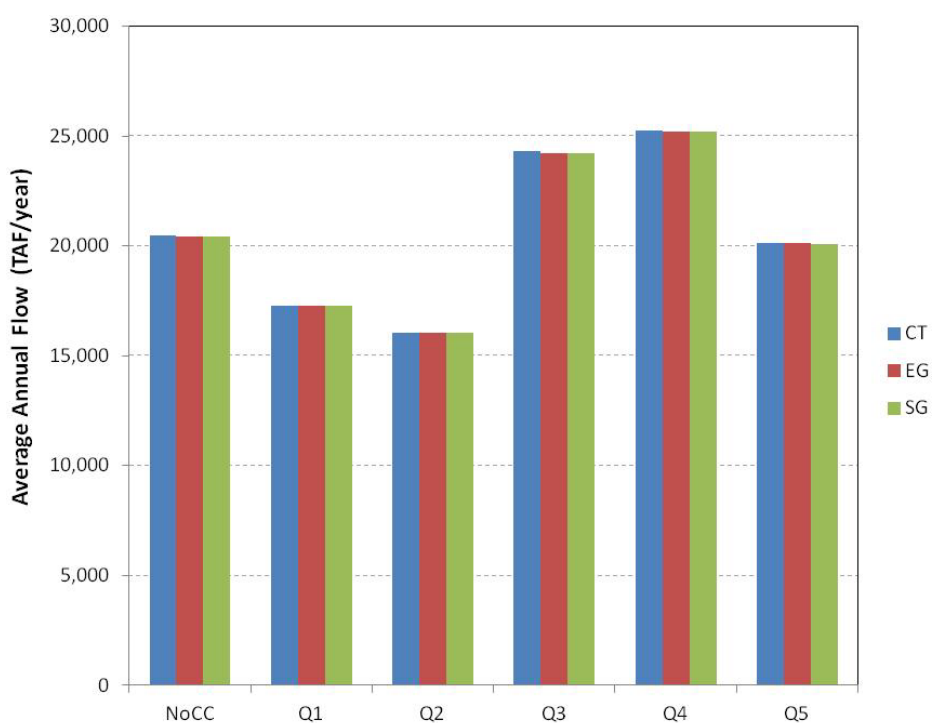

Figure 3-24. Average Annual Runoff in the Sacramento River System in each Scenario

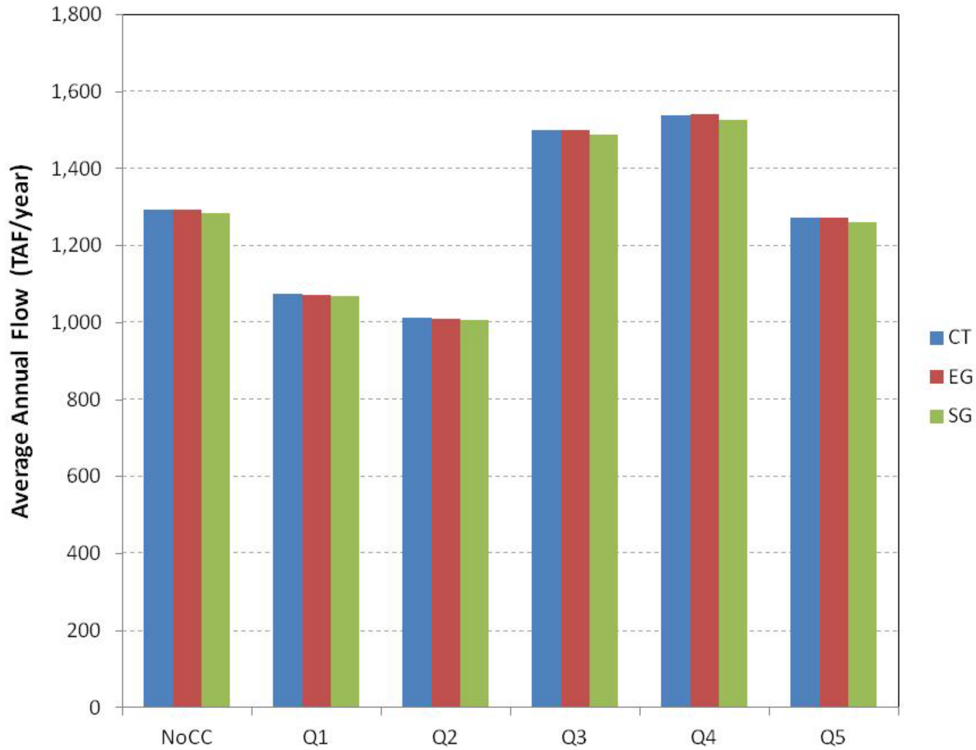

Figure 3-25. Average Annual Runoff in the Eastside Streams and Delta in each Scenario

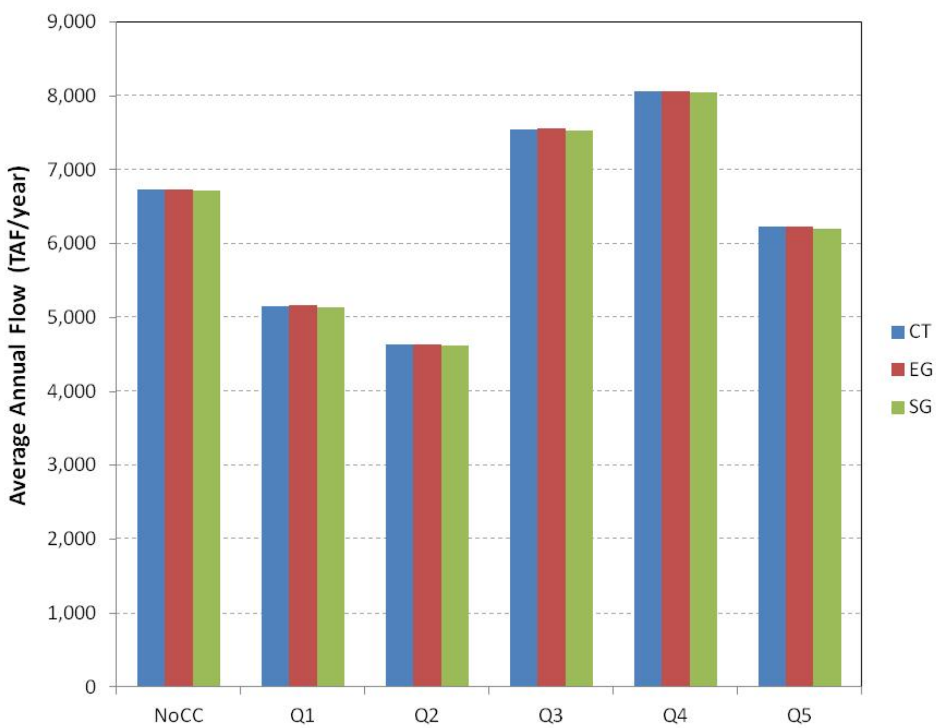

Figure 3-26. Average Annual Runoff in the San Joaquin River System in each Scenario

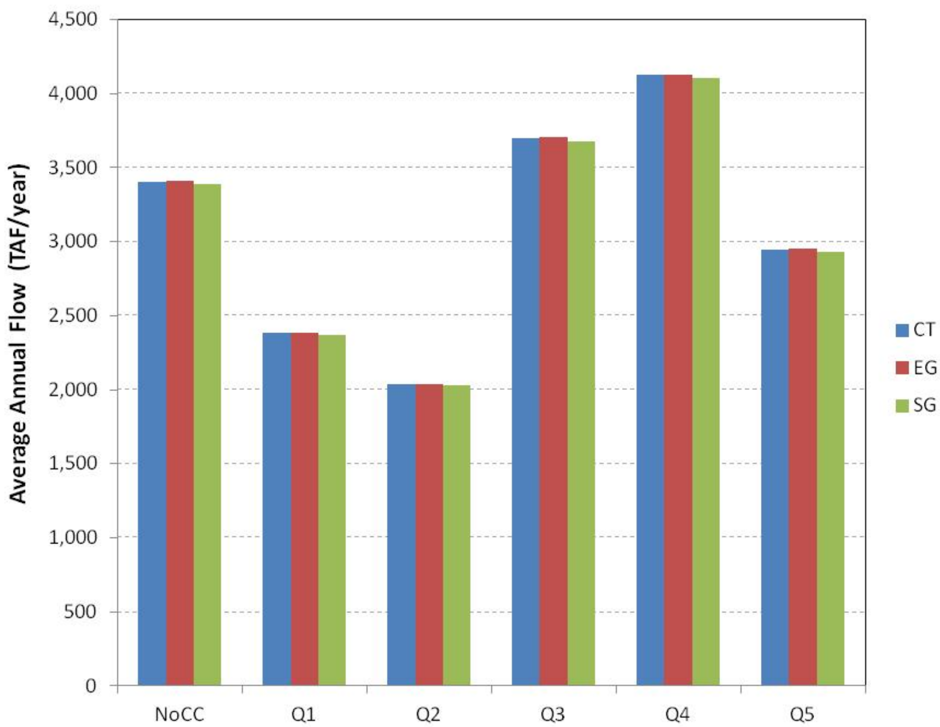

Figure 3-27. Average Annual Runoff in the Tulare Lake Region in each Scenario

Figure 3-28 through Figure 3-31 show the average runoff in each month in the Sacramento River system, the Eastside Streams and the Delta, San Joaquin River system, and Tulare Lake region in each CT scenario for the period of water years 2012 through 2099. Figure 3-32 through Figure 3-36 show the same information for the inflows into each of the major CVP and SWP reservoirs. Each basin has a different monthly pattern reflecting the precipitation-runoff characteristics of the basin. In each basin, the climate scenarios exhibit a similar pattern to the no climate change scenario but with a shift in runoff from the spring months to the winter months, which results from the occurrence of higher temperatures during winter in all the climate projections causing earlier snowmelt runoff. This seasonal shift is greater in basins where the elevation of the historic snowpack area is lower and therefore more effected by warming induced changes of precipitation from snow to rain.

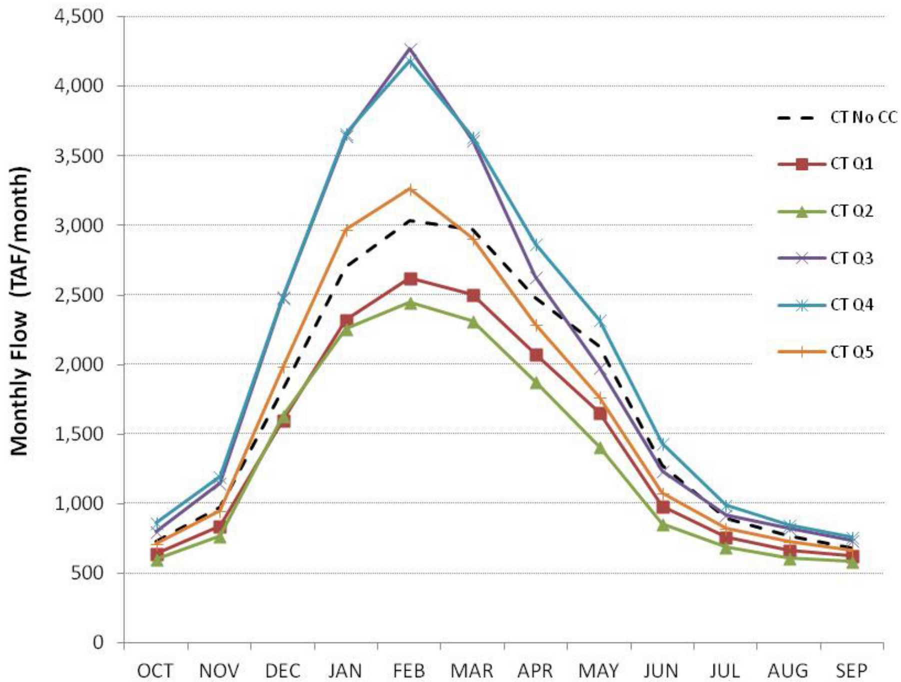

Figure 3-28. Average Runoff in each Month in the Sacramento River System in each Climate Scenario

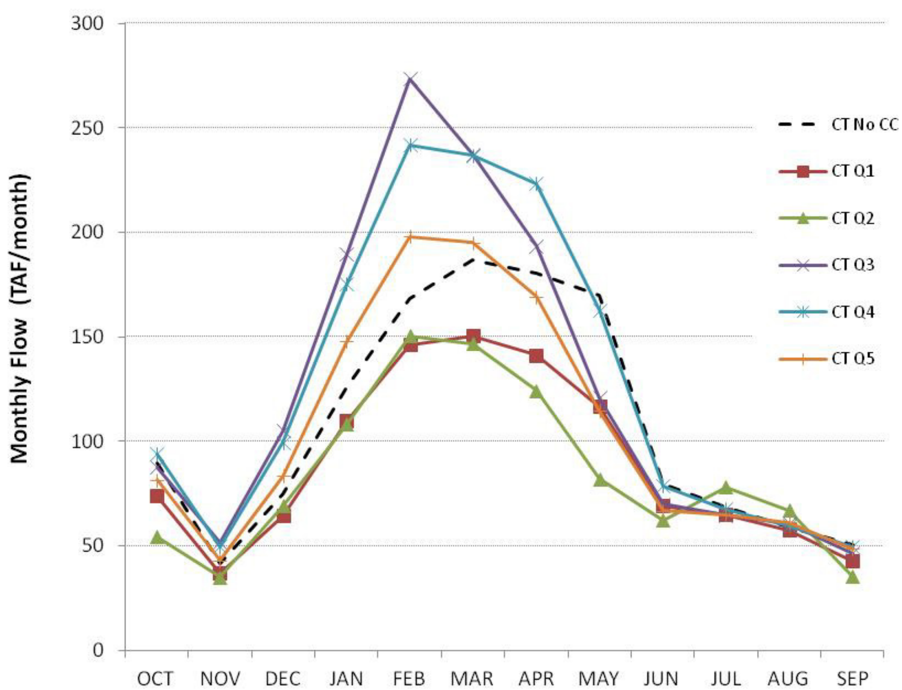

Figure 3-29. Average Runoff in each Month in the Eastside Streams and Delta in each Climate Scenario

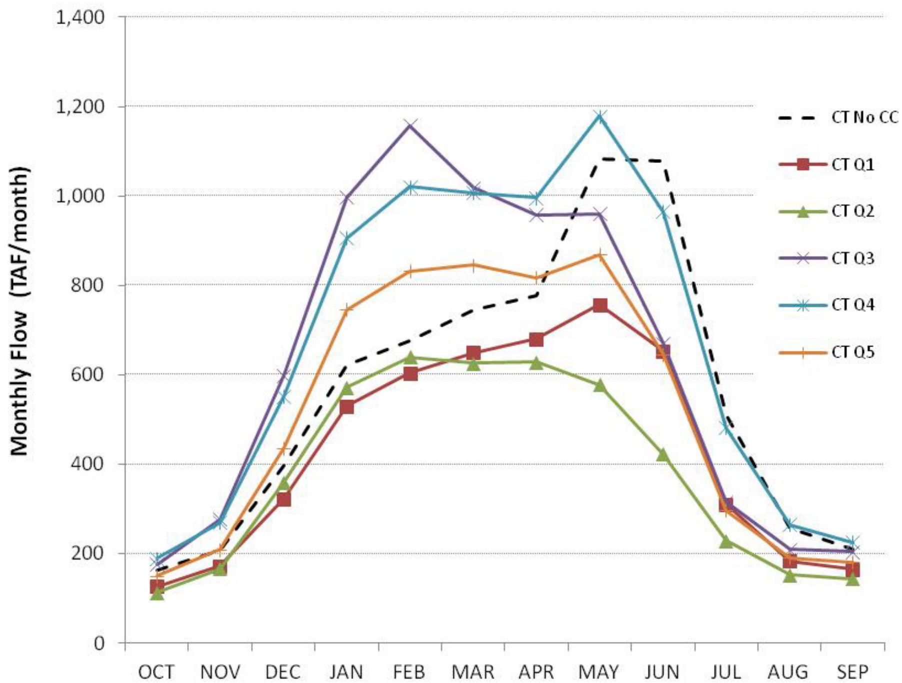

Figure 3-30. Average Runoff in each Month in the San Joaquin River System in each Climate Scenario

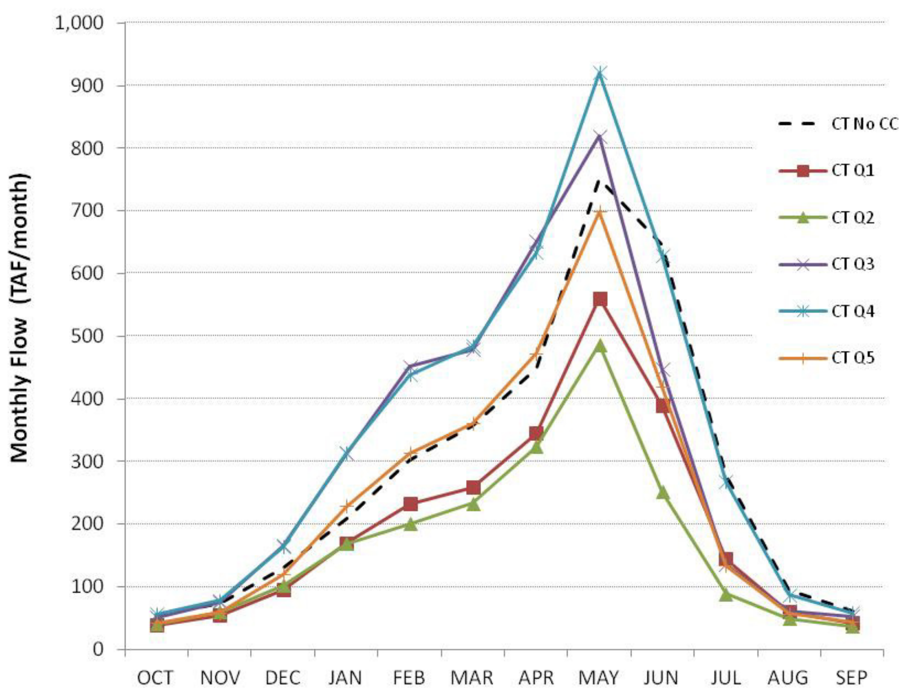

Figure 3-31. Average Runoff in each Month in the Tulare Lake Region in each Climate Scenario

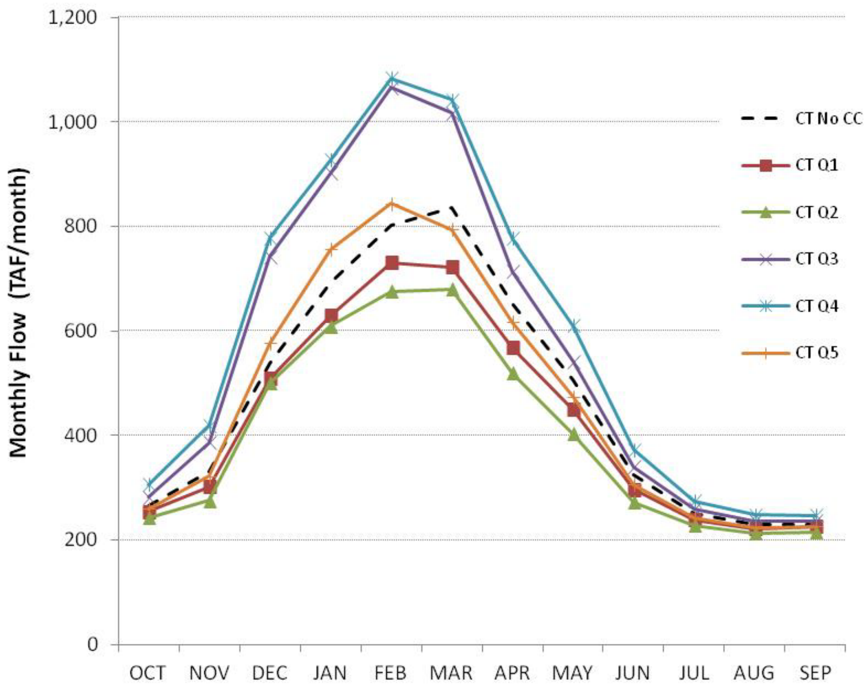

Figure 3-32. Average Runoff in each Month into Lake Shasta in each Climate Scenario

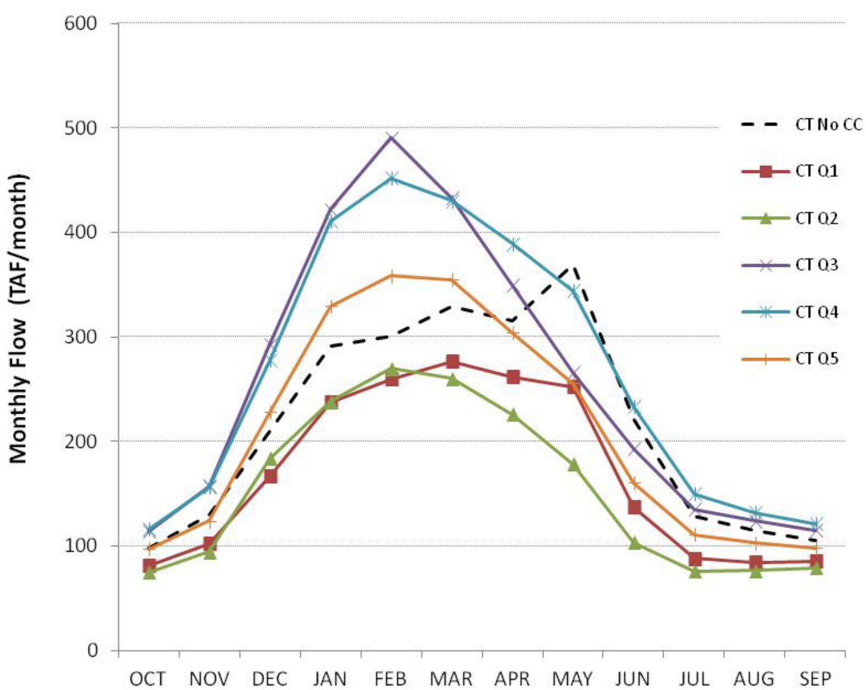

Figure 3-33. Average Runoff in each Month into Folsom Lake in each Climate Scenario

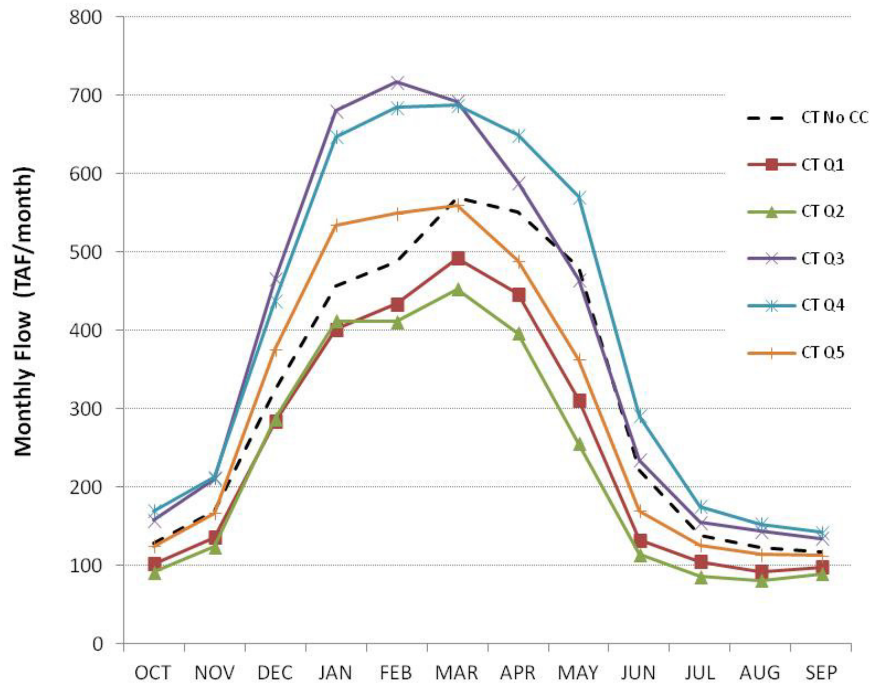

Figure 3-34. Average Runoff in each Month into Lake Oroville in each Climate Scenario

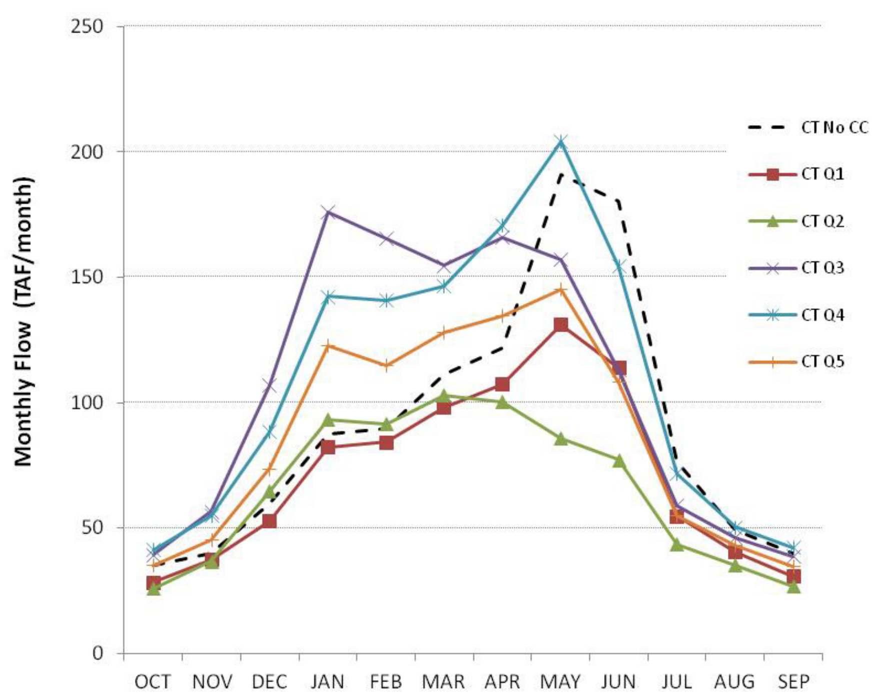

Figure 3-35. Average Runoff in each Month into New Melones Reservoir in each Climate Scenario

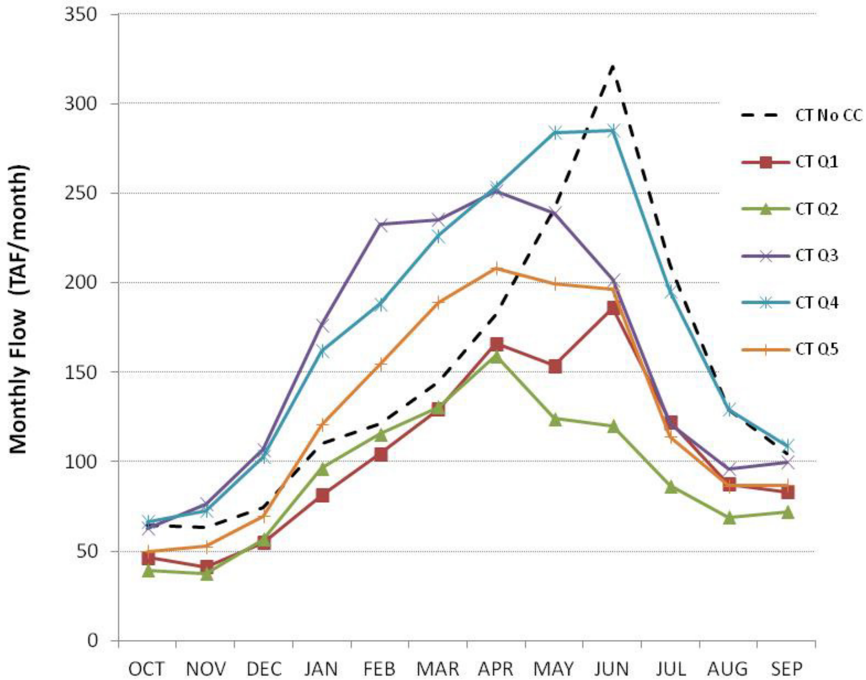

Figure 3-36. Average Runoff in each Month into Millerton Lake in each Climate Scenario

Figure 3-37 through Figure 3-40 show the annual time series of runoff in the Sacramento River system, the Eastside Streams and the Delta, San Joaquin River system, and Tulare Lake regions under each of Current Trends scenarios during the period from 2012 through 2099. The future time series reflect the same inter-annual variability as the historical period because of the methodology used in developing the projections, with extended drought periods with lower runoff values from 2025-2030 (corresponding to 1929-1934 dry period) and from 2083-2088 (corresponding to 1987-1992 drought), and a very substantial dry period from 2072-2073 (corresponding to 1976-1977 minimum precipitation years). However, as can be observed in the figures, the magnitude of the events is different than the historical conditions.

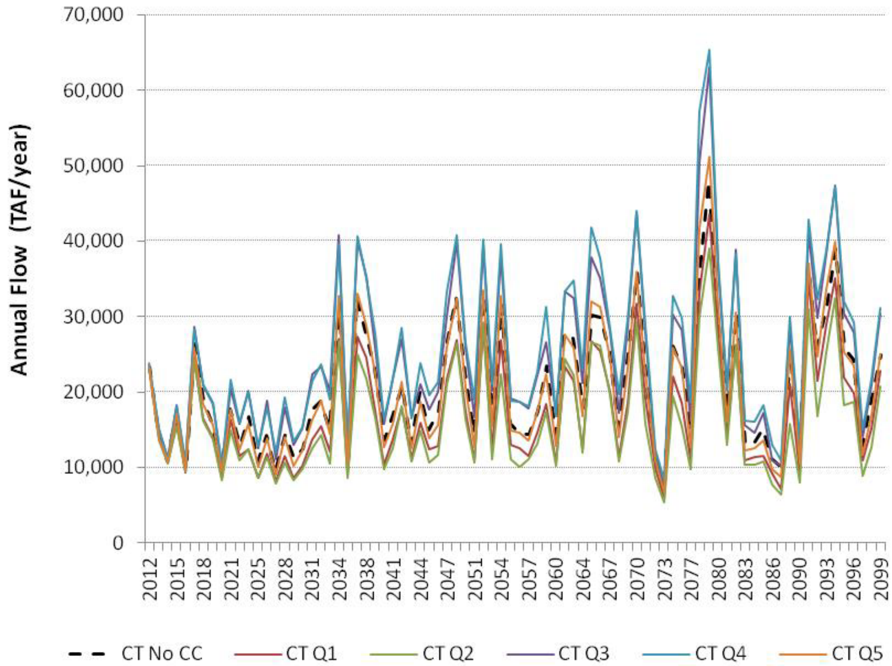

Figure 3-37. Annual Time Series of Runoff in the Sacramento River System in each Climate Scenario

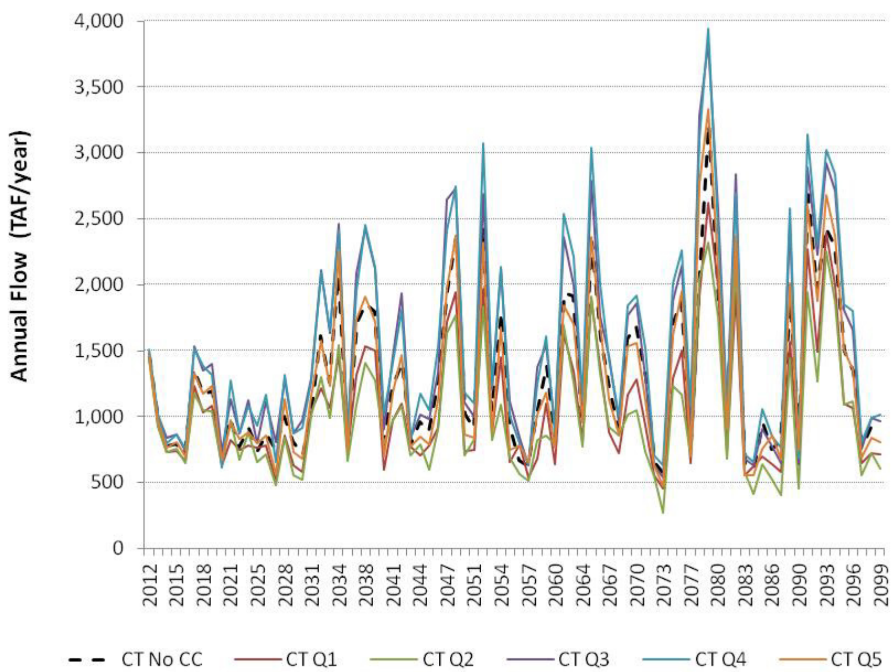

Figure 3-38. Annual Time Series of Runoff in the Eastside Streams and Delta in each Climate Scenario

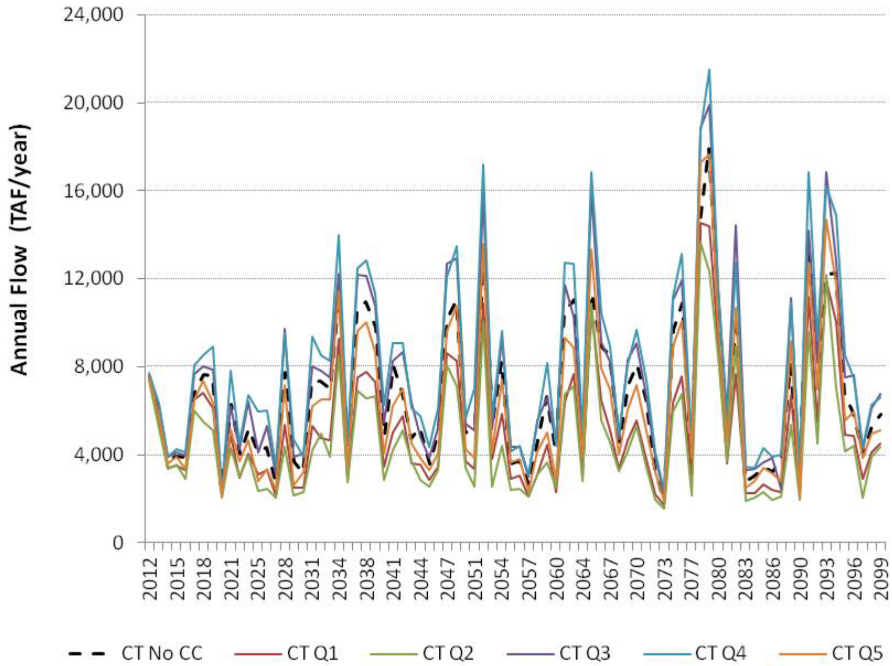

Figure 3-39. Annual Time Series of Runoff in the San Joaquin River System in each Climate Scenario

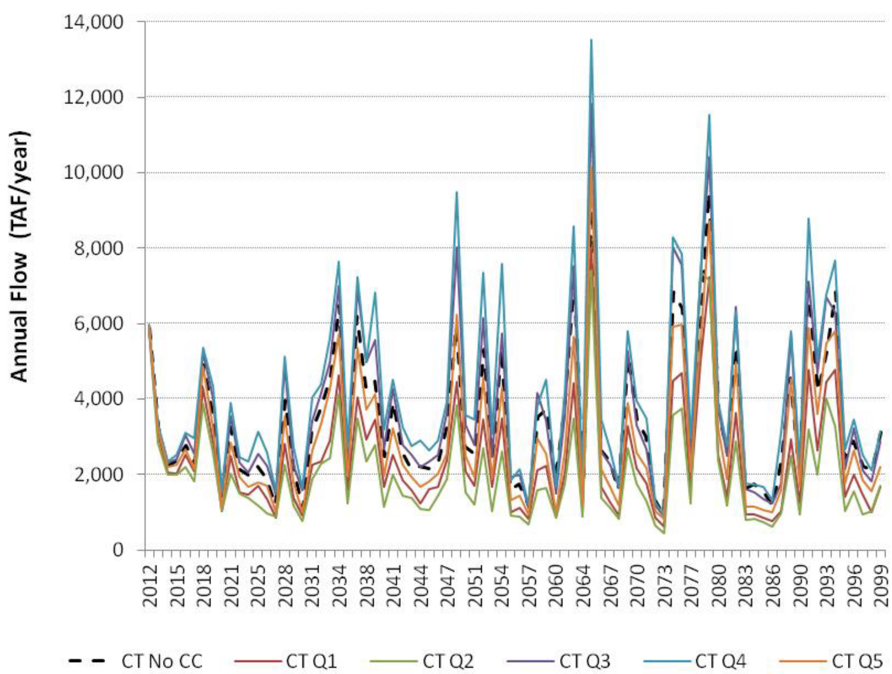

Figure 3-40. Annual Time Series of Runoff in the Tulare Lake Region in each Climate Scenario

Applied Water Demands

Figure 3-41 through Figure 3-48 show the average annual agricultural and urban applied water demands for the CVP, SWP and non-project water users in the Sacramento River system, the Eastside Streams and the Delta, San Joaquin River system, and Tulare Lake region for each of the socioeconomic-climate scenarios over the projected period of water years from 2012 through 2099. Under the no climate change condition, average total average annual demand is about 5.5-5.7 MAF/year in the Sacramento River system, 1.4 MAF/year in the Eastside Streams and Delta, 5.8-6.5 MAF/year in the San Joaquin River system, and 14.7-16.3 MAF/year in the Tulare Lake region.

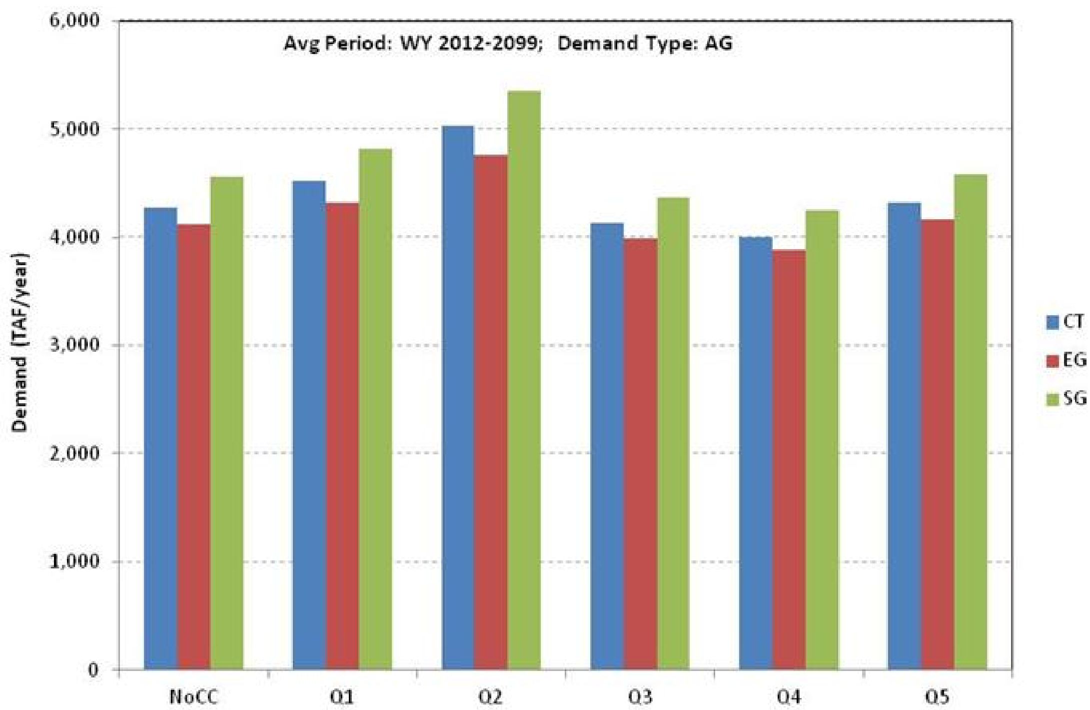

Figure 3-41. Average Annual Agricultural Applied Water Demand in the Sacramento River System in each Scenario

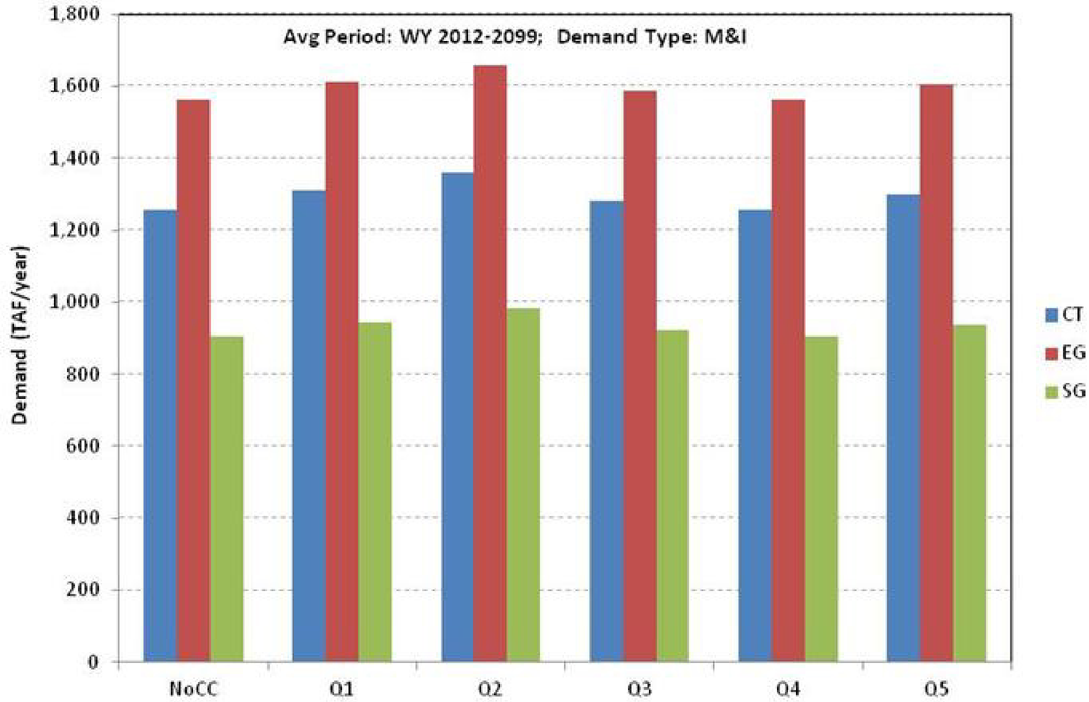

Figure 3-42. Average Annual Urban Applied Water Demand in the Sacramento River System in each Scenario

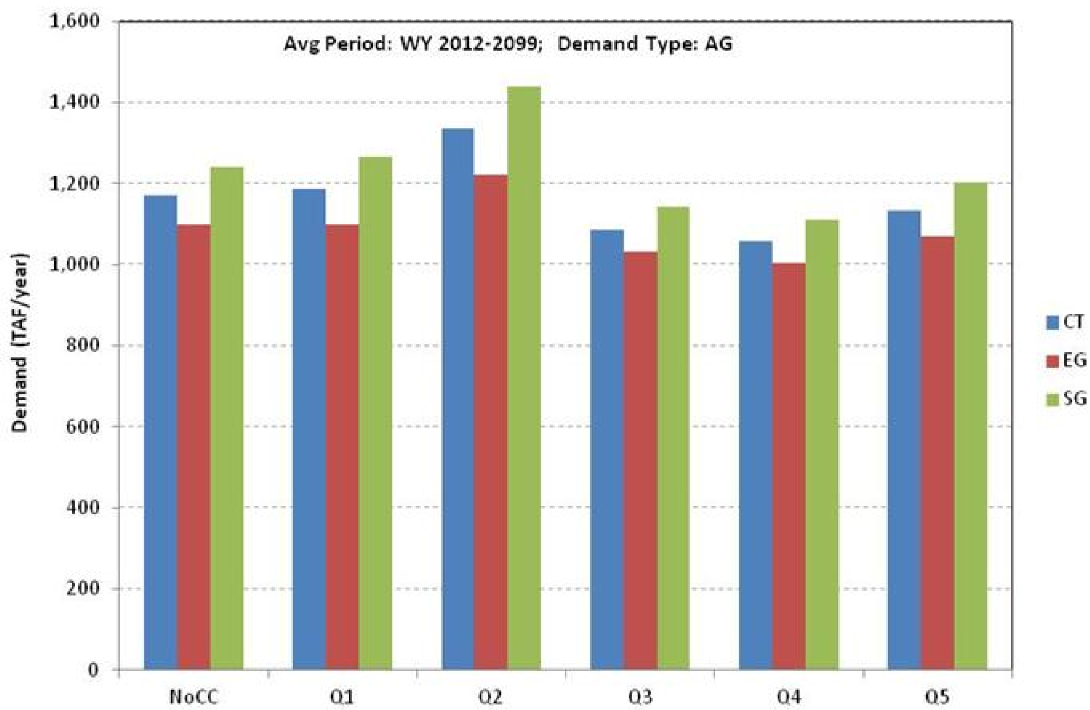

Figure 3-43. Average Annual Agricultural Applied Water Demand in the Eastside Streams and Delta in each Scenario

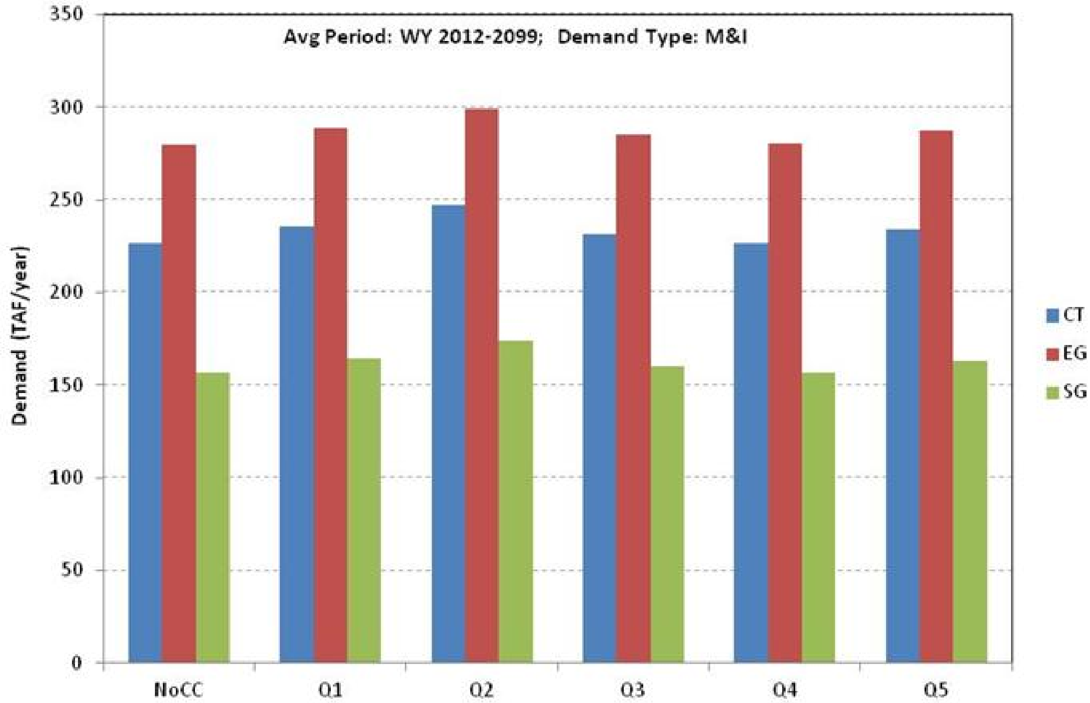

Figure 3-44. Average Annual Urban Applied Water Demand in the Eastside Streams and Delta in each Scenario

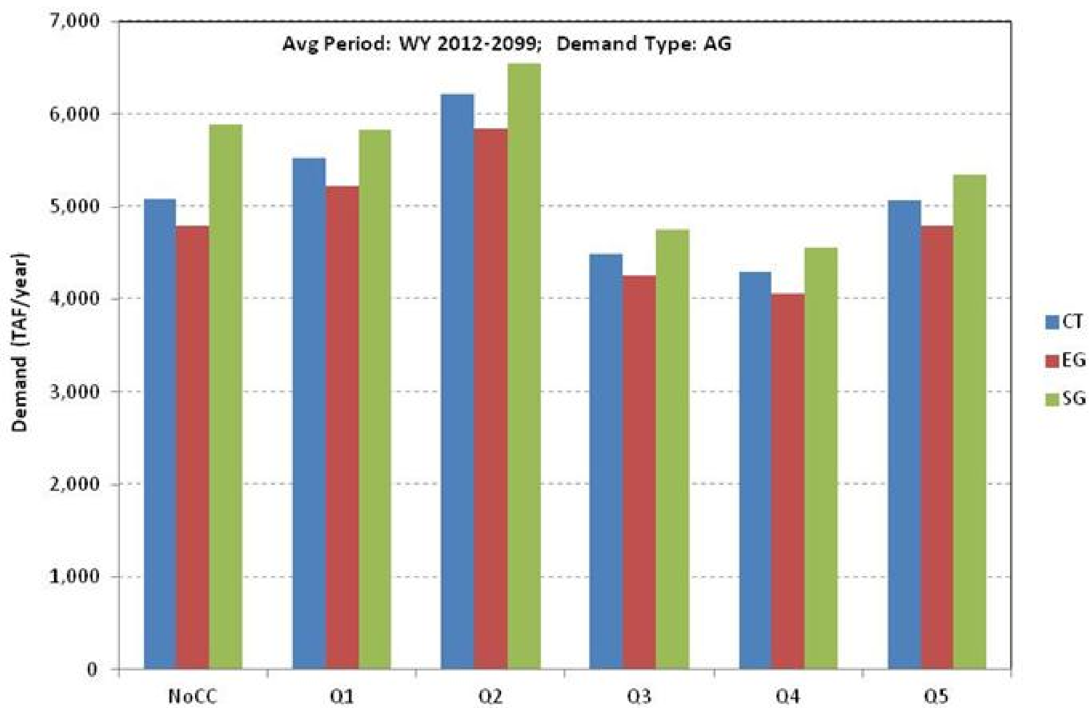

Figure 3-45. Average Annual Agricultural Applied Water Demand in the San Joaquin River System in each Scenario

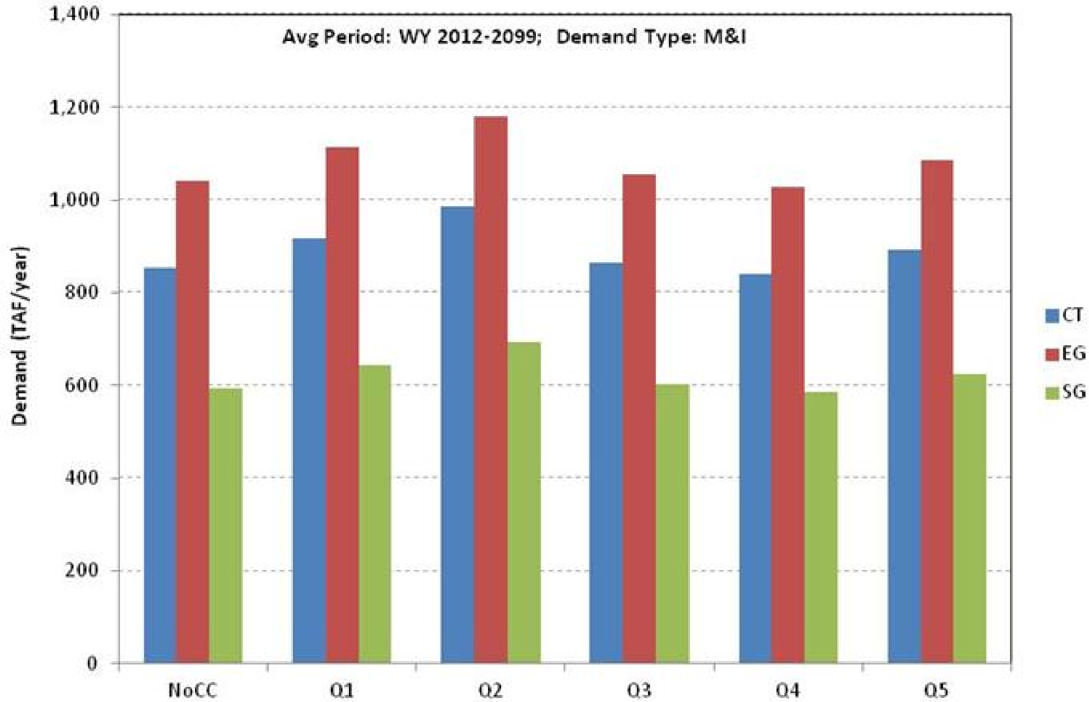

Figure 3-46. Average Annual Urban Applied Water Demand in the San Joaquin River System in each Scenario

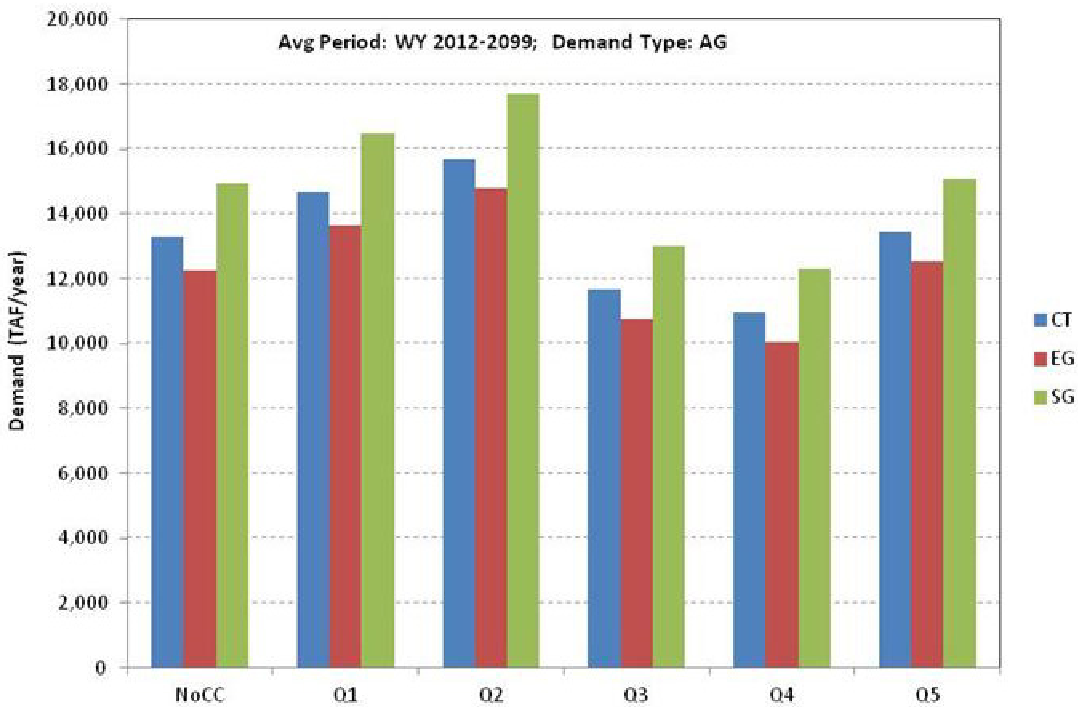

Figure 3-47. Average Annual Agricultural Applied Water Demand in the Tulare Lake Region in each Scenario

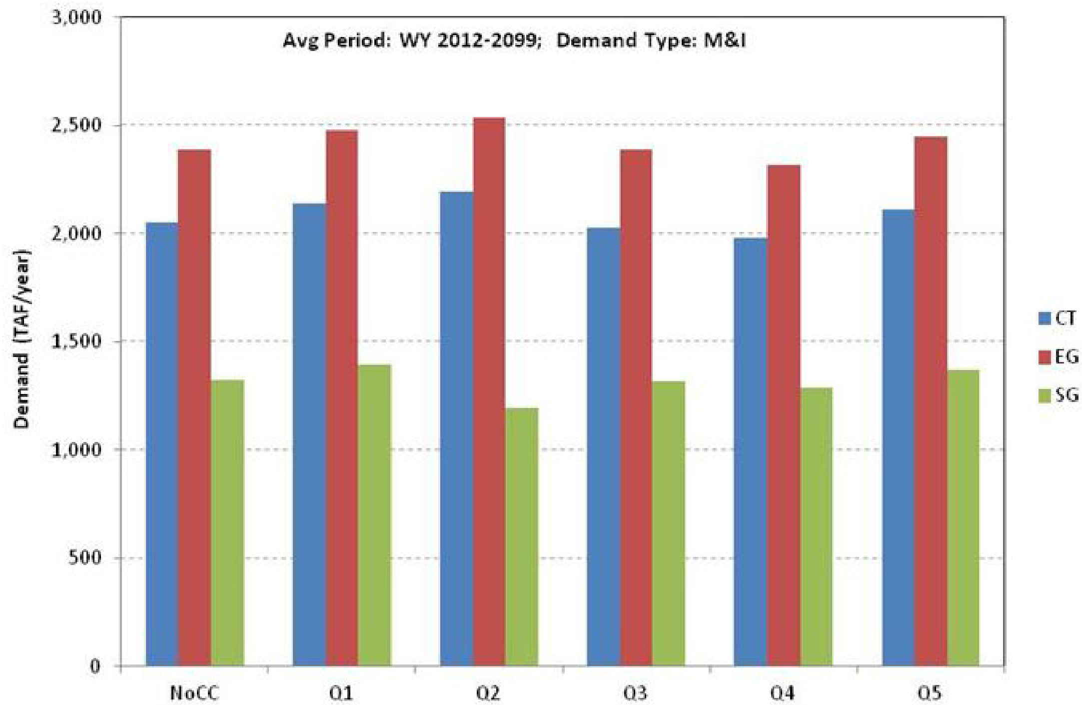

Figure 3-48. Average Annual Urban Applied Water Demand in the Tulare Lake Region in each Scenario

Total agricultural and urban water demands (including CVP, SWP and non-project) vary across both the range of socioeconomic scenarios and across the range of climate scenarios. In all the basins, agricultural demands show a strong relationship with the climate scenarios. Although the magnitudes differ between basins because of differences in crops and acreages, the overall relationship between precipitation and agricultural demand is similar in all the basins. While the median climate scenarios (Q5), have demands that are similar to the no climate change scenario, the drier climate scenarios (Q1 and Q2) have average demands that are higher than the no climate change scenario (ranging from 7-17 percent), while the wetter climate scenarios (Q3 and Q4) have average demands that are less than the no climate change scenario (ranging from 9-13 percent). Among the socioeconomic scenarios, the Expansive Growth scenario has lower agricultural demands than the Current Trends scenario because the assumed rate of urban expansion into agricultural lands is greater. Conversely, the Slow Growth scenario has higher agricultural demands than the Current Trends scenario because of the lesser amount of agricultural to urban land conversion.

In the Sacramento River system, the overall average agricultural demand change including all the socioeconomic scenarios relative to their corresponding no climate change scenarios is about 0-1 percent for the central tendency (Q5) and ranges from –3-7 percent in the wetter Q3 and Q4 scenarios to +5-18 percent in the drier Q1 and Q2 scenarios. In the Eastside Streams and Delta system, the overall average agricultural demand change relative to the no climate change scenario is -3 percent in Q5 and ranges from –6-10 percent in the wetter Q3 and Q4 scenarios to +0-16 percent in the drier Q1 and Q2 scenarios. In the San Joaquin River system, the overall average agricultural demand change relative to the no climate change scenario is -0-9 percent in Q5 and ranges from –11-22 percent in the wetter Q3 and Q4 scenarios to +0-22 percent in the drier Q1 and Q2 scenarios. In the Tulare Lake Region, the overall average agricultural demand change relative to the no climate change scenario is 1-2 percent in Q5 and ranges from –12-18 percent in the wetter Q3 and Q4 scenarios to +10-20 percent in the drier Q1 and Q2 scenarios.

In contrast with agricultural demands, the effect of precipitation variability on urban demands is minimal because it is assumed these demands have a higher delivery priority than agricultural demands. Consequently, the Expansive Growth scenario has the largest urban demands and the Slow Growth scenario the least. Across all climate scenarios and basins, the overall urban demand is about 4.4-4.8 MAF/year the in the Current Trends socioeconomic scenario and ranges from a low of about 2.9-3.1 MAF/year in SG to a high of about 5.2-5.7 MAF/year in EG.

In the Sacramento River system, the overall average urban demand change relative to the corresponding no climate change socioeconomic scenarios is +3-4 percent for the central tendency Q5 scenario and ranges from +0-2 percent in the wetter Q3 and Q4 scenarios to +3-9 percent in the drier Q1 and Q2 scenarios. In the Eastside Streams and Delta system, the overall average urban demand change is +3-4 percent relative to the no climate change scenario in Q5 and ranges from +0-2 percent in the wetter scenarios to +3-11 percent in the drier scenarios. In the San Joaquin River system, the average Q5 urban demand change is +4-5 percent and ranges from –1 percent to +2 percent in the wetter scenarios to +7-17 percent in the drier scenarios. In the Tulare Lake Region, the average Q5 urban demand change is 3-4 percent and ranges from 0 percent to -3 percent in the wetter scenarios to -10 percent to 7 percent in the drier scenarios.

Figure 3-49 through Figure 3-58 show the average annual agricultural and urban demand in each socioeconomic-climate scenario for the total CVP service area and within each CVP Division. Total average annual demands in the CVP service area range from about 10-14 MAF/year across the range of future scenarios. Among the Divisions, the largest demands are in the Friant Division, with total demands of about 4-6 MAF/year across the range of scenarios. The American River and San Felipe Divisions have much higher urban demands than agricultural demands and consequently show the highest total demands in the Expansive Growth scenario and the lowest total demands in the Slow Growth scenarios as the changes in demands are driven primarily by changes in population. The other Divisions have more agricultural demands than urban demands and therefore show little differences in total demands between socioeconomic scenarios, as changes in agricultural demand are offset by corresponding changes in urban demand.

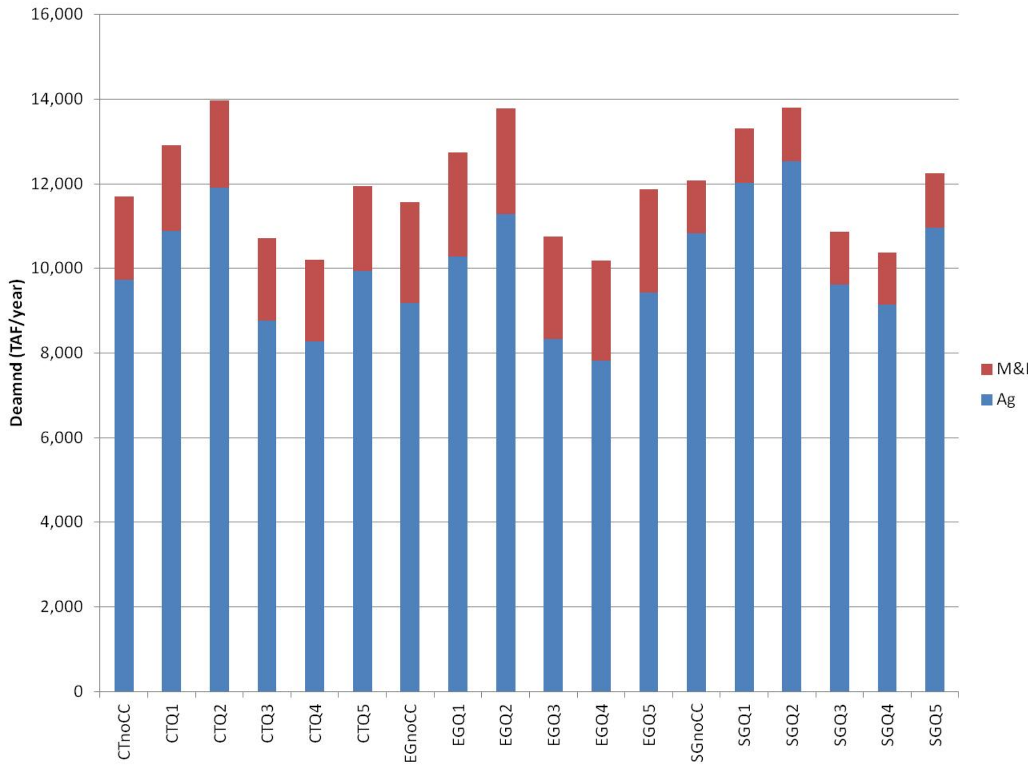

Figure 3-49. Average Annual Agricultural and Urban Demands in the CVP Service Area

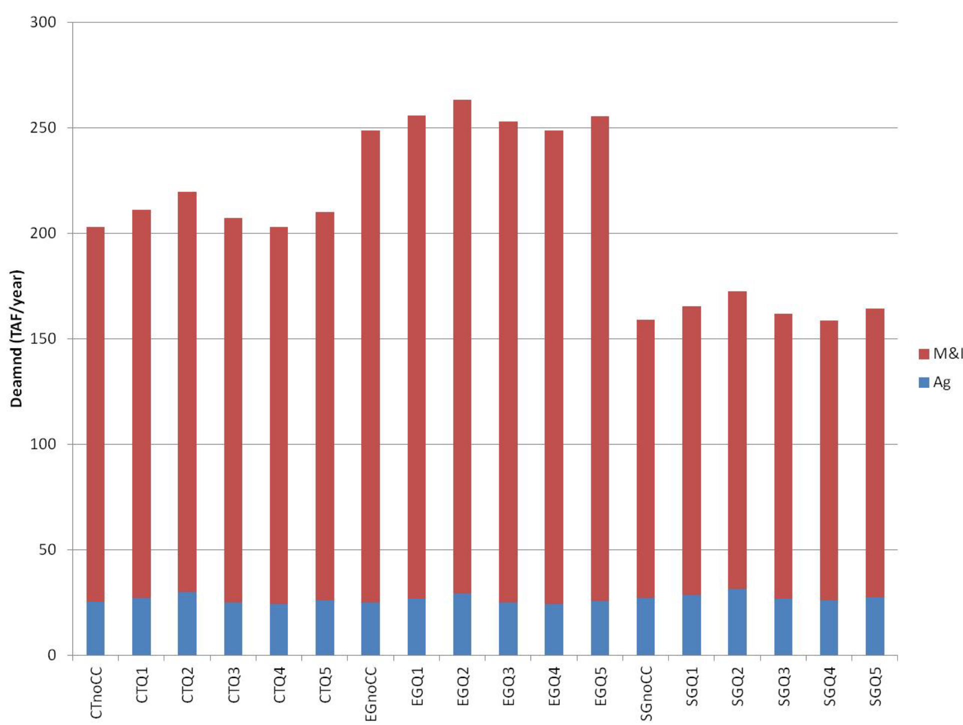

Figure 3-50. Average Annual Agricultural and Urban Demands in the American River Division

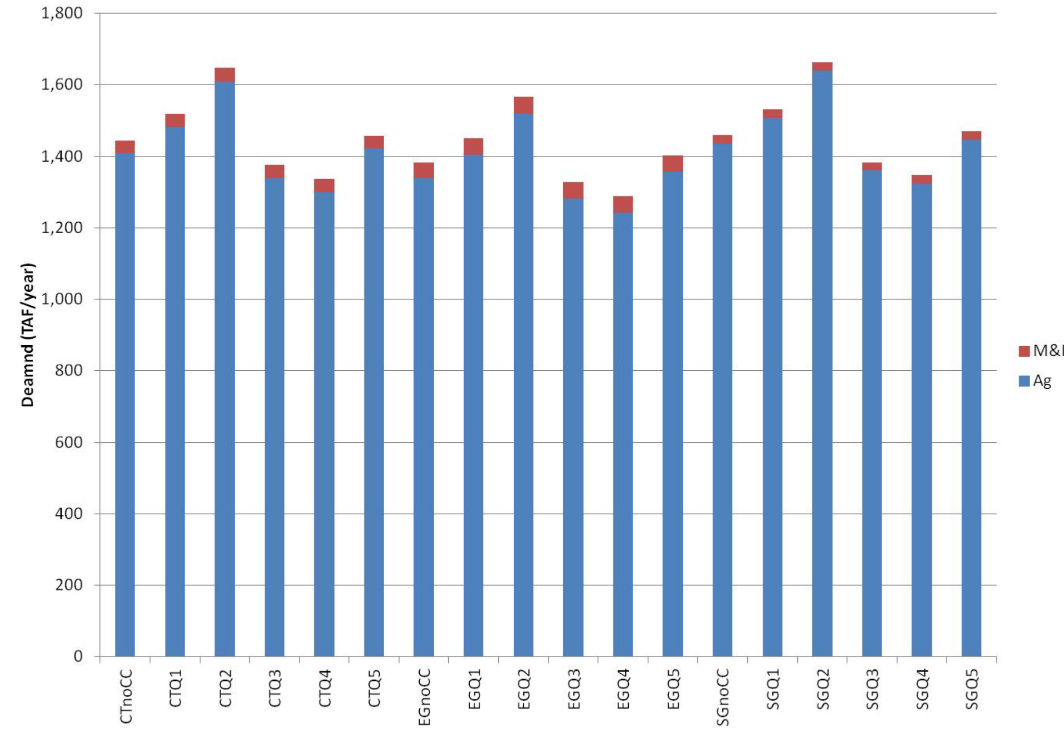

Figure 3-51. Average Annual Agricultural and Urban Demands in the Delta Division

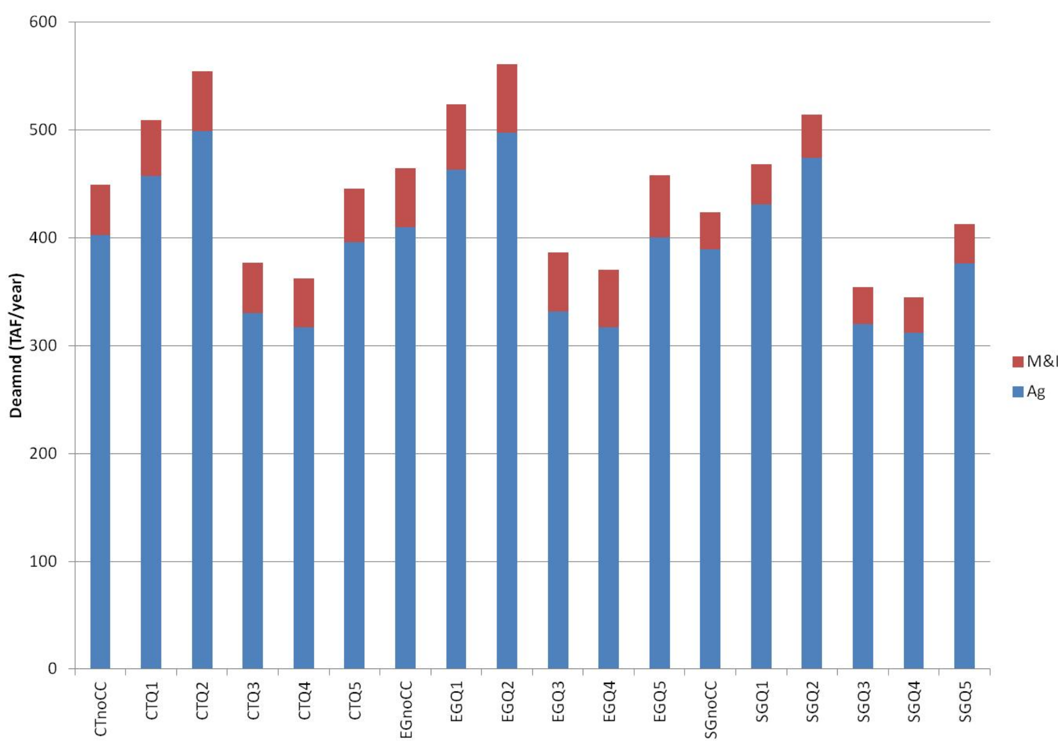

Figure 3-52. Average Annual Agricultural and Urban Demands in the Eastside Division

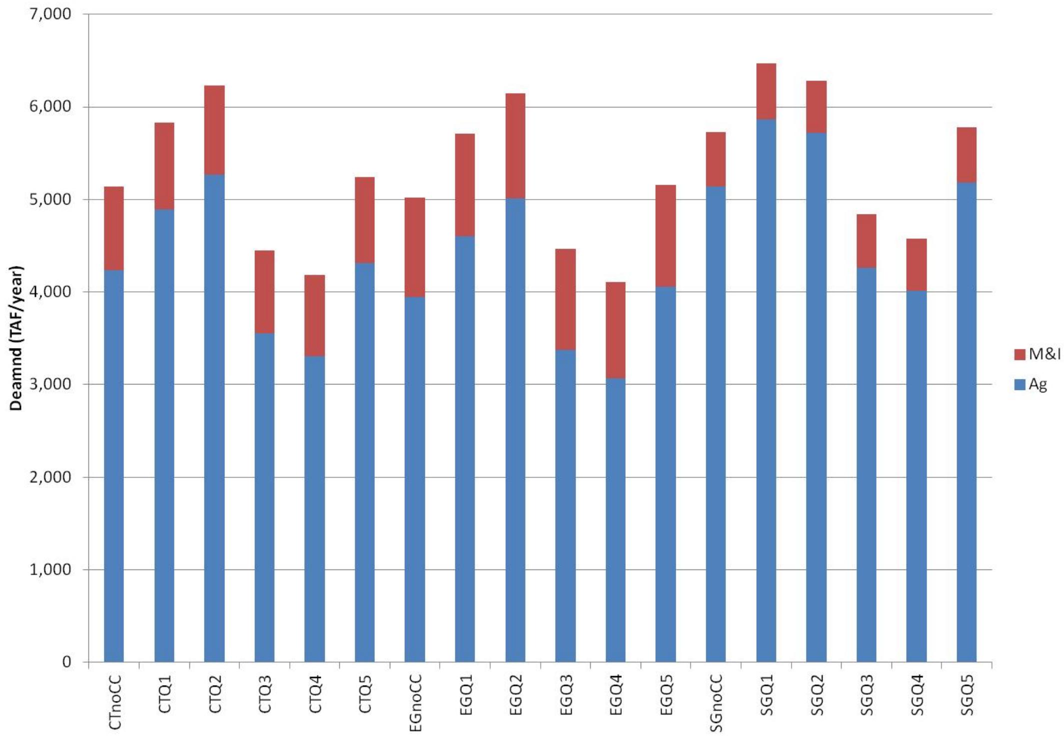

Figure 3-53. Average Annual Agricultural and Urban Demands in the Friant Division

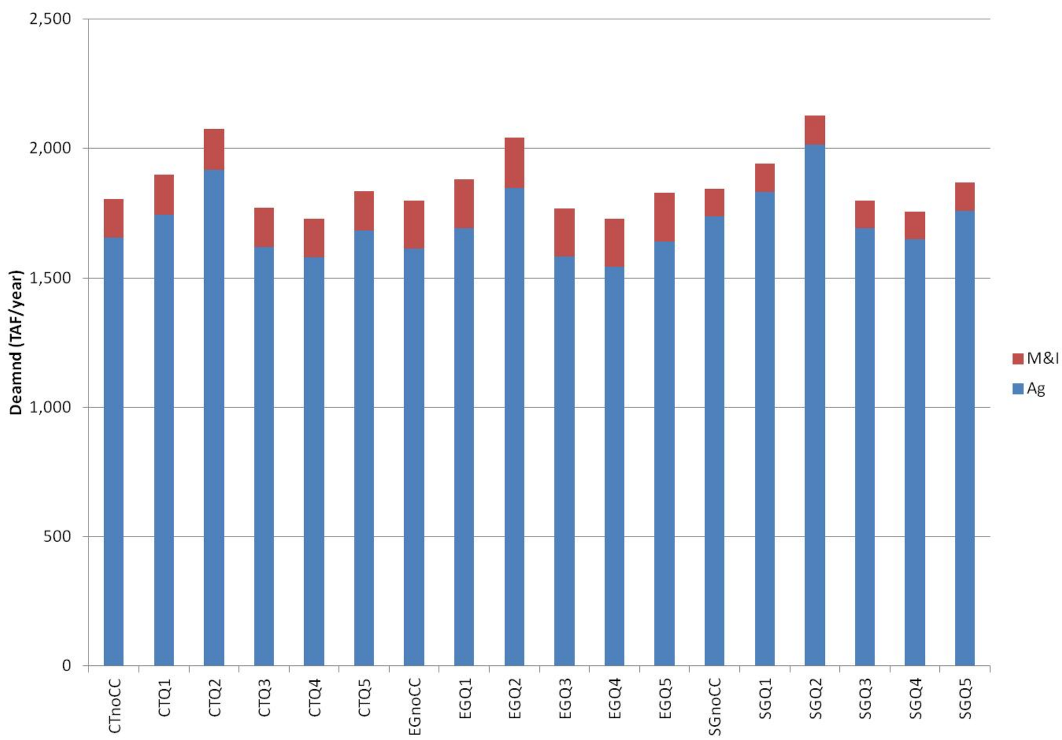

Figure 3-54. Average Annual Agricultural and Urban Demands in the Sacramento River Division

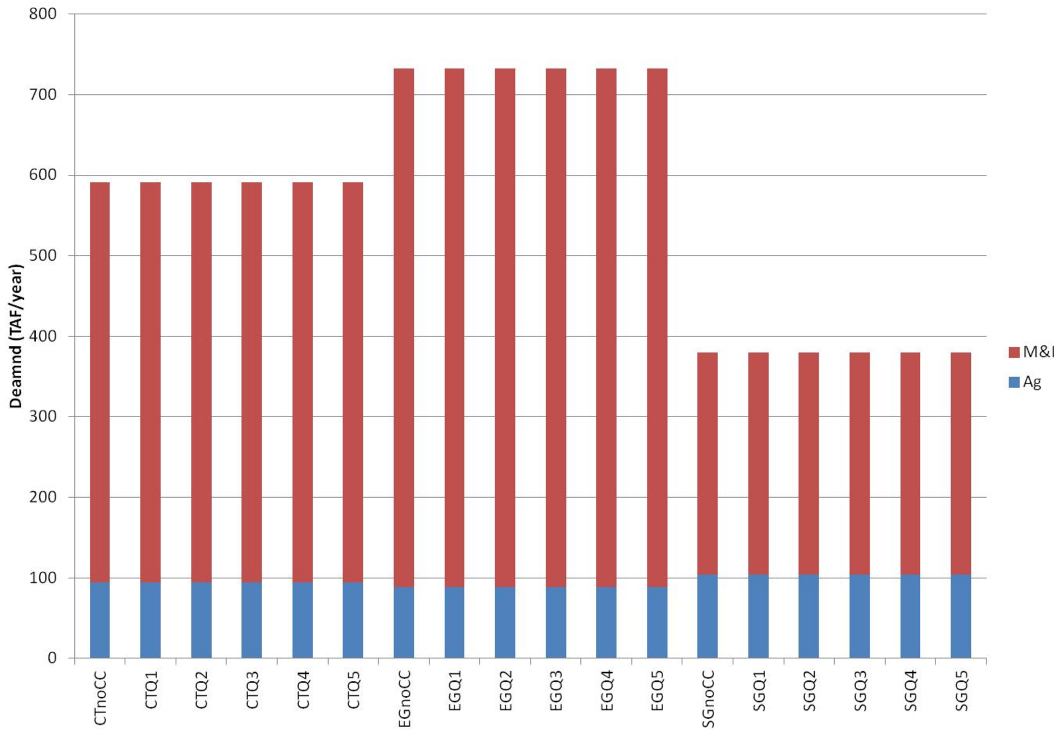

Figure 3-55. Average Annual Agricultural and Urban Demands in the San Felipe Division

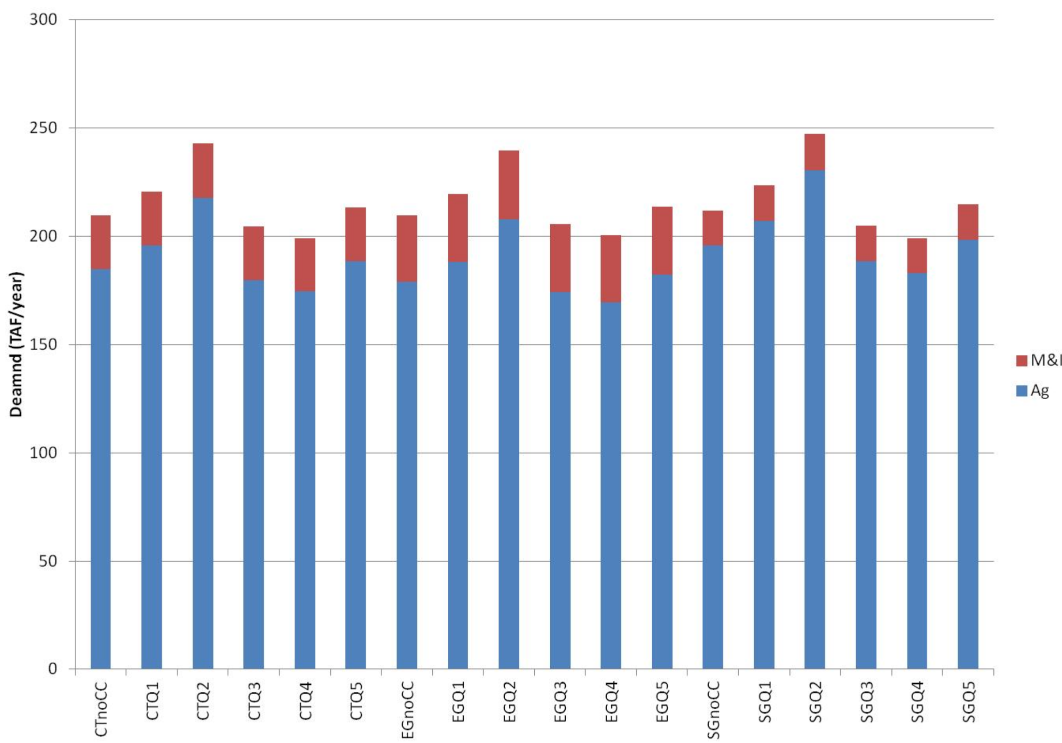

Figure 3-56. Average Annual Agricultural and Urban Demands in the Shasta Division

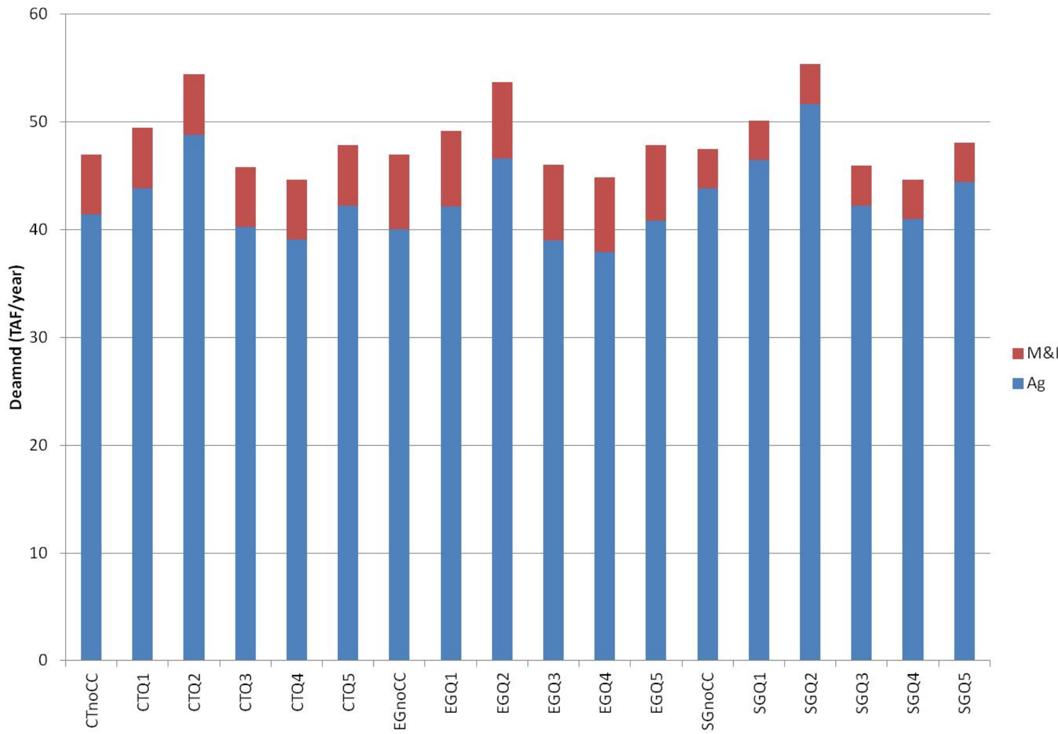

Figure 3-57. Average Annual Agricultural and Urban Demands in the Trinity Division

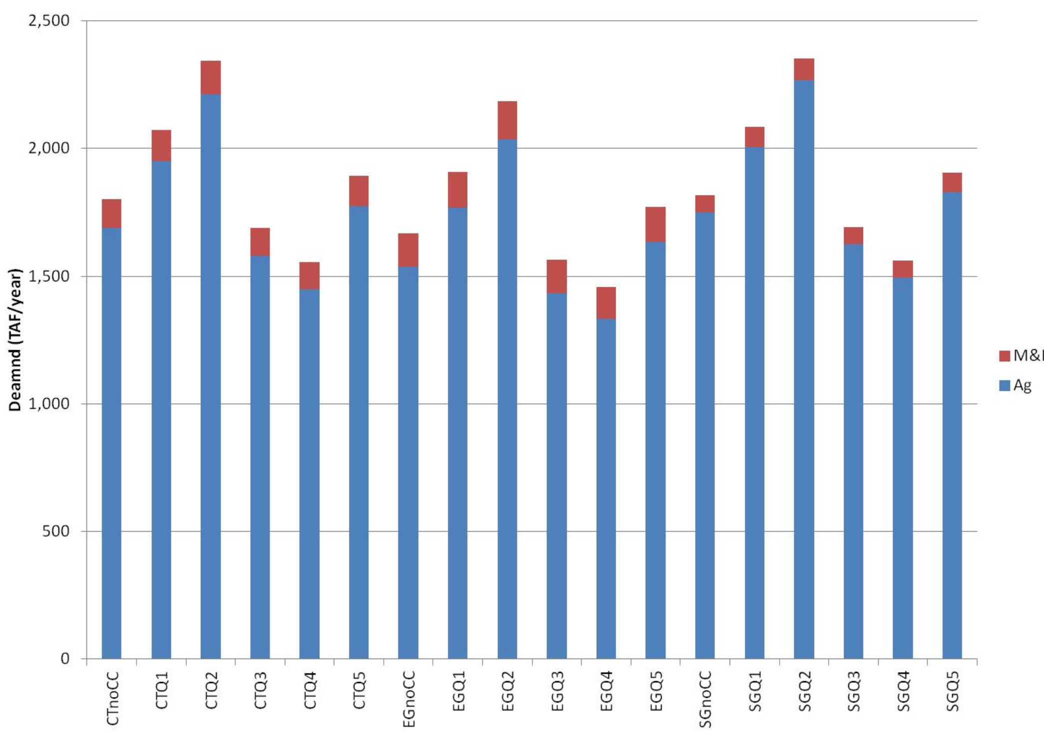

Figure 3-58. Average Annual Agricultural and Urban Demands in the West San Joaquin Division

Figure 3-59 and Figure 3-60 present the annual time series of projected total agricultural and urban demands within the all CVP Service Areas for the eighteen socioeconomic-climate scenarios. As shown on Figure 3-59, there is both short term variability and longer term trends in agricultural water demands. For the agricultural demands it is assumed that there are no changes in the crop types being grown and that changes in acreage are only associated with the socioeconomic scenarios. The short term variability is highly correlated with the variability in annual precipitation. In years of low precipitation, demand is higher while in years of high precipitation agricultural demands decrease. The longer term trends include both a period of increasing demands during the early 21st century followed by declining demands in the latter half of the century. These changes occur across all the future socioeconomic-climate scenario projections. However, it is also important to note that the rapid increase in demands during the early 21st century is partly an artifact of using the historical period precipitation record to create the projected future climate. A better method would be to simulate droughts and wet periods throughout the simulation period. However, this approach was not implemented in this study.

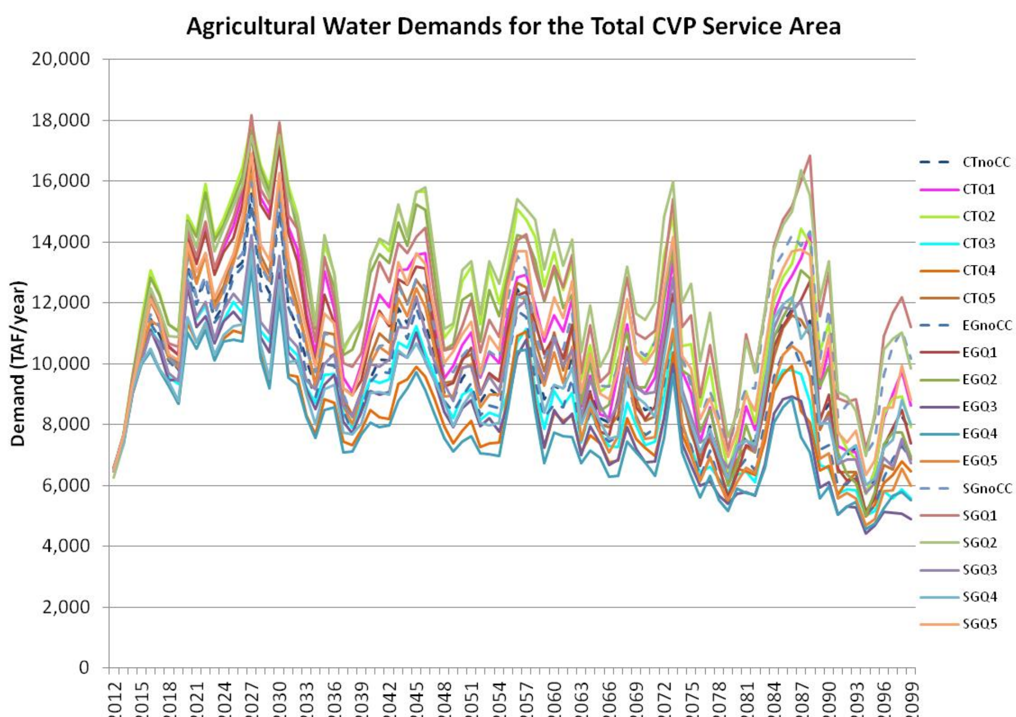

Figure 3-59. Annual Time Series of Agricultural Applied Water Demand in the CVP Service Area in each Scenario

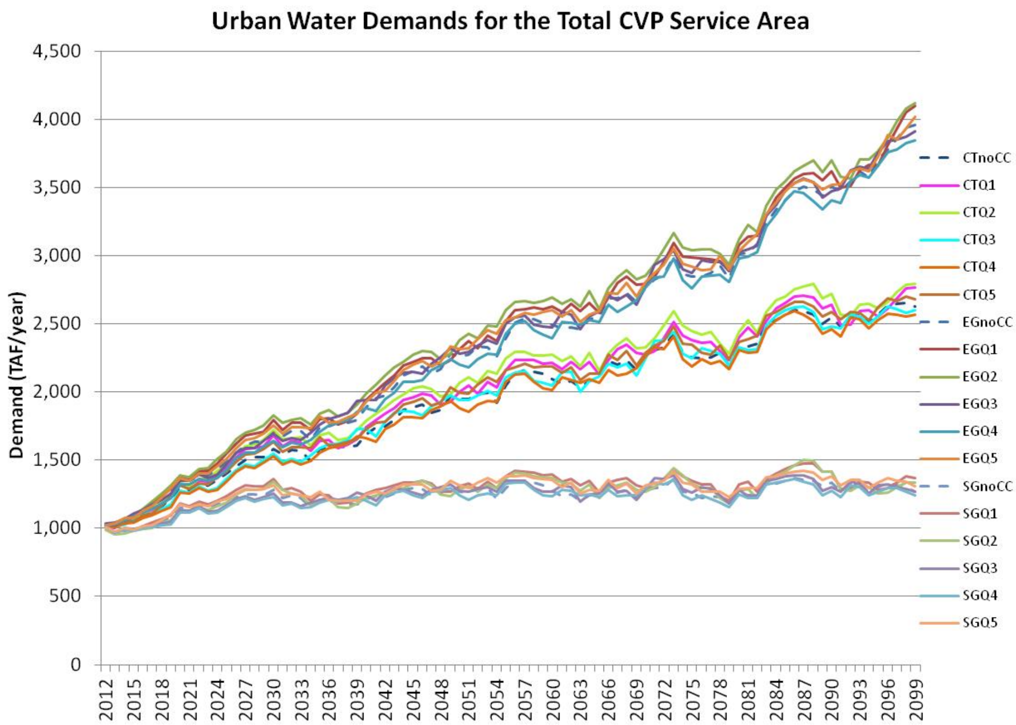

Figure 3-60. Annual Time Series of Urban Applied Water Demand in the CVP Service Area in each Scenario

There are several projected changed climatic conditions that contribute to the long term trends. Increased temperatures during the growing season can have multiple and opposing effects on crop growth, yield and ET. In general as temperatures rises, the rate of plant transpiration increases due an increase in the VPD which is the difference between the vapor pressure in the plant's leaves and the surrounding atmosphere. However, many plants can adapt to increased VPD by reducing their growth and stomatal openings to mitigate this heat stress. This adaptation ability varies between different crops and even amongst crop cultivars. The magnitude of the VPD is also affected by changes in atmospheric humidity. For the climate projections used in this study, both the VPD and atmospheric humidity (dew point temperature is a good indicator) were projected to increase throughout the 21st century. Although atmospheric humidity was projected to increase, the nonlinear nature of effect of temperature on the saturation vapor pressure in the plant's leaves was greater than the potentially offsetting increase in humidity. Increasing temperature may also effect plant growth by causing plants to grow faster. For annual plants like many agricultural crops, the faster growth results in a shorter growth period which reduces the total growing season ET. The yield of many agricultural crops is also negatively affected by overly rapid growth because of inadequate time for seed development. In contrast, increased temperature, providing it is not excessive, extends the growth period for perennial crops such as alfalfa, grasses and some trees which tends to increase total ET. Thus, these temperature related phenological changes can have significant and opposite effects on different types of agricultural crops. The Tmax and Tmin daily average temperatures and VPD associated with the climate projections were presented previously in Figure 3-11, Figure 3-12, and Figure 3-15, respectively. As shown, there is a steadily upward trend projected for both Tmax, Tmin and VPD during the 21st century.

Rs is also a major climatic factor affecting plant growth, yield and ET. As solar radiation increases, ET, growth and yield also generally increase. However, unlike temperature, Rs was projected to decrease during the 21st century. This decrease in Rs is associated with projected increases in atmospheric humidity and cloudiness. These changes are reflected in the rising Tdew shown on Figure 3-14. Consequently, this projected climatic change would tend to reduce the rate of crop growth, yield and ET during the 21st century. The projected changes in solar radiation are shown on Figure 3-13.

CO_2 is an important GHG which effects crop growth, yield, and ET. As CO_2 concentrations increase, most agricultural crops respond by reducing the conductance of the stomatal openings in their leaves which reduces their transpiration rate. The magnitude of the reduction depends somewhat on whether the plant uses the C3 or C4 photosynthetic pathway to assimilate CO_2. In C3 crops such as wheat, stomatal conductance is reduced by an average of 22 percent when CO_2 concentrations increase from 366 to 567 parts per minute (ppm) (current global average concentrations are ~ 385 ppm). For C4 crops such as corn, the average reduction in stomatal conductance was about 30 percent. Based on data from the Free Air Carbon Exchange (FACE) experiments, Ainsworth and Long (2005) reported an overall average reduction in stomatal conductance of between 20 – 22 percent when CO_2 concentrations were increased from 360 to 600 ppm. Furthermore, CO_2 effects on crop yield differ between C3 and C4 crops. For C3 crops, increasing CO_2 tends to increase crop growth. For C4 crops, growth is less affected because the C4 photosynthetic pathway is more efficient and consequently growth is not significantly affected.

In this study, CO_2 concentrations were based on global emission scenarios developed for the IPCC Forth Assessment Report (IPCC, 2007) and are described in the Special Report on Emissions Scenarios (IPCC, 2000). The projected concentrations vary between the scenarios and increase over time. The warmer scenarios Q2 and Q3 have higher CO_2 concentrations than the less warm Q1 and Q4 scenarios. The central tendency, Q5, projection is intermediate between these extremes. The Q5 concentrations increase from approximately 370 ppm at the beginning of the 21st century to about 650 ppm by the late 21st century. The maximum concentrations simulated reach 700 ppm by 2099. The projected CO_2 concentrations associated with each of the climate projection are presented on Figure 3-16.

As shown on Figure 3-59, agricultural demands are projected to increase in the early to middle 21st century because of rising temperatures and increased VPD. During this period, the decreases in Rs intensity and increases in CO_2 concentrations are not yet of sufficient magnitude to offset the temperature and VPD affects on ET and yield. However in the latter half of the 21st century as projected Rs continues to decrease and CO_2 concentrations continue to increase to levels of between 600 to 700 ppm, the ET of many agricultural crops being grown in the Central Valley decline despite the rising temperatures and increasing VPDs. As indicated on Figure 3-59, the overall average CVP Service Area agricultural demands increase from about 6.5 MAF in 2012 to approximately 7.5 MAF in 2099 and range from a minimum of 5.5 to a maximum of 11.2. Over the entire 21st century, the demands range from a minimum of 4.4 to a maximum of 18.2 MAF.

In contrast to the agricultural demands, urban demands are strongly correlated with the socioeconomic scenarios and show only slight variations with changing short term variability and longer term climatic trends. Because the urban demands are mostly indoor M&I, they tend to change steadily over time with the growth in population and expansion in commercial activities. As shown on Figure 3-61, urban demand is only slightly changed under Slow Growth conditions but does increase significantly under the Current Trends and Expansive Growth scenarios. By the end of the 21st century, the overall average of all the socioeconomic scenario urban demands in the CVP service areas is 2.7 MAF and ranges from 1.2 MAF (SG) to 4.1 MAF (EG).

CVP and SWP System Operations

CVP and SWP Project Storage Figure 3-61 through Figure 3-74 are exceedence plots of storage at the end of May and at the end of September in Shasta, Folsom, Oroville, New Melones, Friant, CVP San Luis and SWP San Luis reservoirs under each socioeconomic-climate scenario. For example, the 50 percent probability of exceedence may be interpreted as the average storage volume over the entire 21st century period. The end of May storage typically represents the water supply available for meeting agricultural, urban and environmental water demands while end of September storage is an indicator of carryover storage that is reserved to meet demands in subsequent years. In some instances, reservoir storage reaches a minimum volume (dead pool) below which releases cannot be made. Typically, the CVP and SWP systems are operated to maintain sufficient carryover storage to meet demand requirements during drought periods of several years. The dead pool results presented in these figures do not reflect how the CVP and SWP systems would actually be operated under future changes in climate but rather may be viewed as indicators of the potential need for adaptation under some of the projected future climates should such conditions actually occur.

As seen on the figures, the reservoir storage results reveal only a limited amount of variability between the different socioeconomic scenarios but differ significantly between the different climate scenarios. However, reservoir storages typically are higher under the EG scenario because over time agricultural demands which are the largest demand type decrease the most in this scenario because it assumes the most conversion of agricultural land to urban land.

The median climate scenario (Q5) has storage levels very close to the no climate change (No_CC) scenarios in Lake Oroville and a moderate amount lower than the no climate change scenario in Shasta and Folsom reservoirs. In all the reservoirs, the storage levels in both May and September are higher under the wetter climate scenarios (Q3 and Q4) than under the no climate change scenarios, with the highest storage levels in the wetter, less warming scenario (Q4). Conversely, the storage levels in both months are lower under the drier climate scenarios (Q1 and Q2) than under the no climate change scenarios, with the lowest storage levels in the drier, more warming scenario (Q2). At the end of September under climate scenario Q2, Lake Shasta is at dead storage in about 20 percent of all years and Lake Folsom is at dead storage in about 10 percent of all years. Such conditions also occur but less frequently under the Q1 and Q5 (central tendency) scenarios. As noted previously, the actual operation of these reservoirs would more than likely be adapted to maintain end of September carryover storage greater than the amounts described here.

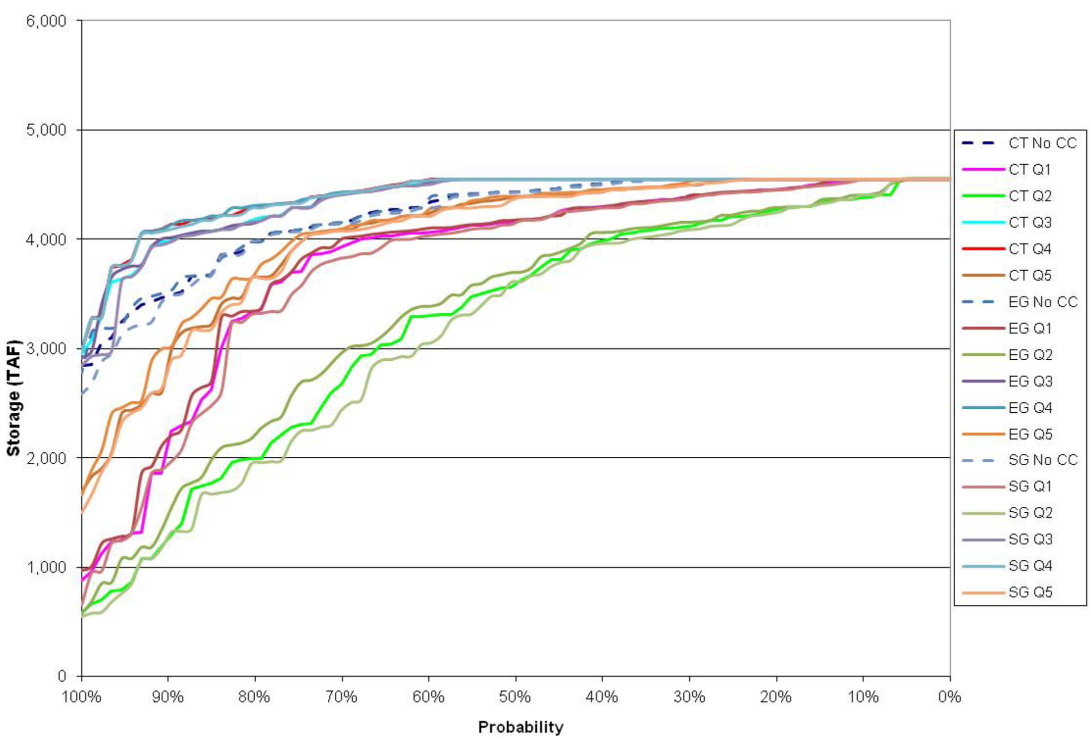

Figure 3-61. Exceedence of Shasta Lake End-of-May Storage in each Scenario

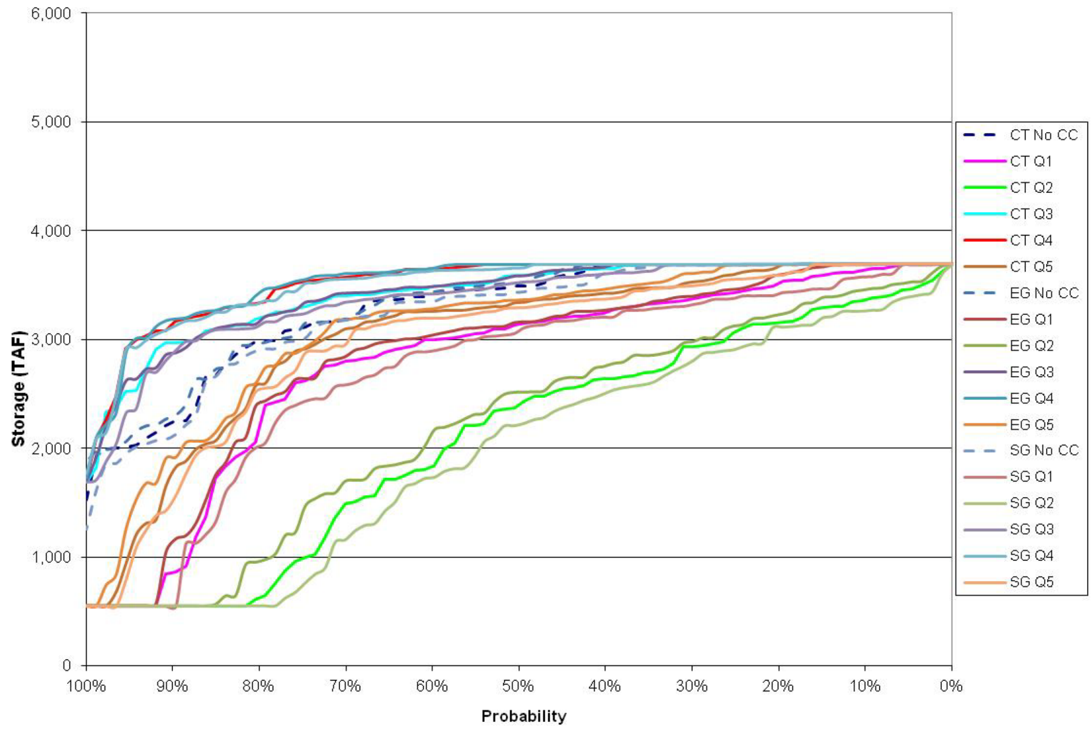

Figure 3-62. Exceedence of Shasta Lake End-of-September Storage in each Scenario

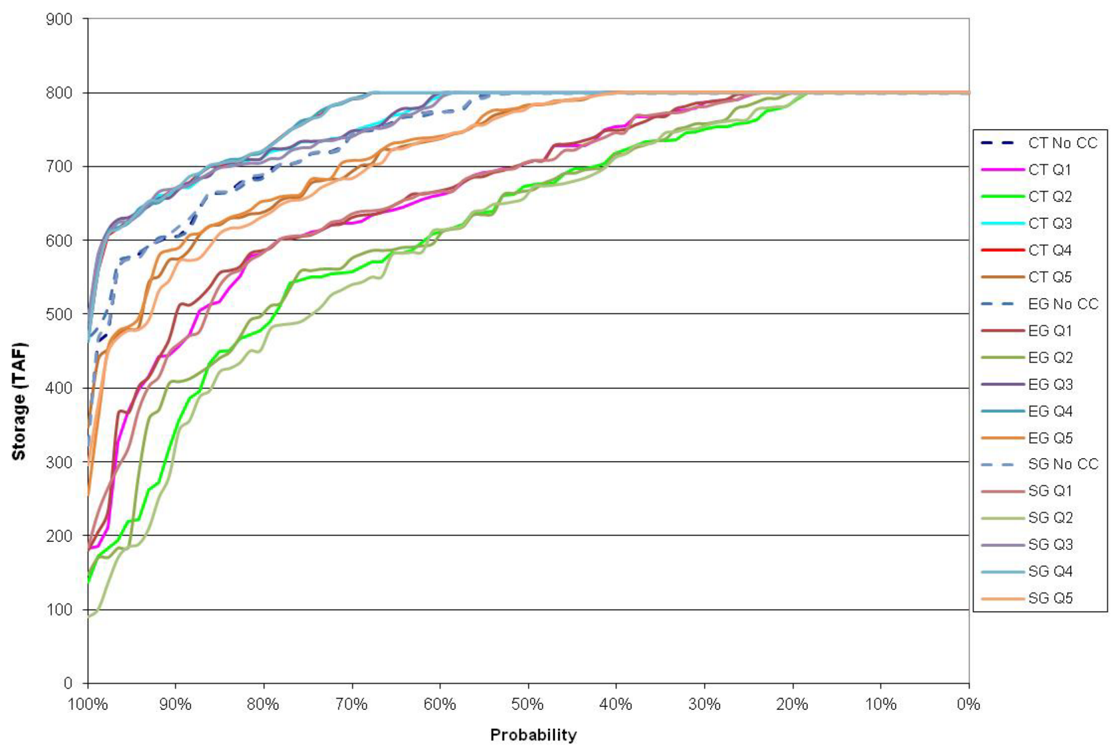

Figure 3-63. Exceedence of Folsom Lake End-of-May Storage in each Scenario

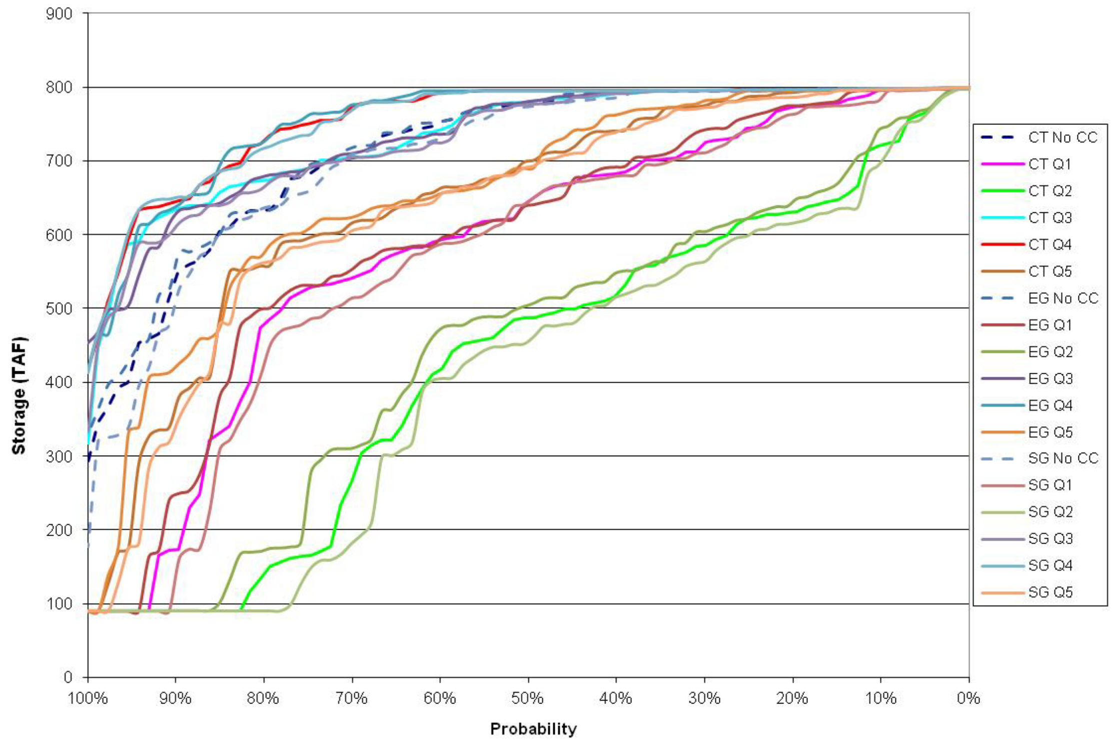

Figure 3-64. Exceedence of Folsom Lake End-of-September Storage in each Scenario

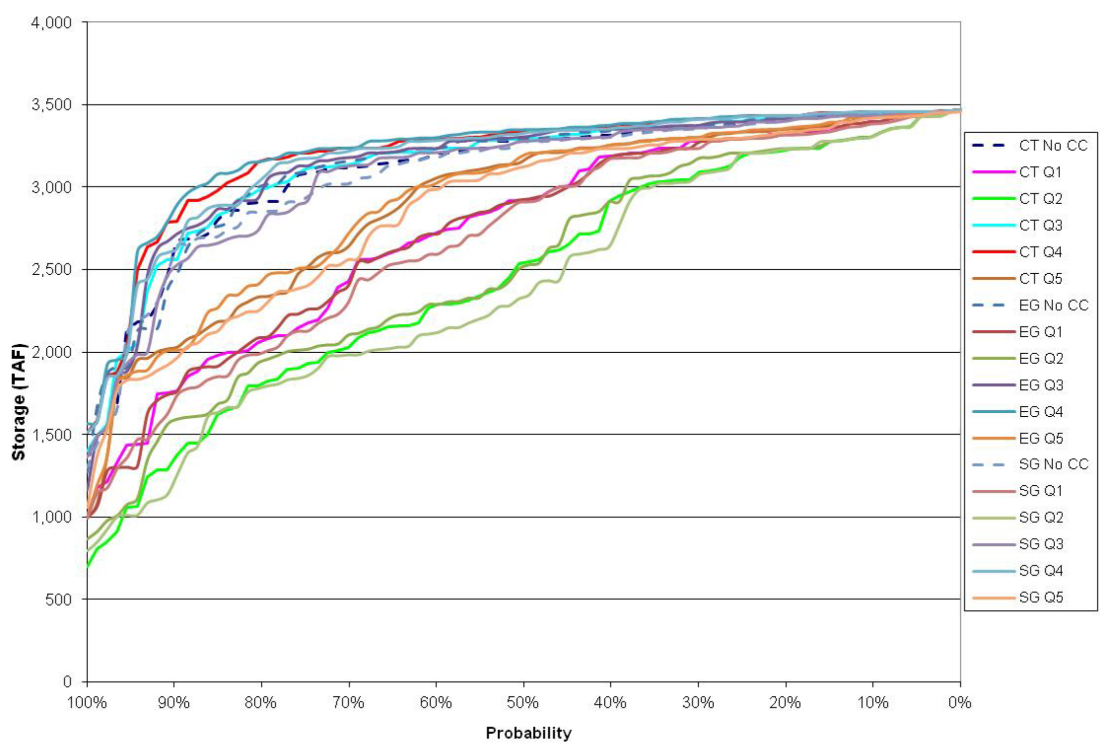

Figure 3-65. Exceedence of Lake Oroville End-of-May Storage in each Scenario

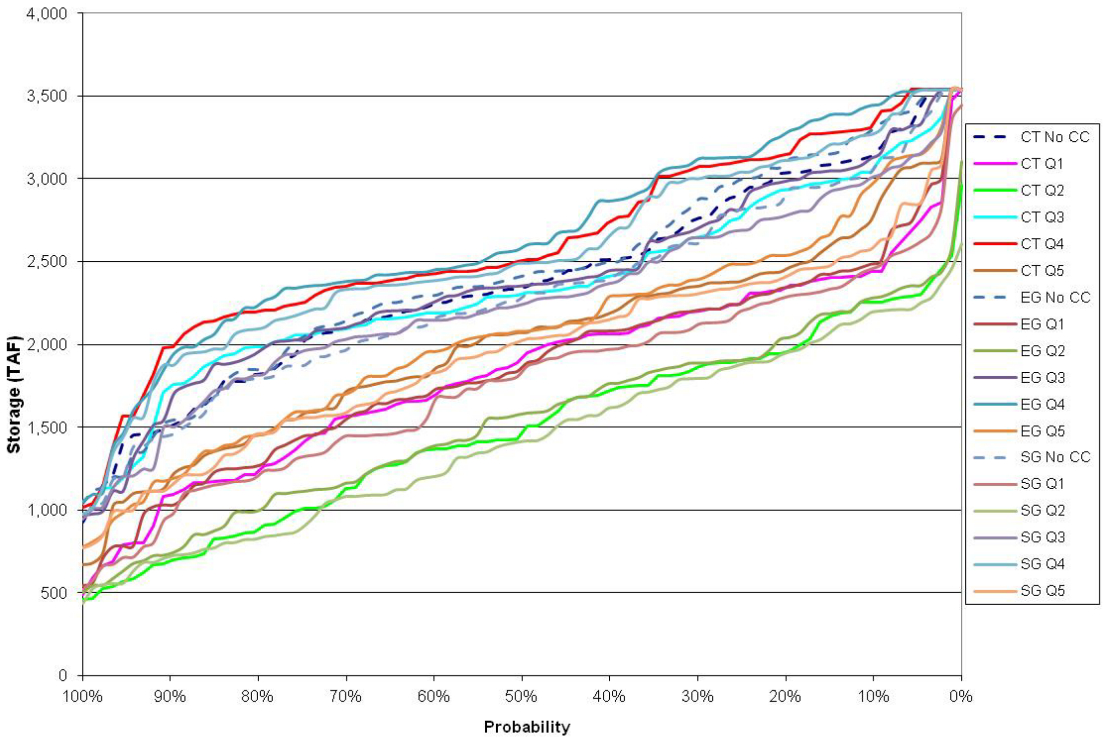

Figure 3-66. Exceedence of Lake Oroville End-of-September Storage in each Scenario

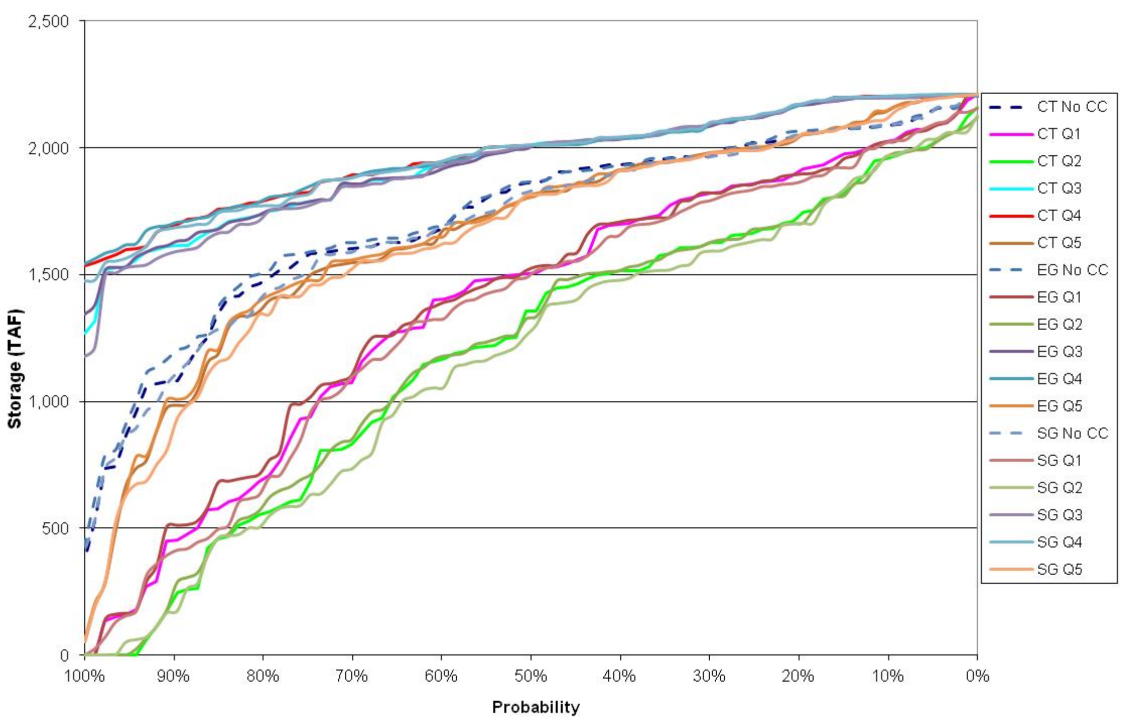

Figure 3-67. Exceedence of New Melones End-of-May Storage Baseline

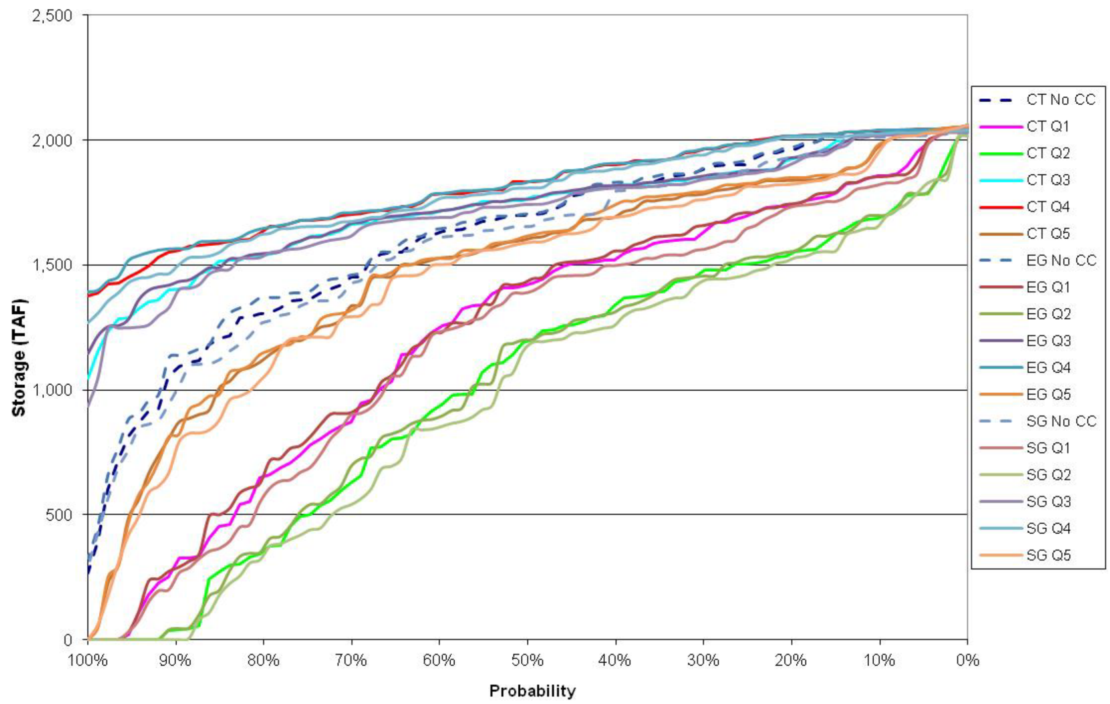

Figure 3-68. Exceedence of New Melones End-of-September Storage Baseline

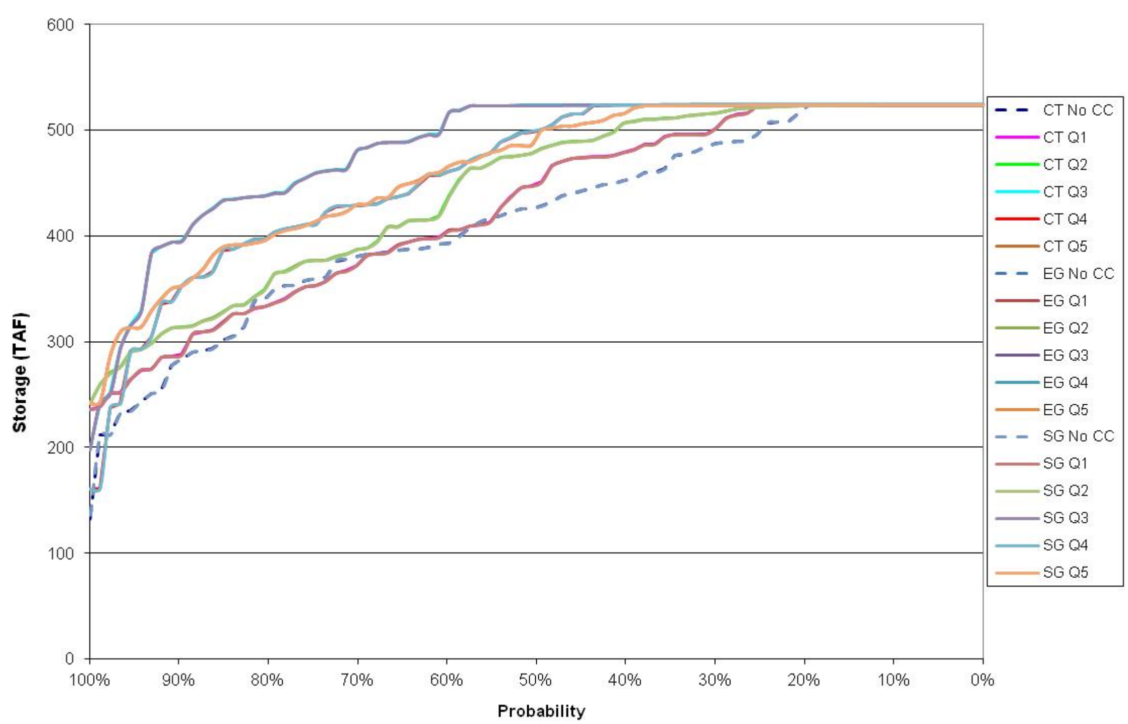

Figure 3-69. Exceedence of Millerton End-of-May Storage Baseline

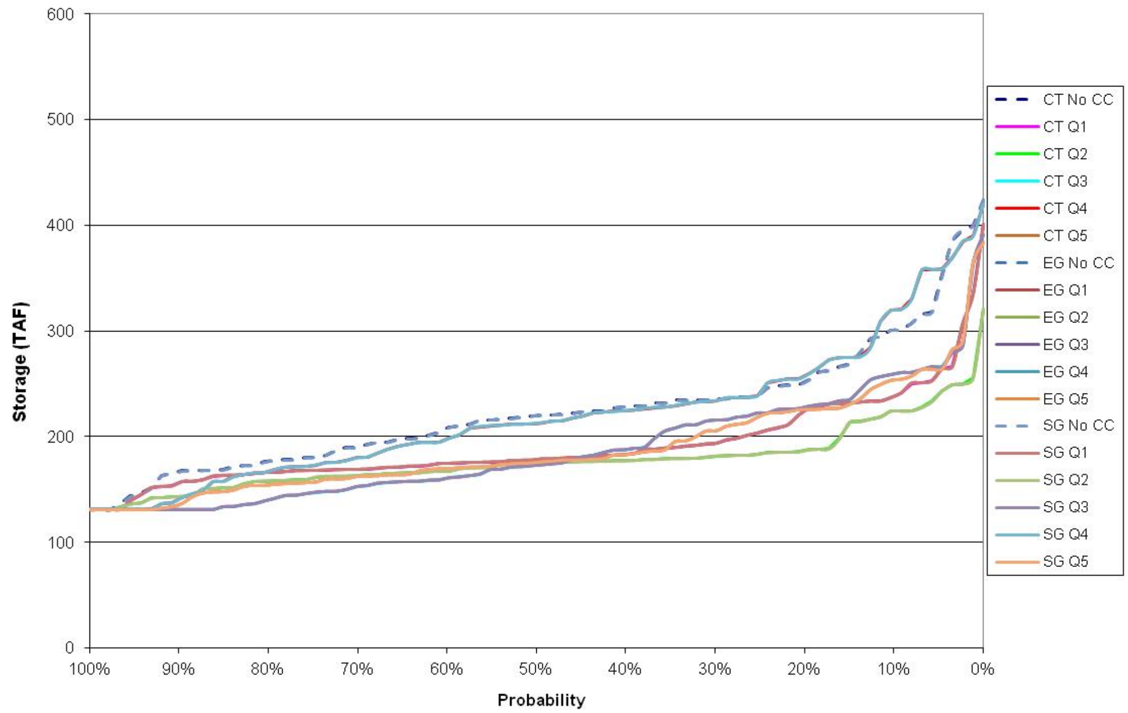

Figure 3-70. Exceedence of Millerton End-of-September Storage Baseline

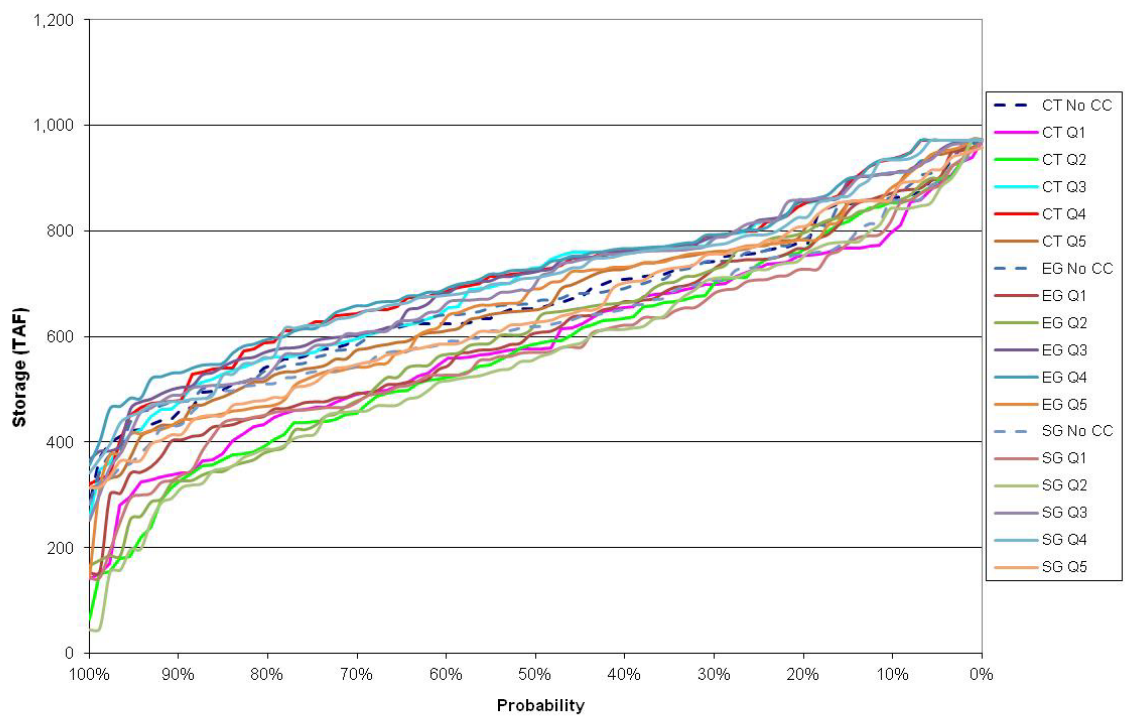

Figure 3-71. Exceedence of CVP San Luis End-of-May Storage Baseline

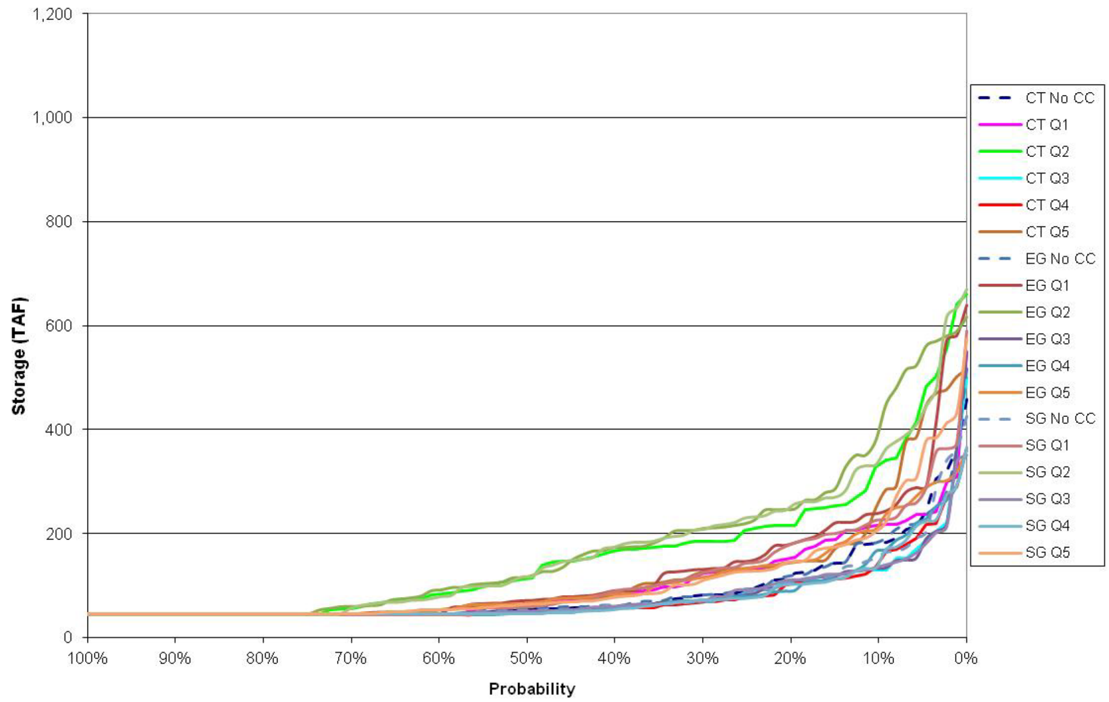

Figure 3-72. Exceedence of CVP San Luis End-of-September Storage Baseline

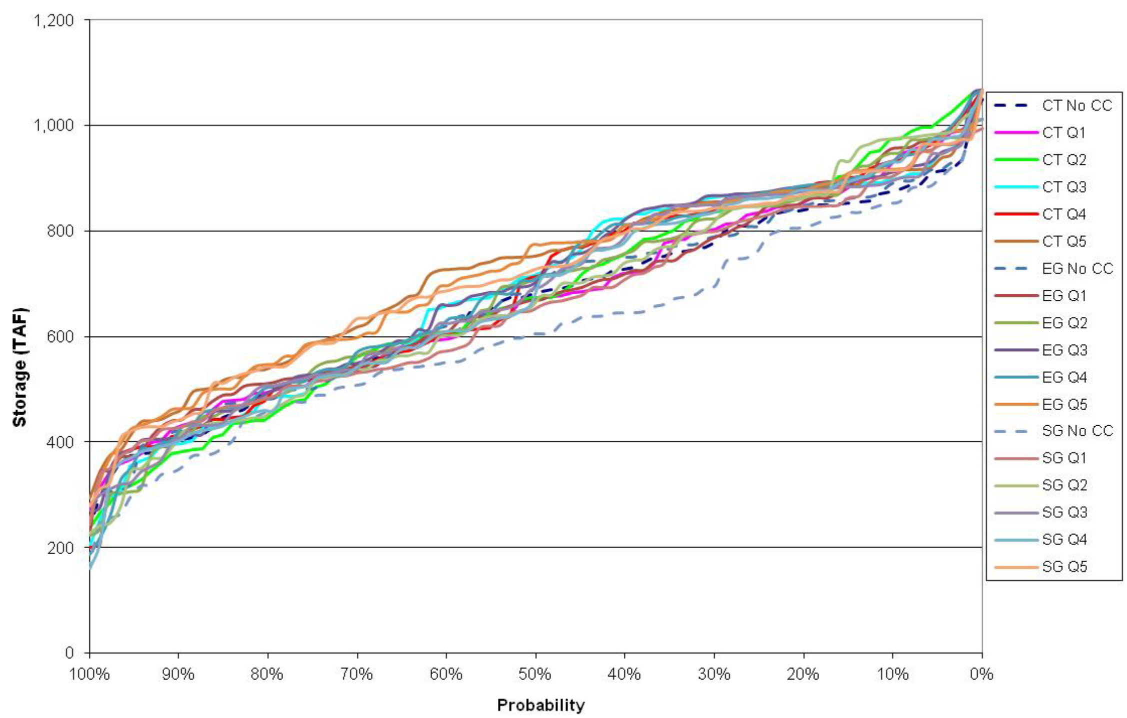

Figure 3-73. Exceedence of SWP San Luis End-of-May Storage Baseline

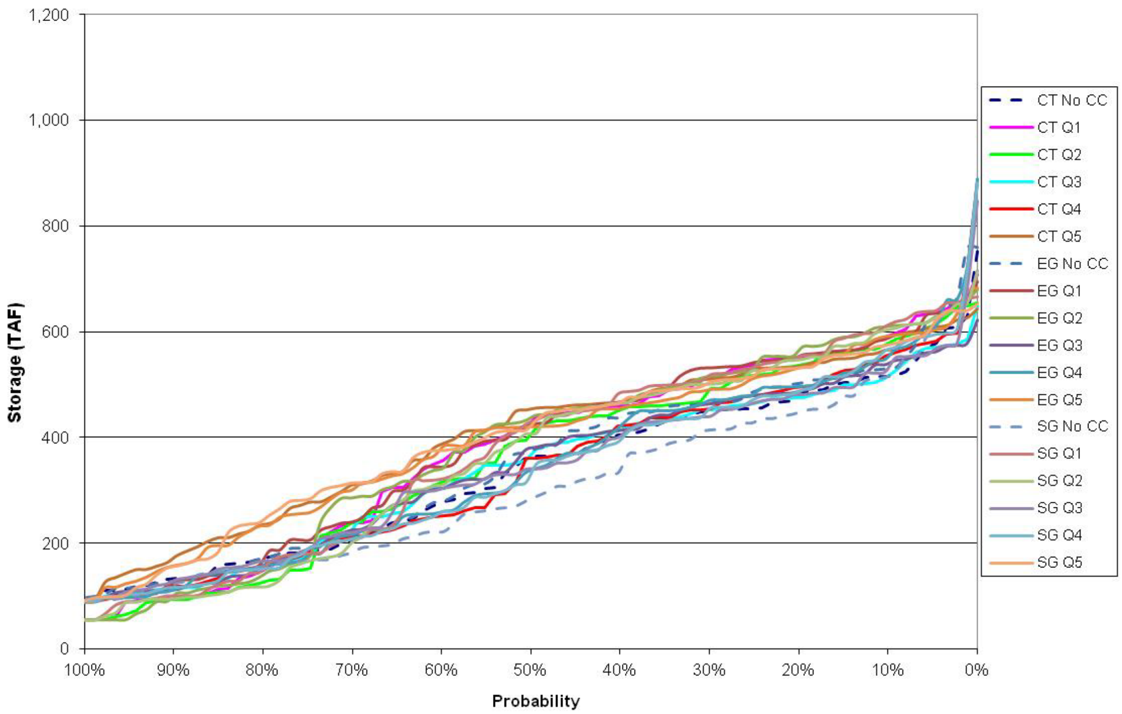

Figure 3-74. Exceedence of SWP San Luis End-of-September Storage Baseline

CVP and SWP Delta Exports and Delta Outflow Figure 3-75 through Figure 3-80 are annual exceedence plots of CVP and SWP exports at H. O. Banks and C. W. Jones pumping plants and Delta outflow. The box plots depict the mean, median, 25th and 75th percentile, minimum and maximum values for the annual flows at these same locations in each socioeconomic-climate scenarios. Like the reservoir storage results, the Delta export and outflow results are very similar with respect to the different socioeconomic scenarios but differ significantly between the different climate scenarios. Banks and Jones pumping and Delta outflow are all lower under climate scenarios Q5, Q1, and Q2 than under the corresponding no climate change scenarios, with the lowest flows occurring in the warmer-drier Q2 scenario. Conversely, the annual flows at all three locations are greater under climate scenarios Q3 and Q4 than under their corresponding no climate change scenarios, with the highest flows occurring in the less warm-wetter Q4 scenario. The drier climate scenarios (Q1 and Q2) show a greater difference in Delta exports relative to the no climate change scenarios than do the wetter climate scenarios (Q3 and Q4) because exports in the wetter climate scenarios are frequently limited by Delta conveyance capacities and Delta regulatory requirements. Total exports are about 1.4 to 1.5 MAF/year lower and Delta outflow is about 4.5 to 5.0 MAF/year lower under Q2 than under the no climate change scenario. Conversely, total exports are about 0.5 to 0.6 MAF/year higher and Delta outflow is about 5.5 to 6.0 MAF/year higher under Q4 than under the no climate change scenario.

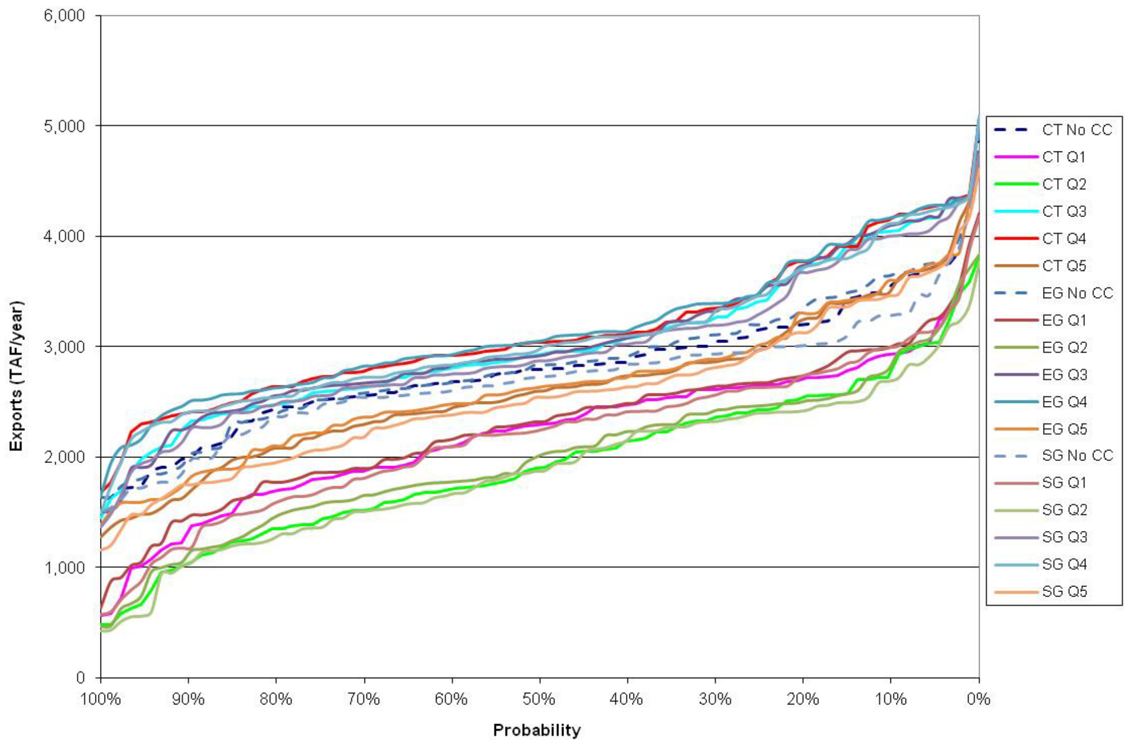

Figure 3-75. Annual Exceedence of Banks Pumping in each Scenario

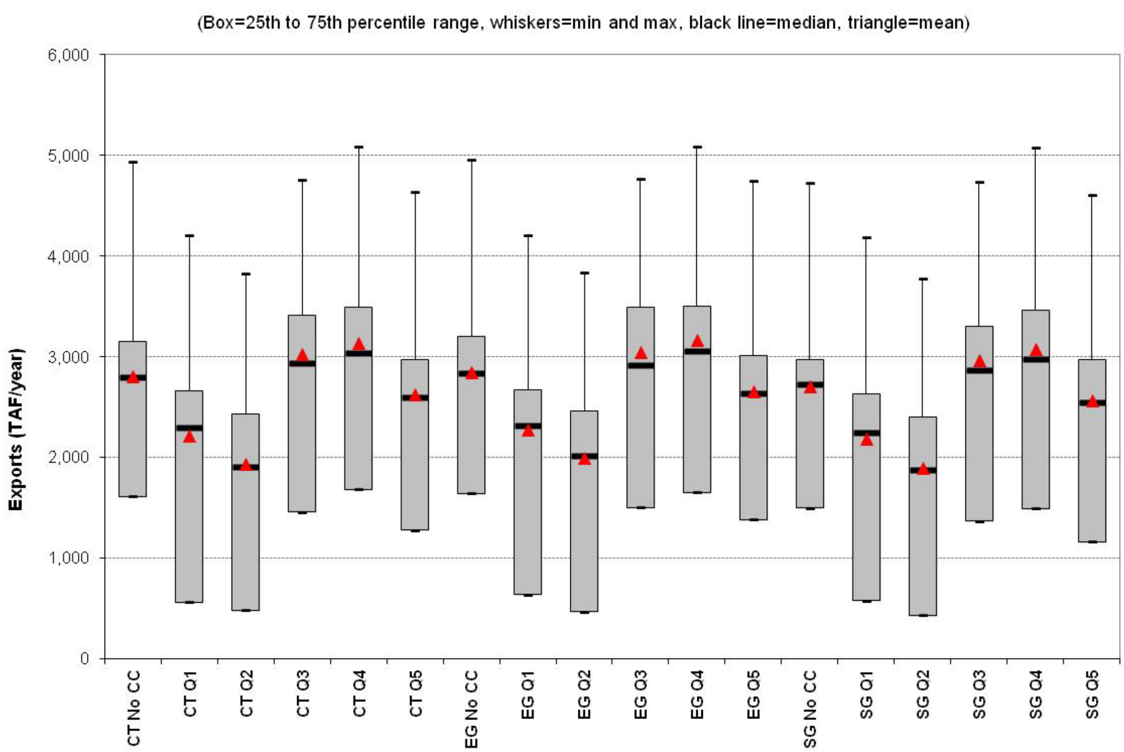

Figure 3-76. Box Plot of Banks Pumping in each Scenario

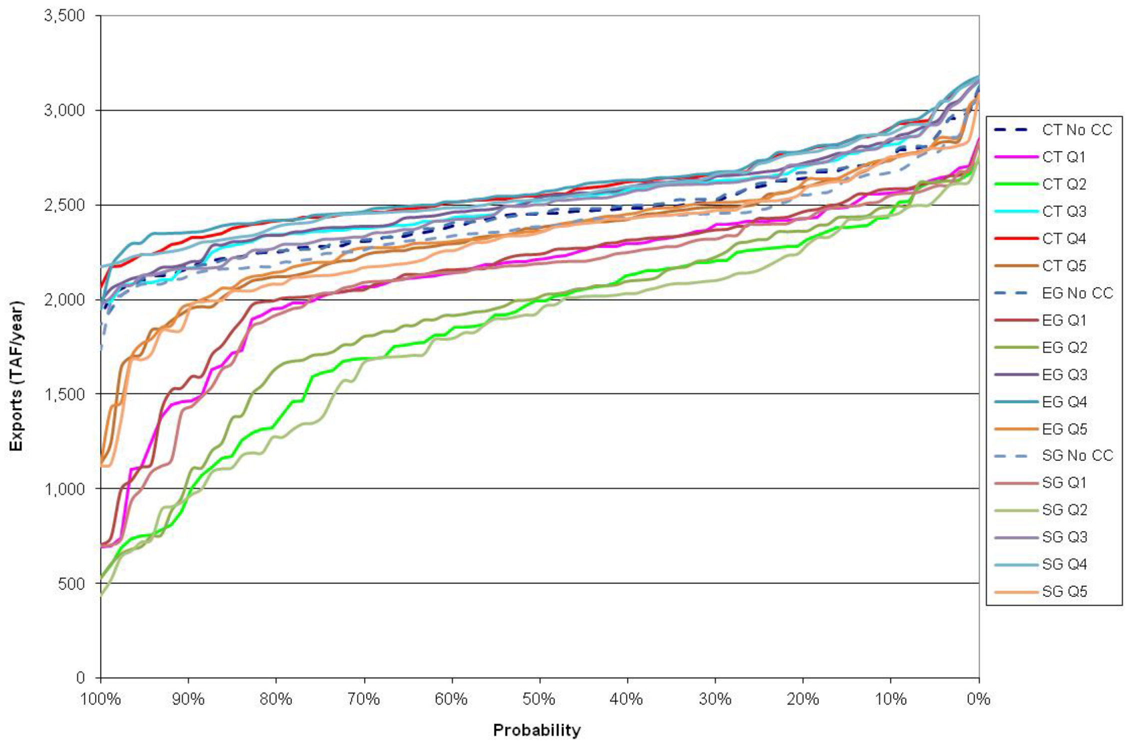

Figure 3-77. Annual Exceedence of Jones Pumping in each Scenario

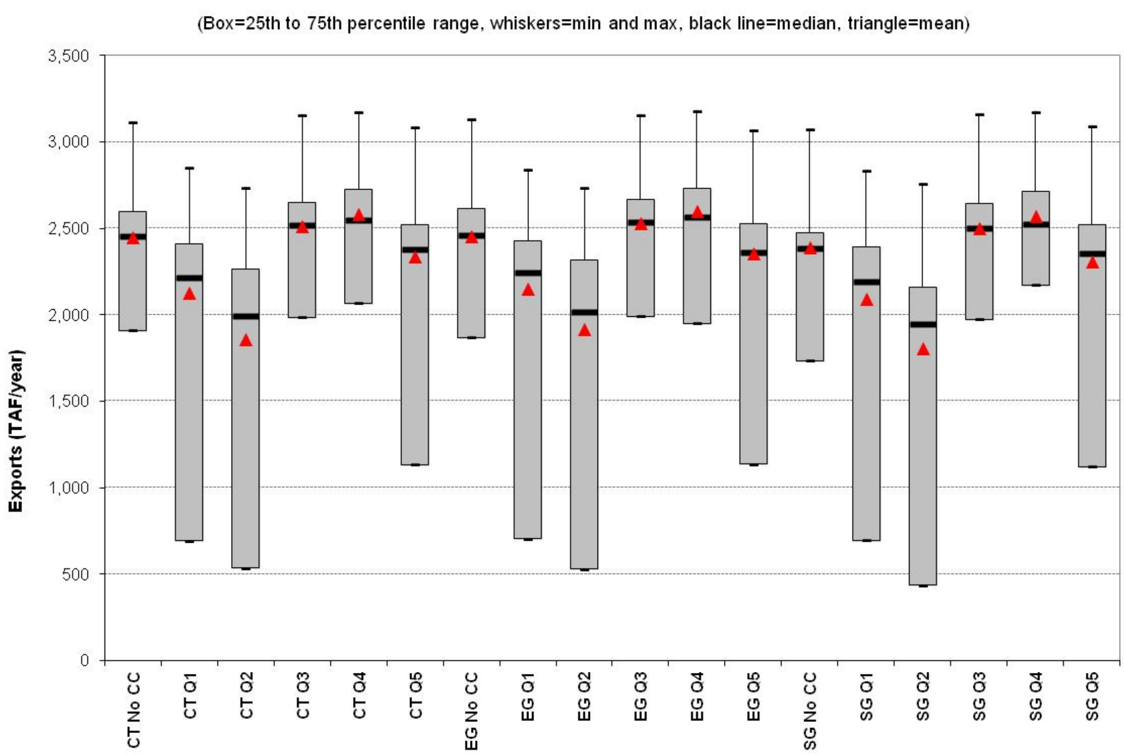

Figure 3-78. Box Plot of Jones Pumping in each Scenario

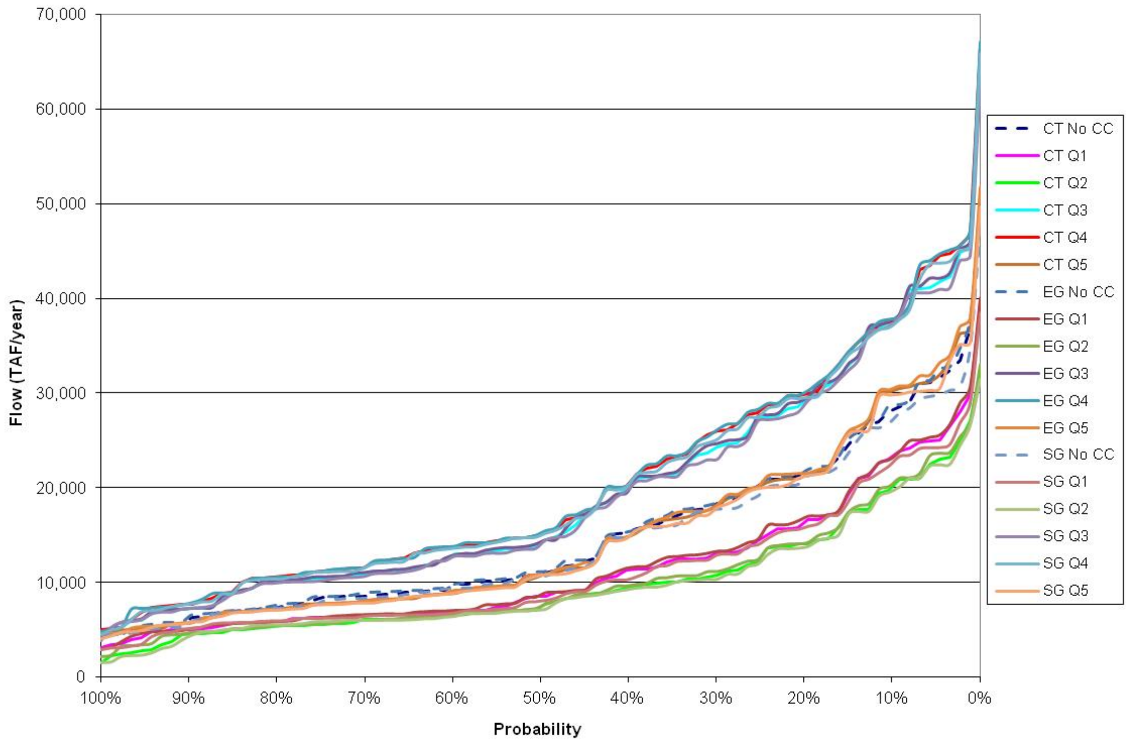

Figure 3-79. Annual Exceedence of Delta Outflow in each Scenario

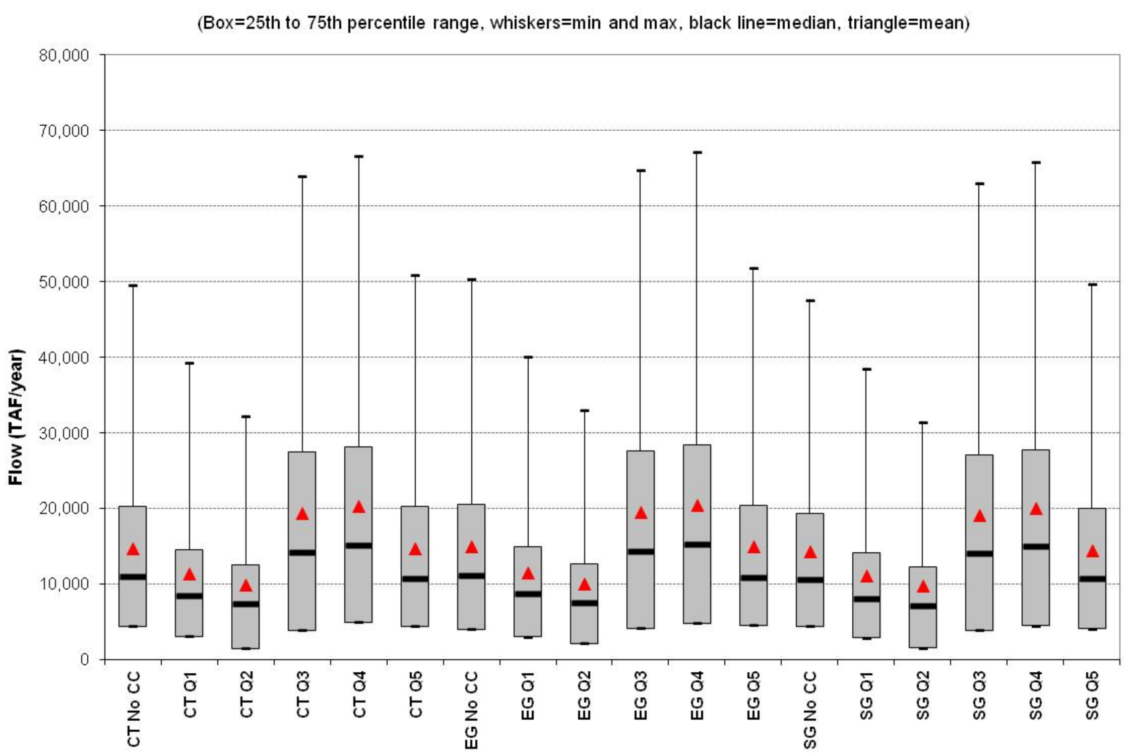

Figure 3-80. Box Plot of Delta Outflow in each Scenario

Delta Salinity Figure 3-81 and Figure 3-82 show exceedence and box plots of the average distance measured from the Golden Gate Bridge of the X2 (2 parts per thousand salinity concentration) position from February through June for each of the socioeconomic-climate scenarios. Greater X2 positions indicate that salinity has moved further eastward into the Delta. The period from February through June is when CVP and SWP reservoirs are operated to maintain certain regulatory requirements concerning the location of X2 within the Delta. As with the other system metrics, the X2 results are very similar between the different socioeconomic scenarios but differ significantly relative to the different climate scenarios. The X2 position results under the wetter climate scenarios (Q3 and Q4) are similar to those of their corresponding no climate change scenarios because the increased flows into the Delta in those wetter scenarios compensate for the increased sea level rise. However, the X2 position is greater under the central tendency Q5 and the drier Q1 and Q2 scenarios where sea level rise combined with reduced Delta inflows relative to the no climate change scenarios results in greater X2 positions., The largest values occur under the warmer-drier Q2 scenario. The average X2 position from February through June under Q2 is about 9-10 kilometers (km) further east than under the no climate change scenario.

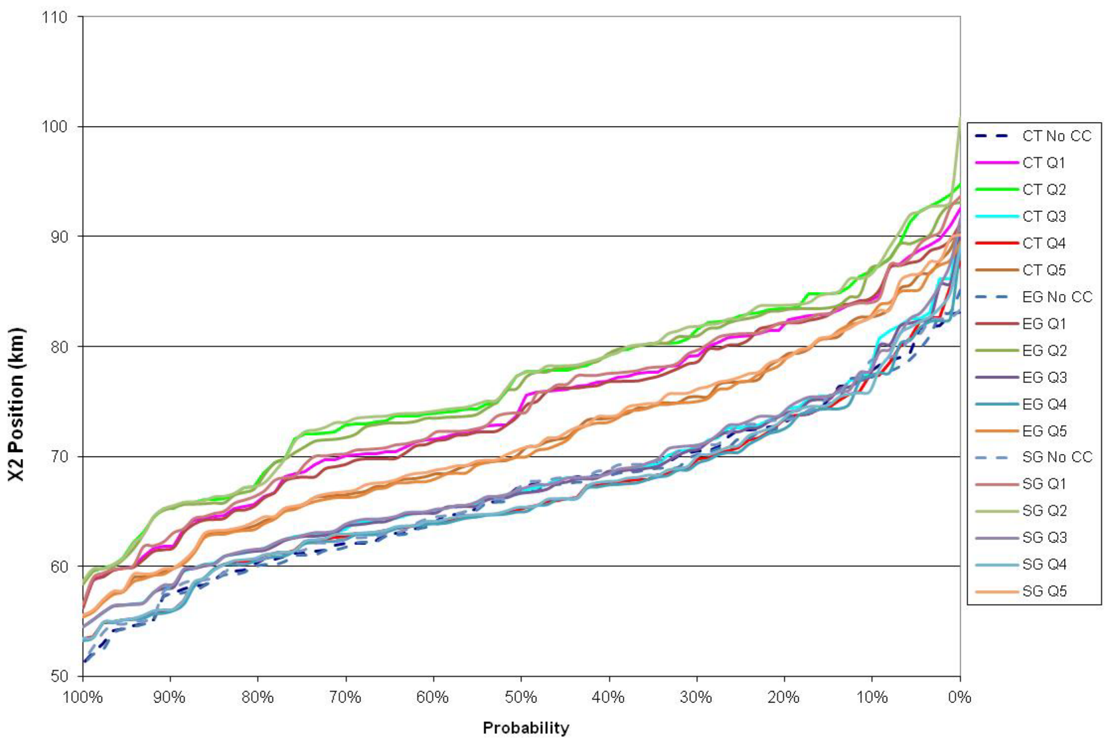

Figure 3-81. Exceedence of Average February-to-June X2 Position in each Scenario

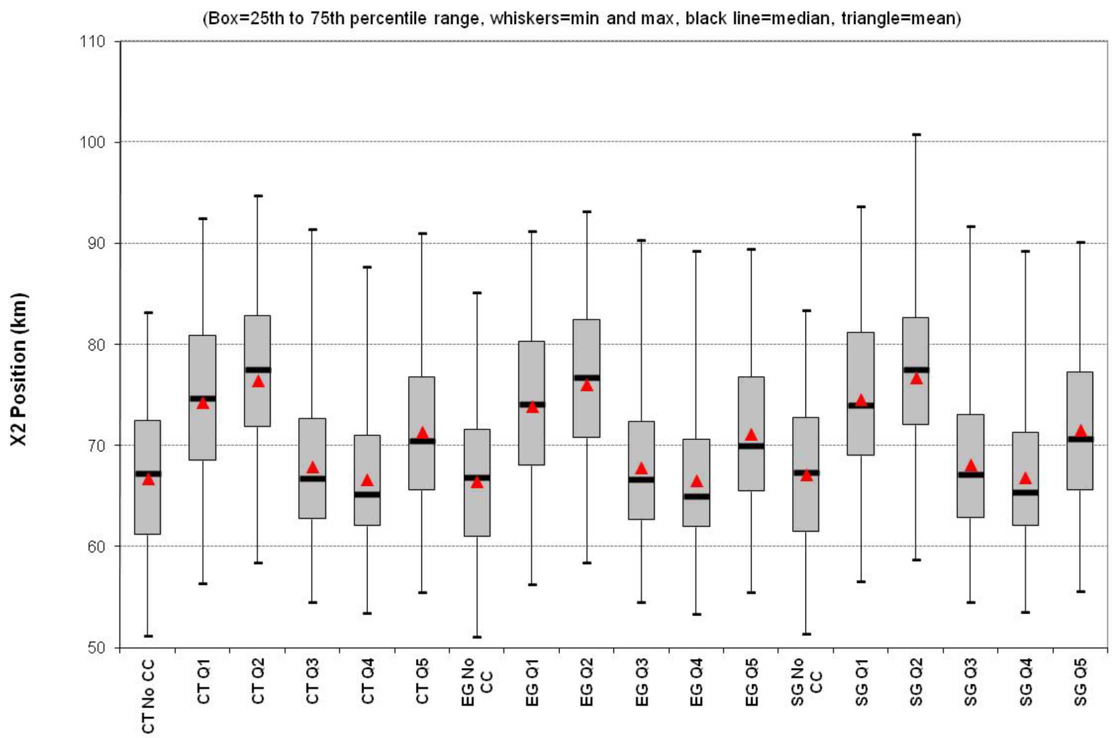

Figure 3-82. Box Plot of Average February-to-June X2 Position in each Scenario

Supplies and Demands in CVP Divisions

Figure 3-83 shows the average annual total CVP Service Area water supplies from various sources during the 21st century including surface water, groundwater and local projects. Also shown on the figure is the average annual unmet demand (defined as total demands minus surface water deliveries, groundwater pumping and the effects of any local actions) for the CVP Service Area under each socioeconomic-climate scenario. The effects of differences in climate are more significant than the socioeconomic scenarios. Local project supplies are relatively small compared to other sources in all the scenarios. Overall groundwater pumping ranges from 1.5 to 2.3 MAF/year. The greatest usage occurs in the wetter Q3 and Q4 scenarios because under these conditions increased aquifer recharge maintains groundwater levels sufficiently high that pumping is not as constrained as in the drier Q1 and Q2 scenarios. In general the central tendency Q5 scenarios are similar to their corresponding no climate change projections. Surface water deliveries range from 3.7-5.1 MAF/year across the range of scenarios. The relationship between deliveries and the climate scenarios is similar to groundwater but the differences between the drier (Q1,Q2) and wetter scenarios (Q3,Q4) is more significant. The central tendency Q5 scenario deliveries are slightly reduced relative to their corresponding no climate change scenarios.

Over the 21st century, the unmet demands range from 2.7-8.2 MAF/year. The largest unmet demands occur in the warmer-drier Q2 scenarios and the least in less warm-wetter Q4 climate scenarios. Overall, the central tendency Q5 unmet demands tend to be slightly greater than their corresponding no climate change scenarios. Because the Slow Growth socioeconomic scenario assumes more agricultural land remains in production, it has the highest unmet demands relative to climate, while Expansive Growth has the least.

Figure 3-83. Average Annual Supplies and Unmet Demand in the CVP Service Area in each Scenario

Figure 3-84 through Figure 3-92 present similar information for each of the CVP Divisions. Simulated unmet demands exist in all CVP Divisions with the exception of the American River Division. The largest unmet demands occur in the Friant Division. In general, the magnitude of unmet demands primarily reflects the amount of agricultural demand in the service area. In most of the Divisions, the differences between socioeconomic-climate scenarios exhibit the same relationships as described above for the overall CVP Service Area. In the San Felipe Division there is more differentiation in total demand between the socioeconomic scenarios as compared to the other Divisions because increases in urban demands are not offset by reductions in agricultural demand. In addition, the San Felipe Division demands do not differ between different climate scenarios because they were not simulated in WEAP-CV. Because of this, in the Slow Growth scenario, the San Felipe Division does not fully use all of its potential groundwater supplies because demands are low enough that not all potential groundwater pumping is required to fully meet demands in most years.

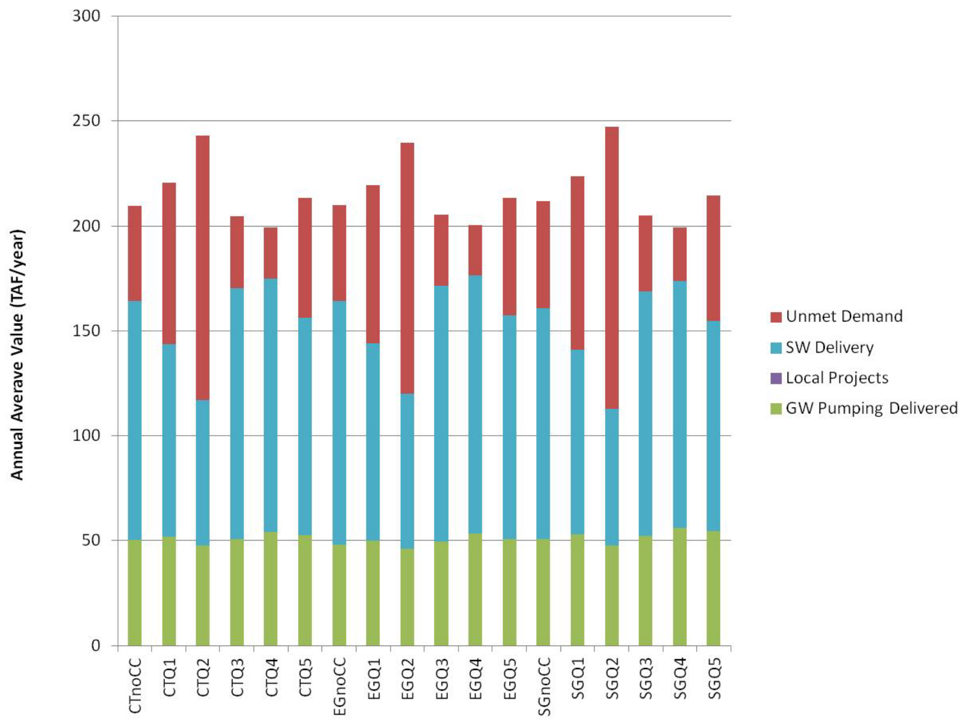

Figure 3-84. Average Annual Supplies and Unmet Demand in the Shasta Division in each Scenario

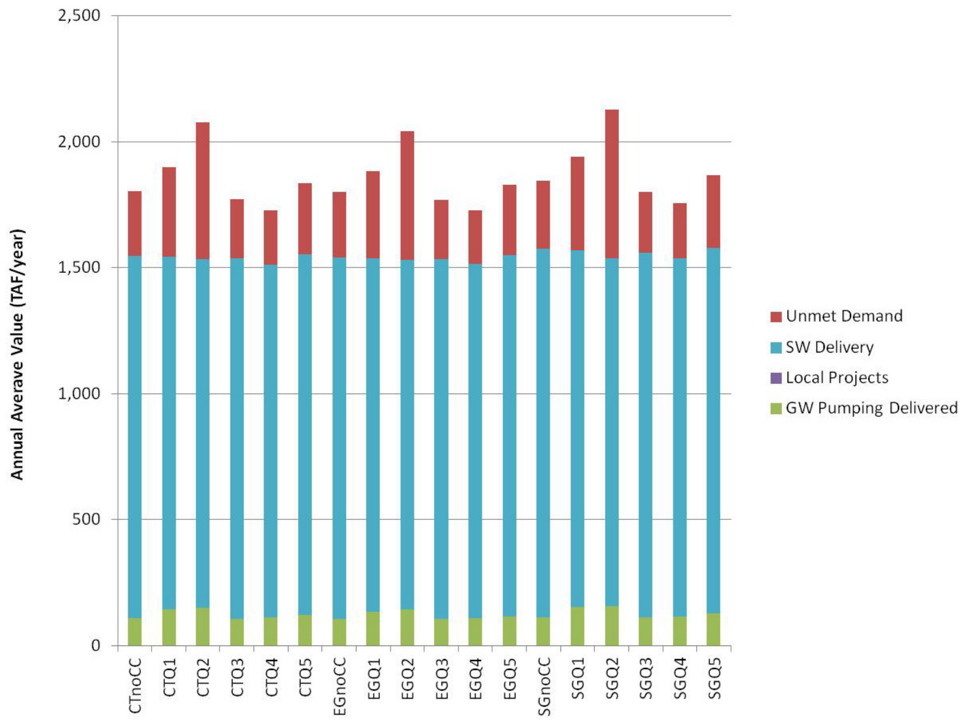

Figure 3-85. Average Annual Supplies and Unmet Demand in the Sacramento River Division in each Scenario

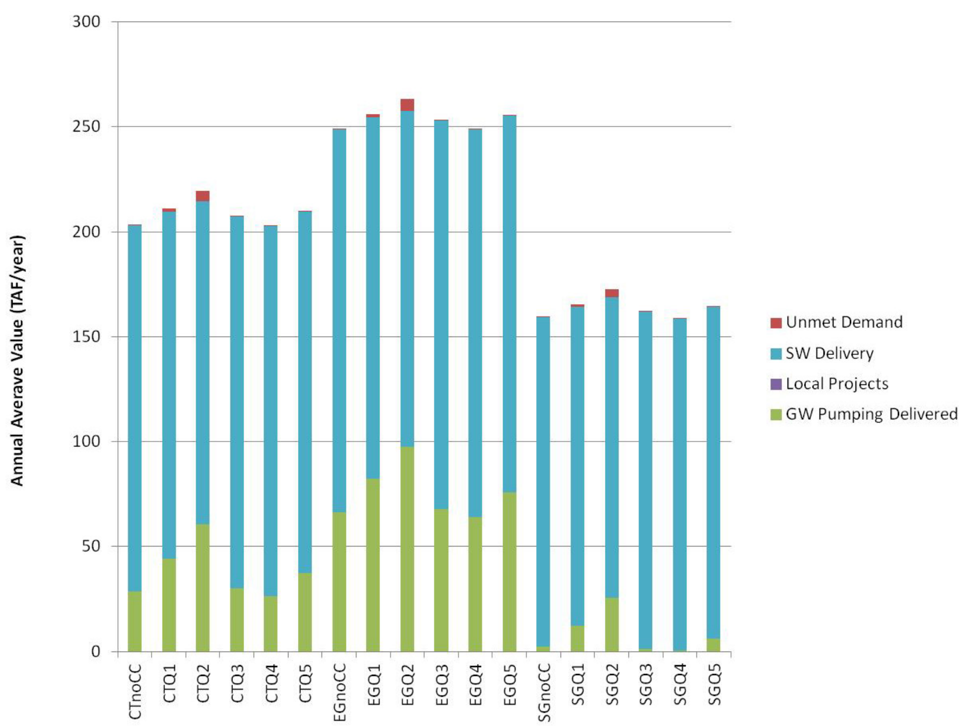

Figure 3-86. Average Annual Supplies and Unmet Demand in the American River Division in each Scenario

Figure 3-87. Average Annual Supplies and Unmet Demand in the Eastside Division in each Scenario

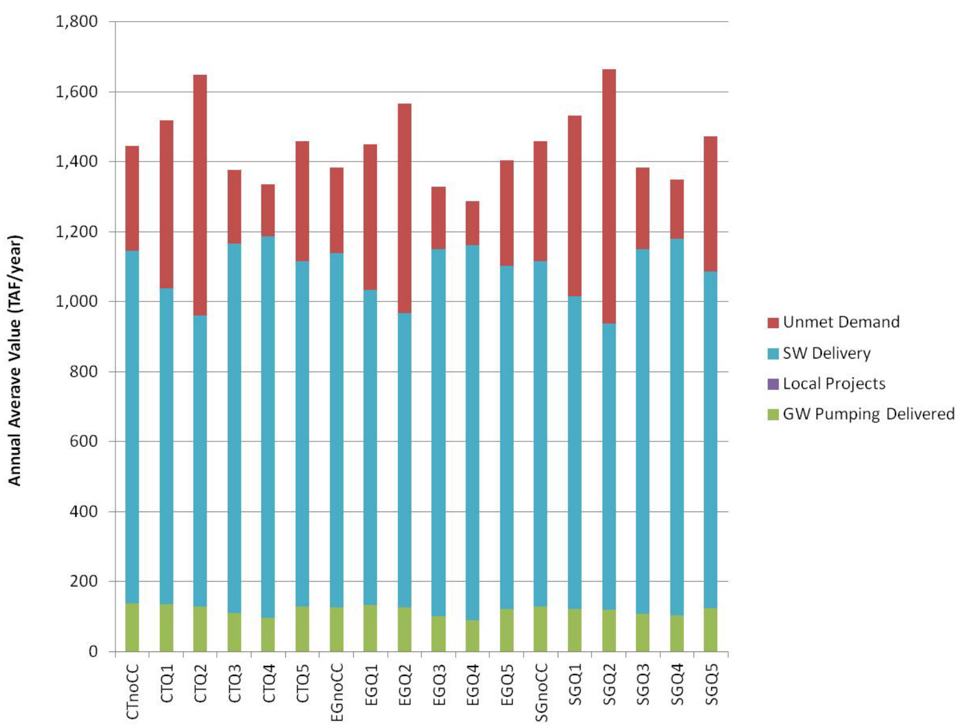

Figure 3-88. Average Annual Supplies and Unmet Demand in the Delta Division in each Scenario

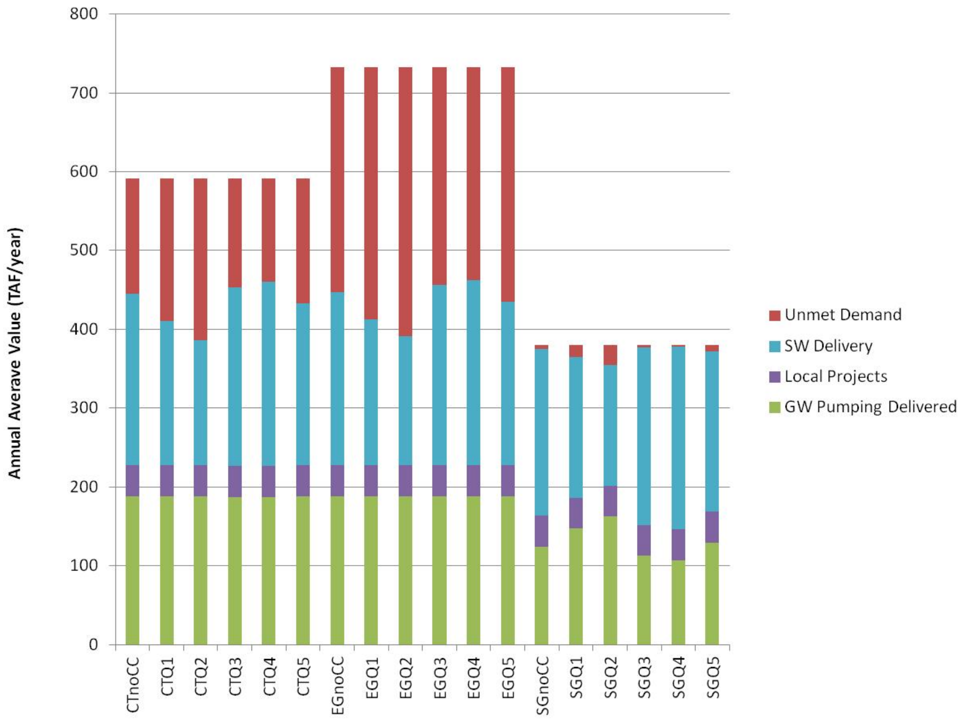

Figure 3-89. Average Annual Supplies and Unmet Demand in the San Felipe Division in each Scenario

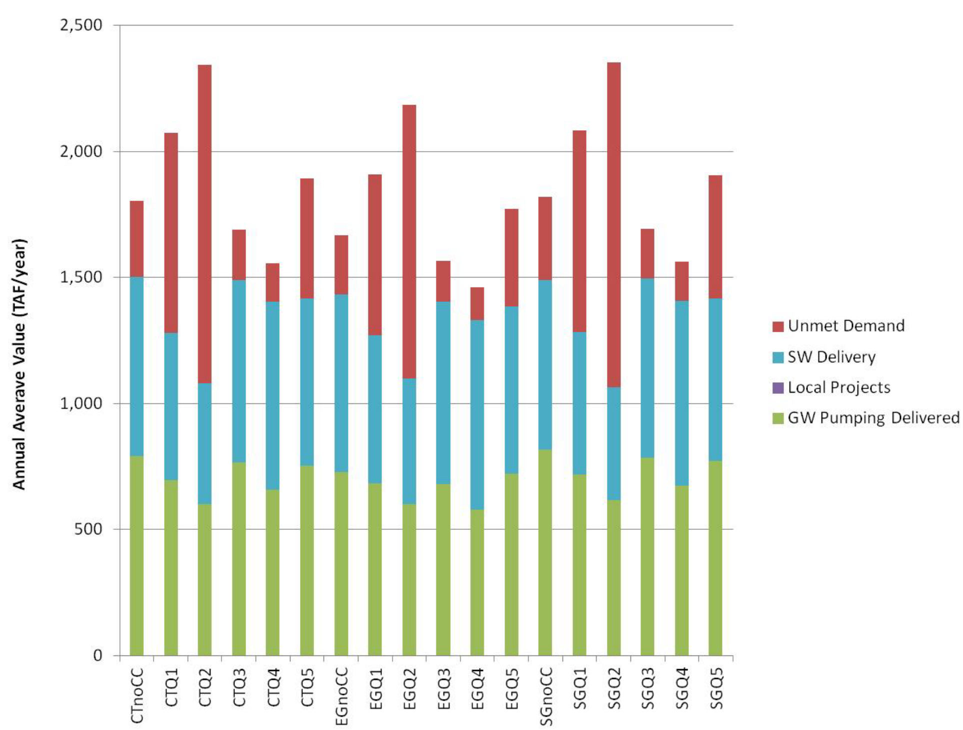

Figure 3-90. Average Annual Supplies and Unmet Demand in the West San Joaquin Division in each Scenario

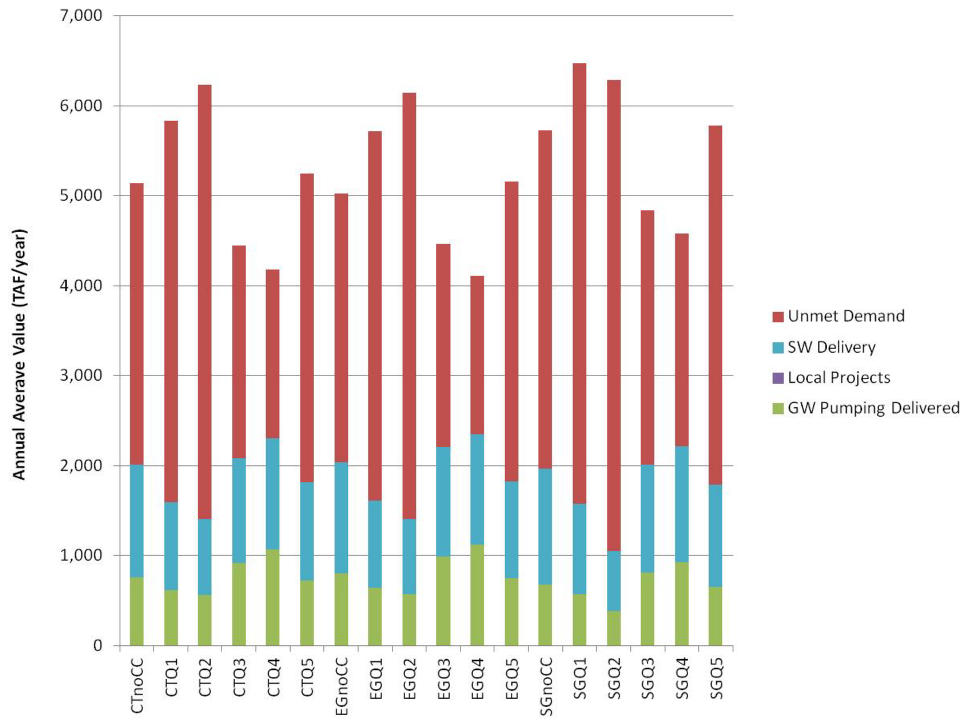

Figure 3-91. Average Annual Supplies and Unmet Demand in the Friant Division in each Scenario

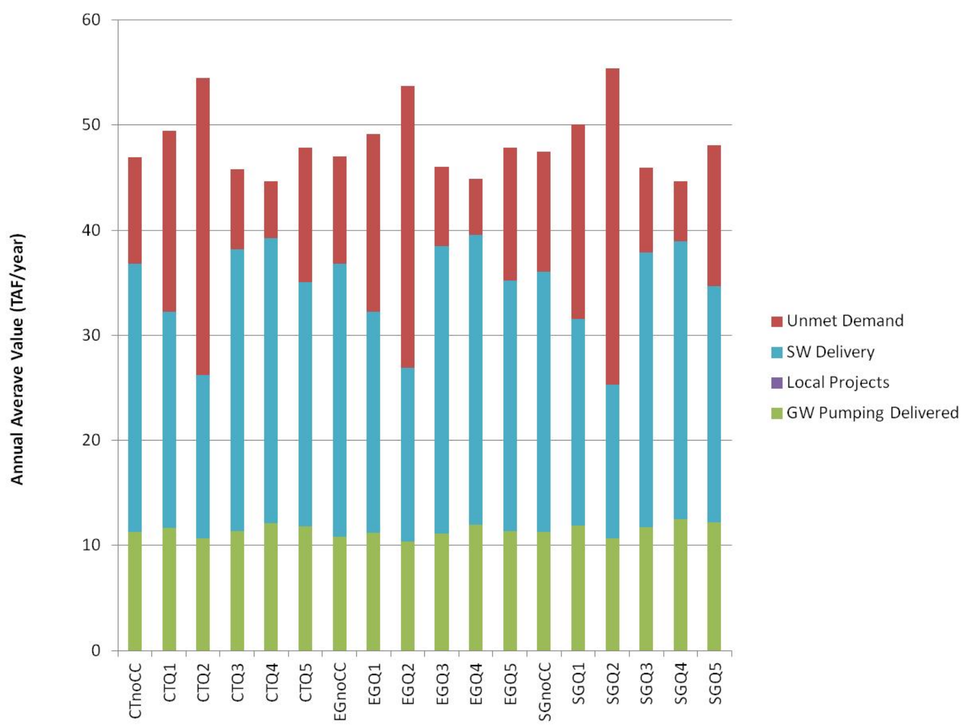

Figure 3-92. Average Annual Supplies and Unmet Demand in the Trinity River Division in each Scenario

Figure 3-93 through 3-96 present annual time series of groundwater, surface water and local project supplies and unmet demand for the entire CVP Service Area. All 4 scenarios show similar year-to-year variability, with demands increasing and surface water supplies decreasing during dry periods and the opposite occurring during wetter years. The Current Trends –Median climate projection (CT-Q5) scenario shows only modest increases in demand reductions in supply relative to the Current Trends no climate change scenario. The Expansive Growth-warmer-drier (EG-Q2) scenario has much greater increases in demand and reductions in supply as compared to the Current Trends-no climate change (CT-noCC) scenario. Conversely, the Slow Growth-less warming-wetter (SG- Q4) scenario has lower demands, higher supplies, and consequently lower unmet demands than the CT-noCC scenario.

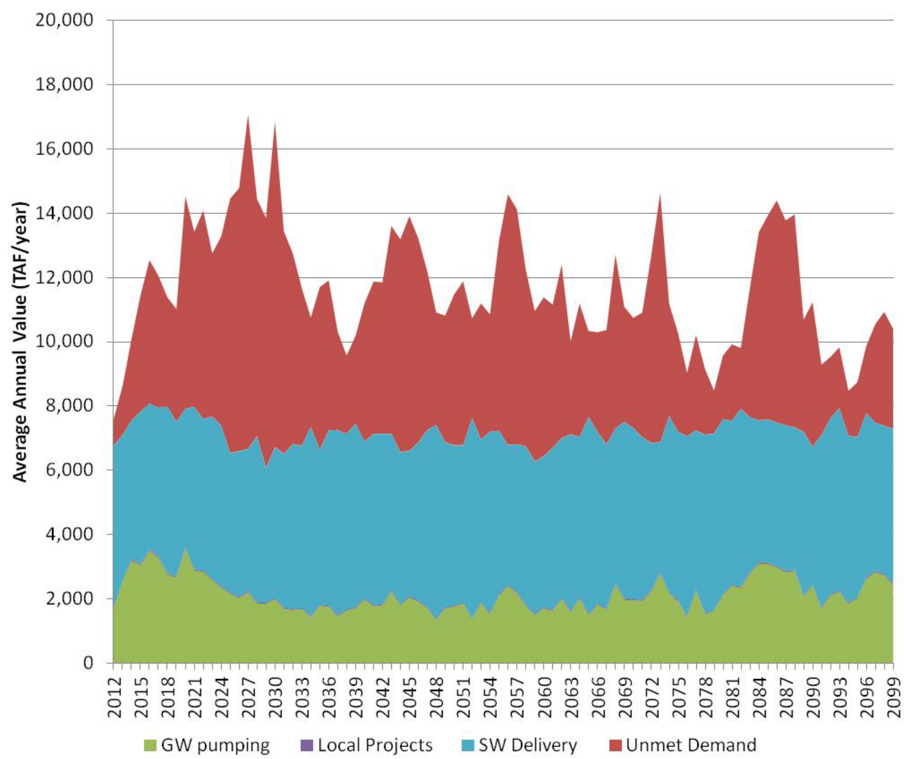

Figure 3-93. Annual Time Series of Supplies and Unmet Demand in CVP Service Area in the CT – NoCC Scenario

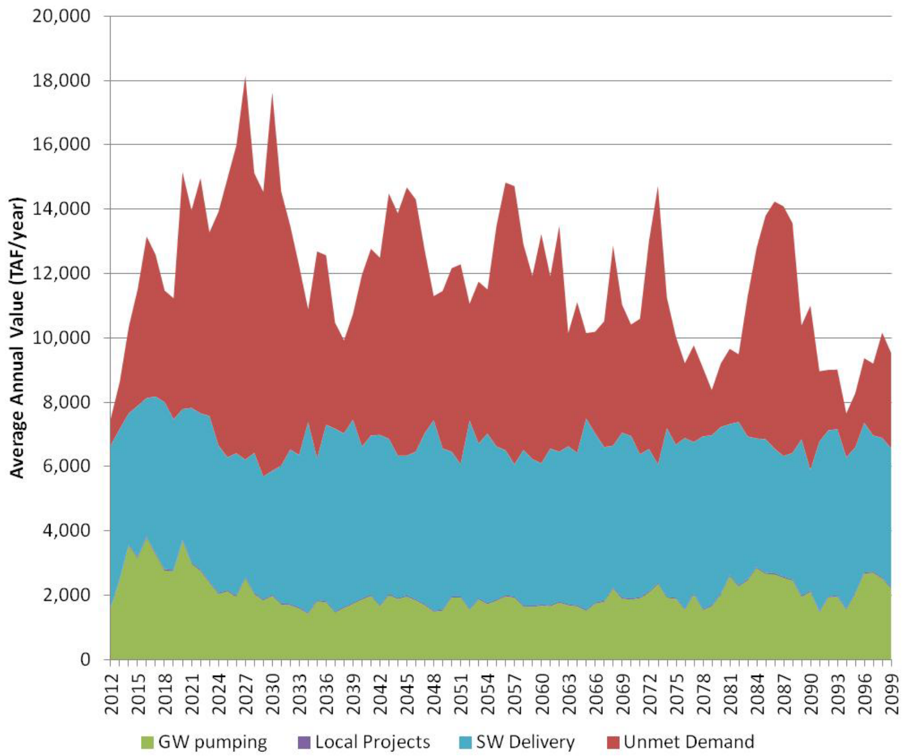

Figure 3-94. Annual Time Series of Supplies and Unmet Demand in CVP Service Area in the CT – Q5 Scenario

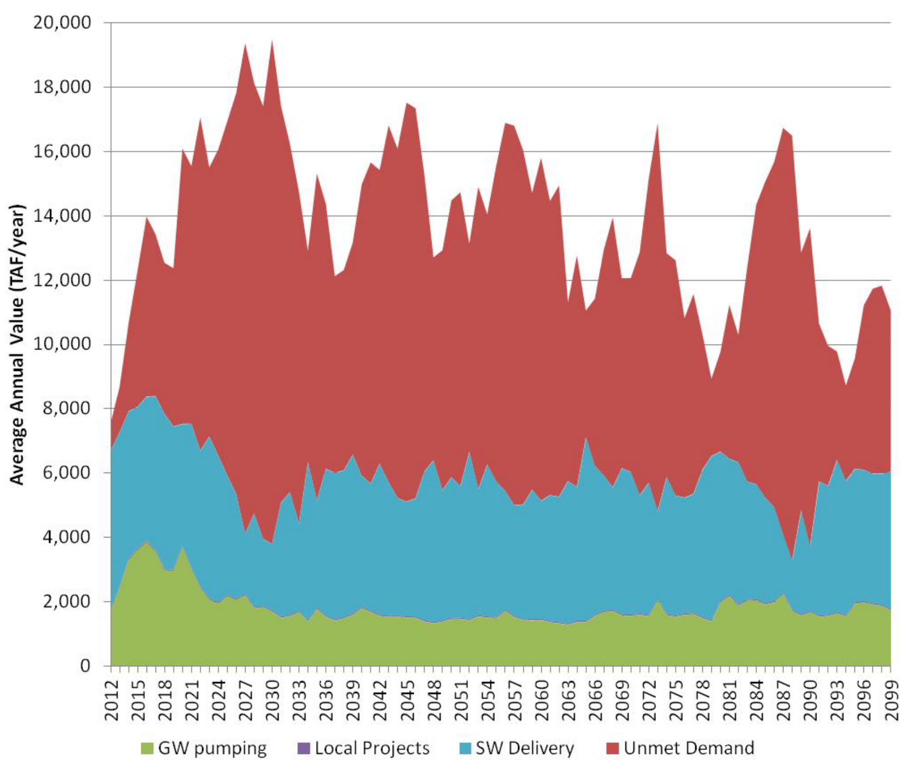

Figure 3-95. Annual Time Series of Supplies and Unmet Demand in CVP Service Area in the EG – Q2 Scenario

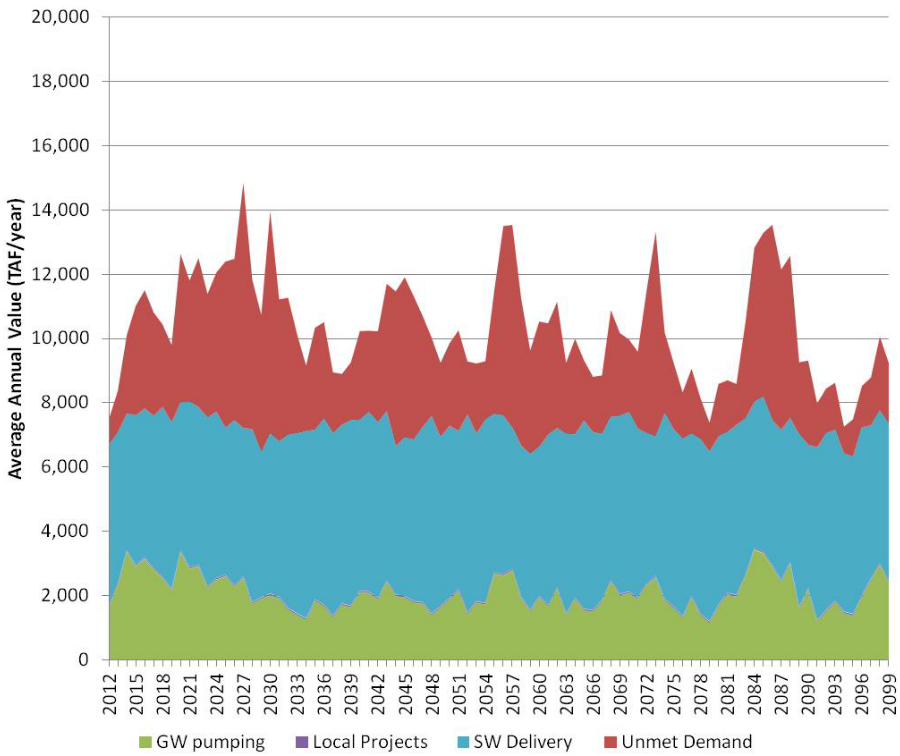

Figure 3-96. Annual Time Series of Supplies and Unmet Demand in CVP Service Area in the SG – Q4 Scenario

Results of Other Performance Assessment Tools

The following sections describe the results of the other performance assessment tools for the Baseline condition. The socioeconomic-climate scenarios analyzed under Baseline conditions include the CT-Q5, to represent a midrange projection of climate effects; EG-Q2, to represent the upper range of effects and SG-Q4 to represent the lower range of climate effects. Because of the sensitivity of the economic and temperature models to climate inputs, additional scenarios were simulated for the economic and temperature models without climate change to better understand the effects of climate change on the results. The results of these simulations are described below. More detailed descriptions of the models are provided in Section entitled Application of Additional Performance Assessment Tools.

Economics The results from four economically based water management models are presented in this section. These models provide the following capabilities:

- LCPSIM provides economic results for the South San Francisco Bay-South Region
- OMWEM provides economic results for urban regions in Central Valley

- SBWQM estimates salinity costs for deliveries to the South San Francisco Bay Region
- SWAP provides economic results for agricultural regions in the Central Valley.

Because these economic models are designed to analyze differences between two different scenarios rather than the absolute values of a single scenario, the results are summarized in terms of differences in average annual net benefit between the different socioeconomic-climate scenarios described above. In addition, the results from these economic models are presented at three future levels of development (LOD). Three LODs were selected to represent early (2025), mid (2050) and late (2085) 21st century socioeconomic and climate conditions. This approach allows for a clearer understanding of how the changes in socioeconomic and climate factors affect the net economic benefits in the CVP Service area over different timeframes during the 21st century.

The following discussion presents the results in two steps because the model inputs differ significantly both between different socioeconomic scenarios and different climate scenarios,

1. Comparisons of the three socioeconomic scenarios without climate change, to understand the effect of socioeconomic changes
2. Comparisons of CT-Q5, EG-Q2, and SG-Q4 scenarios with their corresponding no climate change scenario to understand the effects of climate changes

To evaluate the effects of changes in socioeconomic conditions, simulations of all three growth scenarios without climate change were compared. Figure 3-97 through Figure 3-99 show the changes in net water supply system costs in LCPSIM and OMWEM and in net revenue in SWAP for the Expansive Growth and Slow Growth scenarios relative to the Current Trends at the 3 LODs. (The SBWQM is not capable of producing comparisons between simulations at different socioeconomic conditions and is therefore not included in this comparison.) All three models indicate that there are significantly less net water supply system costs and significantly more net revenue in the Slow Growth scenario than in the Current Trends scenario, and significantly more net water supply system costs and significantly less net revenue in Expansive Growth than in the Current Trends scenario. Furthermore, these differences continue to increase during the 21st century. The primary factors accounting for these differences are the changes in population and corresponding changes in land use from agricultural to urban use that occur in each socioeconomic scenario. The Expansive Growth scenario represents the greatest increase in population and in conversion of agricultural land to urban and consequently has more water supply system costs in the urban models and the lowest net revenue in the agricultural model as compared to the Current Trends scenario. Conversely, Slow Growth has lowest increase in population and the smallest conversion of agricultural land to urban, which results in lower water supply system costs in the urban models and greater net revenue in the agricultural model relative to Current Trends.

Figure 3-97. Change in Average Annual Net Benefit in South San Francisco Bay Region from LCPSIM

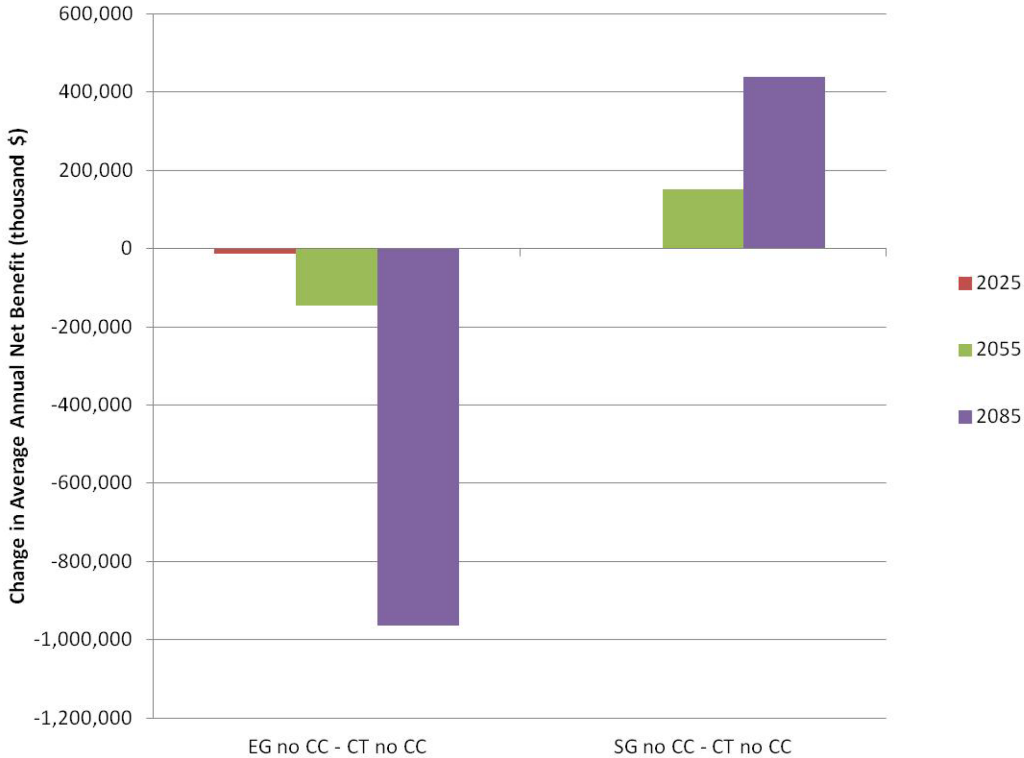

Figure 3-98. Change in Average Annual Net Benefit in Central Valley Urban Areas from OMWEM

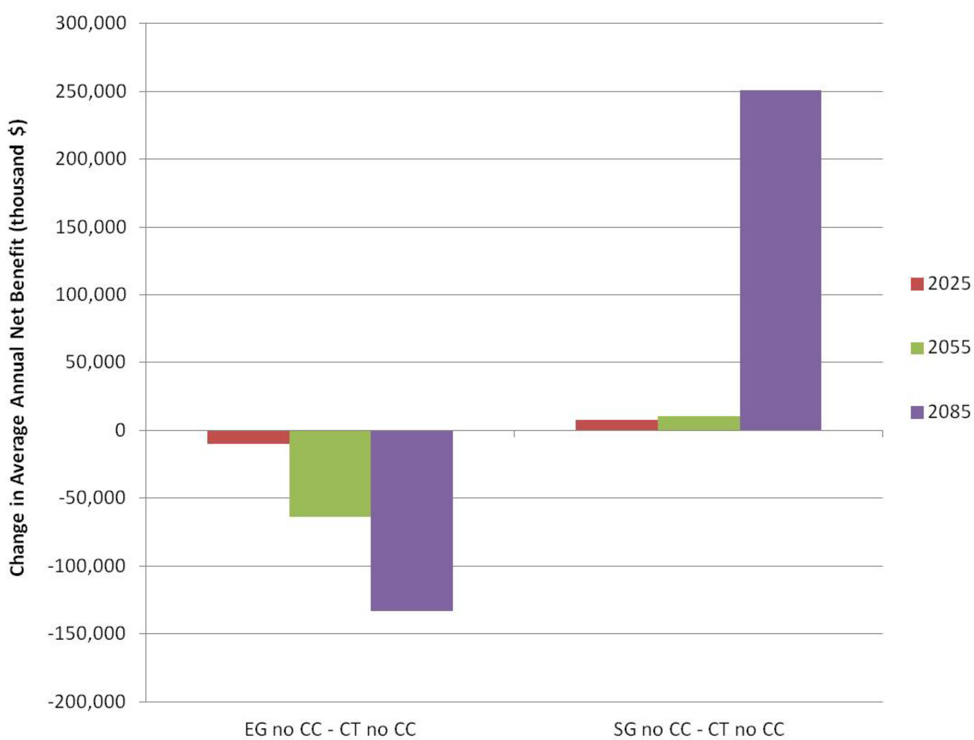

Figure 3-99. Change in Average Annual Net Benefit in Central Valley Agricultural Areas from SWAP

Figure 3-100 through Figure 3-103 show the changes in net economic benefits for scenarios CT-Q5 relative to CT-noCC, EG-Q2 relative to EG-noCC, and SG-Q4 relative to SG-noCC, at the 3 LODs based results from LCPSIM, OMWEM, SBWQM and SWAP. The urban economic models (LCPSIM, OMWEM and SBWQM) show decreases in net economic benefits in CT-Q5 and EG-Q2 due to decreased Delta exports and increased salinity at the Delta pumping locations. OMWEM shows increases in net benefit in SG-Q4 due to increased surface water deliveries in the Central Valley, but LCPSIM has almost no change in benefits because Delta exports in SG-Q4 are almost the same as in SG-noCC. SBWQM shows a net benefit in SG-Q4 relative to SG-noCC because of improved salinity conditions at the Delta exporting locations reduce the salinity costs to the South Bay export regions.

SWAP has similar changes in deliveries as OMWEM, but shows increases in net benefits in all three scenarios because improvements in agricultural production due to climate changes such as increasing CO_2 override the negative effects of reduced SWP and CVP deliveries due to reductions in water supplies in CT-Q5 and EG-Q2.

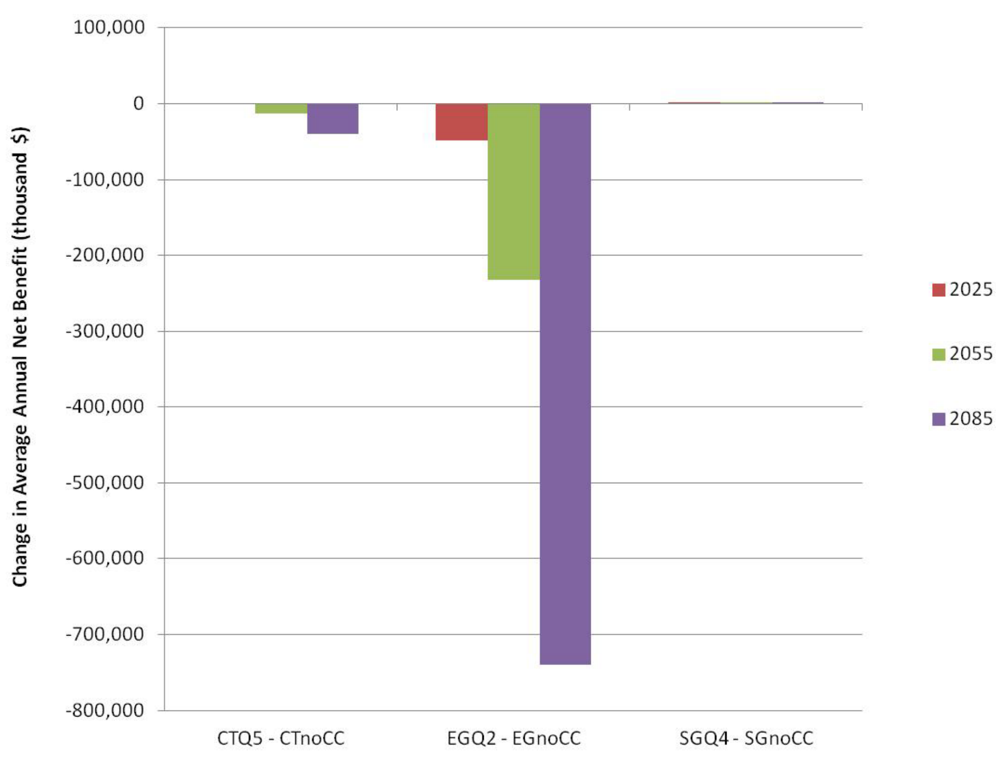

Figure 3-100. Change in Average Annual Net Benefit in South San Francisco Bay Region from LCPSIM

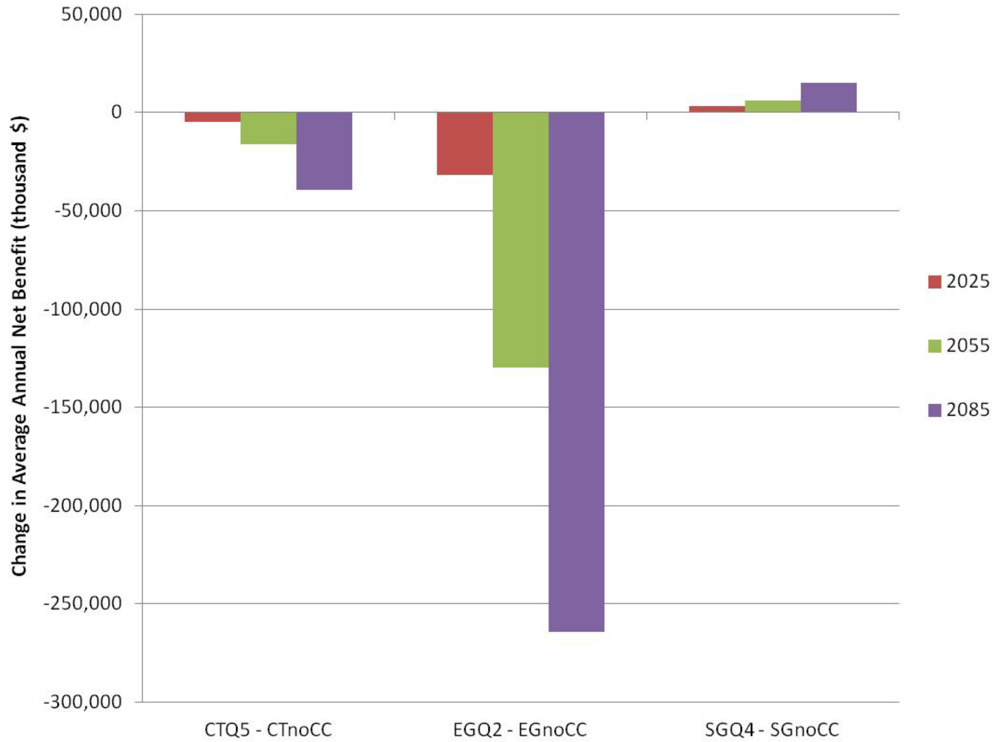

Figure 3-101. Change in Average Annual Net Benefit in Central Valley Urban Areas from OMWEM

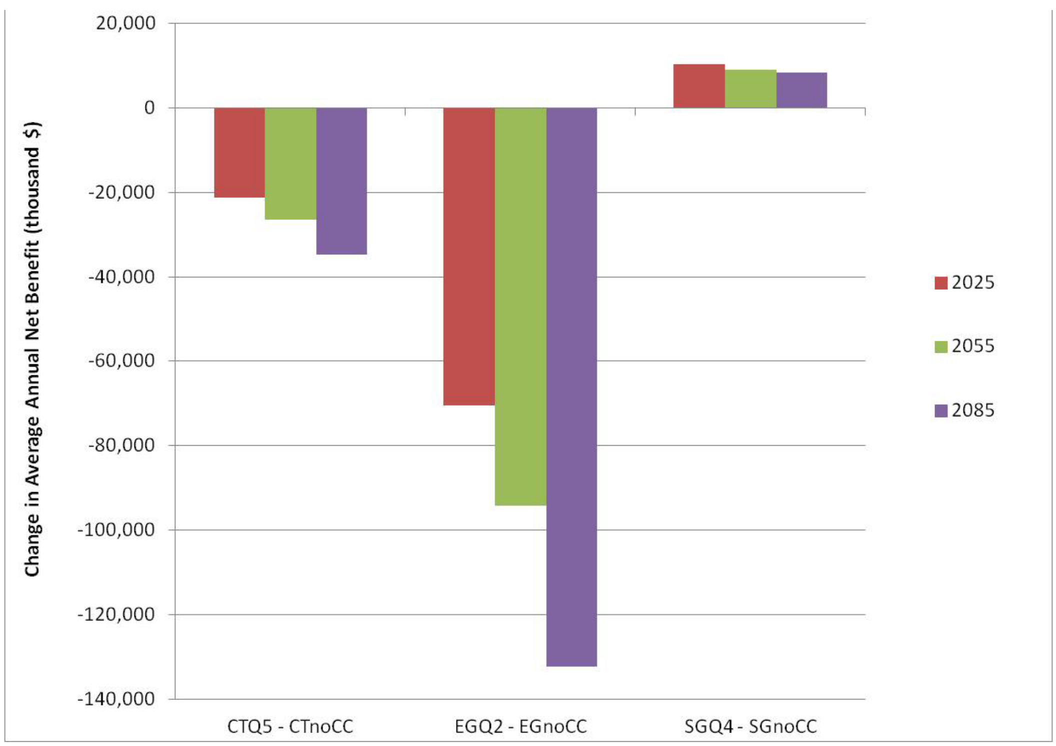

Figure 3-102. Change in Average Annual Net Benefit in South San Francisco Bay Region Salinity Costs from SBWQM

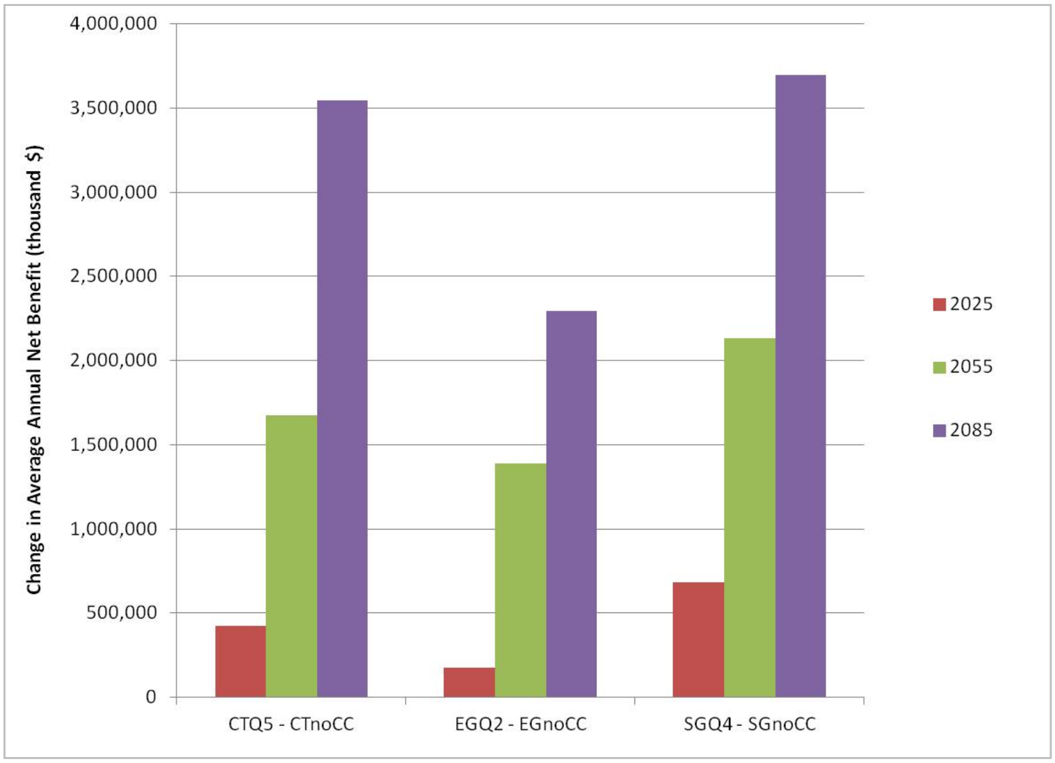

Figure 3-103. Change in Average Annual Net Benefit in Central Valley Agricultural Areas from SWAP

Water Temperature To understand the effects of climate change on river temperatures, the Sacramento (USRWQM) and San Joaquin temperature (SJRWQM) models were simulated for the CT-noCC scenario as well as the CT-Q5, EG-Q2, and SG-Q4 scenarios.

Figure 3-104 through Figure 3-107 show exceedence plots and box plots of daily temperatures from July through September for these four scenarios in the Sacramento River at Keswick and at Jellys Ferry. At both locations the temperatures in SG-Q4 are a modest amount lower than those in CT-noCC, reflecting the effects of increased Shasta cold water pool, and greater flows in the river. Conversely, the temperatures in CT-Q5 are a modest amount higher and the temperatures in EG-Q2 are higher than those in CT-noCC at both locations, also reflecting the changes in the storage and flow levels at each location. The mean July-September temperatures in EG-Q2 are 53.3°F at Keswick and 56.7°F at Jellys Ferry, as compared to 50.7°F at Keswick and 53.7°F at Jellys Ferry in SG-Q4. These reflect a range of about 3 degrees on average between the two most extreme climate conditions and also a difference of about 3 degrees between the two locations indicative of the majority of the spawning and rearing habitat in the upper Sacramento River.

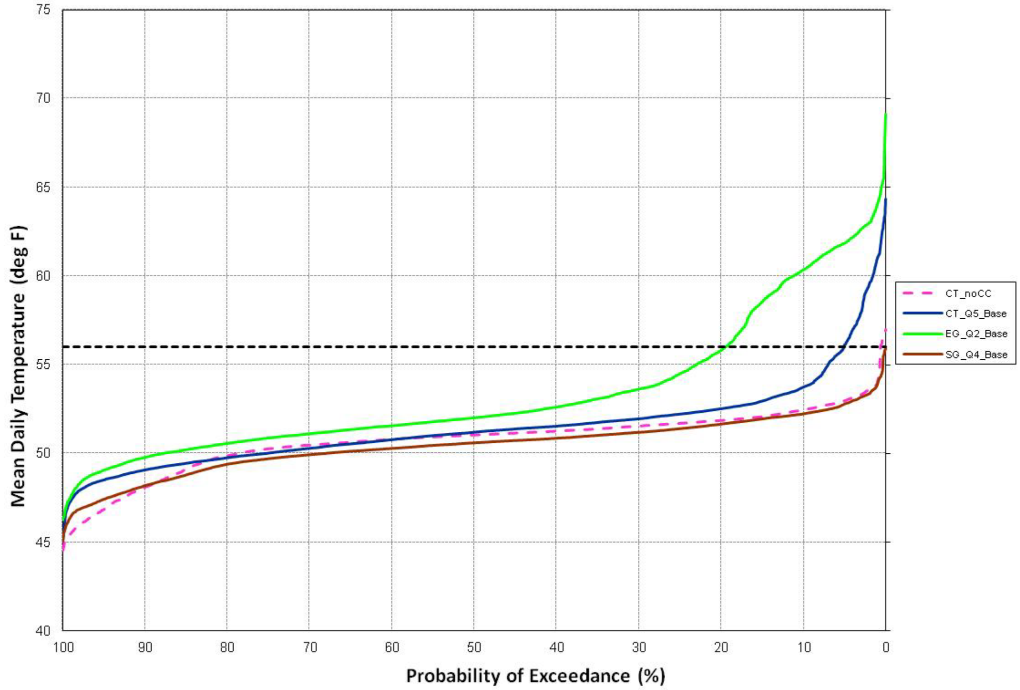

Figure 3-104. Exceedence of Average Daily Water Temperature on Sacramento River at Keswick from July-to-September in each Scenario

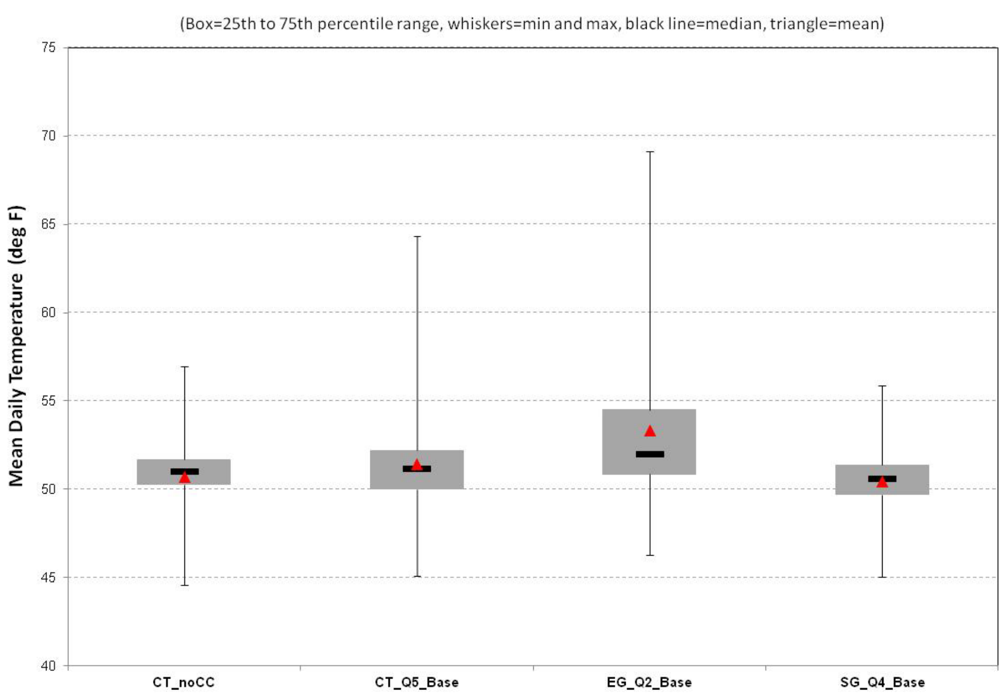

Figure 3-105. Box Plot of Average Daily Water Temperature on Sacramento River at Keswick from July-to-September in each Scenario

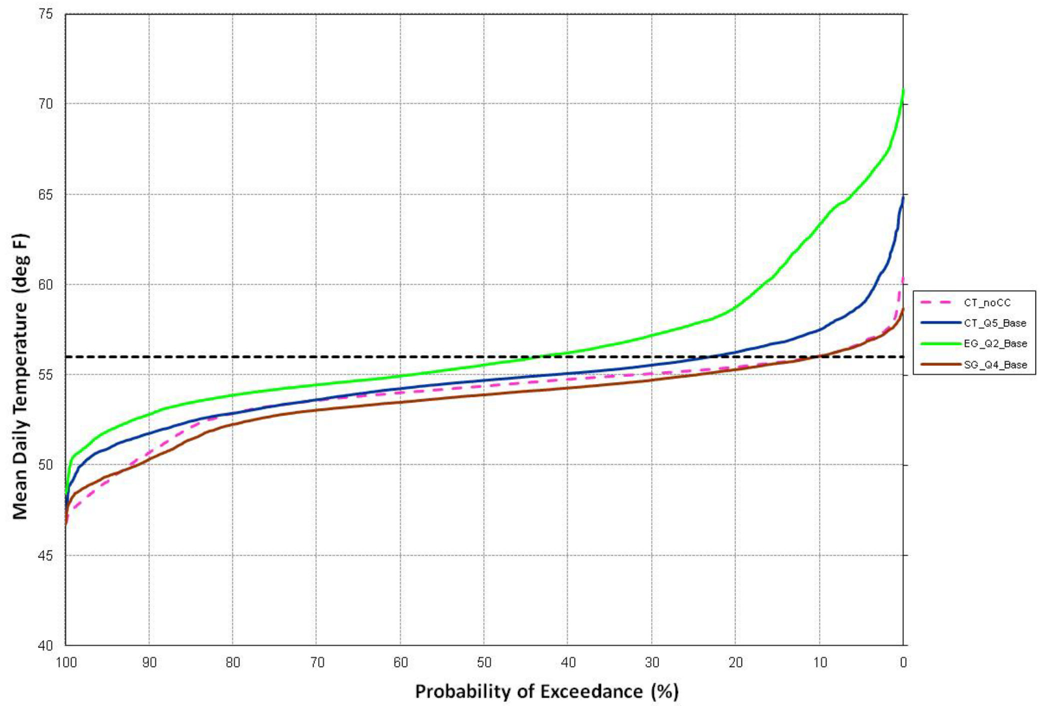

Figure 3-106. Exceedence of Average Daily Water Temperature on Sacramento River at Jellys Ferry from July-to-September in each Scenario

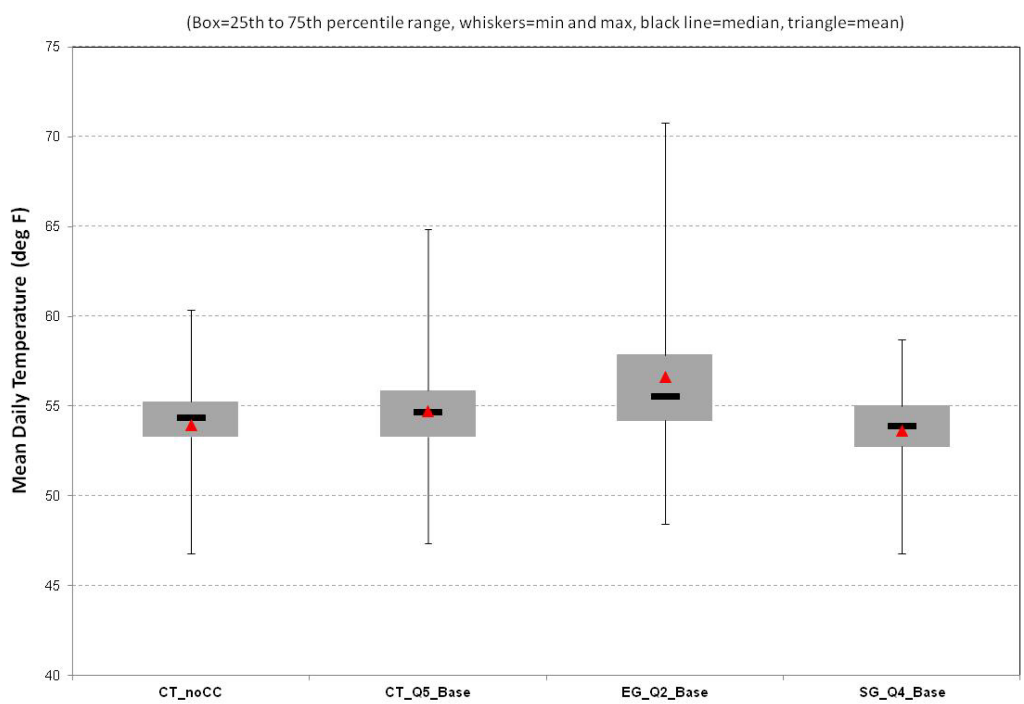

Figure 3-107. Box Plot of Average Daily Water Temperature on Sacramento River at Jellys Ferry from July-to-September in each Scenario

Figure 3-108 through Figure 3-113 show exceedence plots and box plots of daily temperatures for the same four scenarios in the San Joaquin River at Lost Lake, at Gravelly Ford and at Vernalis locations from August through November. The mean daily temperatures at Lost Lake (just downstream from Millerton Lake) during these months range from 53.5 to 54.9°F across the four scenarios. With respect to CT-noCC scenario, scenarios CT-Q5 and EG-Q2 show reduced temperatures at this location, while SG-Q4 shows a small increase. The lowest temperatures are in the EG-Q2 scenario, with the largest temperatures occurring in the SG-Q4 scenario. The warming under SG-Q4 occurs because Millerton Lake has limited capacity to hold high flows, so when there are higher inflows to Millerton (as occurs frequently in climate scenario Q4) the thermocline in the lake is disturbed as the high flows flush out any cold water stored in the Lake. This causes warm flows to be passed down the river, resulting in warmer temperatures at Lost Lake. Conversely, when there are lower inflows into Millerton (as occurs frequently in climate scenario Q2) the thermocline in the Lake is retained and the water released from Millerton is colder, resulting in cooler temperatures at Lost Lake, as observed in the EG-Q2 scenario.

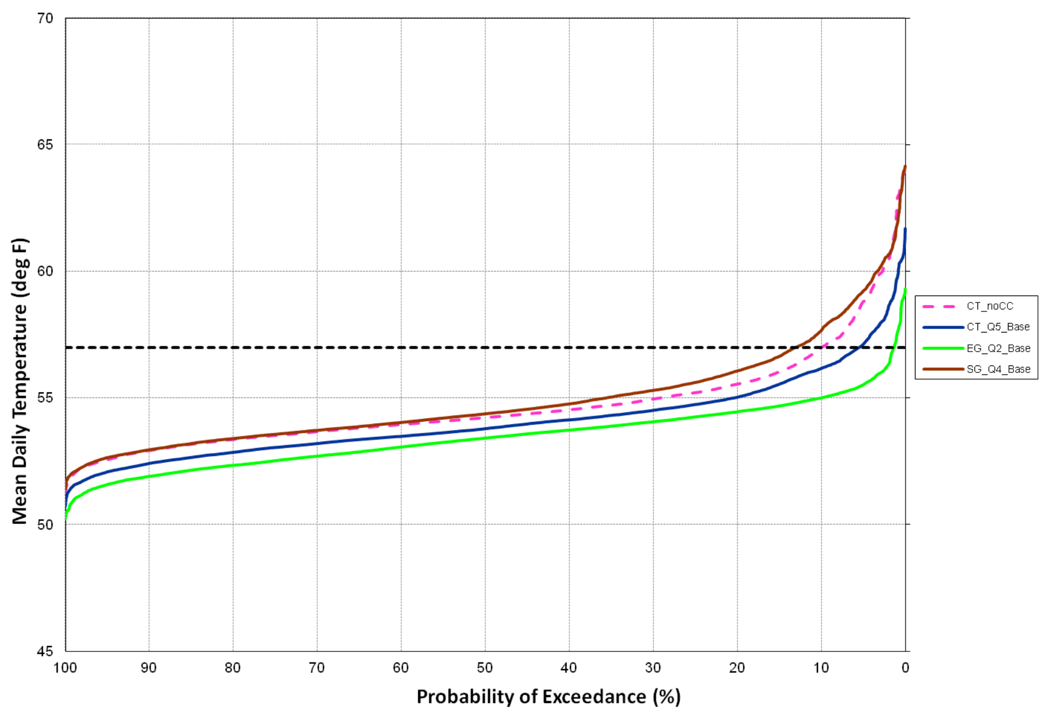

Figure 3-108. Exceedence of Average Daily Water Temperature on San Joaquin River at Lost Lake from August-to-November in each Scenario

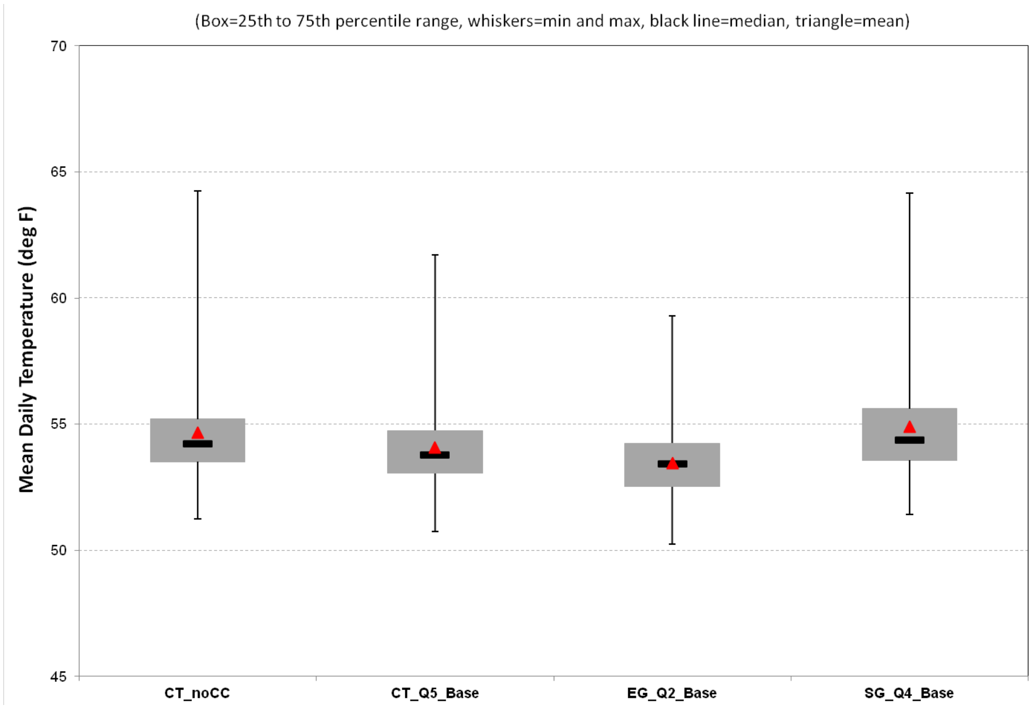

Figure 3-109. Box Plot of Average Daily Water Temperature on San Joaquin River at Lost Lake from August-to-November in each Scenario

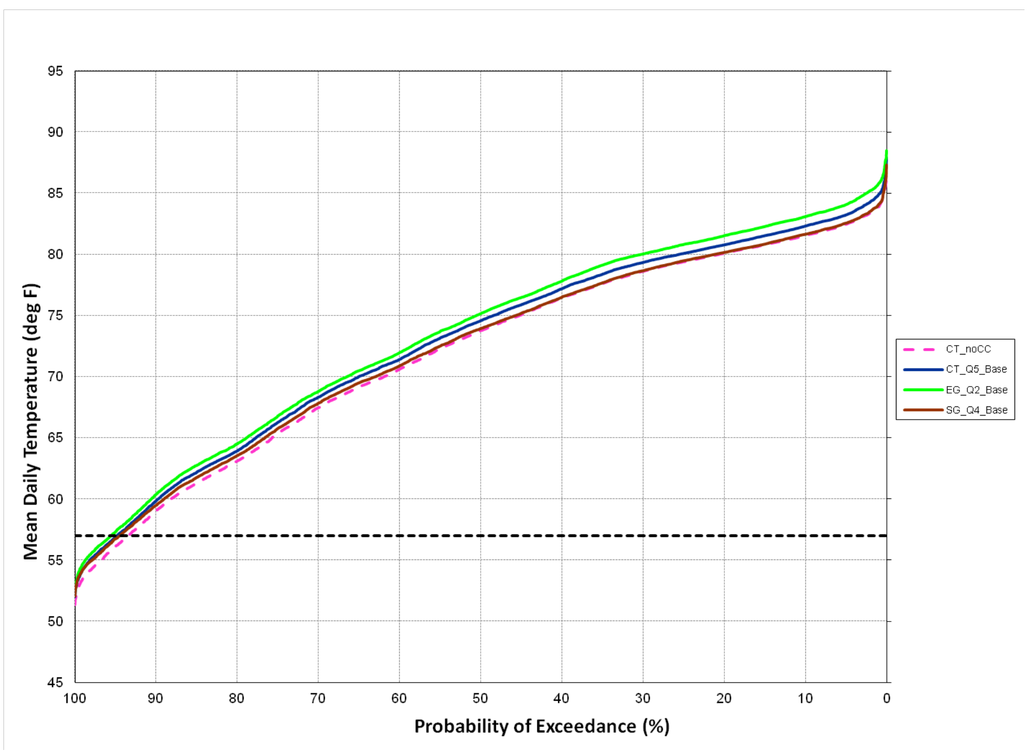

Figure 3-110. Exceedence of Average Daily Water Temperature on San Joaquin River at Gravelly Ford from August-to-November in each Scenario

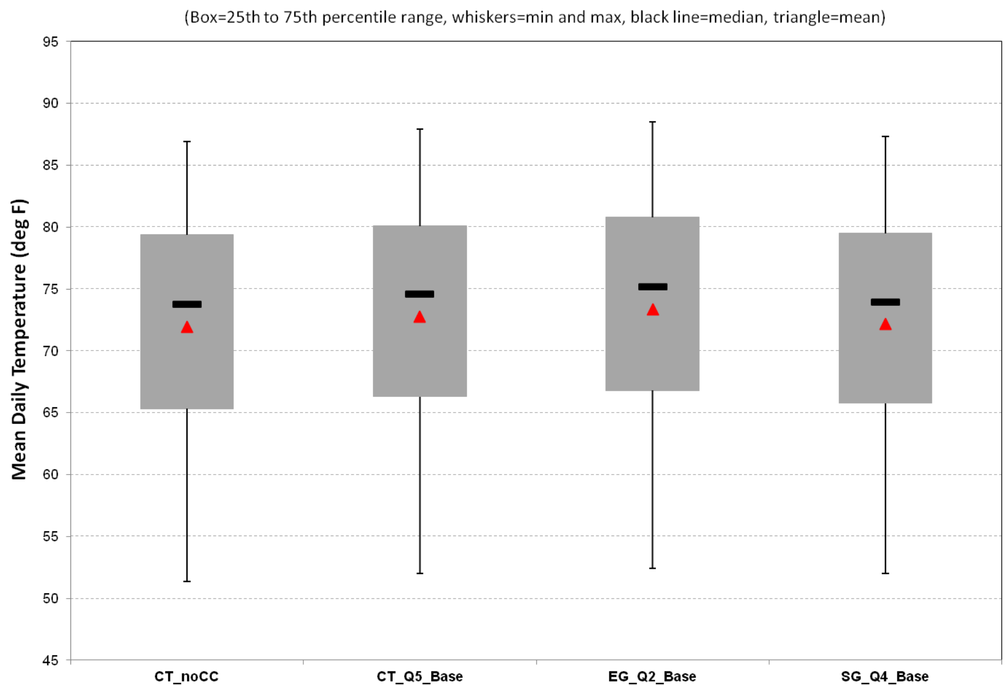

Figure 3-111. Exceedence of Average Daily Water Temperature on San Joaquin River at Gravelly Ford from August-to-November in each Scenario

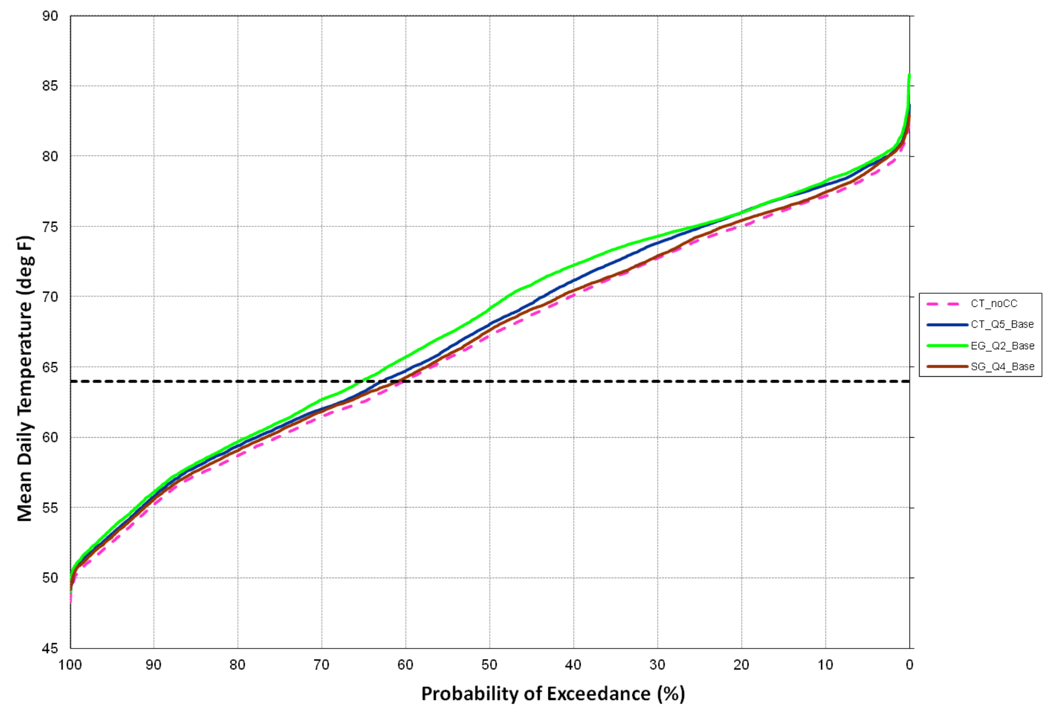

Figure 3-112. Exceedence of Average Daily Water Temperature on San Joaquin River at Vernalis from August-to-November in each Scenario

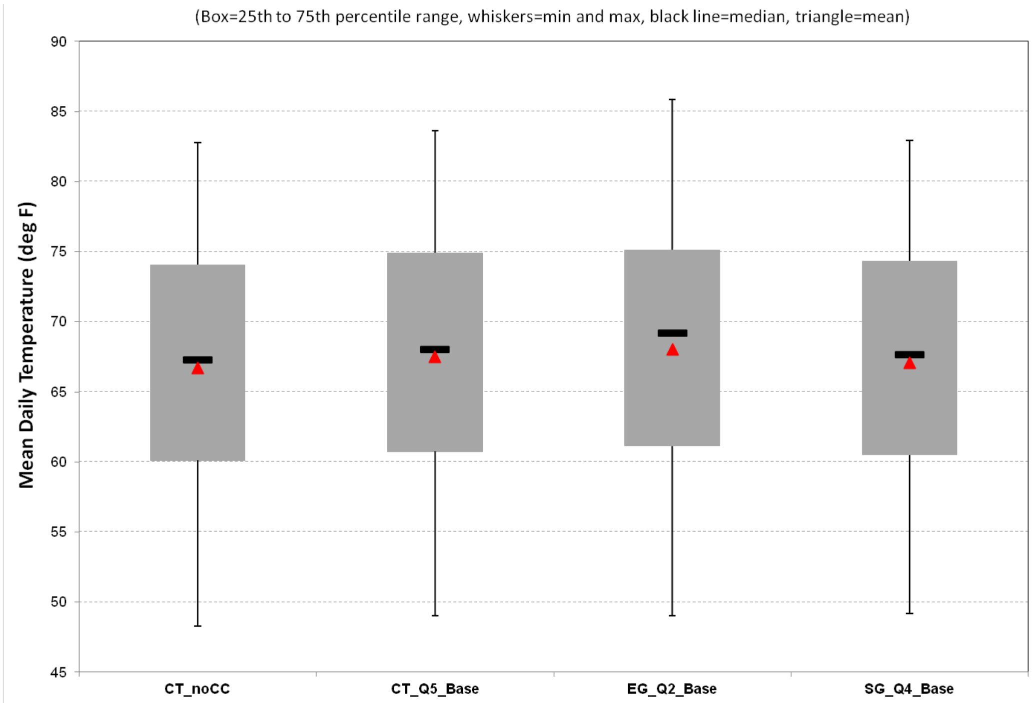

Figure 3-113. Box Plot of Average Daily Water Temperature on San Joaquin River at Vernalis from August-to-November in each Scenario

Further downstream on the San Joaquin River at Gravelly Ford, the mean daily temperatures increase significantly under all climate scenarios due to the effects of diversions in this reach of the San Joaquin River and lower elevation. The warming is greatest in Q2 and smallest in Q4, causing an inverting of the temperature results between scenarios at Gravelly Ford as compared to Lost Lake. At Gravelly Ford, the mean daily temperature in these scenarios during these months range from a low of 72.2°F in SG-Q4 to a high of 73.4°F in EG-Q2, with CT-noCC being at 71.9°F.

At Vernalis, the temperature results show warming under all climate scenarios reflecting the effects of all operations in the San Joaquin River system including the tributaries. The mean daily average temperature at Vernalis in the CT-noCC scenario is 66.7°F. For the three climate scenarios, the mean daily temperatures at Vernalis range from 67°F to 68°F, with lowest in the SG-Q4 scenario, and highest in the EG-Q2 scenario.

Hydro-Power and Green House Gases Figure 3-114 shows the average annual net energy generation for the CVP and SWP systems under the CT_Q5, EG_Q2 and SG_Q4 scenarios based on the results from LT_Gen for the CVP and SWP_Power for the SWP. In all three socioeconomic-climate scenarios, the CVP system has more hydropower generation than energy use while the SWP system has more energy use than hydropower generation. The relative levels of net generation between the three scenarios are consistent with the CVP storage and the Banks pumping results for each scenario. SG_Q4 has the highest storage levels in CVP reservoirs and the greatest amount of Banks pumping and therefore has the most CVP net generation and SWP net energy use. Conversely, EG_Q2 has the lowest storage levels in CVP reservoirs and the lowest amount of Banks pumping and therefore has the least CVP net generation and SWP net energy use.

Figure 3-115 presents the average annual net GHG emissions for the CVP and SWP systems under the CT-Q5, EG-Q2 and SG-Q4 scenarios. These results are consistent with the net generation results for the CVP and SWP in each scenario. The CVP system has negative net GHG emissions (i.e., potential GHG offsets) because it has positive net hydropower generation, while the SWP system has positive net GHG emissions because it has negative net hydropower generation. In addition, the net GHG emission results are greatest in SG-Q4 where the net generation results are greatest and lowest in EG-Q2 where the net generation results are lowest.

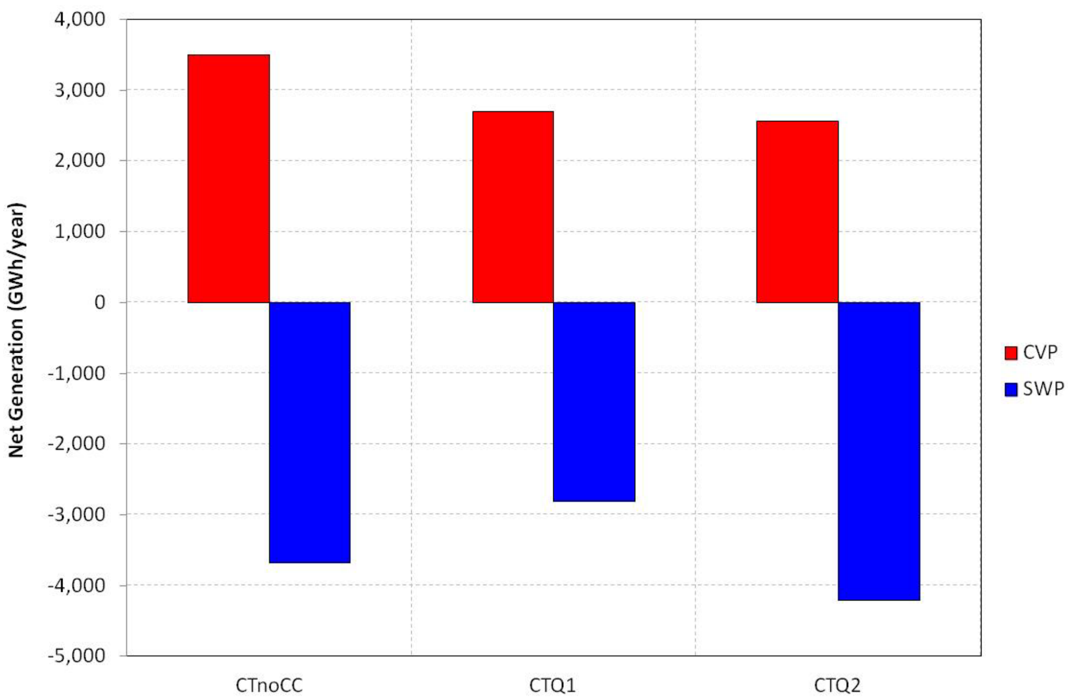

Figure 3-114. Average Annual Net Energy Generation for the CVP and SWP Systems

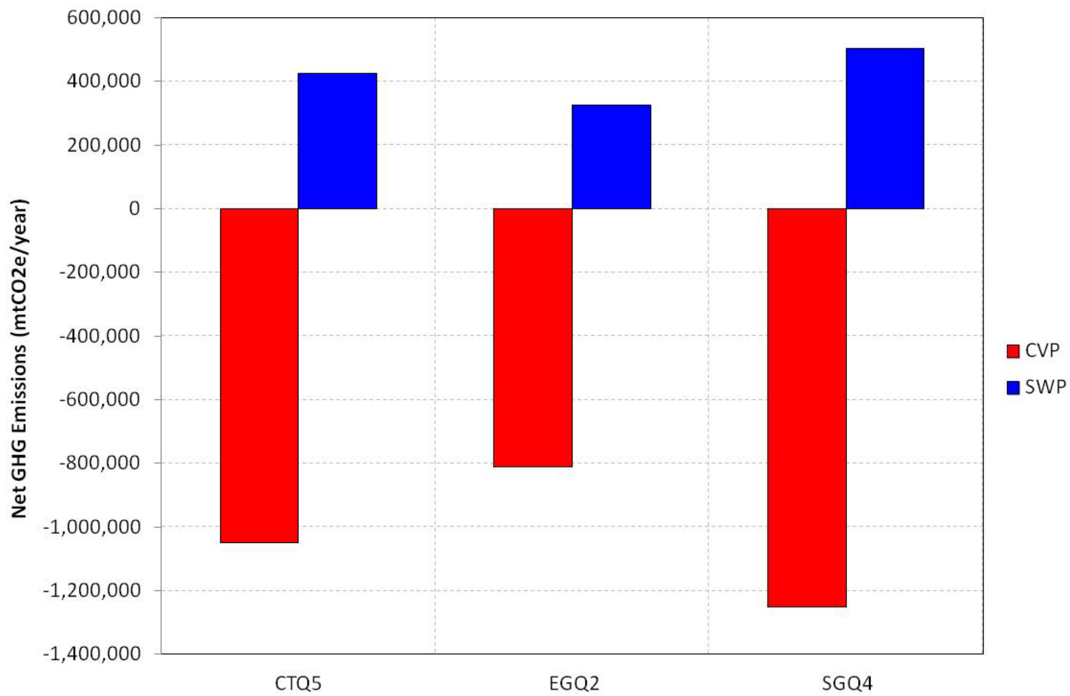

Figure 3-115. Average Annual Net GHG Emissions for the CVP and SWP Systems

Alternative CP5 – Climate Change Analysis

Introduction

The CVP IRP CalLite model was developed and applied to simulate a variety of potential water management actions by combining them into thematic portfolios consisting of a several different types of actions. The primary purpose of the modeling was to analyze the effects of uncertainties in future socioeconomic and climatic conditions on the CVP Service Area. To accomplish these objectives efficiently, the CVP IRP CalLite model was designed to be a comprehensive but simplified representation of the CVP, SWP and non-project water management systems. As such the results presented in this report should not be viewed as fully representative of benefits that might be derived from the alternative CP5 examined in this study.

A graphical user interface was developed for CVP IRP CalLite model to allow users to control which options to include in the simulations. By selecting various combinations of actions from a “dashboard” menu of available actions, users can specify the details of the parameters for particular water management actions. Example dashboards are shown in Figure 3-116 through Figure 3-118.

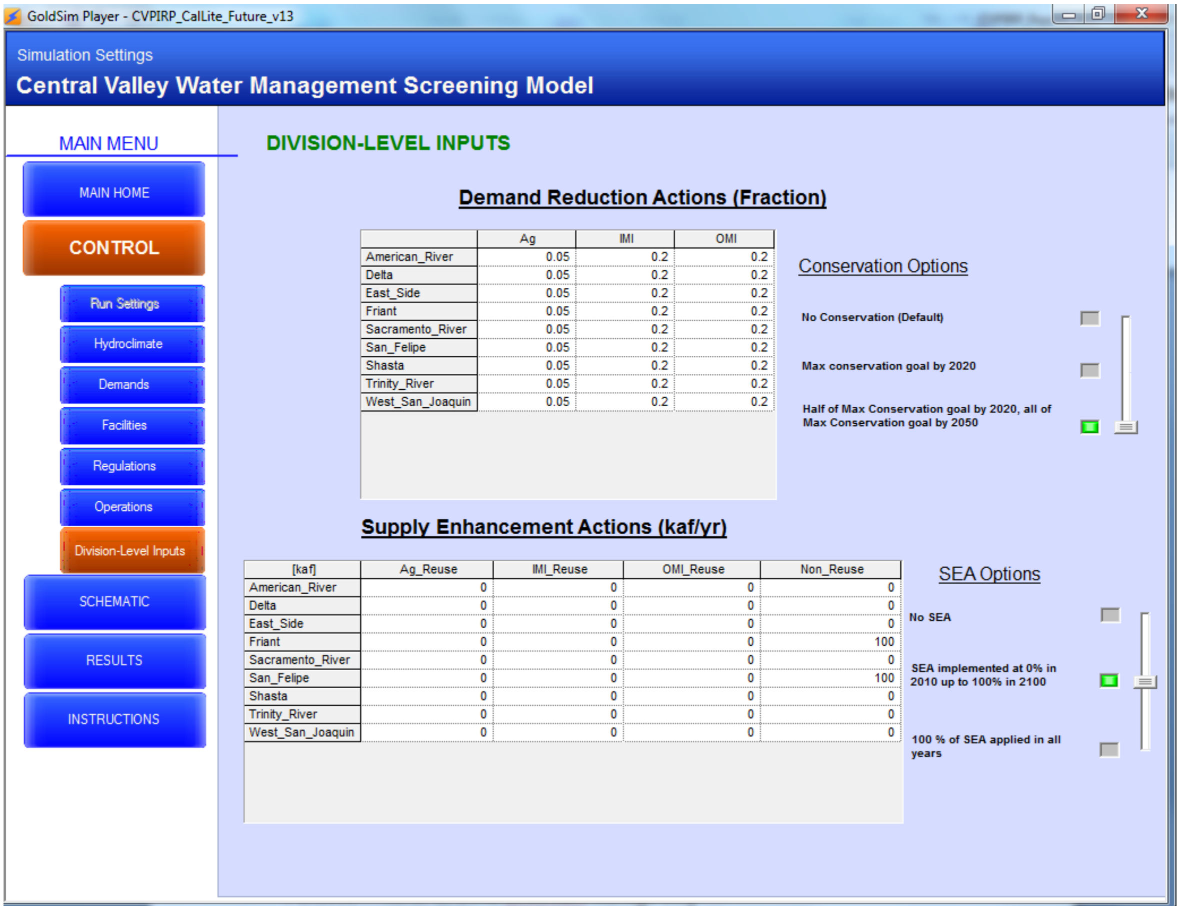

Figure 3-116. Example CalLite Dashboard for Specifying Local Water Management Actions

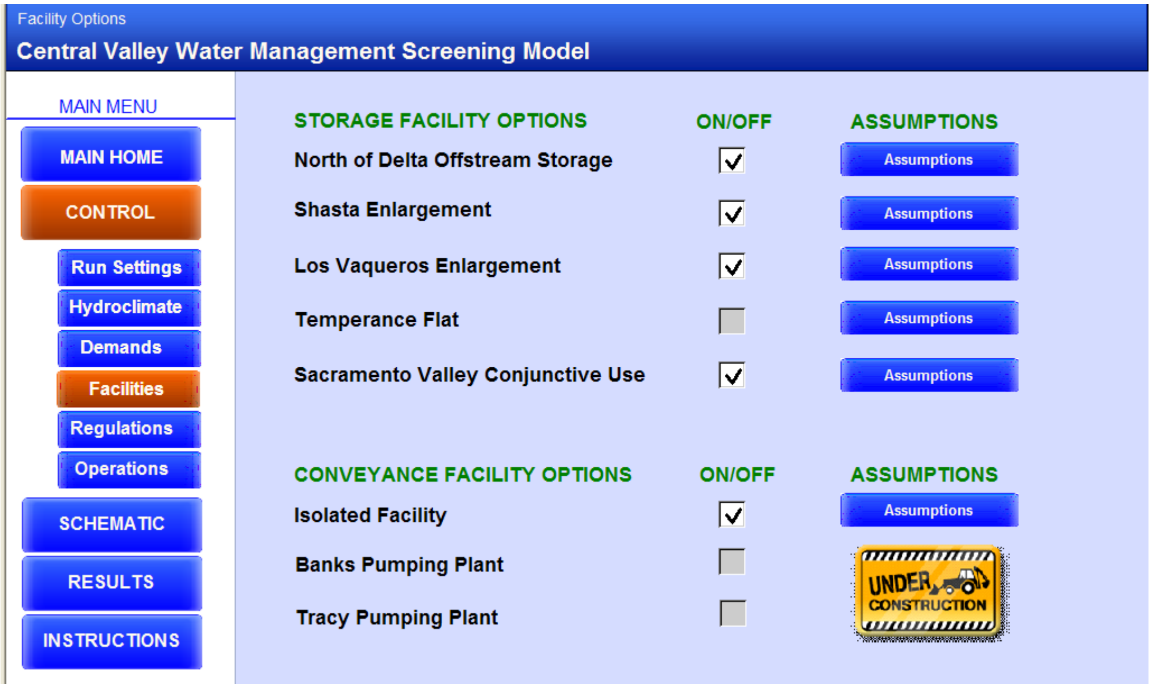

Figure 3-117. Example CalLite Dashboard for Triggering New Storage or Conveyance Facilities

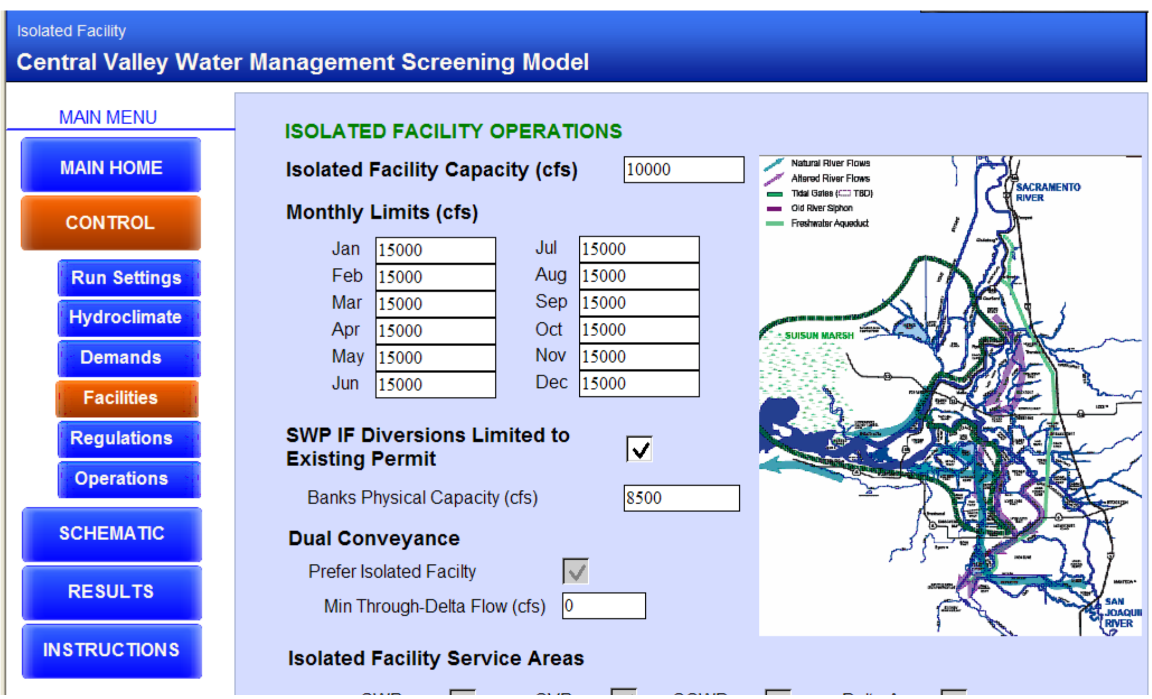

Figure 3-118. Example CalLite Dashboard for Specifying Storage and Conveyance Facility Assumptions (Isolated Facility shown)

The primary objectives of the alternatives identified in the SLWRI are (1) increase survival of anadromous fish populations in the Sacramento River primarily upstream from the Red Bluff Pumping Plant; and, (2) increase water supplies and water supply reliability for agricultural, municipal and industrial, and environmental purposes to help meet future water demands, with a focus on enlarging Shasta Dam and Reservoir.

The Shasta Dam enlargement alternatives available for simulation in CalLite include dam raises of 6.5-feet (256 thousand acre-feet (TAF)), 12.5-feet (443 TAF), and 18.5-feet (634 TAF).

Program Core Elements

The following core elements are included in the CalSim-II SLWRI:

- Enlargement of Shasta Dam and Reservoir, as defined for each SLWRI alternative
- Increased Shasta Reservoir storage identified as a component of the CVP for water supply operation and b2 accounting
- Reserving a portion of the increased storage capacity in Shasta Reservoir to specifically focus on increasing M&I deliveries under CP1, CP2, CP4, and CP5

CalLite representation of SLWRI alternatives excludes Central Valley Project Improvement Act (CVPIA) (b)(2) requirements since the model is currently constructed for D1641 level of requirements.

Options Available in the Model

For the purposes of the screening model implementation, three Shasta Lake enlargement alternative dam raises of 6.5-feet (256 TAF), 12.5-feet (443 TAF), and 18.5-feet (634 TAF) are available. Banks capacity options (6,680 cubic feet per second (cfs) and 8,500 cfs) considered in CalSim-II SLWRI studies are not explicitly included in CalLite.

For the CVP IRP, an 18.5-feet raise is assumed for all simulations in which CP5 is implemented.

Schematic Representation

Unlike the additional storage element in CalSim-II representation (S44), schematic representation in the CVP IRP CalLite model includes a single reservoir with increased capacity.

Facility Operations

To ensure proper operation of the enlarged reservoir, storage-area and storage-elevation curves have been modified, and the target storage level has been adjusted by the user-defined increased storage to ensure that the same flood control space is preserved in Shasta Reservoir. Once these modifications are activated, Shasta Reservoir functions as the original reservoir element and enlargement volumes operate as an additional storage component of the CVP.

Trinity import adjustments are also needed to re-balance the Trinity with the increase in Shasta storage.

Integration with SWP/CVP System

The enlarged portion of Shasta Reservoir under CP5 is considered a component of the CVP as Shasta storage and is directly integrated into COA, water supply indices, operational decisions, etc. CalSim-II WSI-DI curves with alternative CP5 were incorporated into the CVP IRP CalLite model.

Under CP5, Shasta Dam would be raised by 18.5 feet, increasing the storage capacity in Shasta Reservoir by approximately 634 TAF. A portion of the increased storage capacity in Shasta Reservoir under CP5 would be reserved to specifically focus on increasing M&I deliveries in dry and critical water years.[2] Operations targeting increased M&I deliveries were based on existing and anticipated future demands, operational priorities, and facilities of the SWP, which provides M&I water to a majority of the State's population. These operations were simulated by using the reserved storage capacity to provide deliveries for previously unmet SWP demands during dry and critical years. Regardless of Shasta Lake storage condition, a maximum of 75 TAF would be reserved for increasing M&I deliveries in critical years and a maximum of 150 TAF would be reserved for increasing M&I deliveries in dry years. The total annual releases targeting M&I deliveries were limited to the allocation in a given year (from the total storage available under the alternative). However, only about 33 percent of the allocation can be used in the month of June. Following June, only 50 percent of the remaining allocation can be used in the month of July. Following July, the remaining allocation can be used in any month between August and December.

[2] Water year types are defined according to the Sacramento Valley Index Water Year Hydrologic Classification unless specified otherwise.

If the selected alternative was as a dam raise of 6.5-feet (256 TAF increased storage capacity) or 12.5-feet (443 TAF increased storage capacity), the amount of increased storage capacity reserved for targeting M&I deliveries in dry and critical years would be reduced according to the lesser amount of overall increased storage capacity under each alternative.

User Input and Output Requirements

The user is provided with a check box to turn on/off the SLWRI options. If turned on, the user has three more check boxes representing three enlargement alternatives to choose from. Once the user selects a new size, all the related inputs are activated within the model.

Limitations

Limitations of the SLWRI implementation in the CVP IRP CalLite model include exclusion of CVPIA (b)(2) requirements and possible differences with CalSim-II study due to simplified model schematic.

The CVP IRP CalLite model representation of CP5 varies significantly from the CalSim-II model representation. Rule curve and guide curves are adjusted in CalLite to tune the SLWRI operations in the CalLite simulations to be as similar as possible to the operations observed in CalSim-II model simulations; however due to differences in the baseline assumptions of each of these models and differences in how the model implement assumptions and operations criteria, there will be differences in the results of an alternative between the models.

The sections below describe the results of SLWRI Baseline and alternative CP5. The metrics shown are similar to those that are shown above for the Baseline Analysis. To give an overview of the range of results available from the different socioeconomic-climate scenarios, average annual results from CVP IRP CalLite simulations are shown for all scenarios, while time series and exceedence results from CalLite and all results from the other performance assessment tools are shown for the following three scenarios, selected to reflect the full range of potential futures:

- Current Trends with median temperature change and median precipitation future climate (CT-Q5)
- Expansive Growth with higher temperature change and lower precipitation future climate (EG-Q2)
- Slow Growth with lower temperature change and higher precipitation future climate (SG-Q4)

Alternative CP5 Analysis

The SLWRI analysis was designed to investigate potential improvements in water supply reliability from increasing storage capacity in Shasta Reservoir. This report focuses primarily on the effects of socioeconomic–climate changes on the water supply benefits. It is important to acknowledge that the CVP IRP CalLite model is a simplified representation of the CVP/SWP systems and actual SLWRI project operations are not fully captured in these simulations.

CVP and SWP Project Storage

Figures 3-119 through 3-132 show exceedence plots of reservoir storage over the 21st century in the Baseline and CP5 simulations at the end of May, representing storage available for water supply, and at the end of September, representing carryover storage conditions, in Folsom, Oroville, New Melones, Friant, CVP San Luis, and SWP San Luis reservoirs under scenarios CT_Q5, EG_Q2 and SG_Q4. In Lake Shasta, storage is significantly higher than in the Baseline, reflecting the additional capacity of the enlarged reservoir. With alternative CP5, Oroville and Folsom reservoirs have moderately higher storage levels than in the Baseline conditions reflecting the additional overall increased storage available to meet water demands.

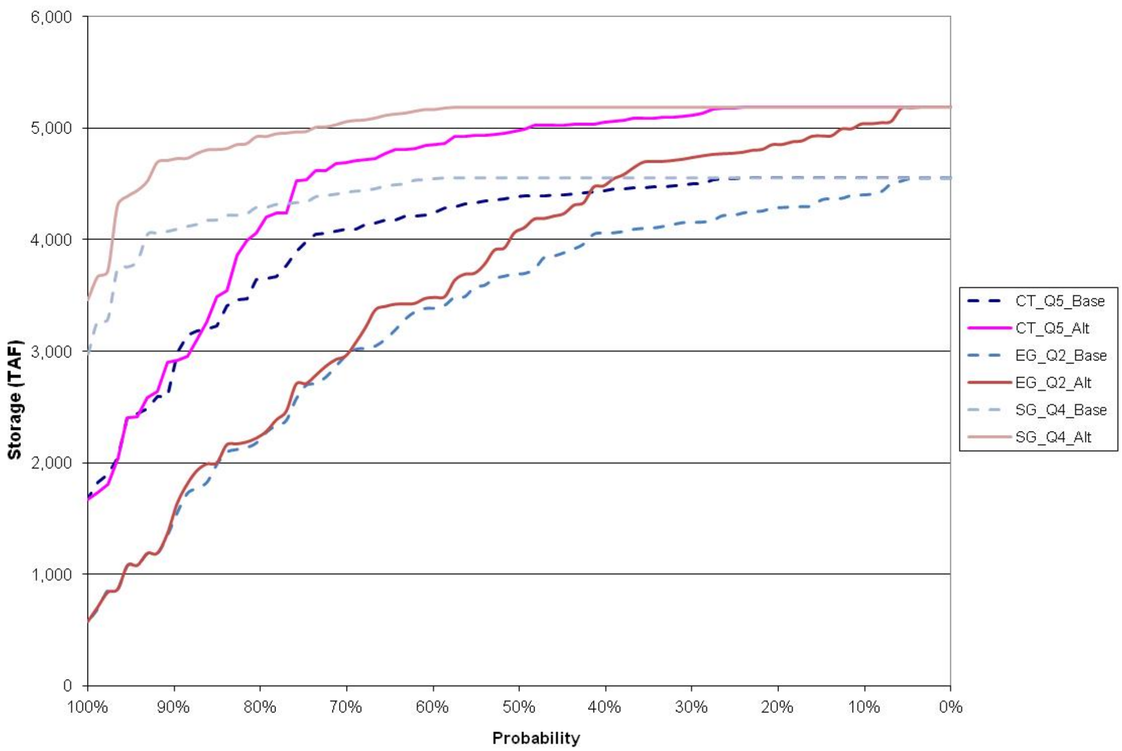

Figure 3-119. Exceedence of Lake Shasta End-of-May Storage with CP5

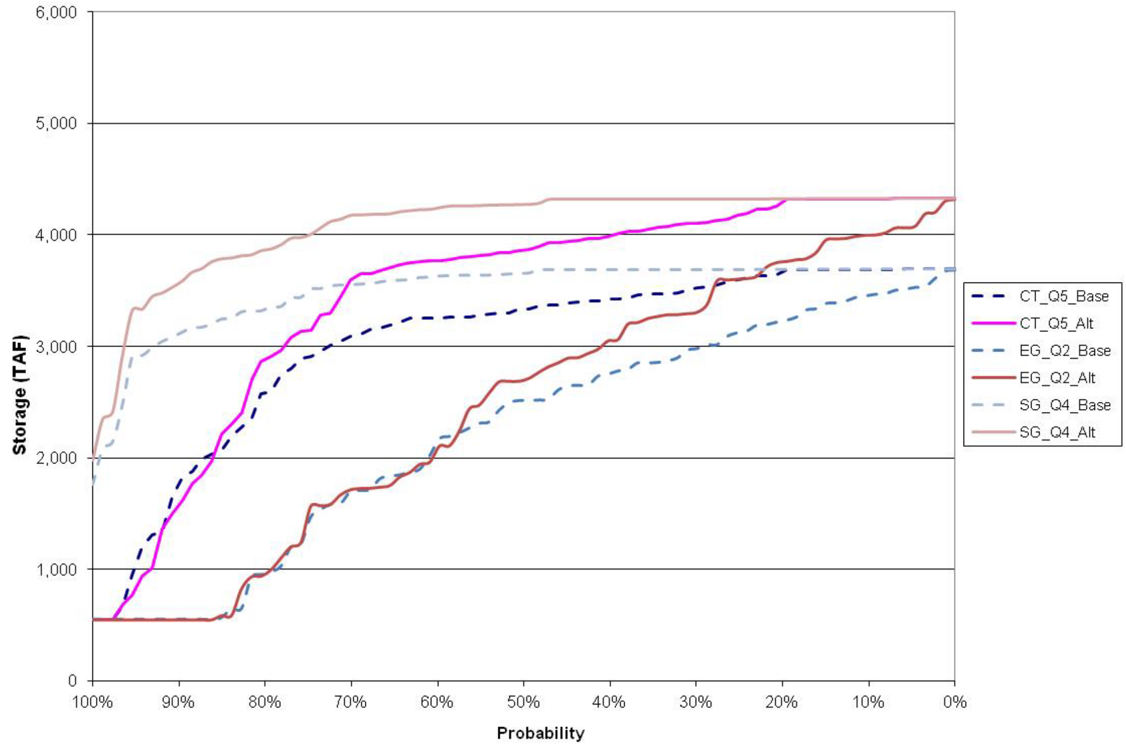

Figure 3-120. Exceedence of Lake Shasta End-of-September Storage with CP5

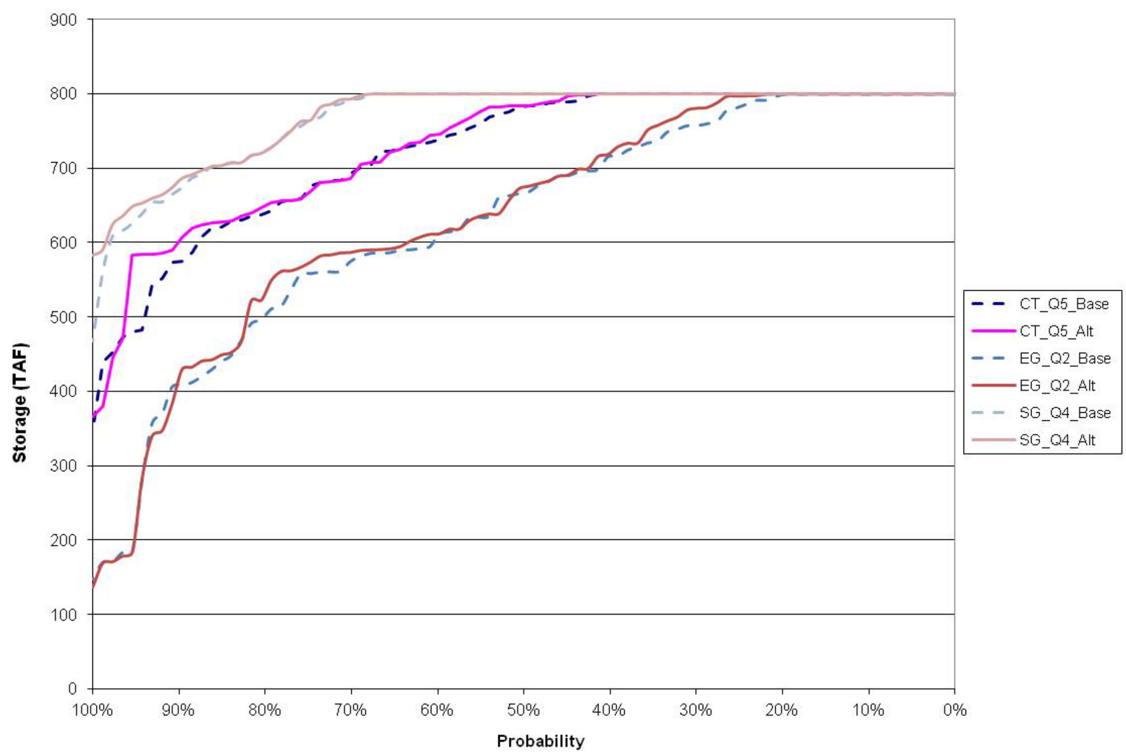

Figure 3-121. Exceedence of Folsom Lake End-of-May Storage with CP5

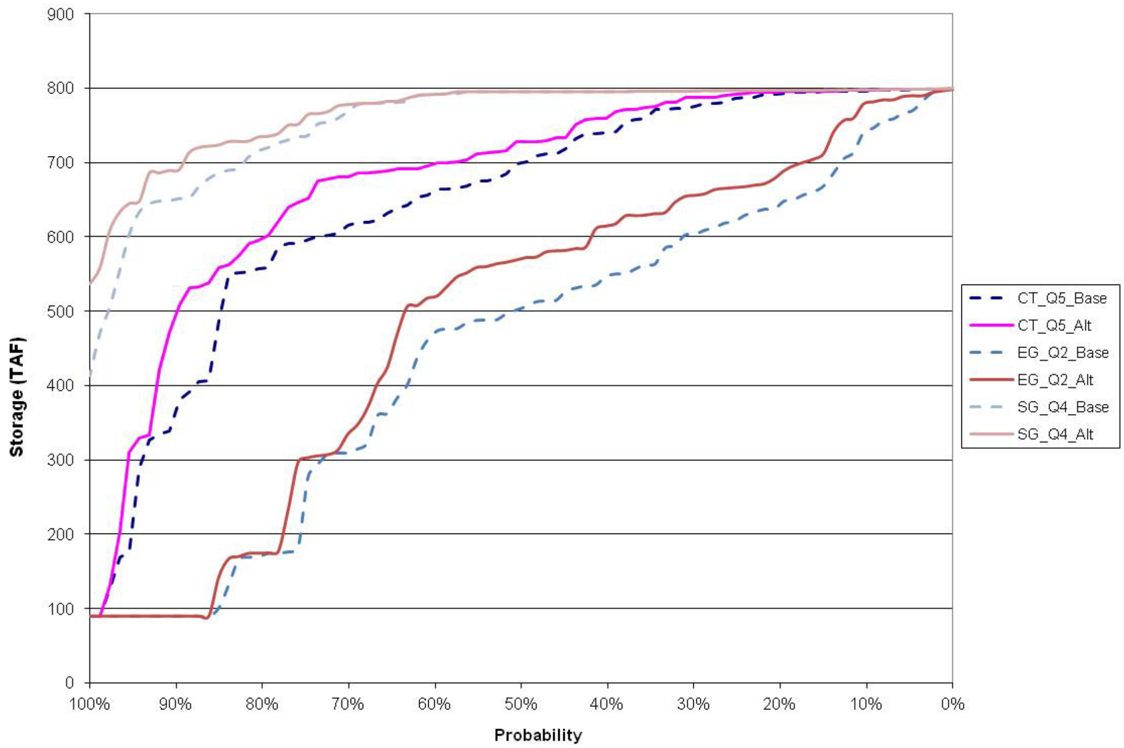

Figure 3-122. Exceedence of Folsom Lake End-of-September Storage with CP5

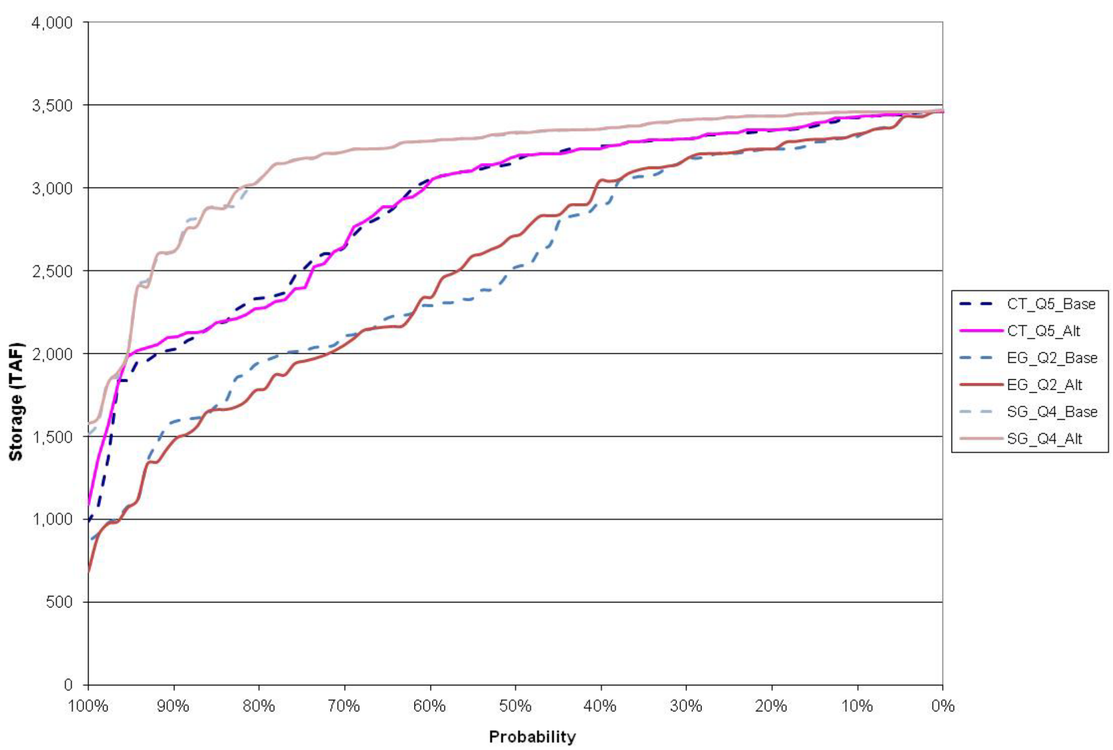

Figure 3-123. Exceedence of Lake Oroville End-of-May Storage with CP5

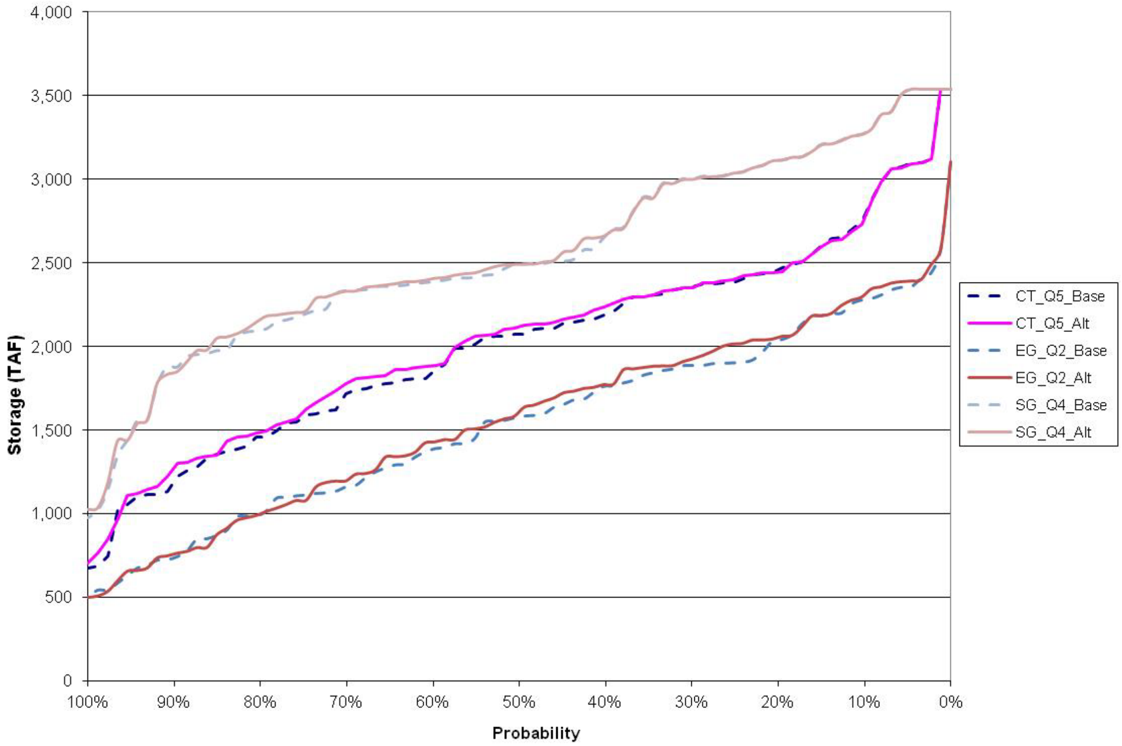

Figure 3-124. Exceedence of Lake Oroville End-of-September Storage with CP5

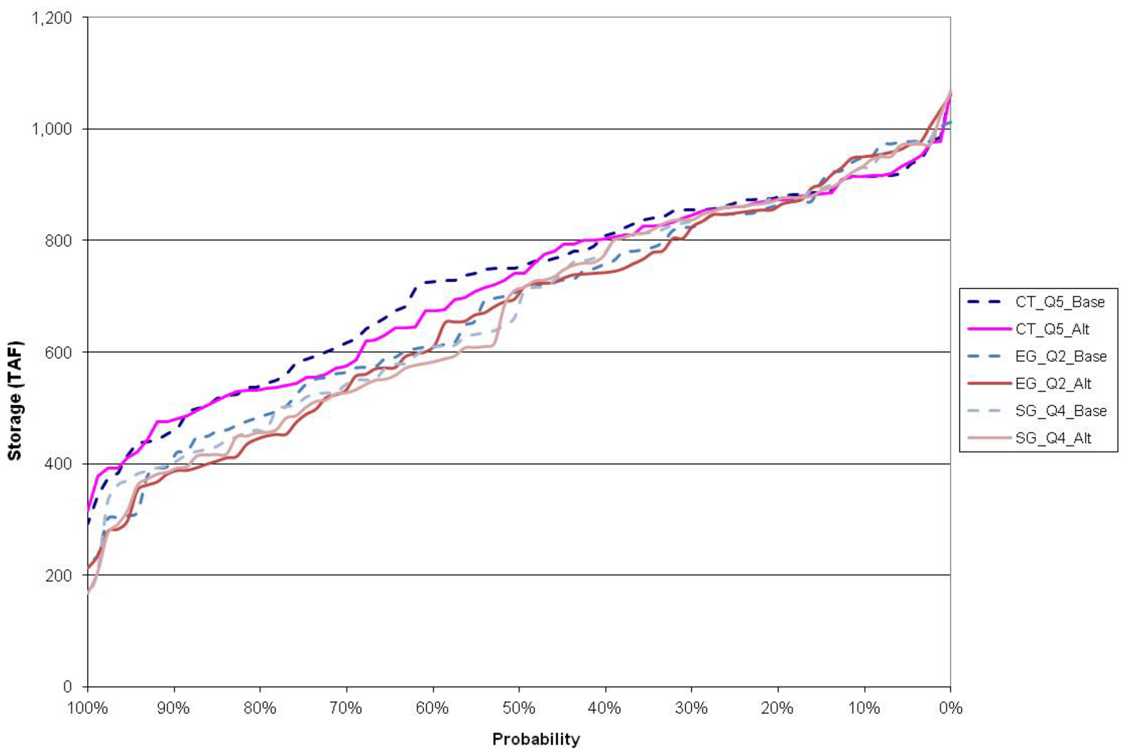

Figure 3-125. Exceedence of SWP San Luis End-of-May Storage with CP5

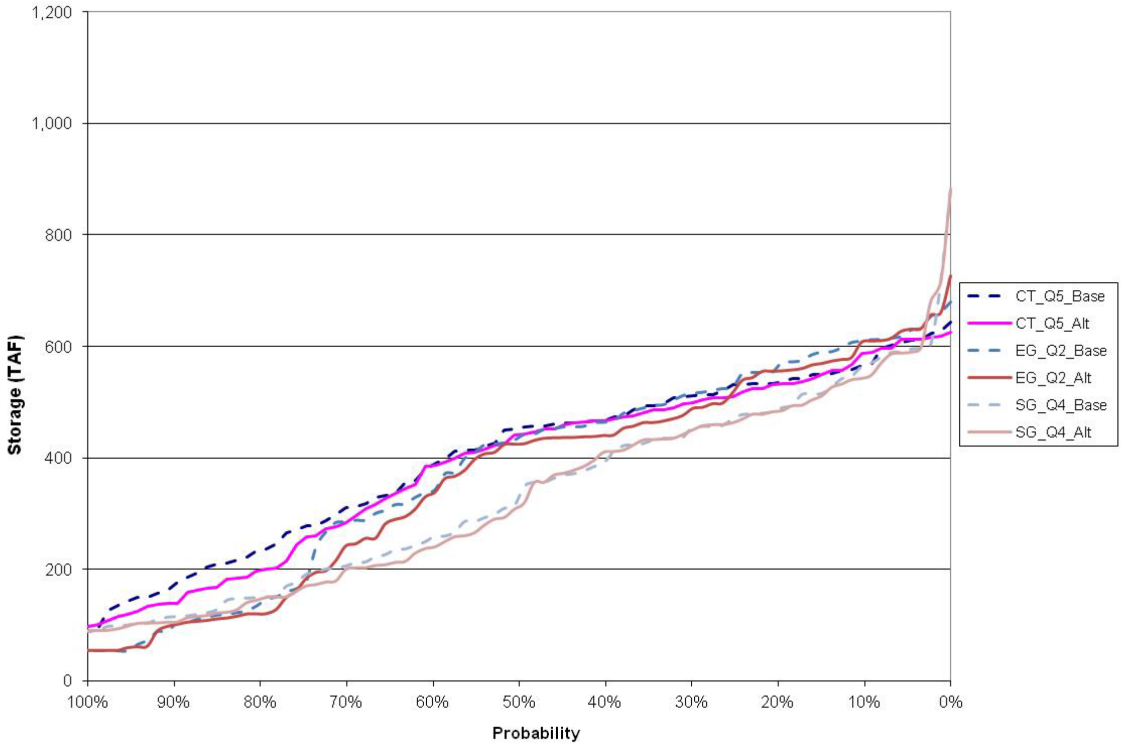

Figure 3-126. Exceedence of SWP San Luis End-of-September Storage with CP5

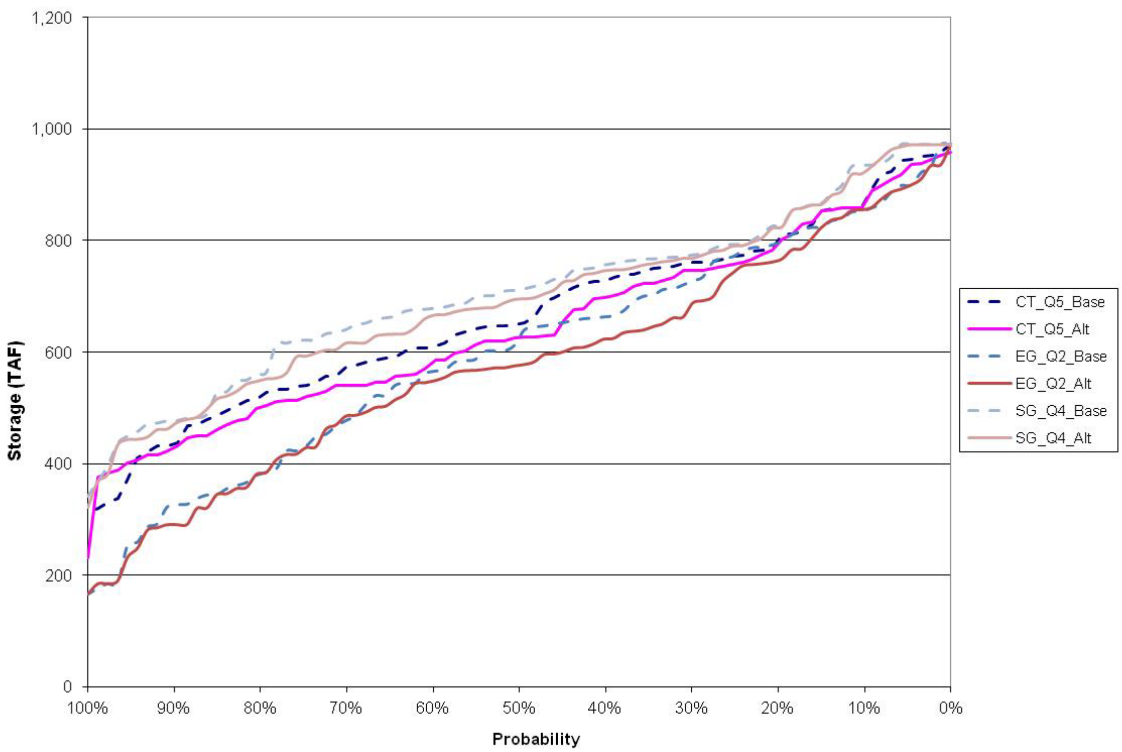

Figure 3-127. Exceedence of CVP San Luis End-of-May Storage with CP5

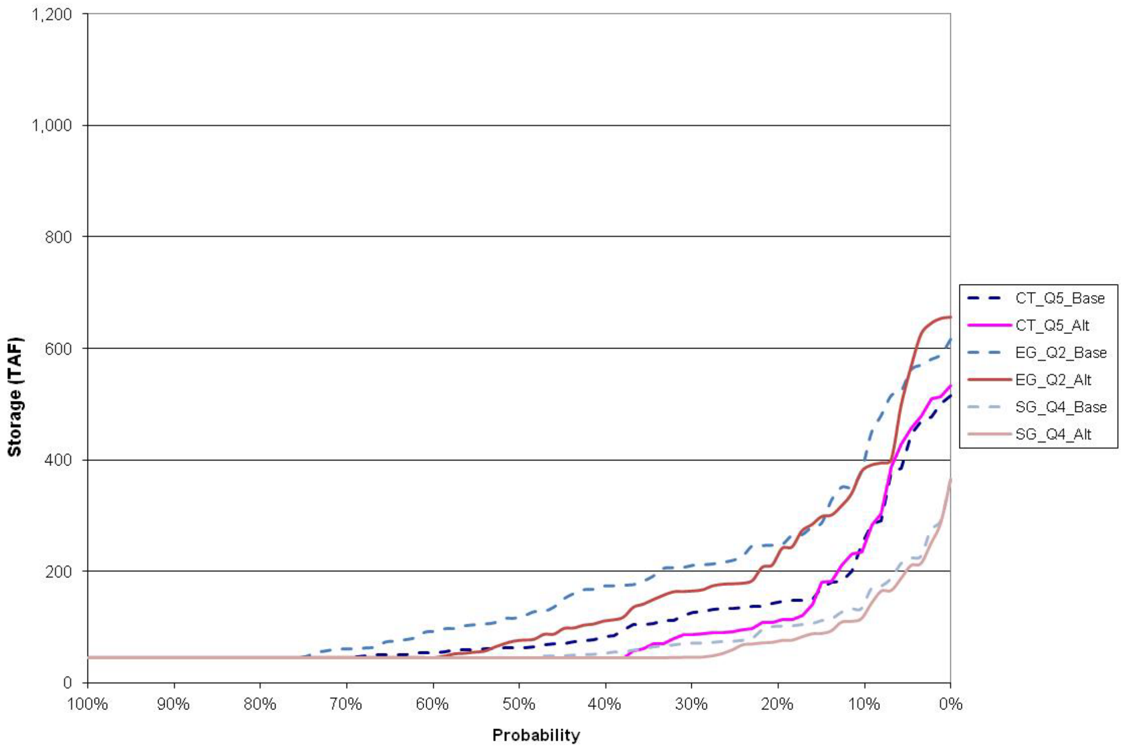

Figure 3-128. Exceedence of CVP San Luis End-of-September Storage with CP5

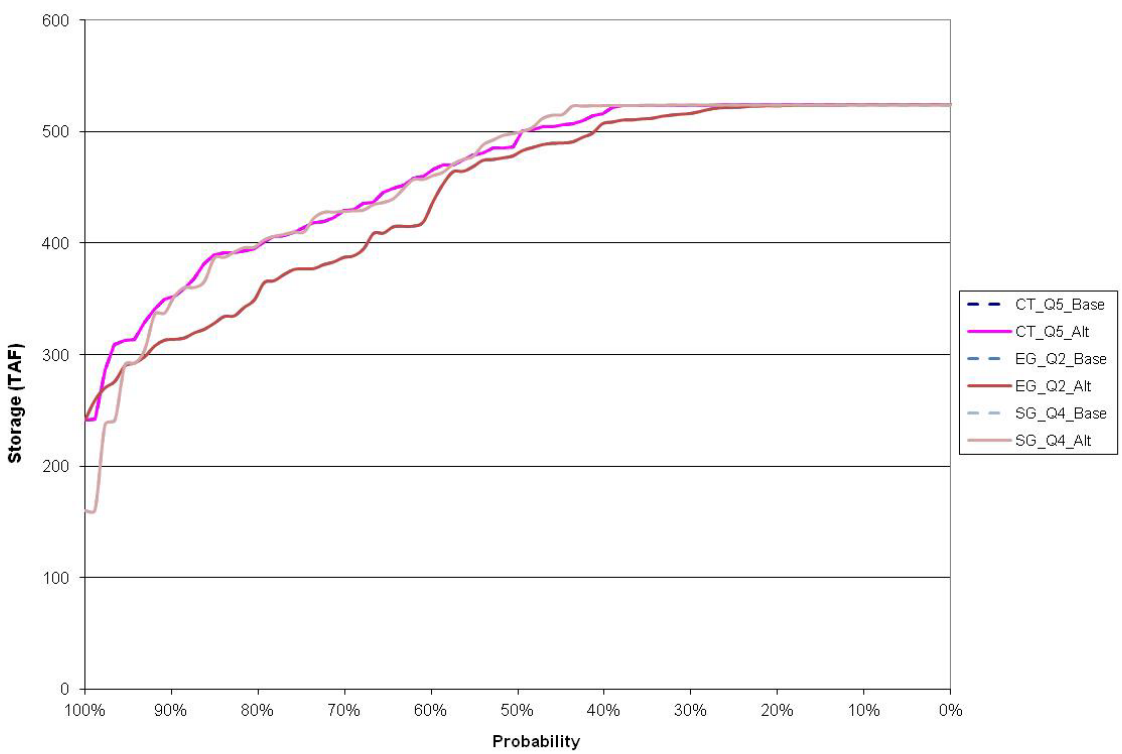

Figure 3-129. Exceedence of Millerton Lake End-of-May Storage with CP5

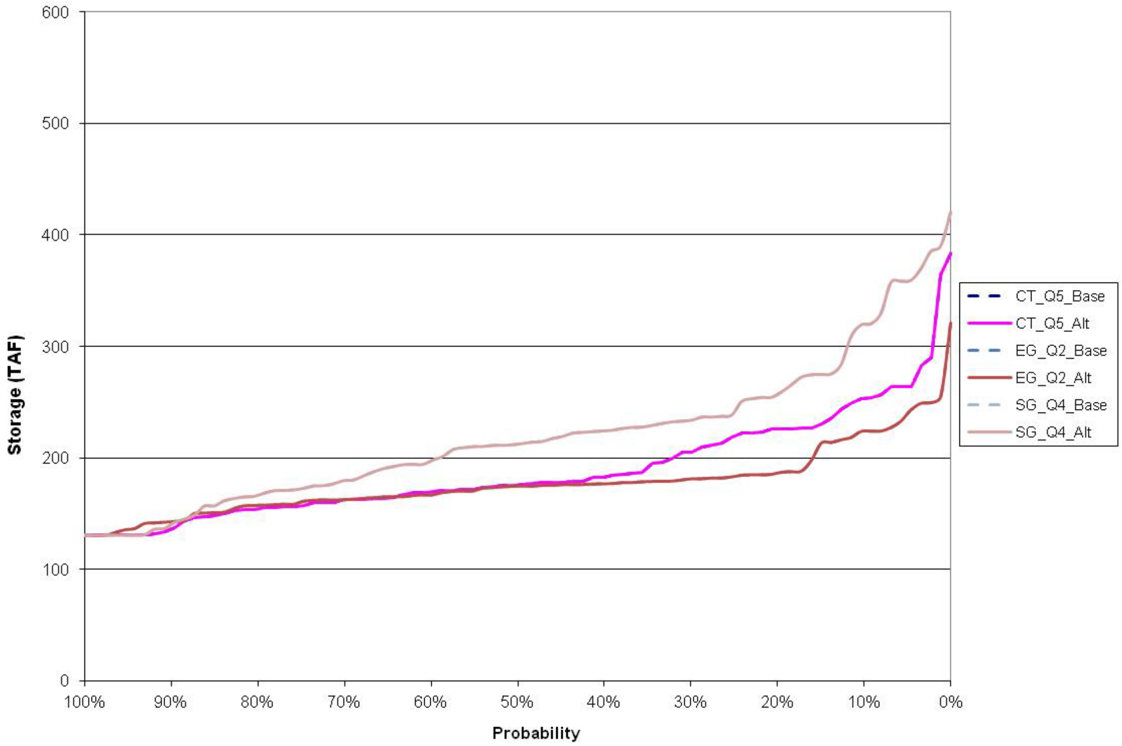

Figure 3-130. Exceedence of Millerton Lake End-of-September Storage with CP5

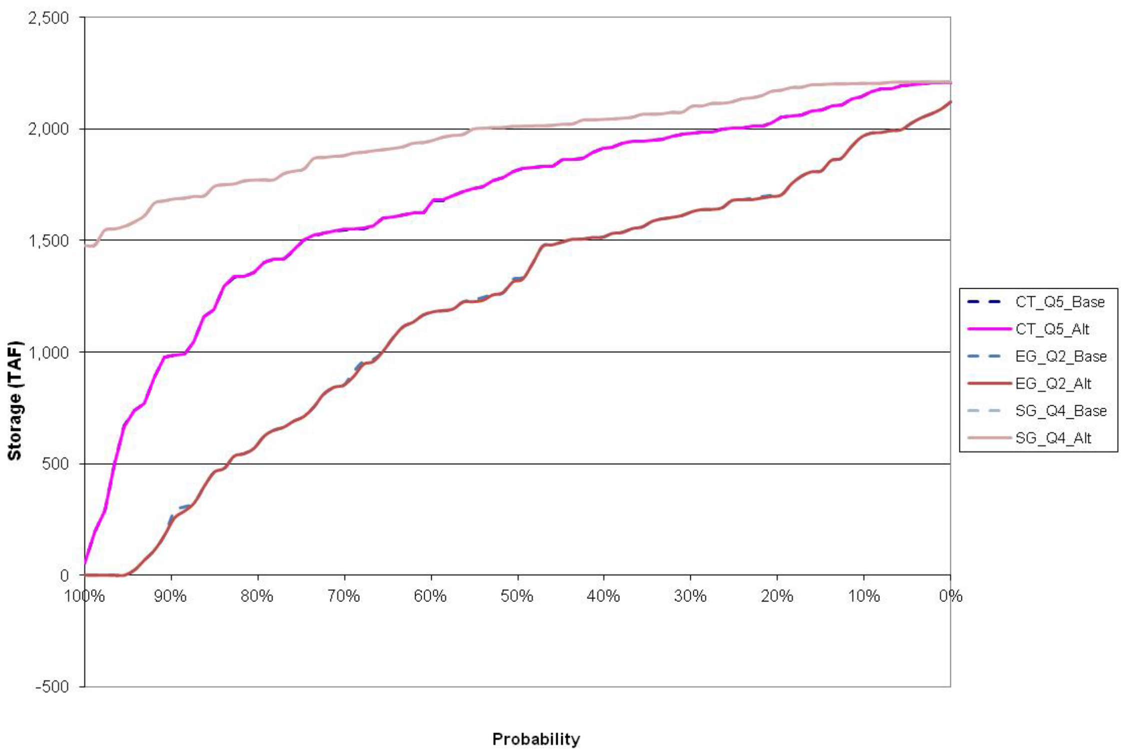

Figure 3-131. Exceedence of New Melones Lake End-of-May Storage with CP5

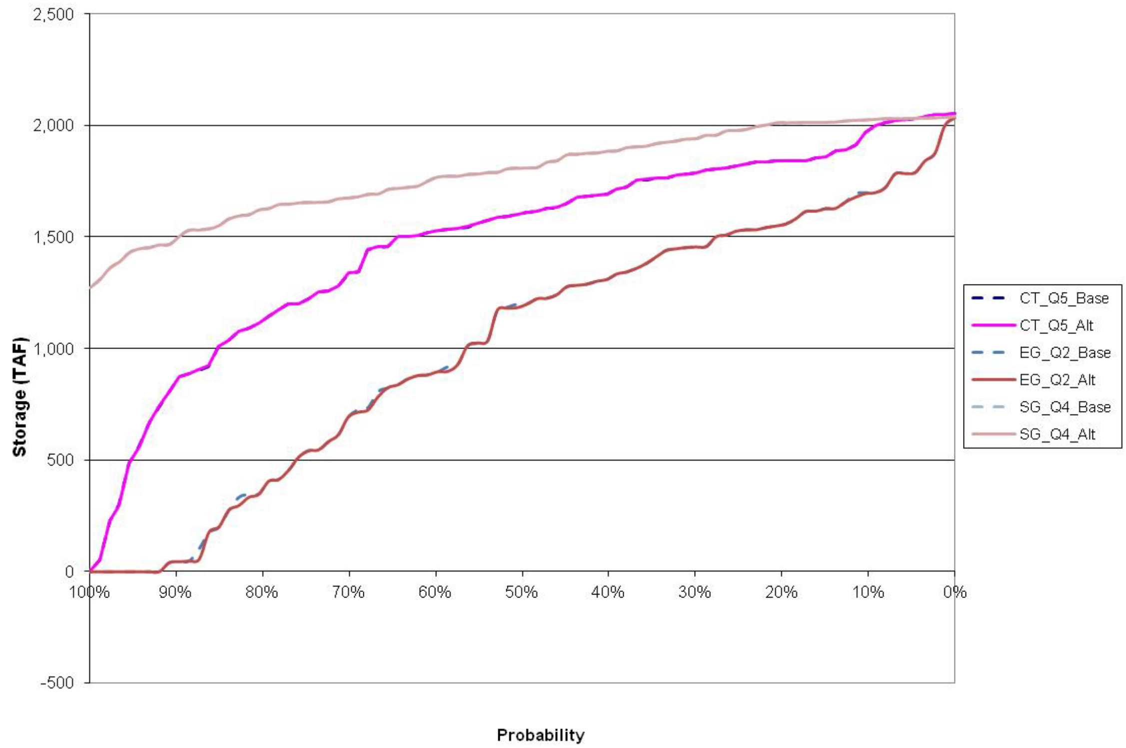

Figure 3-132. Exceedence of New Melones Lake End-of-September Storage with CP5

Delta Exports and Delta Outflow Figure 3-133 through Figure 3-138 are the annual exceedence plots of Delta exports from the H.O. Banks and C.W. Jones pumping plants and of Delta outflow under socioeconomic- climate scenarios CT_Q5 central tendency, EG_Q2 (drier) and SG_Q4 (wetter) and the change in annual average flows relative to their associated Baseline conditions at these locations for all 18 socioeconomic-climate scenarios. Alternative CP5 shows increases in exports and reductions in Delta outflow relative to the Baseline conditions. In both scenarios most of the change in exports occurs at the Banks Pumping Plant under the drier Q1 and Q2 climate projections. Total average annual Delta exports increase by 0 to 68 TAF/year under CP5 across the range of all socioeconomic- climate scenarios. Delta outflows are reduced by 15 to 100 TAF/year with CP5 with largest changes corresponding with the drier Q1 and Q2 climate projections.

With CP5, the greatest increases in exports and reductions in Delta outflow occur with the drier climate scenarios (Q1 and Q2) because the lower export levels in the Baseline in these scenarios allow for more incremental pumping under CP5 simulations. Conversely, the smallest increases in exports occur with the wetter climate scenarios (Q3 and Q4) where pumping is already at the maximum in many years in the Baseline, leaving less room for additional exports under CP5.

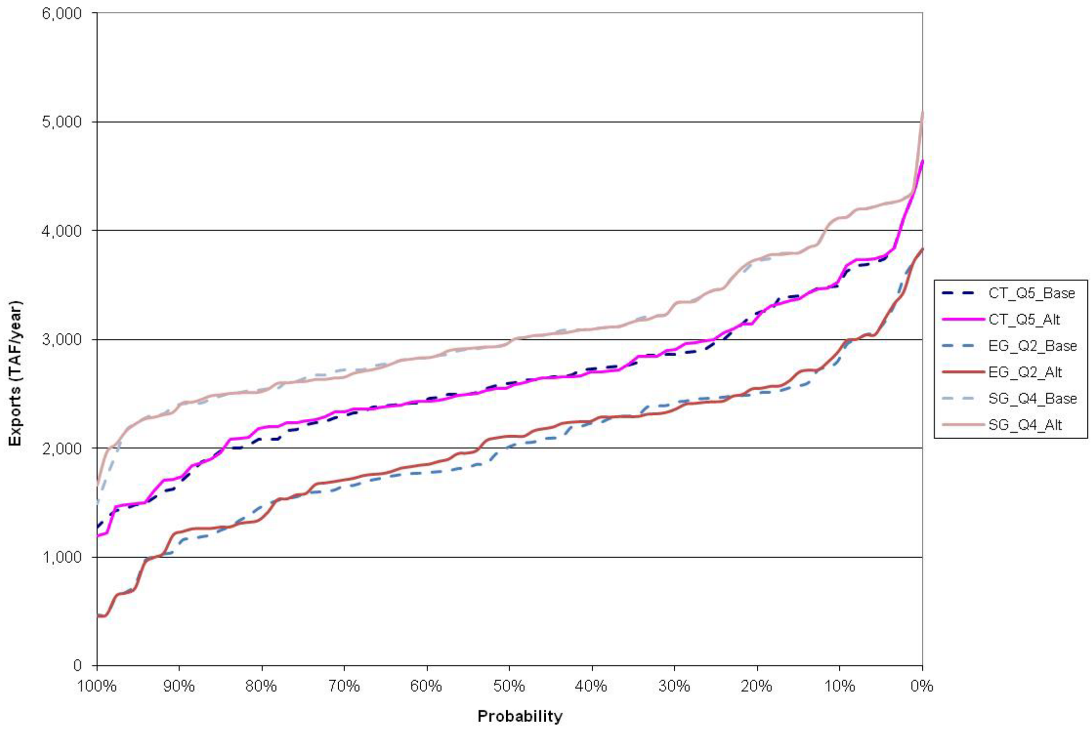

Figure 3-133. Annual Exceedence of Banks Pumping with CP5

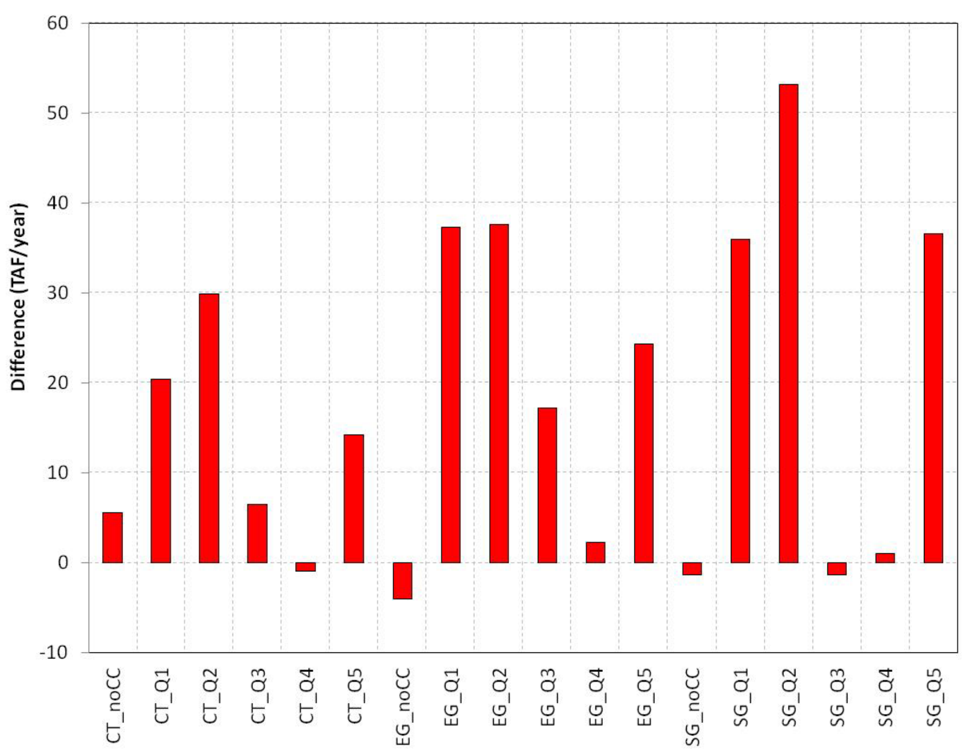

Figure 3-134. Average Annual Change in Banks Pumping for Portfolio B Relative to the Baseline in each Scenario

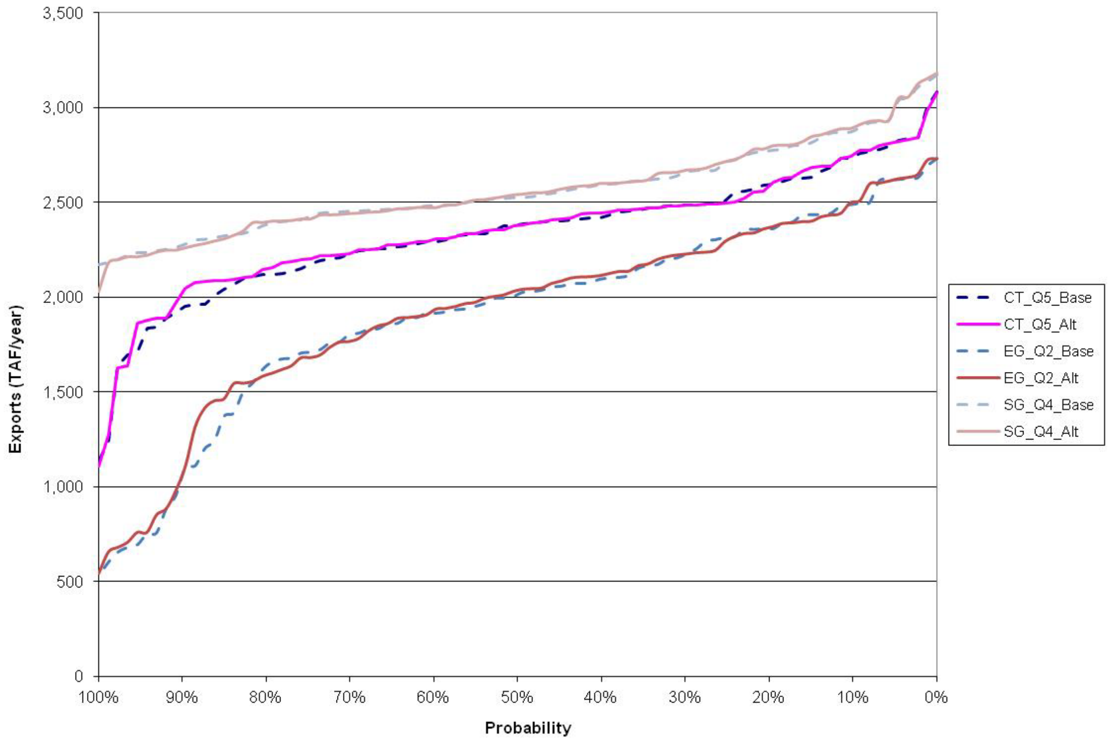

Figure 3-135. Annual Exceedence of Jones Pumping with CP5

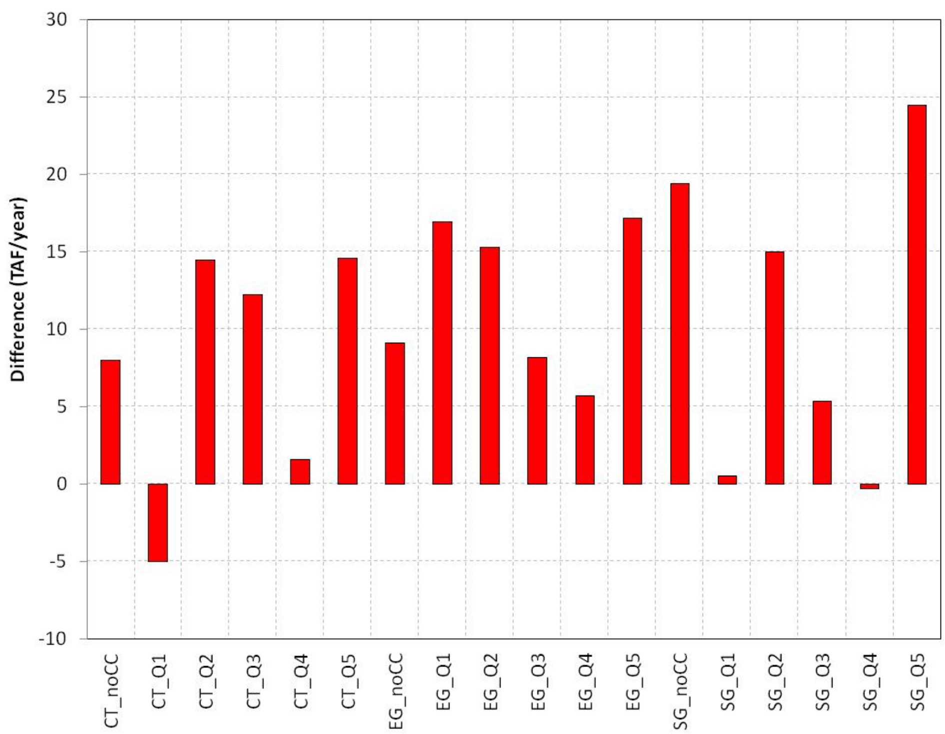

Figure 3-136. Average Annual Change in Jones Pumping for Portfolio B Relative to the Baseline in each Scenario

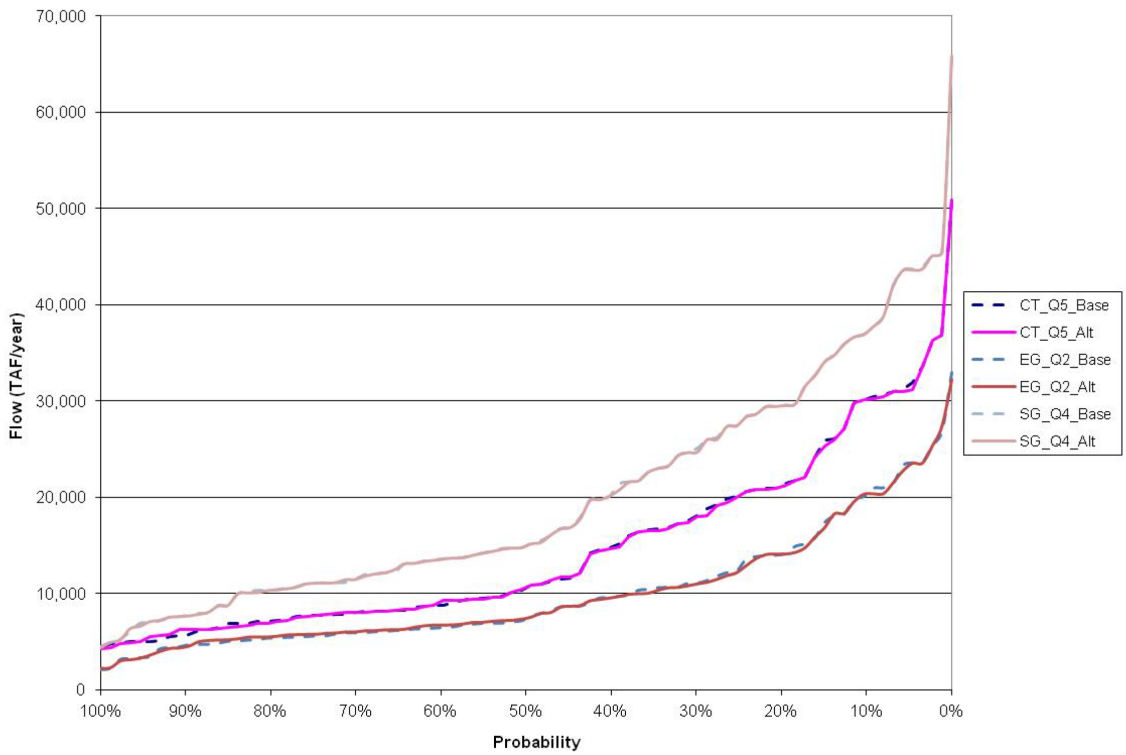

Figure 3-137. Annual Exceedence of Delta Outflow with CP5

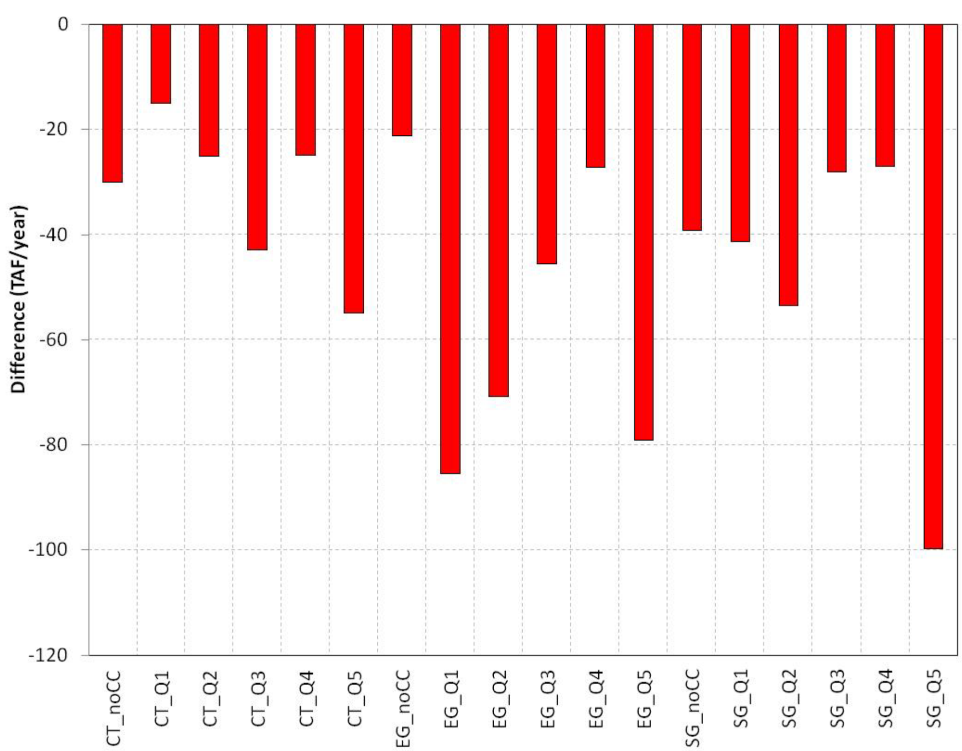

Figure 3-138. Average Annual Change in Delta Outflow for Portfolio B Relative to the Baseline in each Scenario

Delta Salinity Figure 3-139 shows the exceedence plots of average X2 position during the 21st century from February through June under socioeconomic scenarios CT_Q5, EG_Q2 and SG_Q4. Figure 3-140 shows the average X2 position for all 18 socioeconomic-climate scenarios for the months of February through June for Enlarged Shasta. As can be seen on the figures, the changes in X2 position are relatively small, reflecting the small changes in Delta flows resulting from CP5 relative to the Baseline conditions.

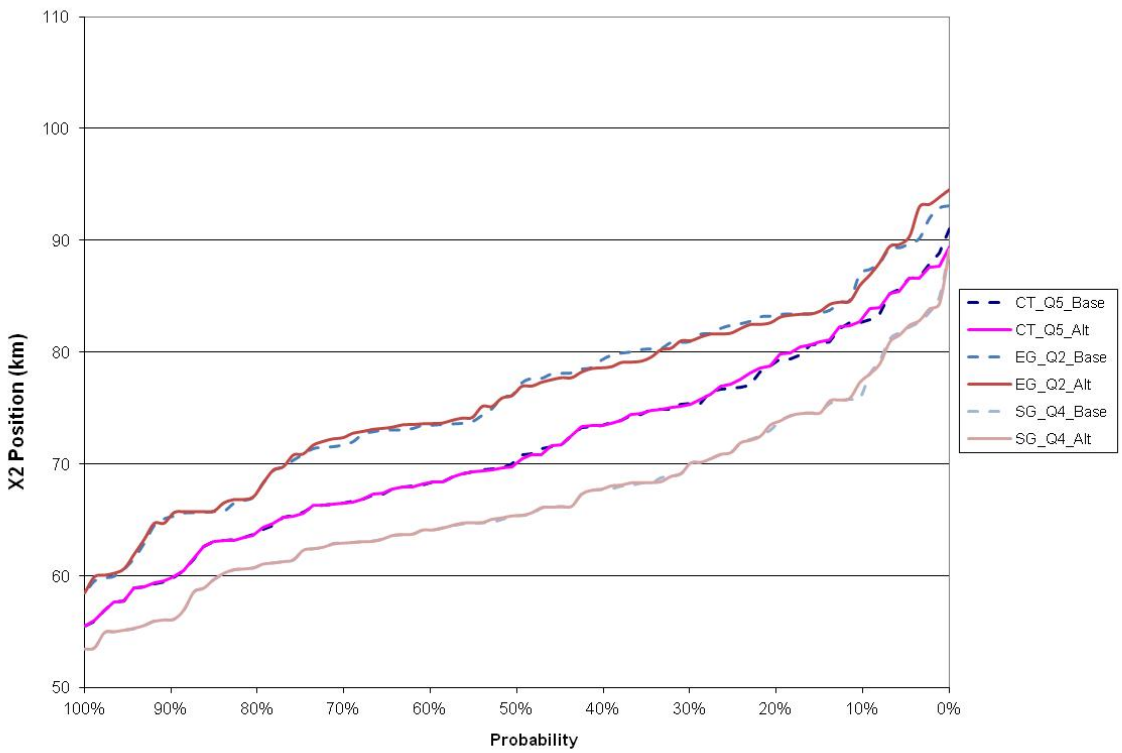

Figure 3-139. Exceedence of Average February-to-June X2 Position with CP5

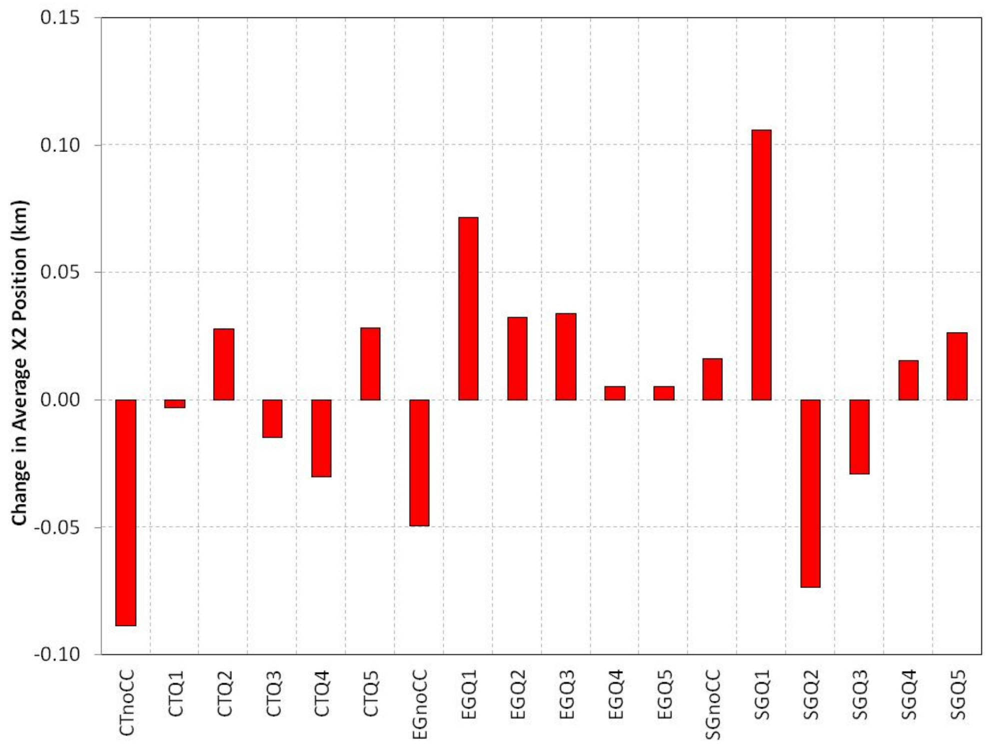

Figure 3-140. Change in Average February-to-June X2 Position for Portfolio B relative to the Baseline in each Scenario

Supplies and Demands in CVP Divisions

Figure 3-141 shows the average reduction in unmet demand in the CVP Service Area in the CP5 scenario. This reduction in unmet demand ranges from 5-33 TAF/year across the range of scenarios. Consistent with the changes in Delta exports, the greatest reductions in unmet demand occurs in Q1 and Q2 while the smallest reductions occur in Q3 and Q4.

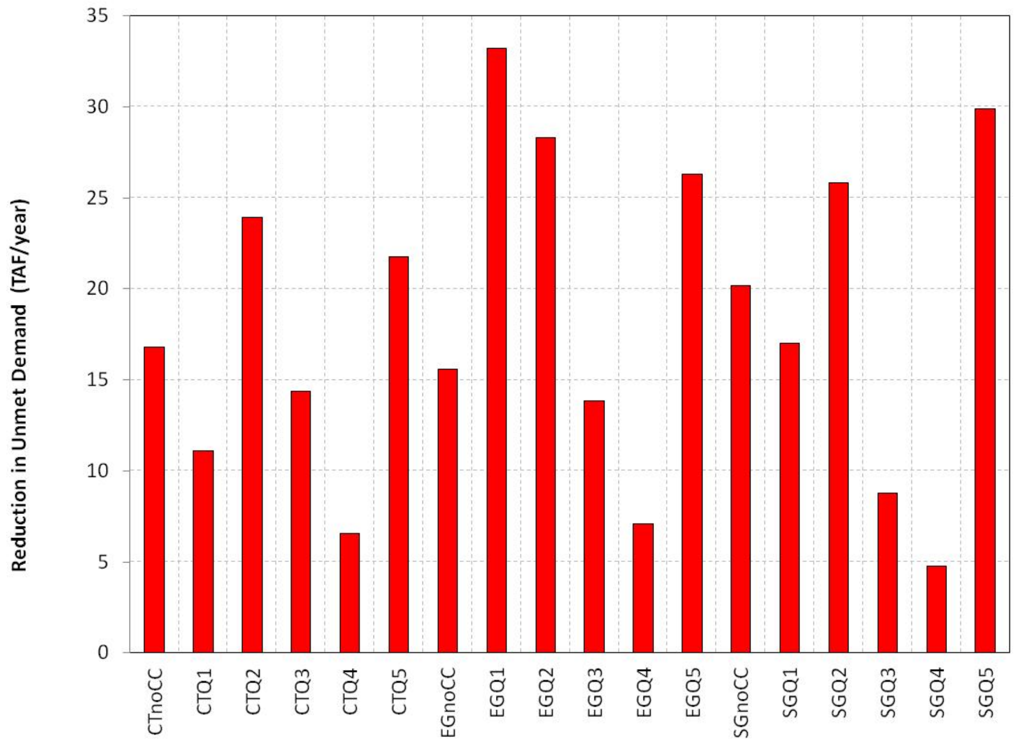

Figure 3-141. Average Annual Reduction in Unmet Demand in the CVP Service Area with CP5 in each Scenario

Results of Other Performance-Assessment Tools

Economics Figure 3-142 through Figure 3-145 show the net improvement in net water supply system costs from the urban economic models LCPSIM and OMWEM, the net improvement in avoided cost from the water quality economic model SBWQM and the net improvement in agricultural net revenue from SWAP for the CP5 simulation suite in the CT-Q5, EG-Q2 and SG-Q4 scenarios at the 2025, 2055, and 2085 LODs.

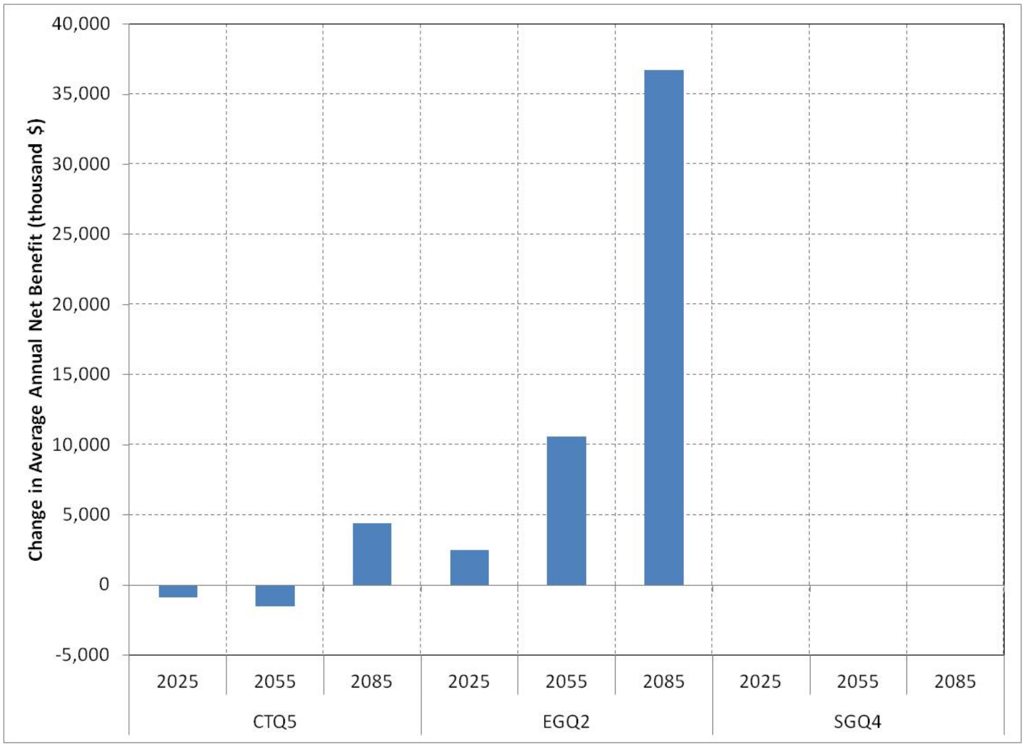

Figure 3-142. Improvement in Average Annual Urban Net Water Supply System Costs in South Bay Region from LCPSIM with CP5

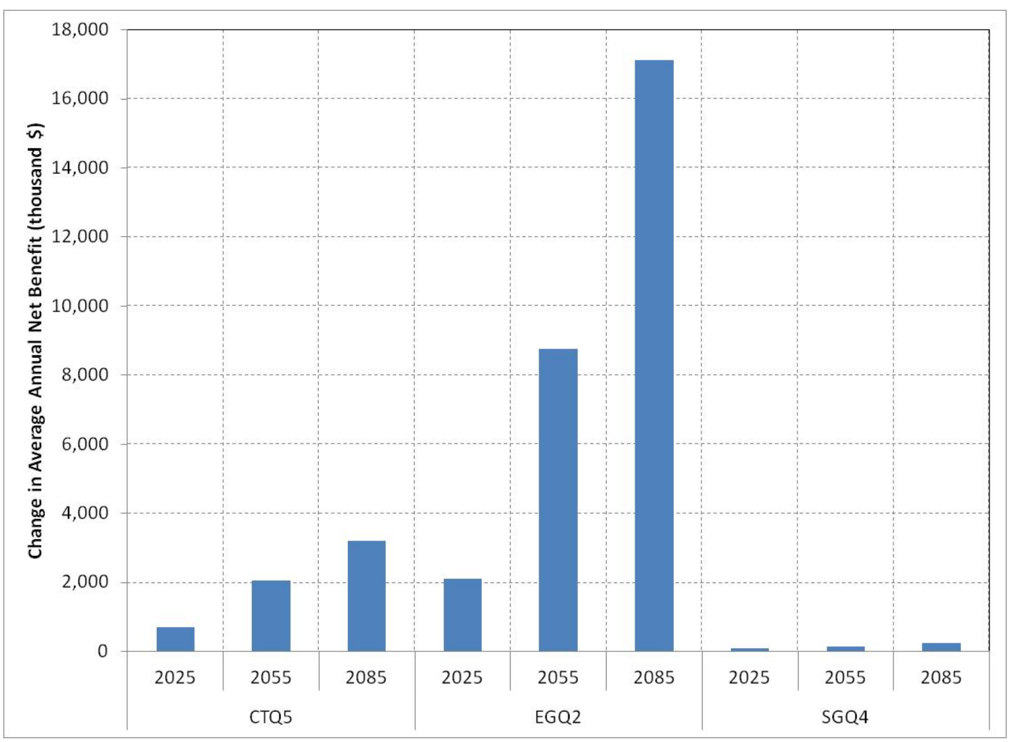

Figure 3-143. Improvement in Average Annual Urban Net Water Supply System Costs in Central Valley from OMWEM with CP5

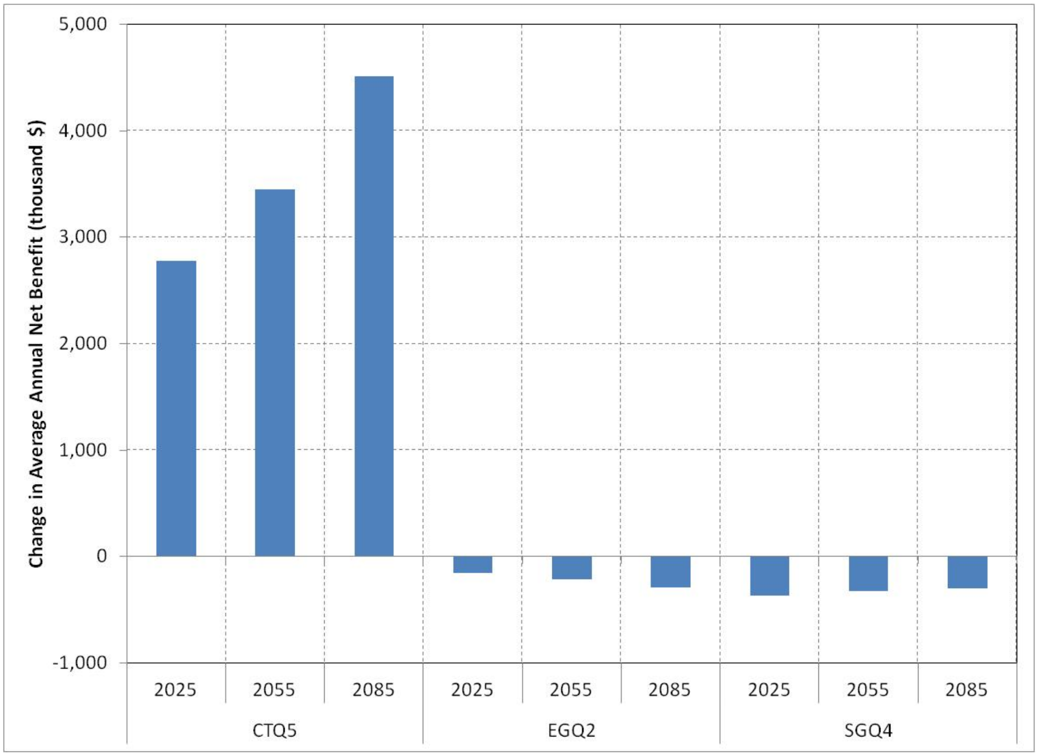

Figure 3-144. Improvement in Average Annual Avoided Water Quality Costs in South Bay Region from SBWQM with CP5

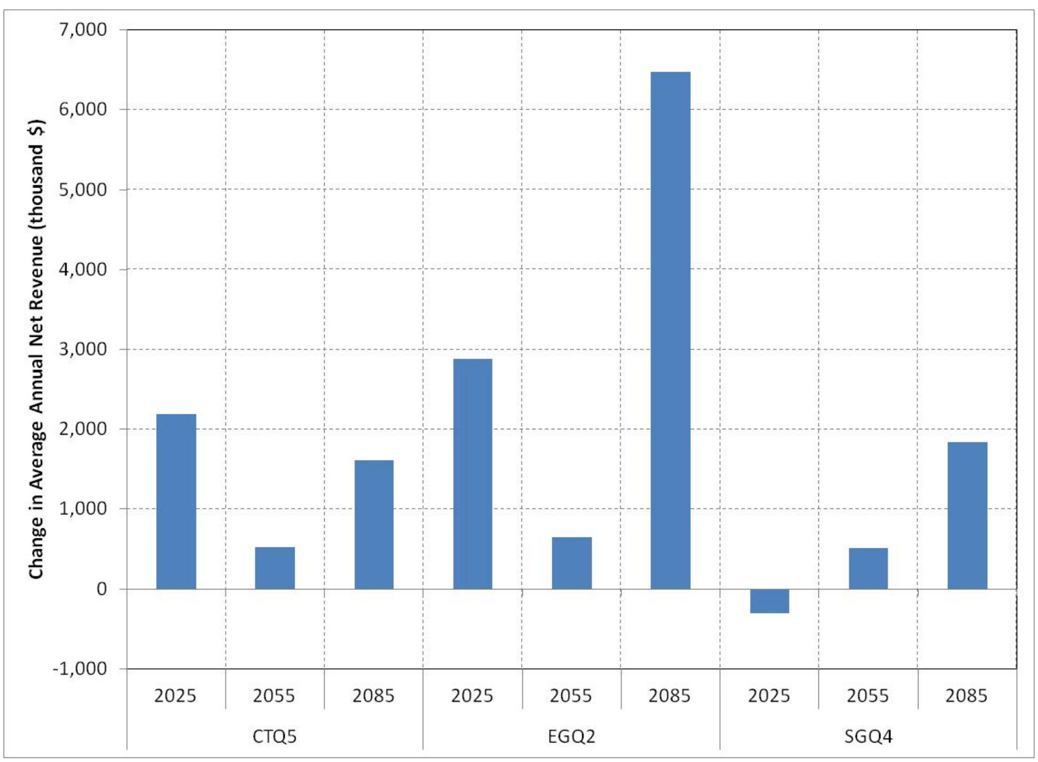

Figure 3-145. Improvement in Average Annual Agricultural Net Revenue in Central Valley from SWAP with CP5

The South Bay urban economic model results from LCPSIM show almost no change in economic values in SG-Q4 scenario with CP5. For CP5, there are economic benefits of up to about $4 million per year in the CT-Q5 scenario and somewhat larger economic benefits in of up to about $37 million per year in the EG-Q2 scenario. These benefits result from the reductions in shortage costs due to the increased deliveries to the South Bay region, and are larger in EG-Q2 because the South Bay has very high urban demands and therefore high marginal shortage costs in EG-Q2 due to the increased population in the Expansive Growth socioeconomic scenario.

South Bay region water quality costs reported by SBWQM show a small increase in costs of up to about $2 million/year with CP5 in the CT-Q5 scenario. In each case, this results from a net increase in total salt load due to increased export levels but not enough salinity reduction at the export locations to reduce the overall salt load. By contrast, in both the EG-Q2 and SG-Q4 scenarios the effects of changes in exports and in salinity result in very little change in water quality costs.

The changes in Central Valley agricultural economic model results from SWAP and urban economic results from OMWEM show only small differences with CP5 as compared to the Baseline, reflecting the small changes in CVP and SWP deliveries in the Central Valley with the implementation of CP5. With CP5, the average annual economic changes across the different scenarios and LODs range from no benefit to a benefit of about $6 million per year for SWAP and from no benefit to a benefit of about $17 million per year for OMWEM.

Water Temperature Figure 3-146 through 3-149 show exceedence plots and average changes relative to the Baseline of daily temperatures from July through September for CT-Q5, EG-Q2 and SG-Q4 scenarios in the Sacramento River at Keswick and at Jellys Ferry. For alternative CP5, the mean daily temperatures in Sacramento River at Keswick are about 0.2-0.25°F lower than in the Baseline and the temperatures at Jelly's Ferry are about 0.2 -0.3°F lower than the Baseline. These modest reductions in temperature occur because of the increased storage and available cold water pool in the Shasta Lake. As observed in the baseline cases, the SG-Q4 scenario has the lowest temperatures and the EG-Q2 scenario has the highest temperatures, with CT-Q5 falling between them.

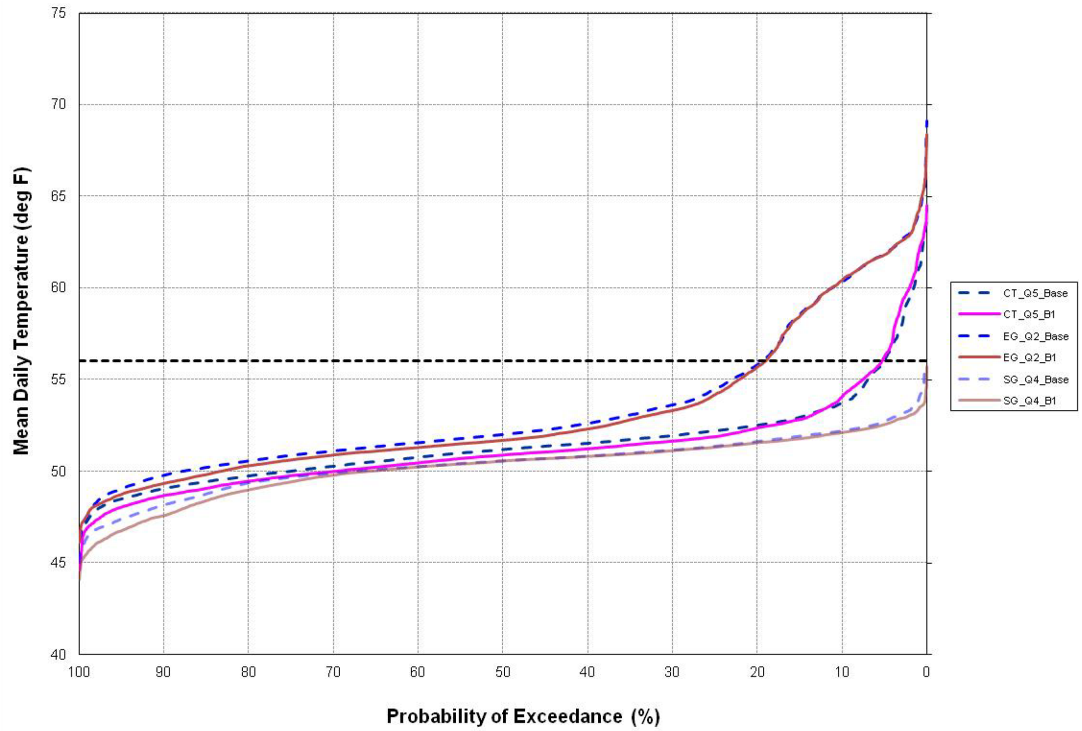

Figure 3-146. Exceedence of Mean Daily Temperature on Sacramento River at Keswick from July to September with CP5

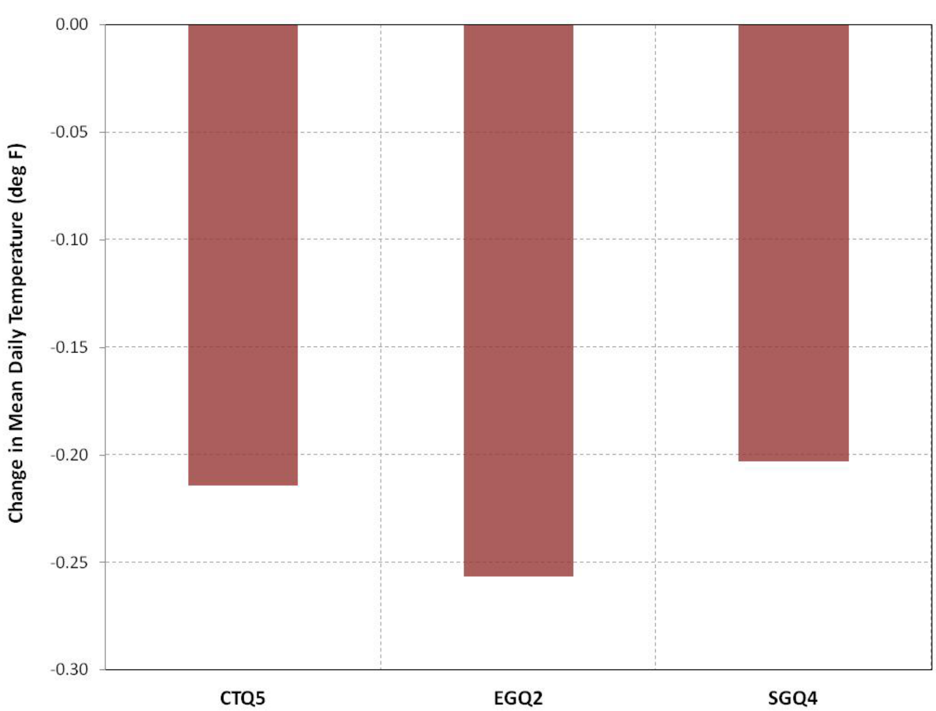

Figure 3-147. Change in Mean Daily Temperature on Sacramento River at Keswick from July to September with CP5

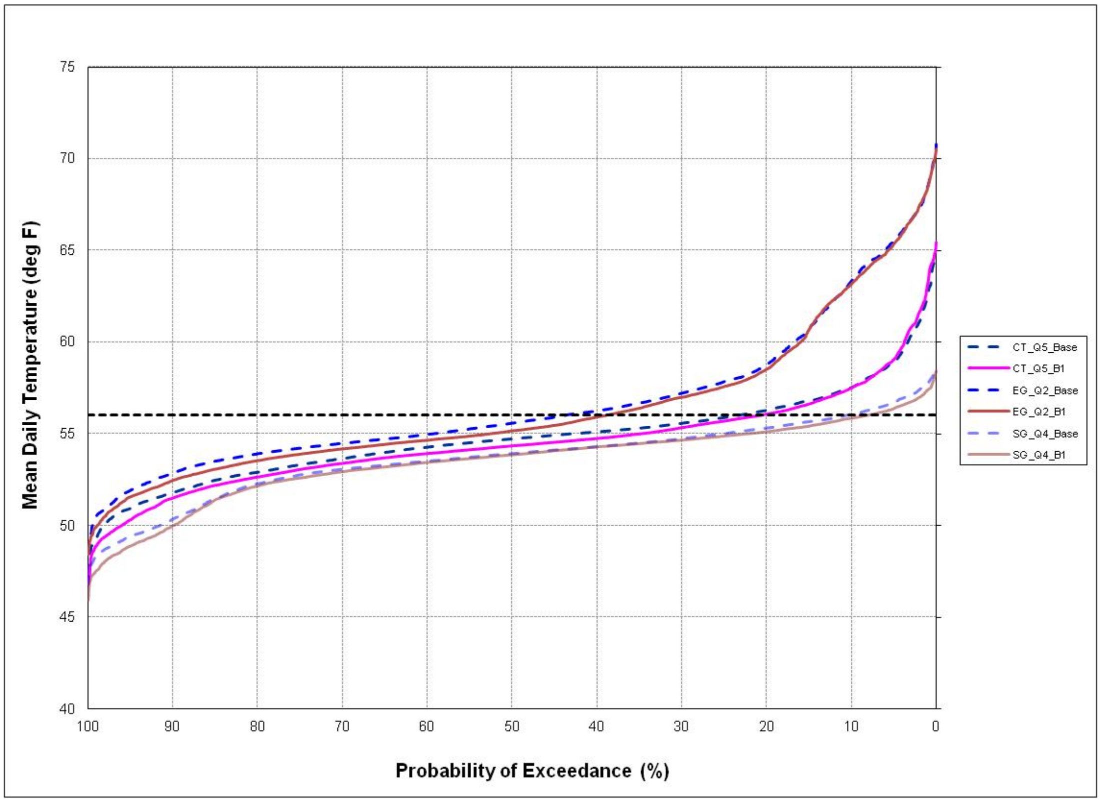

Figure 3-148. Exceedence of Mean Daily Temperature on Sacramento River at Jellys Ferry from July to September with CP5

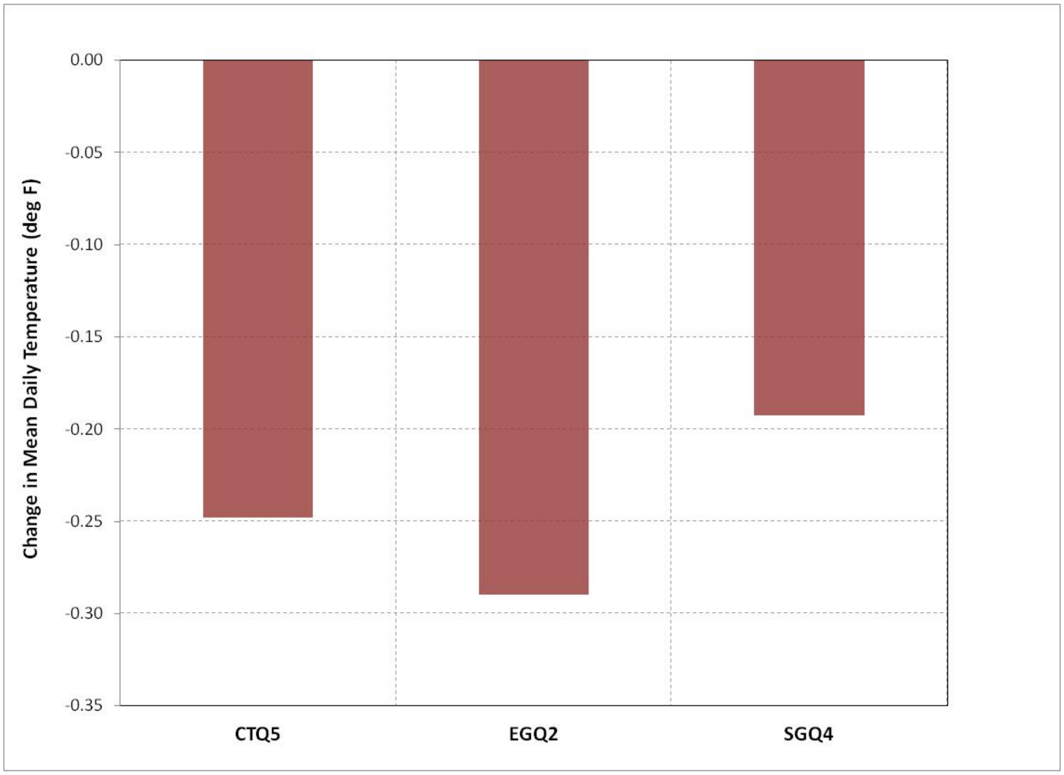

Figure 3-149. Change in Mean Daily Temperature on Sacramento River at Jellys Ferry from July to September with CP5

Figure 3-150 through Figure 3-155 show exceedence plots and average changes relative to the Baseline of daily temperatures for the same three scenarios in the San Joaquin River at Lost Lake, at Gravelly Ford and at Vernalis from August through November. Under all scenarios with CP5, there are only minimal changes in temperatures at all three San Joaquin River locations relative to the Baseline. Therefore, increased storage in Sacramento River system has negligible impacts on temperatures in the San Joaquin River.

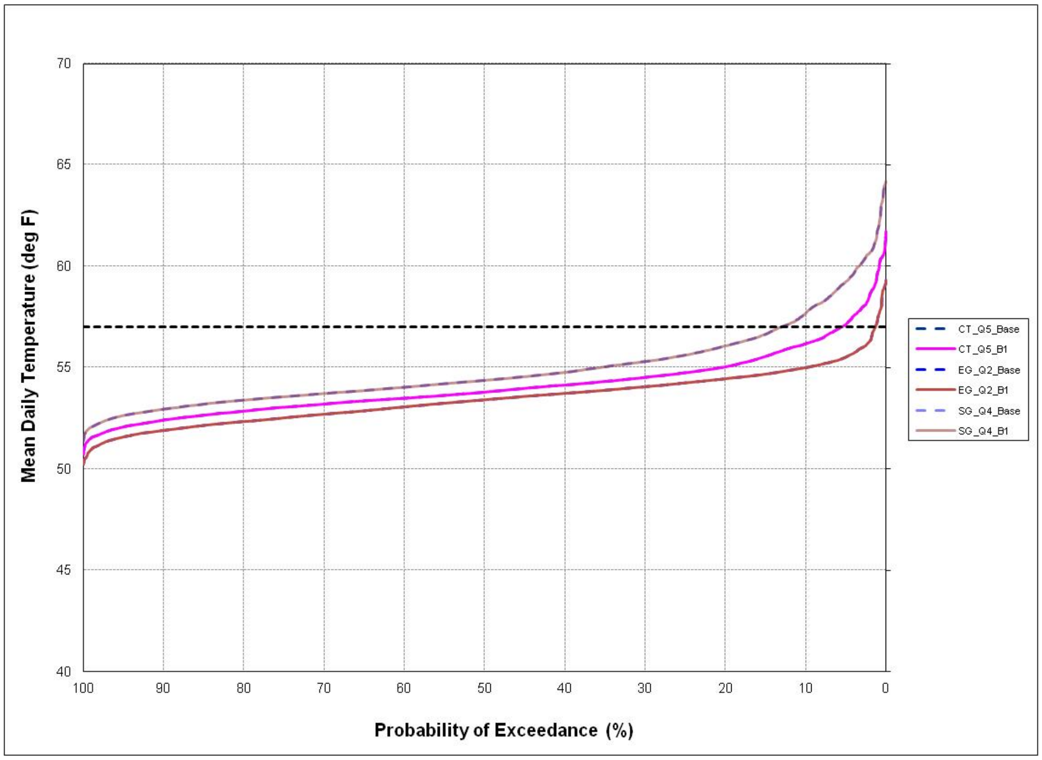

Figure 3-150. Exceedence of Mean Daily Temperature on San Joaquin River at Lost Lake from August to November with CP5

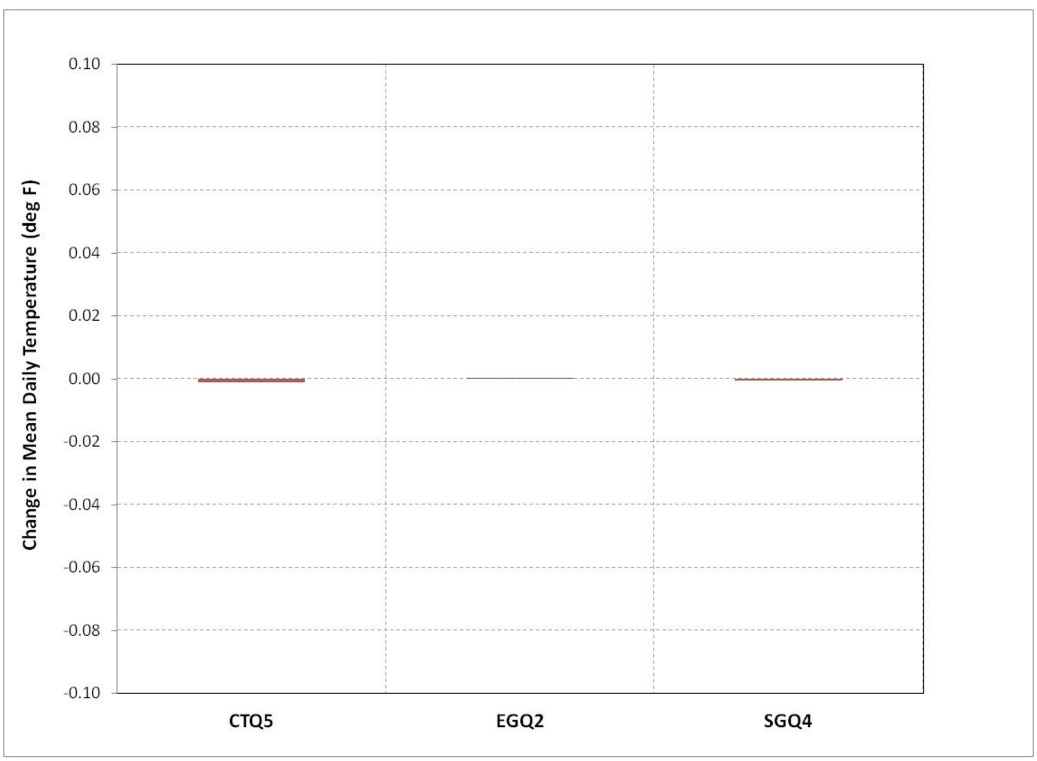

Figure 3-151. Change in Mean Daily Temperature on San Joaquin River at Lost Lake from August to November with CP5

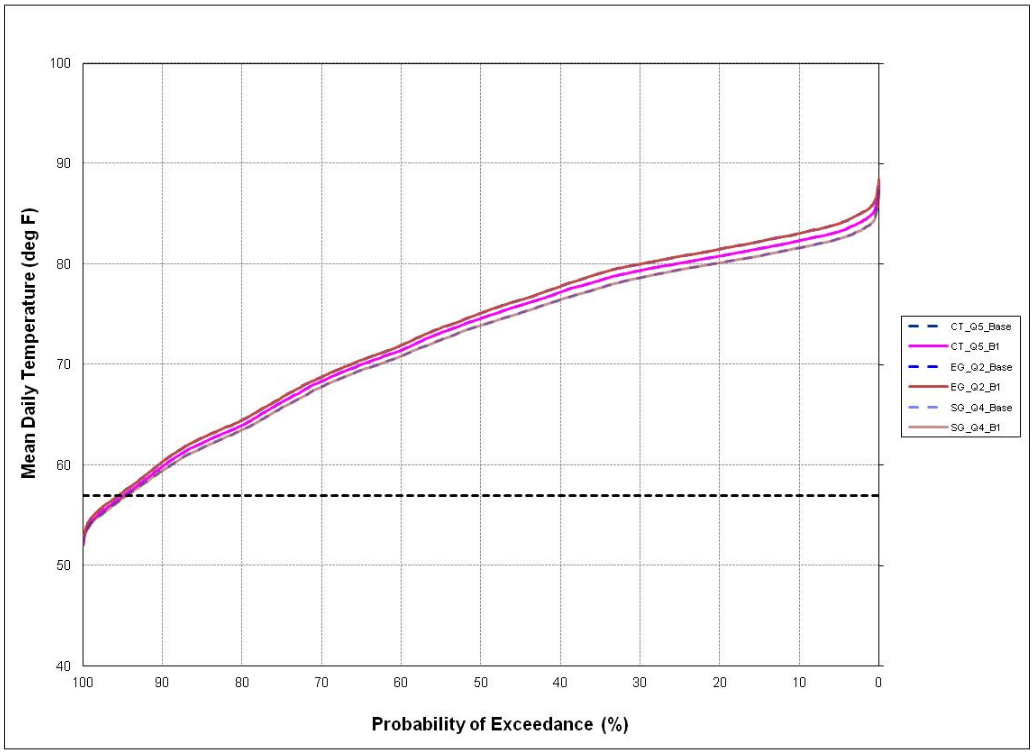

Figure 3-152. Exceedence of Mean Daily Temperature on San Joaquin River at Gravelly Ford from August to November with CP5

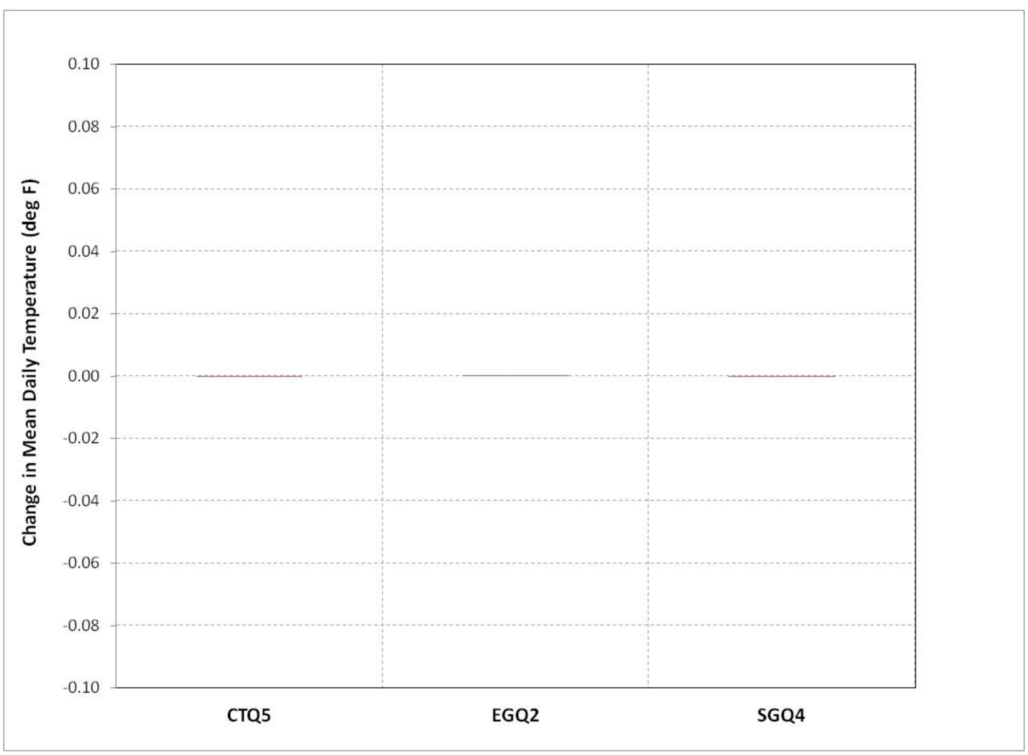

Figure 3-153. Change in Mean Daily Temperature on San Joaquin River at Gravelly Ford from August to November with CP5

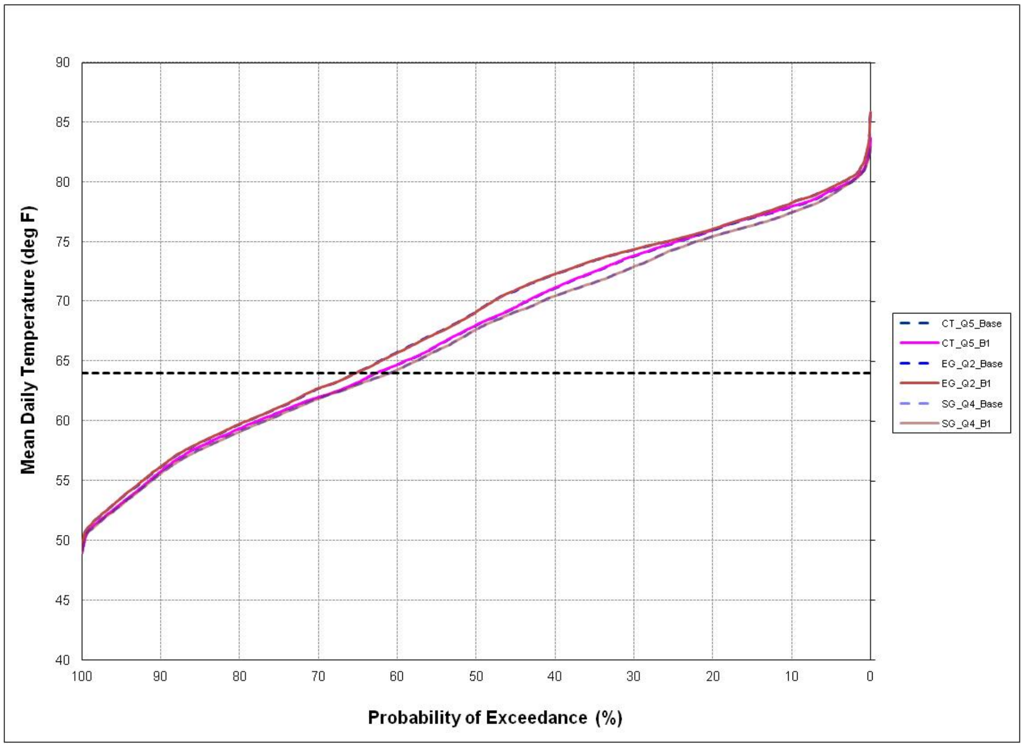

Figure 3-154. Exceedence of Mean Daily Temperature on San Joaquin River at Vernalis from August to November with CP5

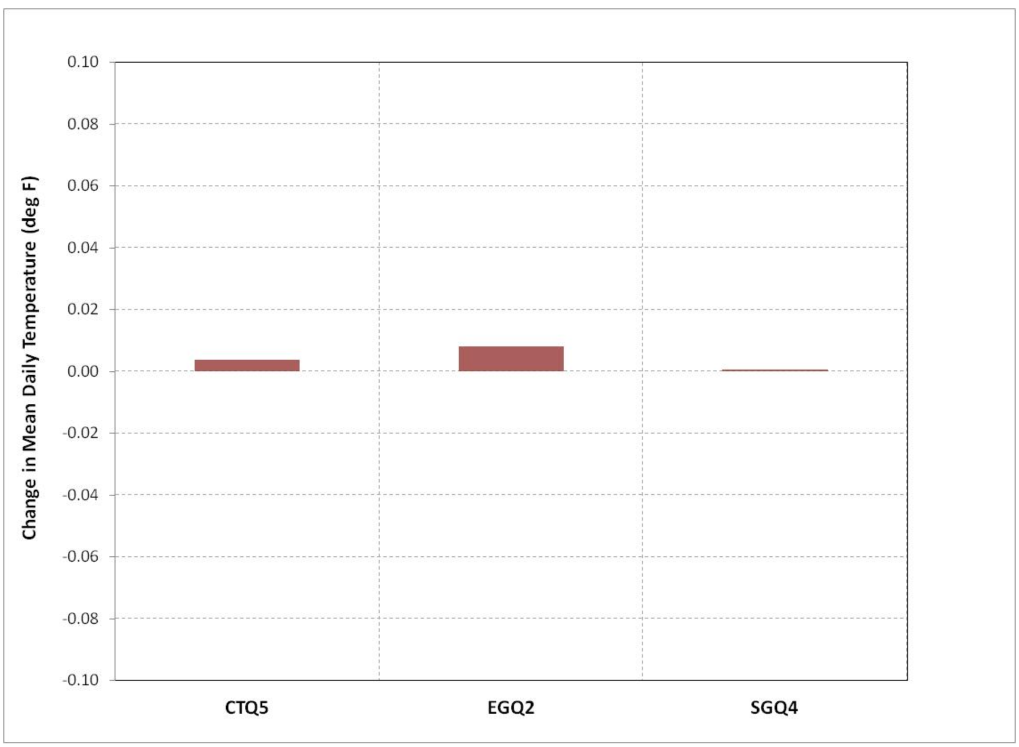

Figure 3-155. Change in Mean Daily Temperature on San Joaquin River at Vernalis from August to November with CP5

Hydropower and GHG Emissions Figure 3-156 and Figure 3-157 show the changes in net generation and net GHG emissions in the CVP and SWP systems with alternative CP5 relative to the Baseline. There is an increase in net generation of about 50-130 gigawatt hours (GWh)/year and a decrease in net GHG emissions of about 16,000-40,000 metric tons of carbon dioxide equivalents (mT CO_2e) as a result of increased storage levels in Lake Shasta.

In the SWP system there is a reduction in net generation and an increase in net GHG emissions with CP5, which is caused by the increase in Delta export levels relative to the Baseline. The SWP's reduction in net generation is about 0-90 GWh/year while the net GHG emissions increase by about 0-16,000 mT CO_2e across the three scenarios.

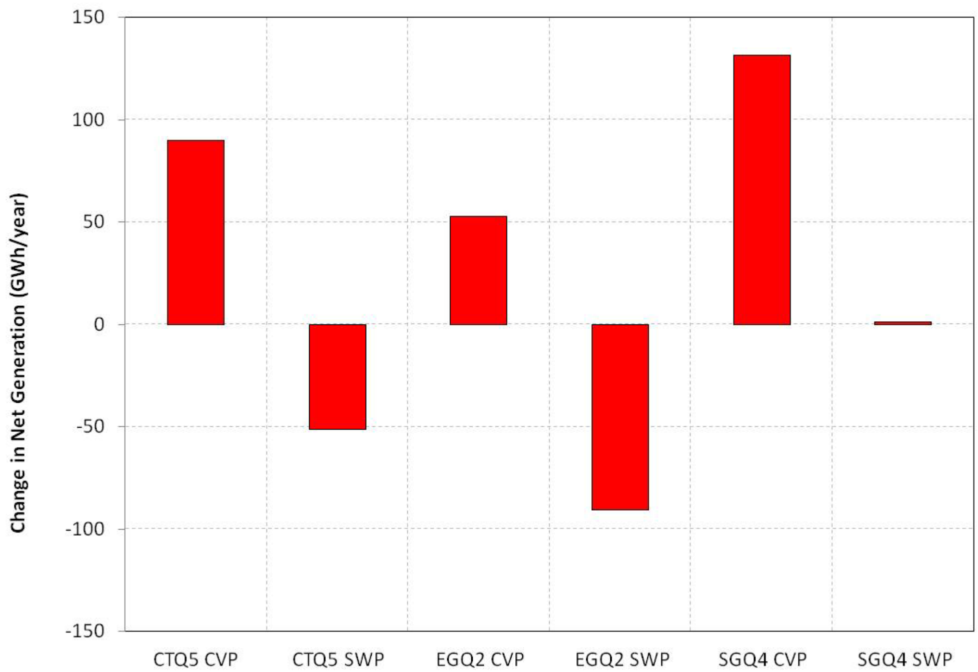

Figure 3-156. Change in Average Annual Net Energy Generation for the CVP and SWP Systems with CP5

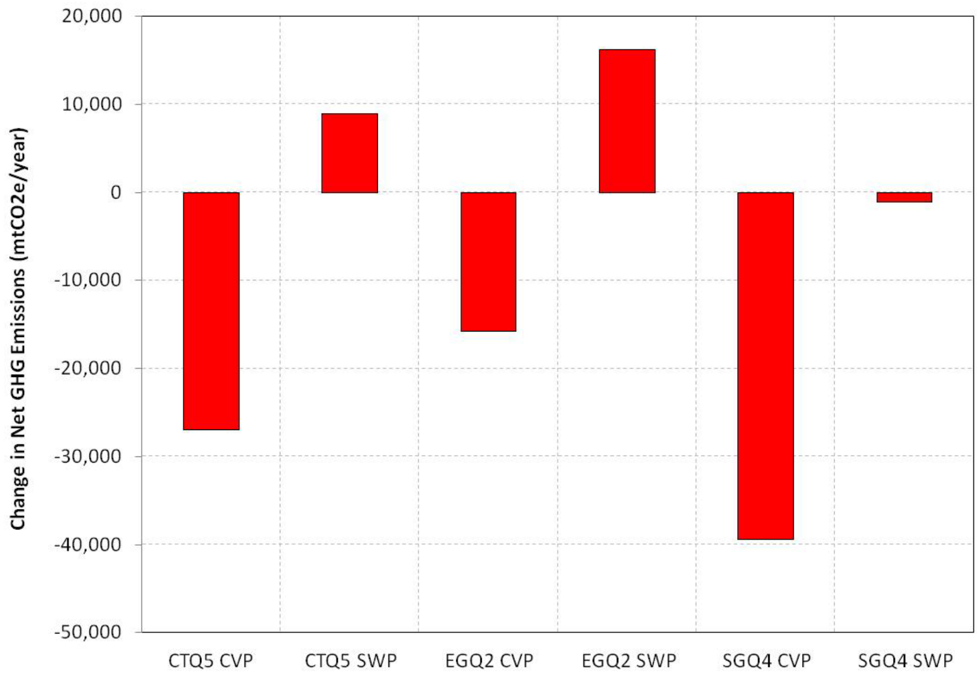

Figure 3-157. Change in Average Annual Net GHG Emissions for the CVP and SWP Systems with CP5

This page left blank intentionally.

Chapter 4 Potential to Achieve Anadromous Fish Survival Objective Under Climate Change

This chapter presents an assessment of the potential to achieve the anadromous fish survival objective under climate change. SLWRI alternative CP4 was selected for this assessment as it maximizes survivability of anadromous fish survival. The following sections describe the methodology applied in the assessment of the influence of climate change on fish survival followed by the modeling results. This method applies the same set of 112 climatic projections for climate change described in Chapter 3. However, unlike the previous method, this method adjusts temperature and/or precipitation by the mean shift from one historical 30-year period to a future 30-year period.

Climate change pertains to the entire planet, with regional variations that stem from the combination of regional and global conditions. Reclamation and DWR perform routine assessments on the sensitivity of California's water resources to climate change. These assessments require a multi-step analysis with significant uncertainty being introduced in each step of the analysis chain. The process for evaluating water resource sensitivities involves the following, general steps:

1. The rate and volume of global GHG emissions is selected from a common set of emissions projections.

2. Complex Global Circulation Models (GCM) use the atmospheric composition of GHG identified in the first step as input, and simulate the resulting patterns of global atmospheric, oceanic and land surface conditions.

3. In a process referred to as downscaling, hydroclimatic outputs from the GCMs (e.g., precipitation) are adjusted from the large spatial scale of GCMs to a spatial scale appropriate for use in hydrologic models.

4. Hydrologic models simulate local conditions (e.g., stream flows, evapotranspiration) that result from the downscaled hydroclimatic parameters.

5. Simulated stream flows from the hydrologic models are used as input to water supply and operations models and fisheries models, which quantify the ability of a particular water resource system to meet performance objectives under the given hydrologic regime (i.e.,

reliability). Results from these models are the basis for assessing the sensitivity of particular water resource systems to changes in climate.

For SLWRI, a similar approach was followed in performing climate change analyses.

Methodology

This report presents only a brief documentation of the methods used for this climate change analysis. The methodologies for developing input hydrologies, retraining CalSim-II Artificial Neural Networks (ANN) for flow-salinity responses under sea level rise, and adjusting temperature modeling inputs are the same as those described in the approach to climate change evaluations in the April 2012 Bay Delta Conservation Plan (BDCP) Administrative Draft EIS. Detailed descriptions of these methodologies are included in the Appendix 5.A.2 of the BDCP Administrative Draft EIS (ICF, 2012). Detailed descriptions of the CalSim-II, SRWQM, and SALMOD models used for this climate change evaluation are included in Chapters 2, 3, 4 and 5 of the Modeling Appendix to this DEIS.

Selection of Emission and Climate Change Scenarios

Climatic Projections

This section discusses emissions and climate change scenarios that were selected for this climate change analysis. Three emission scenarios (A2, A1B and B1) were selected from the four SRES families developed by IPCC. For the three SRES emission scenarios, 112 future climate projections were developed using 16 different GCMs developed by national climate centers all around the world. The 112 climate projections were bias corrected and spatially downscaled to 1/8 degree (~12km) resolution over the contiguous United States through methods described in detail in Wood et al. 2002, Wood et al. 2004, and Maurer 2007. Climatic projections data from GCMs were obtained from Lawrence Livermore National Laboratory under the World Climate Research Program's (WCRP) Coupled Model Intercomparison Project Phase 3 (CMIP3).

A multi-model approach was selected for integrating the information from the 112 downscaled climatic projections. In this approach, the group of multi-model, multi-emission scenario projections termed the ensemble was grouped into four quadrants (Q1 through Q4) using values of simulated changes in annual temperature and precipitation compared to an historical reference period for each climatic projection. Each quadrant consisted of a set of climatic projections based of a nearest neighborhood analysis that represent (1) drier, less warming, (2) drier, more warming, (3) wetter, more warming, and (4) wetter, less warming than the ensemble median values.

In addition, a fifth region (Q5) was developed from inner-quartiles (25^{th} to 75^{th} percentile) of the ensemble and represents a central region of climate change. The Q5 scenario is derived from the central tending climate projections and thus favors the consensus of the ensemble which is evaluated in this study. The Q5 scenario was the only scenario applied for this SLWRI climate change analysis.

Sea Level Rise Scenarios

Projected sea level rise in the future was computed using empirical models based on the degree of global warming developed by Ramsdorf (2007). This method better reproduces historical sea levels and generally produces larger estimates of sea level rise than those indicated by the IPCC (2007). For the year 2060, the projected sea level rise is approximately 30 cm to 60 cm (12 inches to 24 inches). These sea level rise estimates are also consistent with those outlined in the recent U.S. Army Corps of Engineers guidance circular for incorporating sea-level changes in civil works programs (USACE 2009). The mid-range sea-level rise value of 45 cm for year 2060 is applied in this climate change analysis for the SLWRI.

Implementation of Climate Variability

Natural variability in historical observed records were incorporated into the projected climate data using an approach called “quantile mapping.” This technique maps the statistical properties of climate variables from one data subset with the time series of events from a different subset. In this fashion, the approach allows the use of a shorter period to define the climate state, yet maintains the variability of the longer historic record. The quantile mapping approach involves the following steps:

1. Extract a 30-year slice of downscaled climate projections based on the ensemble subset for the quadrant of interest and centered on the year of investigation (i.e., 2025 or 2060)

2. For each calendar month (i.e., January) of the future period, determine the statistical properties (CDF) of temperature and precipitation at each grid cell

3. For each calendar month of the historical period (1971-2000 in this assessment), determine the statistical properties (CDFs) of temperature and precipitation at each grid cell

4. Develop quantile maps between the historic observed CDFs and the future downscaled climate CDFs, such that the entire probability distribution (including means, variance, skew, etc.) at the monthly scale is transformed to reflect the climate scenario.

Regional Hydrologic Modeling

The GCM downscaled climate projections (DCP), developed through the process described above, were then used to create modified temperature and precipitation inputs for the Variable Infiltration Capacity (VIC) hydrology model. The VIC model simulates hydrologic processes on the 1/8 degree scale to produce watershed runoff (and other hydrologic variables) for the major rivers and streams in the Central Valley. The VIC model simulations produce outputs of hydrologic parameters for each 1/8 grid cell and daily and monthly streamflows at key locations in the Sacramento and San Joaquin River watersheds. The changes in "natural" flow at these locations between the observed and climate scenarios are then applied to adjust monthly historical inflows to CalSim-II.

Hydrology and Systems Operations Modeling

Systems operations modeling was performed using the SLWRI 2012 Benchmark Version CalSim-II model, with adjusted input parameters as described below. CalSim-II provides information about the CVP and SWP operations, including reservoir storages, river and canal flows, and project deliveries. The CalSim-II model simulates the response of the river-reservoir-conveyance system to the climate change derived hydrologic patterns.

Two scenarios were simulated to evaluate SLWRI project benefits under climate change which are listed below.

1. Future No Action Scenario with climate change (Q5 Climatic Hydrology with 45 cm sea level rise by 2060) (**FUT_NA_2060Q5**)

2. Future CP4 alternative scenario without climate change (Q5 Climatic Hydrology with 45 cm sea level rise by 2060) (**FUT_CP4_2060Q5)**

Climate change scenario "Q5" represents the central estimate of future climate change for the 30-year climatological period centered on the analysis year 2060.

Determination of flow-salinity relationships in the Delta is critical to both project and ecosystem management. Operation of the SWP/CVP facilities and management of Delta flows is often dependent on Delta flow needs for salinity standards. Salinity in the Delta for operational decisions in CalSim-II is obtained using ANN that mimics the flow-salinity relationships as simulated in Delta Simulation Model (DSM2). A more detailed description of the use of ANNs in the CalSim-II model is provided in Wilbur and Munévar (2001) (ICF, 2012).

The following is a list of input parameters that were adjusted in CalSim-II to incorporate the effects of climate change for this analysis:

- Inflow time series records for all major and minor streams in the Central Valley from a the procedure described above

- Sacramento and San Joaquin Valley water year types adjusted to reflect new runoff patterns

- Runoff forecasts used for reservoir operation and allocation decisions
- Delta water temperature as used in triggering biological opinion smelt criteria
- Modified ANNs to reflect the flow-salinity response under 45 cm sea level rise by 2060

Reservoir and system operation rules were not modified in an attempt to "optimize" system operations under the revised conditions. Thus, the CalSim-II results represent the risks to operations, water users, and the environment in the absence of dynamic adaptation for climate change.

Reservoir and River Water Temperature Modeling

The SRWQM was applied to simulate water temperatures in the upper Sacramento River system. Detailed information on the SRWQM and on the methodology applied for temporal downsizing of monthly outputs from CalSim-II to daily values for use in temperature modeling can be found in the Modeling Appendix to the DEIS.

For the climate change scenarios, the Sacramento River equilibrium temperatures used in the SRWQM model were adjusted using projected changes in air temperatures with climate change. Temperatures for local tributary creek inflows were not changed.

Fisheries Modeling

The freshwater production potential for the four runs of Chinook salmon (*Oncorhynchus tshawytscha*) that inhabit the Sacramento River was evaluated using the SALMOD model. A complete description of SALMOD is included in both Chapter 11 of the DEIS and in Chapter 5 of the Modeling Appendix to the DEIS.

Method Summary

The overall process for assessing anadromous fish survival under climate change for the SLWRI is summarized in Figure 4-1. Figure 4-1 presents the various sequential steps beginning from identification of emission scenarios to simulation of salmon mortalities using SALMOD model.

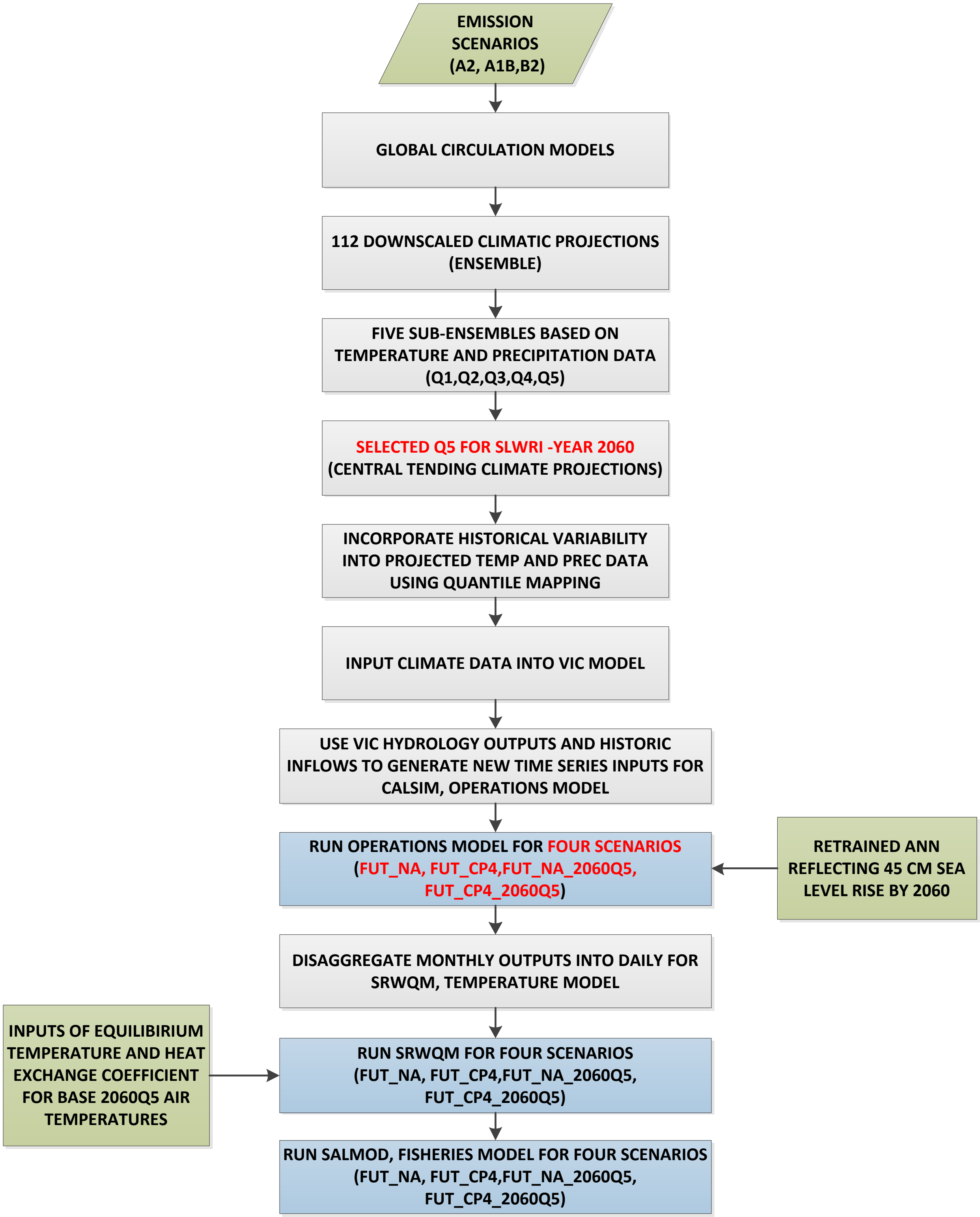

Figure 4-1. Schematic of Overall Methodology for Climate Change Assessment

Hydrology and Operations

Figure 4-2 shows projected inflows into Shasta reservoir based on the central estimate (Q5) of climatic projections. Figure 4-2 indicates a shift in runoff timing with higher inflows in December, January, and February from rainfall and reduced snowmelt runoff between April and June. Under this scenario, annual Shasta Reservoir inflows would increase slightly by 2 percent (98 TAF) due to climate change by 2060. Winter flows are likely to increase in magnitude followed by a decline in snowmelt runoff in spring and summer. This shift in timing of runoffs and reservoir inflows could affect the CVP and SWP system operations.

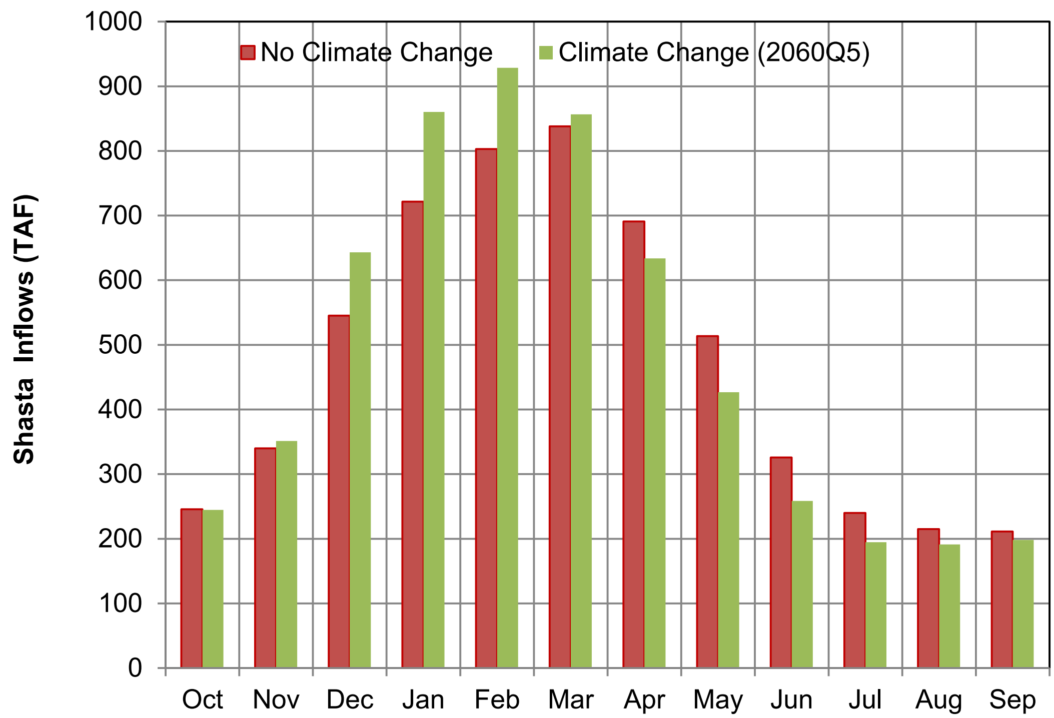

Figure 4-2. Comparison of Shasta Reservoir Inflows with and Without Climate Change in the Future

Figure 4-3 shows an exceedence plot of end-of-month Shasta storages with and without project under projected future climatic conditions. Shasta storage would remain higher under CP4 than under the future No-Action Alternative in the Q5 climatic scenario. The projected shift in timing of runoffs and reservoir inflows would result in changes in system operations. Higher sea levels in the future could increase salinity intrusions in the Sacramento-San Joaquin Delta which could trigger more releases from upstream reservoirs to meet water quality objectives in the Delta. Figure 4-4 shows a comparison of average monthly Shasta releases with and without alternative CP4 under the Q5 climatic scenario.

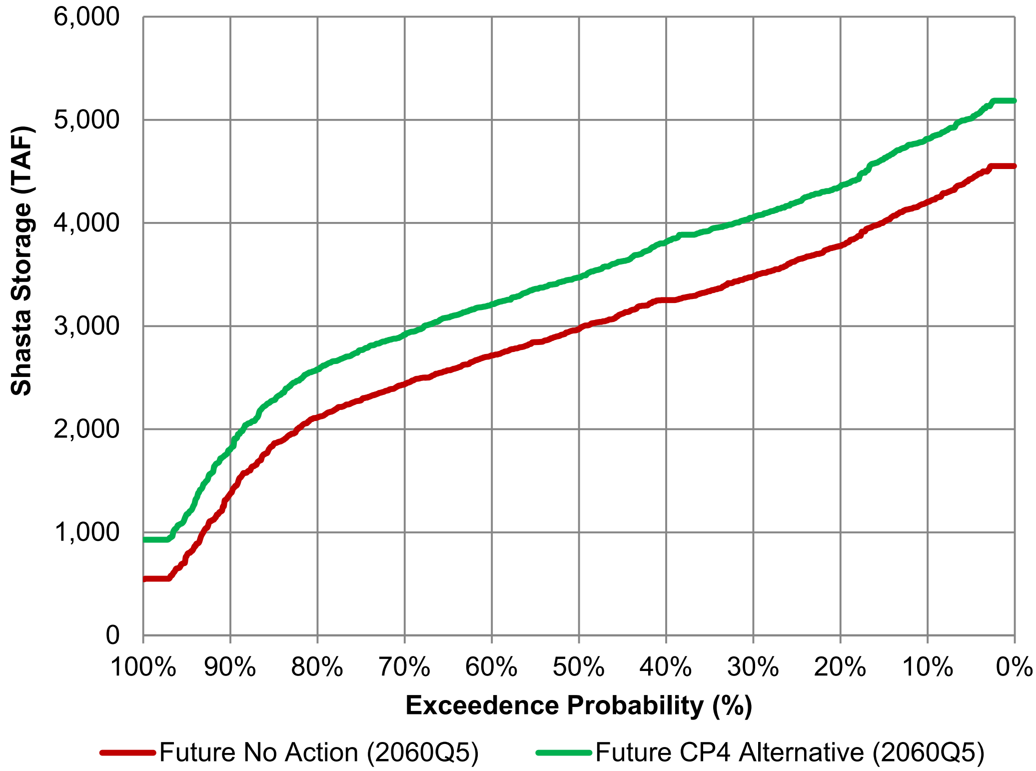

Figure 4-3. End of Month Shasta Storages

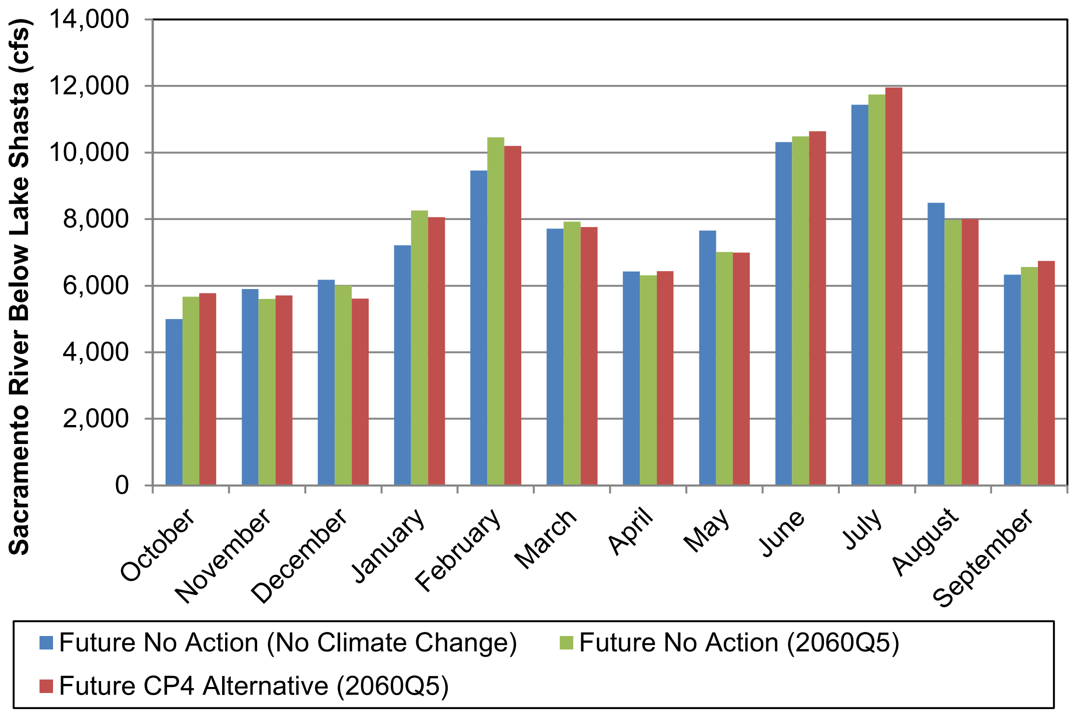

Figure 4-4. Sacramento River Flow Below Shasta

Upper Sacramento River Temperature

Changes in future climatic conditions (year 2060-Q5 scenario) could increase upper Sacramento River temperatures by up to 2.2°F on a monthly average basis compared to conditions without any changes in climate. Average monthly river temperatures for CP4 would be up to two degrees colder than under the future No-Action Alternative under future climatic conditions between August and October. The differences between with and without project conditions under climate change diminish with distance downstream from Shasta Dam to Balls Ferry as the system approaches equilibrium conditions, as shown in Figures 4-5 through 4-8. Overall, the temperatures under CP4 would decrease by nearly 0.5°F compared to the future No-Action Alternative under climatic conditions based on long-term monthly average at the Sacramento River locations shown in Figure 4-5 through Figure 4-8. Benefits of CP4 under projected climatic changes on anadromous fish survival are evaluated using the fisheries model SALMOD, described in the following sections.

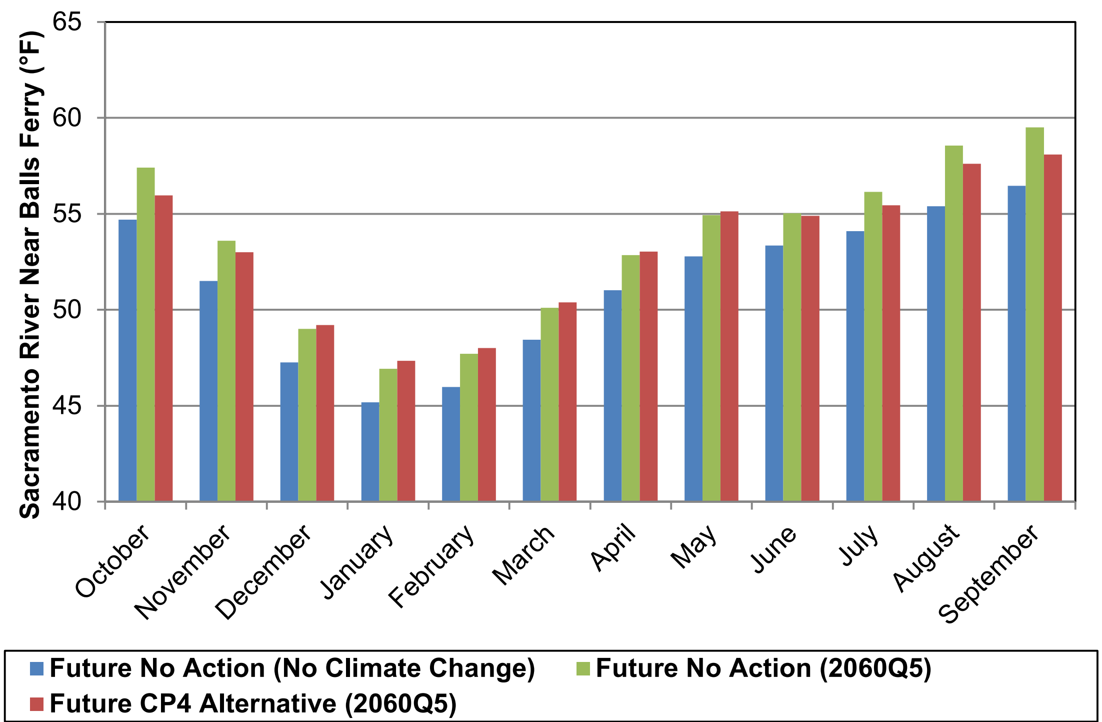

Figure 4-5. Sacramento River Temperature near Balls Ferry

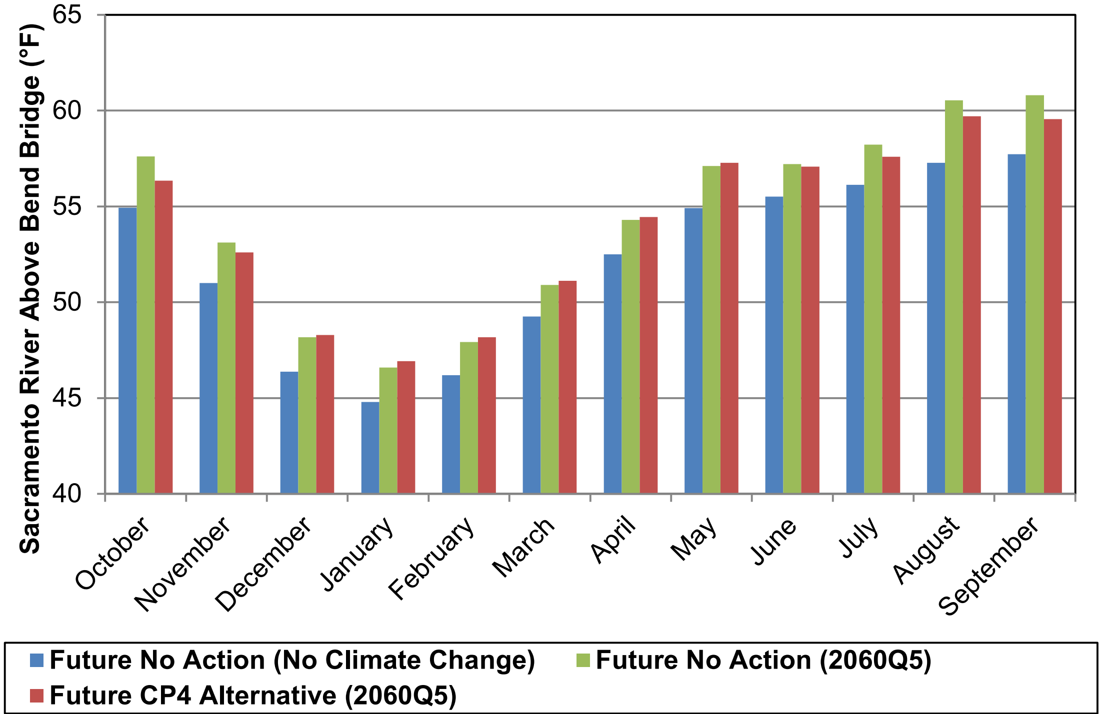

Figure 4-6. Sacramento River Temperature above Bend Bridge

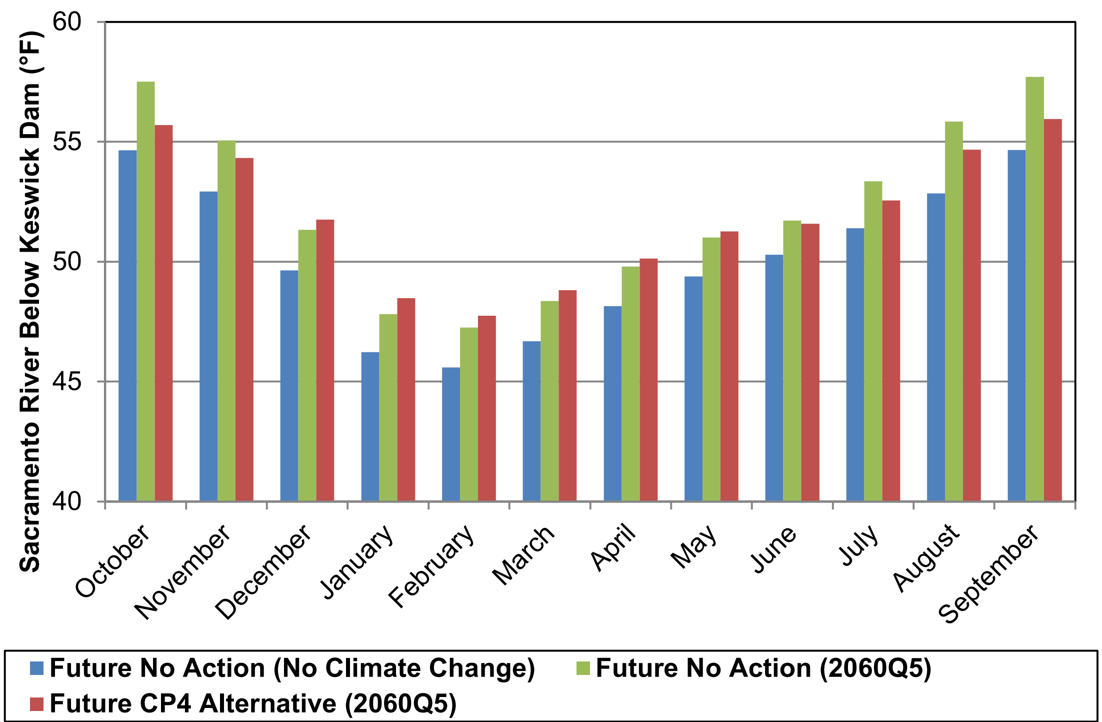

Figure 4-7. Sacramento River Temperature Below Keswick Dam

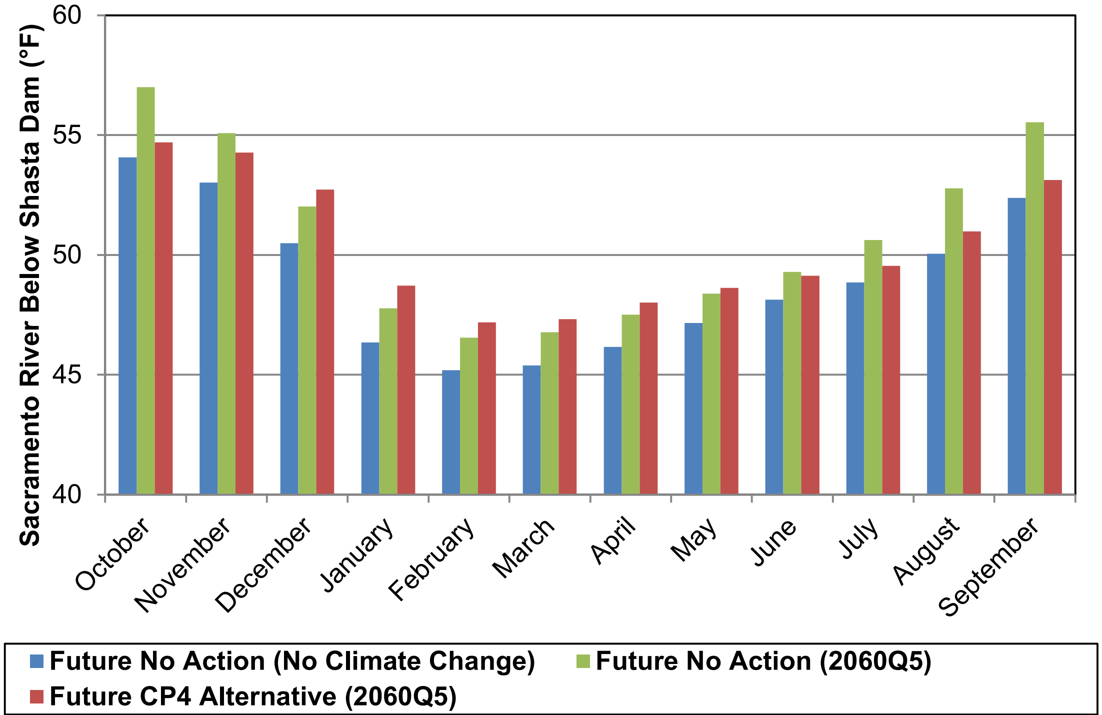

Figure 4-8. Sacramento River Temperature Below Shasta Dam

Fisheries

The need for improved cold water storage in Shasta Lake was identified early in the SLWRI evaluation, and in both the National Marine Fisheries Service 2009 Biological Opinion (BO) and the 2009 Draft Recovery Plan. Key text from the 2009 BO describing how to benefit Chinook salmon in the upper Sacramento River includes:

- *Ensure a sufficient cold water pool to provide suitable temperatures for winter-run spawning between Balls Ferry and Bend Bridge in most years, without sacrificing the potential for cold water management in a subsequent year.*

- *Ensure suitable spring-run temperature regimes, especially in September and October.*

- *Need for stable Sacramento River level/stage to increase habitat for optimal spring-run and fall-run redds/egg incubation and minimization of redd dewatering and juvenile stranding.*

- *Depending on hydrology and air temperature, from May through October, it is necessary to use the cold water* *pool in Shasta Reservoir to provide cold water releases to maintain suitable water temperatures for listed anadromous fish below Shasta. Without access to the cold water pool, suitable temperatures for egg incubation are not attainable.*

- ***Action I.2.2.****B 1) Maintain Keswick releases between 7000 cfs and 3250 cfs to reduce adverse effects on mainstem spring-run and conserve storage for next year's cold water pool…… 3) Be more conservative in Keswick releases throughout fall and early winter if hydrology is dry, and release more water for other purposes if hydrology becomes wet. For example, release no more than 4,000 cfs if hydrology remains dry.*

- ***Action I.2.3.*** *2) Reclamation shall make releases to maintain a temperature compliance point not in excess of 56 degrees between Balls Ferry and Bend Bridge from April 15 through May 15.*

- ***Action 1.2.4*** *Reclamation shall manage operations to achieve daily average water temperatures in the Sacramento River between Keswick Dam and Bend Bridge as follows:*

1) Not in excess of 56°F at compliance locations between Balls Ferry and Bend Bridge from May 15 through September 30 for protection of winter-run, and not in excess of 56°F at the same compliance locations between Balls Ferry and Bend Bridge from October 1 through October 31 for protection of mainstem spring run, whenever possible.

Key text from the 2009 Draft Recovery Plan referencing the risks to salmonids from climate change includes:

- *If air temperatures in California rise significantly, it will become increasingly difficult to maintain appropriate water temperatures in order to manage coldwater fisheries, including winter-run Chinook salmon. A reduction in snowmelt and increased evaporation could lead to decreases in reservoir levels and, perhaps more importantly, coldwater pool reserves (California Energy Commission 2003). As a result, water temperatures in rivers supporting anadromous salmonids, including winter-run Chinook salmon, could potentially rise and no longer be able to support over-summering life stages (i.e., winter-run Chinook salmon embryo incubation, fry* *emergence, and juvenile emigration). The California Department of Water Resources suggests that under a warmer climate scenario, water temperature standards in the upper Sacramento River likely could not be maintained.*

- *Winter-run Chinook salmon are especially vulnerable to climate warming, prolonged drought, and other catastrophic climate events, because they have only one remaining population that spawns in the hottest time of the year*

- ***Upper Sacramento River Action 2.6.2.1** Implement a river flow management plan that balances carryover storage needs with instream flow needs for winter-run Chinook salmon based on runoff and storage conditions, including flow fluctuation and ramping criteria (USFWS 2001).*

- *The embryo incubation life stage of winter-run Chinook salmon is the most sensitive to elevated water temperatures. Preferred water temperatures for Chinook salmon egg incubation and embryo development range from 46°F to 56°F (NMFS 1997). A significant reduction in egg viability occurs at water temperatures above 57.5°F and total mortality may occur at 62°F (NMFS 1997). Additionally, several diseases that can adversely affect developing embryos become more virulent as water temperatures increase. For example, Saprolegnia is a common fungal disease, which spreads rapidly and suffocates developing eggs in a redd. The rate of fungal growth rises exponentially as water temperatures increase from the mid-50s to the low-60s (NMFS 1997). Historically, water temperatures in the middle Sacramento River typically exceeded 60°F from July through September and in drier years may have exceeded 66°F (NMFS 1997). Winter-run Chinook salmon that spawned downstream of the RBDD normally did not produce viable offspring because of lethal water temperatures (Hallock and Fisher 1985). However, with implementation of the TCD* [temperature control device] *at Shasta Dam in 1997 suitable water temperatures for embryo incubation may extend downstream of Bend Bridge. Currently, river water temperatures just below the RBDD only marginally exceed the incipient lethal level for incubating eggs during June through September, by reaching 57°F to*

58°F. These water temperatures are in the range that would typically cause mortality for 10 to 20 percent of eggs (Cramer et al. 2003).

Based on the need to protect listed Chinook salmon in the Sacramento River watershed, an assessment similar to that presented in the DEIS was used to evaluate potential implications of raising Shasta Dam to Chinook salmon production. Using the results from SALMOD, it is clear that climate change will impact Chinook salmon production in the Sacramento River upstream from Red Bluff Pumping Plant (RBPP) by altering flow and water temperatures in a manner that would result in reduced Chinook salmon survival. Implementation of CP4 would result in the ability to increase the cold water storage needed to release cold water and meet the water temperatures at the Bend Bridge compliance point to benefit both spring-run and winter-run Chinook salmon, per the 2009 BO requirement.

Figures 4-9 through 4-12 show the differences in production between the No-Action Alternative with no climate change, the No-Action Alternative with climate change, and CP4 with climate change. For most runs, the greatest differences occur in critical and dry water years. Production under CP4 with climate change is greater than under the No-Action Alternative with climate change. Therefore, under climate change conditions, implementing CP4 would result in an increased likelihood of species preservation, whereas under the No-Action Alternative, most of the races in the Sacramento River would be at risk of extirpation.

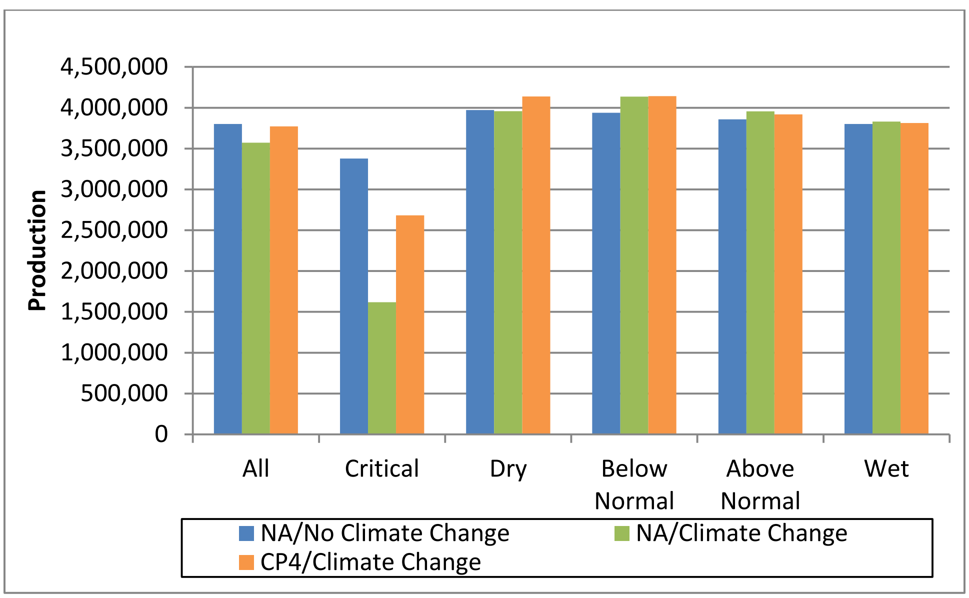

Figure 4-9. Winter-Run Chinook Production Under the No-Action Alternative with and without Climate Change and Under CP4 with Climate Change

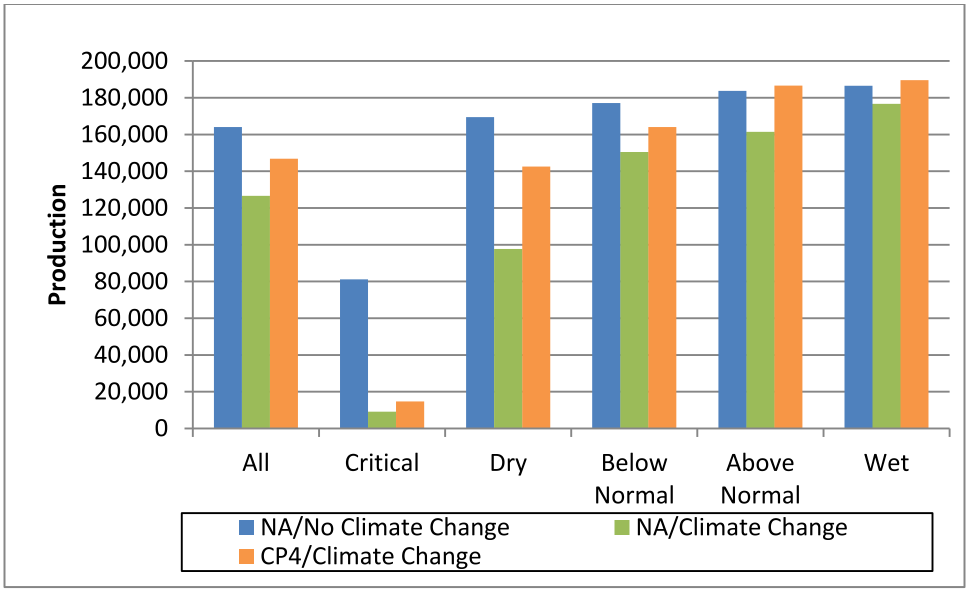

Figure 4-10. Spring-Run Chinook Production Under the No-Action Alternative with and without Climate Change and Under CP4 with Climate Change

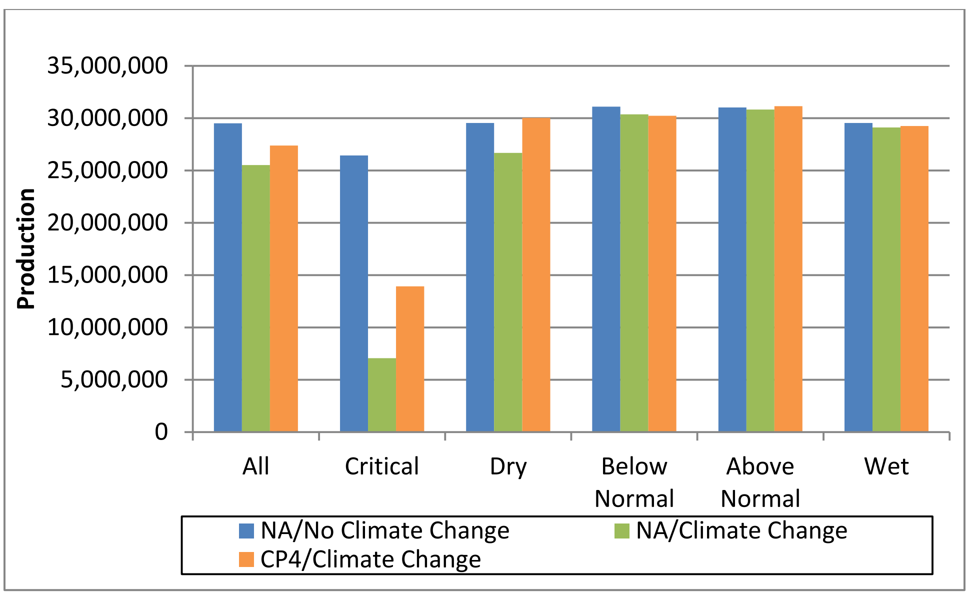

Figure 4-11. Fall-Run Chinook Production Under the No-Action Alternative with and without Climate Change and Under CP4 with Climate Change

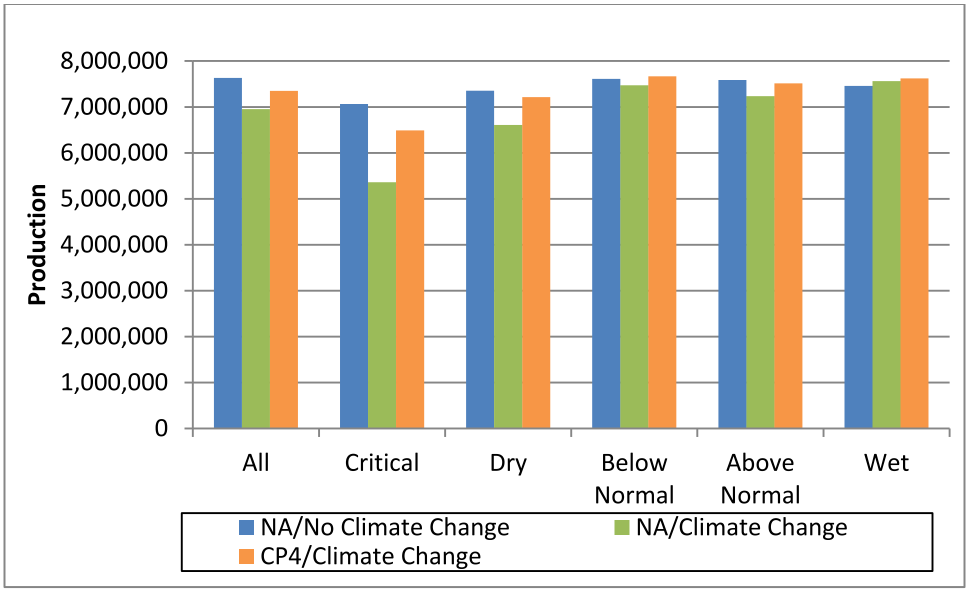

Figure 4-12. Late Fall-Run Chinook Production Under the No-Action Alternative with and without Climate Change and Under CP4 with Climate Change

Under the No-Action Alternative with climate change, the average annual production for winter-run Chinook salmon is over 3.5 million juveniles reaching the RBPP. However, 6 of the simulated 83 years (all critical water years) have productions under 1 million fish with three of those under 20,000 fish. Implementing CP4 with climate change would result in only 1 year with productions less than 1 million fish. Under the No-Action Alternative with climate change, late fall-run would experience 3 years under 2 million fish, but CP4 would result in production of not less than 2 million fish. Late fall-run Chinook salmon would have the lowest risk of extirpation from climate change. Late fall-run Chinook salmon would benefit from implementation of CP4, but would be less affected by implementation of CP4 as compared with the other runs.

Both spring-run and fall-run would be the most significantly impacted from climate change if alternative CP4 is not implemented. In all but two critical water years, spring-run Chinook salmon populations would likely be extirpated. Under the No-Action Alternative, water years 1931 through 1934 and 1990 to 1992 would have zero fish surviving through the egg life stage. Given that the majority of Chinook salmon return as 3 year olds to spawn, a prolonged drought with unsuitable conditions could wipe out spring-run Chinook salmon in the upper Sacramento River. Under CP4, however, while productions are overall lower in 1931 through 1934 and 1990 through 1992 compared with all the other simulated years, there are juveniles surviving during these drought years and migrating downstream from RBPP, thus giving spring-run Chinook salmon improved chances of returning as adults to spawn in later years.

Fall-run Chinook salmon production follows a similar pattern as that for spring-run Chinook salmon. Under the No-Action Alternative, water years 1931, 1933 and 1934 would have zero eggs surviving, and only just under 8,600 eggs surviving in 1932. Additionally, in 1990, just under 16,000 eggs survived, but 1991 and 1992 had zero eggs surviving. These trends could result in extirpation of naturally spawning fall-run Chinook salmon in the upper Sacramento River, and would be dependent on straying adults to repopulate fall-run Chinook salmon in the upper Sacramento River.

Comparisons of mortalities under the No-Action Alternative and CP4 show that without implementing CP4, climate change has very significant impacts to each of the four runs, particularly at the prespawn and egg life stages.

Under CP4 relative to the No-Action Alternative, winter-, spring-, fall-, and late fall-run Chinook salmon experience a significant decrease in water temperature-related mortality under all water year types, but an insignificant change in flow-related mortality. The increase in mortality resulting from flows (impact) is far less overall than the decrease in mortality from water temperatures and flows (benefit). Therefore, all four runs of Chinook salmon would experience a benefit from alternative CP4 relative to the No-Action Alternative under climate change conditions and the risk of extirpation would be greatly reduced.

Under CP4 relative to the No-Action Alternative, winter-run Chinook salmon would experience a significant decrease in water temperature-related mortality under all water year types, a significant increase in flow-related mortality under dry water year types, and a significant decrease during critical water year types due to climate change. In above-normal year types, spring-run Chinook salmon would experience a significant decrease in flow-related mortality under CP4 relative to the No-Action Alternative with climate change. For fall-run Chinook salmon, mortality resulting from flows increases significantly in critical and dry water years, but increases by much less in below-normal, above-normal and wet water years. Late fall-run Chinook salmon experience a significant decrease in water temperature-related mortality under all water year types, but an insignificant change in flow-related mortality under all water year types under CP4 relative to the No-Action Alternative with climate change.

Although not modeled in SALMOD, increasing water temperatures in the Sacramento River would likely result in more fish spawning in the upper reaches of the river. This could lead to increased competition for spawning and rearing habitat, potentially leading to increased mortality. Therefore, increasing cold water reliability in the upper Sacramento River will improve spawning and rearing conditions, and help minimize any impacts resulting from competition or reduced habitat availability. By increasing the cold water pool in Shasta Lake, CP4 also provides for the potential for adaptive management to accommodate the potential impacts of climate change to fisheries.

Based on the results of SALMOD, without increasing the cold water pool in Shasta Lake, Chinook salmon would suffer extreme losses, likely even extirpation, from climate change. Implementation of CP4 would benefit Chinook salmon by modifying water temperatures in the Sacramento River, potentially preserving the runs, particularly winter-run, spring-run and fall-run Chinook salmon.

Chapter 5 References

Ainsworth, E.A., & Long, S.P. (2005). What have we learned from 15 years of free-air CO_2 enrichment (FACE)? A meta-analytic review of the responses of photosynthesis, canopy properties and plant production to rising CO_2. New Phytologist, 165(2), 351-372.

Anderson, M.T.; J.F. Stamm, P.A. Norton. 2008a. "Changes in Monthly Streamflow Conditions in the Missouri River Basin from 1957 to 2007," *American Geophysical Union*, Fall Meeting 2008, abstract #H11I-02.

Anderson, J., F. Chung, M. Anderson, L. Brekke, D. Easton, M. Ejeta, R. Peterson, and R. Snyder. 2008. "Progress on Incorporating Climate Change into Management of California's Water Resources." *Climatic Change*, Springer, Netherlands, Volume 89, Supplement 1, pp. 91–108. Published online 12-22-2007. ISSN: 0165-0009 (Print) 1573–1480 (Online) DOI: 10.1007/s10584-007-9353-1.

Barnett, T.P., D.W. Pierce, H.G. Hidalgo, C. Bonfils, B.D. Santer, T. Das, G. Bala, A. Wood, T. Nazawa, A. Mirin, D. Cayan, and M. Dettinger. 2008. "Human-induced changes in the hydrology of the Western United States." *Science*, 319(5866), 1080–1083, doi:10.1126/science.1152538.

Beckley, B.D., F.G. Lemoine, S.B. Luthcke, R.D. Ray, and N.P. Zelensky. 2007. "A reassessment of global and regional mean sea level trends from TOPEX and Jason-1 altimetry based on revised reference frame and orbits." *Geophysical Research Letters* 34:L14608.

Bonfils, C., D.W. Pierce, B.D. Santer, H. Hidalgo, G. Bala, T. Das, T. Barnett, C. Doutriaux, A.W. Wood, A, Mirin, and T. Nazawa. 2008. "Detection and attribution of temperature changes in the mountainous Western United States." *Journal of Climate* 21(23): 6404–6424, doi:10.1175/ 2008JCLI2397.1.

CALFED Independent Science Board (CALFED). 2007. Sea Level Rise and Delta Planning. Memorandum to Michael Healey, Lead Scientist of the CALFED Bay-Delta Program. September 6, 2007.

Cayan, D.R., S.A. Kammerdiener, M.D. Dettinger, J.M. Caprio, and D.H. Peterson. 2001. "Changes in the Onset of Spring in the Western United States." *Bulletin of the American Meteorology Society* 82(3): 399–415.

California Energy Commission. 2003. Climate Change and California Staff Report. Prepared in Support of the 2003 Integrated Energy Policy Report Proceeding (Docket # 02-IEO-01).

California Energy Commission (CEC). 2006. Inventory of California Greenhouse Gas Emissions and Sinks: 1990 to 2004. (Staff Final Report). Publication CEC-600-2006-013-SF. Available: <http://www.climatechange.ca.gov/policies/ greenhouse_gas_inventory/index.html> and <http://www.energy.ca.gov/global_ climate_change/inventory/documents/index.html>. Last updated July 2008. Accessed April 20, 2009

CEC. *See* California Energy Commission.

Church, J.A., and N.J. White. 2006. "A 20th century acceleration in global sea-level rise." *Geophysical Research Letters* 33: L01602.

Cramer, S.P, M. Daigneault, M. Teply, and R2 Resource Consultants, Inc. 2003. Step 1 Report, Conceptual Framework for an Integrated Life Cycle Model of Winter-Run Chinook Salmon in the Sacramento River. Prepared for California Urban Water Agencies. Sacramento, California.

Daly, C., Neilson, R.P., & Phillips, D.L. (1994). A statistical-topographic model for mapping climatological precipitation over mountainous terrain. Journal of applied meteorology, 33(2), 140-158.

Das, T., H.G. Hidalgo, M.D. Dettinger, D.R. Cayan, D.W. Pierce, C. Bonfils, T.P. Barnett, G. Bala and A. Mirin. 2009. "Structure and Detestability of Trends in Hydrological Measures over the Western United States." *Journal of Hydrometeorology*, Vol. 10, doi:10.1175/2009JHM1095.1.

Dettinger, M.D., and D.R. Cayan. 1995. "Large-scale Atmospheric Forcing of Recent Trends toward Early Snowmelt Runoff in California." *Journal of Climate*, Vol. 8(3).

Gibson, W.P., C. Daly, T. Kittel, D. Nychka, C. Johns, N. Rosenbloom, A. McNab, and G. Taylor. 2002. Development of a 103-year high-resolution climate data set for the conterminous United States. In: Proc., 13th AMS Conf. on Applied Climatology, Amer. Meteorological Soc., Portland, Oregon, May 13–16, 181–183.

DWR. 2009. The California Water Plan, Update, Bulletin 160-09. Sacramento, California. December.

DWR. 2010. Least-Cost Planning Simulation Model (LPCSIM). Division of Planning and Local Assistance. Sacramento, California.

Hallock, R.J, and F.W. Fisher. 1985. Status of Winter-Run Chinook Salmon, Oncorhynchus tshawytscha, in the Sacramento River. Prepared for the Anadromous Fisheries Branch of the California Department of Fish and Game. January.

Hidalgo H.G., T. Das, M.D. Dettinger, D.R. Cayan, D.W. Pierce, T.P. Barnett, G. Bala, A. Mirin, A.W. Wood, C. Bonfils. 2009. "Detection and Attribution of Streamflow Timing Changes to Climate Change in the Western United States." *Journal of Climate* 22(13): 3838. doi:10.1175/2008JCLI2470.1.

Hoerling M., J. Eischeid and J. Perlwitz. 2010. "Regional Precipitation Trends: Distinguishing Natural Variability from Anthropogenic Forcing." *Journal of Climate* (in press).

Howitt, R.E., J. Medellin-Azuara, D. MacEwan, J.R. Lund. 2012. "Calibrating Disaggregate Economic Models of Agricultural Production and Water Management." Environmental Modeling and Software. 38: 244–258.

ICF International. 2012. Appendix 5.A.2. Climate Change Approach and Implications for Aquatic Species, Administrative Draft, Bay Delta Conservation Plan. April.

ICF. *See* ICF International.

IPCC. 2000. IPCC Special Report, Emissions Scenarios, Summary for Policy Makers. Intergovernmental Panel on Climate Change. Available at: http://www.ipcc.ch/pdf/special-reports/spm/sres-en.pdf. Accessed: April 2012.

IPCC. 2007. "The Physical Science Basis," contribution of Working Group I to *The Fourth Assessment Report of the Intergovernmental Panel on Climate Change*. Solomon, S., D. Qin, M. Manning, Z. Chen, M. Marquis, K.B. Averyt, M. Tignor, and H.L. Miller (eds.).

Irrigation Training and Research Center. 2003. "California Crop and Soil Evapotranspiration for Water Balances and Irrigation Scheduling/Design." Irrigation Training and Research Center Report No. R 03-001. California Polytechnic State University San Luis Obispo, California.

Kapnick, S., and A. Hall. 2009. *Observed Changes in the Sierra Nevada Snowpack: Potential Causes and Concerns*. California Energy Commission CEC-500-2009-016-F.

Knowles, N., and D. Cayan. 2002. Potential Effects of Global Warming on the Sacramento/San Joaquin Watershed and the San Francisco Estuary. Geophysical Research Letters 29:38-1–38-4.

Knowles, N., M. Dettinger, and D. Cayan. 2007. *Trends in Snowfall Versus Rainfall for the Western United States, 1949–2001*. Prepared for California Energy Commission Public Interest Energy Research Program, Project Report CEC-500-2007-032.

Maurer, E.P. 2007. "Uncertainty in hydrologic impacts of climate change in the Sierra Nevada, California under two emissions scenarios." *Climatic Change*, Vol. 82, No. 3–4:309–325, doi: 10.1007/s10584-006-9180-9.

MacWilliams, M., F. Salcedo, and E. Gross. 2008. San Francisco Bay-Delta UnTRIM Model Calibration Report. Prepared for California Department of Water Resources. December.

Miller, N.L., K.E. Bashford and E. Strem. 2003. Potential Impacts of Climate Change on California Hydrology. *J. Amer. Water Resour. Assoc.* 39, 771–784.

Moser, S., G. Franco, S. Pittiglio, W. Chou, D. Cayan. 2009. *The Future Is Now: An Update on Climate Change Science Impacts and Response Options for California*. California Energy Commission, PIER Energy-Related Environmental Research Program. CEC-500-2008-071.

Mote, P.W., A.F. Hamlet, M.P. Clark, and D.P. Lettenmaier. 2005. "Declining mountain snowpack in western North America." *Bull. Amer. Meteor. Soc.,* 86:39–49.

National Marine Fisheries Service. 1997. Proposed Recovery Plan for the Sacramento River Winter-Run Chinook Salmon. Long Beach, CA: National Marine Fisheries Service, Southwest Region.

———. 2009 (October). Public Draft Recovery Plan for the Evolutionarily Significant Units of Sacramento River Winter-run Chinook Salmon and Central Valley Spring-run Chinook Salmon and the Distinct Population Segment of Central Valley Steelhead. Sacramento Protected Resources Division.

NMFS. *See* National Marine Fisheries Service.

Null, S.E., J.H. Viers and J.F. Mount. 2010. "Hydrologic Response and Watershed Sensitivity to Climate Warming in California's Sierra Nevada." *PLoS One.* Vol. 5(4): e9932. doi:10.1371/journal.pone.0009932.

Peterson, D.H., I. Stewart, and F. Murphy. 2008. "Principal Hydrologic Responses to Climatic and Geologic Variability in the Sierra Nevada, California." *San Francisco Estuary and Watershed Science* 6(1): Article 3.

Pierce, D.W., T. Barnett, H. Hidalgo, T. Das, C. Bonfils, B.D. Santer, G. Bala, M. Dettinger, D. Cayan, A. Mirin, A.W. Wood, and T. Nazawa. 2008. “Attribution of declining Western U.S. snowpack to human effects.” *Journal of Climate* 21(23): 6425–6444, doi:10.1175/2008JCLI2405.1.

Ramsdorf, S. (2007). A semi-empirical approach to projecting future sea level. Science, vol 315. January.

Reclamation. 2011a. *West-Wide Climate Risk Assessments: Bias-Corrected and Spatially Downscaled Surface Water Projections*, prepared by the U.S. Department of the Interior, Bureau of Reclamation, Technical Services Center, Denver ,Colorado. March 2011.

———. 2011b. *Literature Synthesis on Climate Change Implications for Water and Environmental Resources*. Second Edition. Available at: http://www.usbr.gov/research/docs/climatechangelitsynthesis.pdf.

———. 2011c. SECURE Water Act Section 9503(c) – Reclamation Climate Change and Water 2011.

———. 2013. Central Valley Project Integrated Resource Plan: Technical Modeling Report. Prepared by CH2MHill for the U.S. Department of Interior, Bureau of Reclamation. February.

Regonda, S.K., B. Rajagopalan, M. Clark, and J. Pitlick. 2005. “Seasonal Cycle Shifts in Hydroclimatology Over the Western United States.” *Journal of Climate* 18(2): 372–384.

Roos, M. 1991. “A trend of decreasing snowmelt runoff in northern California.” *Proceedings of 59th Western Snow Conference*, Juneau, Alaska, pp 29–36.

Tansey, M.K., C.A. Young, J. F. DeGeorge, and S. Larson. 2011. Land Atmosphere Water Simulator (LAWS) Version 2.0. Bureau of Reclamation, Mid-Pacific Region.

Thornton, P.E. and S.W. Running. 1999. *An Improved Algorithm for Estimating Incident Daily Solar Radiation from Measurements of Temperature, Humidity, and Precipitation*. Agricultural and Forest Meteorology. 93: 211–228.

U.S. Fish and Wildlife Service. 2001. Final Restoration Plan for the Anadromous Fish Restoration Program: A Plan to Increase Natural Production of Anadromous Fish in the Central Valley of California. Prepared for the Secretary of the Interior by the U.S. Fish and Wildlife Service.

USFWS. *See* U.S. Fish and Wildlife Service.

This page left blank intentionally.